SPATIOTEMPORAL DYNAMICS OF INSECTS IN LARGE-SCALE AGRICULTURAL SYSTEMS: METHODOLOGY AND ANALYSIS WITH THE SILVERLEAF WHITEFLY, *BEMISIA ARGENTIFOLII* (BELLOWS AND PERRING)

By

CARLYLE CHRISTOPHER BREWSTER

A DISSERTATION PRESENTED TO THE GRADUATE SCHOOL
OF THE UNIVERSITY OF FLORIDA IN PARTIAL FULFILLMENT
OF THE REQUIREMENTS FOR THE DEGREE OF
DOCTOR OF PHILOSOPHY

UNIVERSITY OF FLORIDA

1996

ACKNOWLEDGMENTS

I would like to thank my advisor and committee chairperson, Dr. Jon C. Allen, for giving me the opportunity to study under his direction for a second time. Jon and I have worked together before, but the experience on this occasion was unique since it gave me an opportunity to know him on a more personal level. It is always a great pleasure for me to work with someone that I can relate to both professionally and personally. I was particularly intrigued by his drive, determination, and passion for the things in which he believes. Some of his views at times seemed abstract and required some imagination. They have always turned into good ideas based on sound scientific principles and have allowed me, as a scientist, to see the advantages of an imagination. For this I thank him.

I also extend my sincere thanks to the members of my committee, Drs. Heather J. McAuslane, Jerry L. Stimac, Jim W. Jones , and Robert M. Peart, for agreeing to be members of my committee, keeping me focused during the course of my studies, and for providing some useful insights into the challenges that lie ahead.

Many thanks also go out to a number of people who supported this project in one way or another. Dr. Dennis Kopp is the national program leader of the National Agricultural Pesticide Impact and Assessment Program (NAPIAP) that provided most of the funding for this project. Dr. Kopp believed in this project from the start and offered

his encouragements on many occasions. I am also indebted to Dr. Jack Paris for his tutoring and guidance in remote sensing technology, and Drs. David Schuster, David Riley and Philip Stansly for support in field work and data collection.

I would like to also thank my parents for their patience , encouragement and support. I know at times they wondered whether I would ever finish my schooling. Finally, I thank my wife, Charlene, and son, Stephen, for their love, patience and sacrifice. My studies have separated me from Charlene for extended periods on at least two occasions during our marriage. Throughout these difficult periods, I was fortunate to have received nothing but the strongest support from her. All my love and thanks go to her. Stephen has been my official time-keeper, constantly inquiring about the progress of each chapter in this study. I hope in time he comes to understand the tremendous encouragement that those inquiries provided.

TABLE OF CONTENTS

ACKNOWLEDGMENTS ii

TABLE OF CONTENTS iv

LIST OF TABLES viii

LIST OF FIGURES x

ABSTRACT xix

CHAPTERS

1. INTRODUCTION AND LITERATURE REVIEW 1

Origin, Distribution and Taxonomic History of Whiteflies 4
Whitefly Biology and Host Preferences 7
Life Stages 7
Development 9
Survival and Mortality 10
Fecundity and Longevity 11
Sex Ratio 12
Host Plant Specificity, Suitability and Preferences 13
Economic Importance 15
Whitefly Induced Host Injury 15
Economic Losses 16
Population Dynamics 17
Factors Affecting Whitefly Dynamics 17
Spatial Distribution of Whiteflies 18
Monitoring Whitefly Population 19
Dispersal and Migration 21
Whitefly Population Models 23
Management of Whitefly Populations 25
Chemical Control 25
Biological Control 27
Cultural and Other Control Strategies 28

Integrated Control 29

2. A SPATIOTEMPORAL INSECT SPECIES INTERACTION MODEL FOR LARGE-SCALE DYNAMICS 40

Introduction 40
Model Formulation, Development and Description 43
Spatially Explicit Population Models 43
Coupled Map Lattices 44
Integrodifference Equations and Discrete Space Counterparts .. 46
Nicholson-Bailey Model Examined 48
The Spatiotemporal Insect Model 50
Prey reproduction 51
Natural enemy attack function 52
Dispersal or redistribution kernels 53
Solving the convolutions 56
The Resource Map 58
Discussion 59

3. EQUILIBRIUM, STABILITY AND CHAOS IN DISCRETE-TIME MODELS OF INSECT SPECIES INTERACTIONS 64

Introduction 64
Equilibrium and Stability in Nonspatial Discrete-Time Systems 66
Single Species First-Order Difference Equations 66
Systems of Two and Three First-Order Difference Equations .. 68
Systems of Order Greater than Three 71
Nonspatial Age-Structured Systems of Interacting Species 77
Stabilizing an Unstable System: Model Modification 79
Equilibrium, Persistence and Dynamics in Spatial Systems 81
Dynamics of Interacting Species in 2-D Systems 84
Study 1: Spatially Varying Initial Populations: Homogeneous System 84
Study 2: Initial Populations at a Single Location: Homogeneous system 85
Study 3: Spatially Varying Initial Populations: Heterogeneous System 87
Study 4: Prey Refuge 87
Discussion 89

4. CONSTRUCTION AND ANALYSIS OF RESOURCE MAPS FOR HERBIVOROUS INSECTS 107

Introduction 107
Farm-Level Whitefly Resource Maps 108
Remote Sensing and Large-scale Resource Maps 110
Remote Sensing Data 110
Data Acquisition and Display 111
Feature Classification 114
Data Preparation for Classification 115
Feature Classification: The San Joaquin Valley Agricultural System .. 116
Data Acquisition 116
Preprocessing and Supporting Data 116
Classification Procedure: K-Means and ISODATA 117
Classification Results and Interpretation 122
San Joaquin Valley Resource Map 125
Feature Classification: The Imperial Valley Agricultural System 125
Data Acquisition 125
Preprocessing and Supporting Data 126
Classification Procedure: Maximum Likelihood 128
Classification Results and Interpretation 129
Imperial Valley Resource Maps 131
Experimental Resource Maps 132
Discussion 132

5. SIMULATING THE DYNAMICS OF THE SILVERLEAF WHITEFLY IN AN ORGANIC CROPPING SYSTEM 173

Introduction 173
Materials and Methods 174
Study Site and Farm Layout 174
Insect Population Sampling and Field Data 174
The Spatially Explicit Whitefly Model 175
Reproductive and attack functions 176
Whitefly resource map 177
Insect dispersal 177
Model parameters 178
Simulations 180
Comparing model output and sampling data 181
Simulation experiments 182
Results and Discussion 183
Concluding Remarks 187

6. SIMULATING THE DYNAMICS OF THE SILVERLEAF WHITEFLY IN THE IMPERIAL VALLEY AGRICULTURAL SYSTEM 199

Introduction 199
Materials and Methods 200
Study Site: The Imperial Valley 200
The Spatially Explicit Whitefly Model 200
Model Parameters and Parameter Maps 205
Simulating Whitefly Dynamics in the Imperial Valley System .. 209
The Model by Wilhoit et al. (1994) 210
Results and Discussion 211

7. SUMMARY AND DISCUSSION 232

The Silverleaf Whitefly Problem 233
The Spatially Explicit Population Model 235
Resource Maps 237
Applying the Model to Whiteflies in Two Spatial Systems 238
Final Considerations 239

APPENDIX EQUILIBRIUM AND STABILITY ANALYSIS 240

LITERATURE CITED 274

BIOGRAPHICAL SKETCH 302

LIST OF TABLES

Table		Page
1-1.	Mean duration of development for *Bemisia tabaci* and *Bemsia argentifolii* at various temperatures and on various host plants	30
1-2.	Economically important viruses and phytotoxic disease disorders resulting from feeding by *Bemisia tabaci* and *Bemisia argentifolii* on agricultural crops	39
3-1.	Parameter values for *Trialeurodes vaporariorum* and *Encarsia formosa* in the simplifed non-spatial age-structured model.	93
3-2.	Spatiotemporal patterns observed in discrete-time coupled systems with species interaction.	94
4-1.	Characteristics of remotely sensed Landsat Thematic Mapper data.	135
4-2.	Green Soil, Bright Soil and Dark Soil sample values obtained from raster correlation, that were used in the Graham-Schmidt™ Orthogonalization transformations of the San Joaquin Valley Landsat TM subscenes.	136
4-3.	Mean radiance for TM bands 3 and 4, and feature class characteristics from the ISODATA classification of Landsat TM data on the San Joaquin Valley.	137
4-4.	Factor loadings and correlation between Landsat TM bands and Principal Component axes for Landsat TM data on the Imperial Valley, California.	140
4-5.	Confusion matrix and accuracy estimates from classification of the February 23, 1995 Landsat TM data on the Imperial Valley, CA.	141
4-6.	Classification accuracy estimates for Landsat TM data on the Imperial Valley, California.	142
4-7.	Earth observation satellites planned for the next decade.	145

5-1. State variables, parameters and functions in the spatiotemporal model for *Bemisia argentifolii* at Pine Island Organics. 189

5-2. Standard parameter values used for *Bemisia argentifolii* and the natural enemy in the Pine Island simulations. 190

6-1. State variables, parameters and functions in the spatiotemporal model for the silverleaf whitefly, *Bemisia argentifolii* in the Imperial Valley, CA. 215

6-2. Parameter values for *Bemisia argentifolii* reproduction, immature survival and development in the Imperial Valley whitefly simulation model 216

LIST OF FIGURES

Figure		Page
2-1.	Redistribution kernels generated from two-dimensional normal density functions. (a) symmetric redistribution; (b) and (c), direction-biased redistribution (d), wind blown redistribution kernel from (a).	62
2-2.	Dispersal patterns for whiteflies. (a) bimodal redistribution showing the dispersal pattern for trivial fliers and migrators; (b) a repulsive dispersal pattern or ripple density function.	63
3-1.	Spatiotemporal dynamics on a 64 x 64 grid with a 2-D integrodifference equation Nicholson-Bailey model. One cell initially seeded and prey and predator dispersal is Gaussian with equal standard deviations (1:1 grid cell); $r = 2.0$, $a = 0.5$. (a) prey and predator interaction--high prey density (red), high predator density (dark-blue); (b) simulation time plot--prey (red), predator (black); (c) phase-plane plot; (d) Lyapunov exponent.	95
3-2.	Spatiotemporal dynamics on a 64 x 64 grid with a 2-D integrodifference equation Nicholson-Bailey model. One cell initially seeded and prey and predator dispersal is Gaussian with the standard deviation of predator dispersal twice that of prey (2:1 grid cells); $r = 2.0$, $a = 0.5$. (a) prey and predator interaction--high prey density (red), high predator density (dark-blue); (b) simulation time plot--prey (red), predator (black); (c) phase-plane plot,; (d) Lyapunov exponent.	96
3-3.	Spatiotemporal dynamics on a 64 x 64 grid with a 2-D integrodifference Nicholson-Bailey model. One cell initially seeded and prey and predator dispersal is Gaussian with the standard deviation of predator dispersal four times that of prey (4:1 grid cells); $r = 2.0$, $a = 0.5$. (a) prey and predator interaction--high prey density (red), high predator density (dark-blue); (b) simulation time plot--prey (red), natural enemy (black); (c) phase-plane plot; (d) Lyapunov exponent.	97

3-4. Spatiotemporal dynamics on a 64 x 64 grid with a 2-D integrodifference equation Nicholson-Bailey model. All cells initially seeded and prey and predator dispersal is Gaussian with equal standard deviations (1:1 grid cell) ; r varies spatially with Uniform distribution as $1 < r < 2.0$, $a = 0.5$ (a) prey and predator interaction--high prey density (red), high predator density (dark-blue); (b) simulation time plot--prey (red), predator (black); (c) phase-plane plot; (d) Lyapunov exponent. 98

3-5. Spatiotemporal dynamics on a 64 x 64 grid with a 2-D integrodifference equation Nicholson-Bailey model. All cells initially seeded and prey and predator dispersal is Gaussian with the standard deviation of prey dispersal twice that of predator (2:1 grid cells); r varies spatially with Uniform distribution as $1 < r < 2.0$, and $a = 0.5$. (a) prey and predator interaction--high prey density (red), high predator density (dark-blue); (b) simulation time plot--prey (red), predator (black); (c) phase-plane plot; (d) Lyapunov exponent. 99

3-6. Spatiotemporal dynamics on a 64 x 64 grid with a 2-D integrodifference equation Nicholson-Bailey model. All cells initially seeded and prey and predator dispersal is Gaussian with the standard deviation of predator dispersal twice that of prey (2:1 grid cells); $r = 2.0$, a varies randomly with Uniform distribution as $0 < a < 0.5$. (a) prey and predator interaction--high prey density (red), high predator density (dark-blue); (b) simulation time plot--prey (red), predator (black); (c) phase-plane plot; (d) Lyapunov exponent. 100

3-7. Spatiotemporal dynamics on a 64 x 64 grid with a 2-D integrodifference equation Nicholson-Bailey model. All cells initially seeded and prey and predator dispersal is Gaussian with the standard deviation of predator dispersal four times that of prey (4:1 grid cells) ; r =2.0 , a varies spatially with Uniform distribution as $0 < a < 0.5$. (a) prey and predator interaction--high prey density (red), high predator density (dark-blue); (b) simulation time plot--prey (red), predator (black); (c) phase-plane plot; (d) Lyapunov exponent. 101

3-8. Varying prey refuge in a 64 x 64 spatial grid. Black areas represent refuge cells with predator searching efficiency $a = 0.0$; White areas are non-refuge with $a > 0$. The amount of refuge is obtained fromthe equation, $a = \overline{a}\,[(1 + \Delta)*U(0,1) - \Delta\,]$. Negative a values are reassigned to 0.0. In the refuge maps shown (a) $\Delta = 0.05$, (b) $\Delta = 0.10$, (c) $\Delta = 0.25$, and(d) $\Delta = 1.00$. 102

3-9. Spatiotemporal dynamics on a 64 x 64 grid with a 2-D integrodifference equation Nicholson-Bailey model. No prey refuge ($\Delta = 0.00$). Prey and predator dispersal is Gaussian with the standard deviation of prey dispersal twice that of predator (2:1 grid cells); r and a vary spatially with Uniform distribution as $1 < r < 2.0$, $0 < a < 1$. (a) prey and predator interaction--high prey density (red), predator density (dark-blue); (b) simulation time plot--prey (red), predator (black); (c) phase-plane plot; (d) Lyapunov exponent. 103

3-10. Spatiotemporal dynamics on a 64 x 64 grid with a 2-D integrodifference equation Nicholson-Bailey model. Approximately 9% of cells are prey refuge ($\Delta = 0.10$). Prey and predator dispersal is Gaussian with the standard deviation of prey dispersal twice that of predator (2:1 grid cells); r and a vary spatially with Uniform distribution as $1 < r < 2.0$, $0 < a < 1$. (a) prey and predator interaction--high prey density (red), high predator density (dark-blue); (b) simulation time plot--prey (red), predator (black); (c) phase-plane plot; (d) Lyapunov exponent. 104

3-11. Spatiotemporal dynamics on a 64 x 64 grid with a 2-D integrodifference equation Nicholson-Bailey model. Approximately 12 % of cells are prey refuge ($\Delta = 0.15$). Prey and predator dispersal is Gaussian with the standard deviation of prey dispersal twice that of predator (2:1 grid cells); r varies spatially with Uniform distribution as $1 < r < 2.0$ and average $a = 0.5$. (a) prey and predator interaction--high prey density (red), high predator density (dark-blue); (b) simulation time plot--prey (red), predator (black); (c) phase-plane plot; (d) Lyapunov exponent. 105

3-12. Spatiotemporal dynamics on a 64 x 64 grid with a 2-D integrodifference equation Nicholson-Bailey model. Approximately 50% of cells are prey refuge ($\Delta = 1.0$). Prey and predator dispersal is Gaussian with the standard deviation of prey dispersal twice that of predator (2:1 grid cells); r varies spatially with Uniform distribution as $1 < r < 2.0$ and average $a = 0.5$. (a) prey and predator interaction--high prey density (red), high predator density (dark-blue); (b) simulation time plot--prey (red), predator (black); (c) phase-plane plot; (d) Lyapunov exponent. 106

4-1. Map of Florida showing Pine Island on the west coast near Fort Myers. 146

4-2. Maps of Pine Island Organics, Pine Island, FL. (a) scaled map; (b) color-coded whitefly resource map created from the scaled-map. 147

4-3. Index to Landsat Worldwide Reference Systems showing the United States west coast and part of Mexico. Gray dots are Landsat scene centers located along specific rows (R) and paths (P). The red dot is the scene center (P42:R35) for the San Joaquin Valley, CA. The magenta dot is the scene center (P39:R37) for the Imperial Valley, CA. 148

4-4. Images created from Landsat TM data on Crow Butte, Nebraska (30 July, 1986). Original data supplied by MicroImages, Inc., Lincoln, Nebraska. (a) Normalized Difference Vegetation Index raster with scale equal 2; (b) Transformed Vegetation Index raster; (c) natural color image with band 3 (red), band 2 (green), and band 1 (blue) assigned to RGB; (d) enhanced vegetation color image with band 5 (Mid IR), band 4 (Near IR), and band 3 (red) assigned to RGB. 149

4-5. Landsat TM subscenes of the San Joaquin Valley, CA. Bands 5, 4 and 3 were assigned to Red, Green and Blue (RGB). Each image covers approximately 100 km x 100 km (62 mi x 62 mi) and consists of 3510 x 3510 pixels (cells). Vegetated areas appear in green, non-vegetated areas in shades of red and purple, and water in black. Image dates are (a) April 27, 1993; (b) June 30, 1993; (c) October 20, 1993 150

4-6. Results of the Graham-Schmidt™ Orthogonalization of TM data on the San Joaquin Valley, CA. (a), (c), (e) Greenness rasters for April 27, June 30, and October 20, 1993, respectively. Areas with active vegetative growth are whiter. (b), (d), (f) Soil brightness rasters for April 27, June 30, and October 20, 1993, respectively. High intensity white indicates bare soil 151

4-7. Ground truth data in the San Joaquin Valley, CA. (a) Air-Ways Farms Inc. ranches and crop types; (b) ranches overlaid on June 30, 1993 satellite image of the valley (yellow vector objects). 152

4-8. MicroImages Inc. TNTmips™ automatic classification window with parameters used in the ISODATA classification of 18 TM bands of Landsat data on the San Joaquin Valley, CA. 153

4-9. ISODATA classification rasters for the San Joaquin Valley, CA. (a) classified raster with 100 classes assigned to different colors; (b) distance raster. Darker pixels are closer to their class mean than lighter pixels. 154

4-10. Characteristic zones in a TM3 (Red) and TM4 (Near Infrared) radiance plot. 155

4-11. TM band 3 and 4 radiance plots from the ISODATA classification of Landsat data on San Joaquin Valley, CA. Letters a, j and o in data plot labels represent April 27, June 30 and October 20, 1993, respectively. Numbers next to letters represent classes 1 to 100; Classes are plotted (a) 1-10; (b) 11-20; (c) 21-30; (d) 31-40; (e) 41-50; (f) 51-60; (g) 61-70; (h) 71-80; (i) 81-90; (j) 91-100. 156

4-12. Result of class aggregation on the classified raster of the San Joaquin Valley, CA. (a) classified raster merging similar classes. Major classes include cotton (white), soil (tan), grapes (brown & purple), water (blue), safflower (yellow), natural vegetation (light green); (b) the final resource map created by filtering the raster in (a) with a 3 x 3 majority filter and nearest neighbor resampling to 128 x 128 raster cells. 161

4-13. Landsat TM subscenes of the Imperial Valley, CA. TM bands 5, 4 and 3 displayed in RGB. Each image is 100 km x 100 km (62 mi x 62 mi) and consist of close to 3510 x 3510 pixels (cells). Green indicates active plant growth; unvegetated areas are in shades of purple. The Salton Sea (black area) is located at the top left corner, and Mexico in the lower portion of each image. Images are from satellite data taken on (a) August 31, 1994; (b) December 21, 1994; (c) February 23, 1995; (d) May 30, 1995. 162

4-14. Georeferencing of the Imperial Valley satellite data using TigerLine vector data. (a) TigerLine overlaid on a subscene; (b) close up of an area near the Salton Sea showing the agreement between TigerLine vector, roads and field boundaries in the image. 163

4-15. Location of ground truth sample points in the Imperial Valley, CA. Only TM band 1 from Landsat subscenes on each date is shown. (a) August 31, 1994 image--samples taken on September 1, 1994; (b) December 21, 1994 image--samples taken on December 10-11, 1994; (c) February 23, 1995 image--samples taken on February 1-2, 1995; (d) May 30, 1995 image--samples taken on May 13-14, 1995. 164

4-16. Training rasters in MicroImages Inc. TNTmips™. (a) using feature mapping to create training sets (rasters). A portion of August 31, 1994 principal component RGB image with feature samples shown as colored specks. (b) training raster image. The position of each colored feature sample gives the location of feature cells in the TM data. 165

4-17. Principal component rasters from four Landsat satellite subscenes on the Imperial Valley, CA. PC bands 2, 1 and 3 assigned to RGB. (a) August 31, 1994; (b) December 21, 1994; (c) February 23, 1995; (d) May 30, 1995. 166

4-18. Classified rasters and dendrograms from maximum likelihood classification of Landsat TM data on the Imperial Valley, CA. Number of cells in each class is in square brackets. Data are for (a & b) August 31, 1994; (c & d) December 21, 1994; (e & f) February 23, 1995; (g & h) May 30, 1995. 167

4-19. Whitefly resource maps. Classified rasters for the Imperial Valley, CA. were clipped close to the Mexican border, filtered with a 3 x 3 majority filter and resampled (nearest neighbor) to 100 x 100 cells. Map dates are (a) August 31, 1994; (b) December 21, 1994; (c) February 23, 1995; (d) May 30, 1995. 171

5-1. Color-coded whitefly resource maps at Pine Island Organics, Pine Island, FL. (a) original resource map; (b) experimental resource map with resources grouped by plant family; (c) experimental resource map with sugarcane barriers removed. 191

5-2. Forcing or driving variables for parameters in the spatiotemporal model on whiteflies at Pine Island Organics, Pine Island, FL. (a) weekly average temperature; (b) an example of a crop growth cycle and that cycle 180° out-of-phase and shifted. The phase-shifted cycle forces dispersal. 193

5-3. Number of adult whiteflies collected by beat-pan sampling on various crops at Pine Island Organics. Letters and numbers in the Fields, Crops, & Indices axis represent the crops and their resources indices, respectively. C16&T for example is cucumber, resource 16 followed by tomato; E06 is eggplant, resource 6; Z is zucchini, and P is pepper. 194

5-4. Comparison of scaled beat-pan sampling data (----) with scaled simulation results (—) for adult whiteflies at Pine Island Organics; (a) tomato, resource 4 ($r = 0.85$, $P < 0.001$); (b) tomato, resource 5 ($r = 0.90$, $P < 0.001$); (c) tomato, resource 11 ($r = 0.82$, $P < 0.01$); (d) eggplant, resource 6 ($r = 0.92$, $P < 0.001$); (e) eggplant, resource 12 ($r = 0.89$, $P < 0.001$); (f) cucumber, resource 3 ($r = 0.88$, $P < 0.005$); (g) zucchini, resource 13 ($r = 0.98$, $P < 0.001$); (h) pepper, resource 7 ($r = 0.88$, $P < 0.001$). 195

5-5. Parasitism of whiteflies on tomato and eggplant at Pine Island Organics. 196

5-6. Examples of comparisons of observed with simulated adult whitefly density maps at Pine Island Organics. In all cases, the 2-dimensional correlation coefficients were greater than 0.70. Highest densities are white. Map dates are (a) 17 November, 1992; (b) 24 November, 1992; (c) 1 December, 1992; (d) 7 December, 1993. 197

5-7. Relative differences in whitefly and natural enemy densities at Pine Island Organics in simulations with the original and experimental resource maps. RDs = 0 indicate no differences in densities with the original versus the experimental maps; positive RDs indicate that densities with the original map were higher; negative RDs indicate that densities with the experimental maps were higher. (a) RDs between the original map and an experimental map where resources were grouped by plant Family; (b) RDs between the original map and an experimental map with no sugarcane barriers. . . . 198

6-1. Silverleaf whitefly reproduction parameter (*r*) maps for the Imperial Valley, CA. The colorbar next to each map shows the range of *r* values per week at 27 °C. Total weekly egg production per female on each resource is *exp(r)*. Map dates are (a) August 31, 1994; (b) December 21, 1994; (c) February 23, 1994; (d) May 30, 1995 219

6-2. Silverleaf whitefly immature stage development parameter (*DY2*) maps for the Imperial Valley, CA. The colorbar next to each map shows the proportion of immature whiteflies that develop each week on each resource at 27 °C. Map dates are (a) August 31, 1994; (b) December 21, 1994; (c) February 23, 1994; (d) May 30, 1995 220

6-3. Silverleaf whitefly immature stage survival parameter (*SY2*) maps for the Imperial Valley, CA. The colorbar next to each map shows the proportion of immature whiteflies that survive each week on each resource at 27 °C. Map dates are (a) August 31, 1994; (b) December 21, 1994; (c) February 23, 1994; (d) May 30, 1995 221

6-4. Temperature at three weather stations in the Imperial Valley, CA. for the period July 1994 to June 1995. (a) minimum, maximum, and average temperature at Calipatria; (b) minimum, maximum, and average temperature at Meloland; (c) minimum, maximum, and average temperature at Seeley; (d) average temperature for all three sites, and a fitted temperature cycle. The fitted daily temperature cycle is given by 21.5(1+0.6 cos (((2*pi)/365)*(day - 192)), while

21.5(1+0.6 cos(((2*pi)/52)*(week - 27)) can be used to obtain a weekly temperature cycle 222

6-5. Wind Rose diagrams for three weather stations in the Imperial Valley, CA. Each plot presents wind data collected between 6 a.m. and 10 a.m. for July 1, 1994 to June, 30 1995. The bars indicate the direction from which the wind is coming, and their lengths indicate frequency. (a) Calipatria--mean 179° (± 46.33 SD), speed 2.4 m/s; (b) Meloland--mean 238.9° (± 51.47 SD), speed 2.4 m/s; (c) Seeley--mean 283° (± 61.53 SD), speed 2.3 m/s; (d) average of the three stations--mean 226.9° (± 52.44 SD), speed 2.3 m/s 223

6-6. Montage of images showing the effects of variability in wind direction and speed on the pattern of adult whitefly dispersal in a spatiotemporal model for the insect in the Imperial Valley, CA. Sixteen consecutive dispersal steps in the model are presented. the central distribution in each subimage represents the dispersal pattern of trivial fliers at the source, while the other distribution is the wind-shifted dispersal pattern of migrators. 224

6-7. Dynamics of the silverleaf whitefly from simulation on the Imperial Valley, CA. Average whitefly density in the system has been scaled to the carrying capacity in a quarter section (one cell) in the spatial grid. (a) result of a five year simulation in the Valley ; (b) adult whitefly dynamics in a single year. 225

6-8. Dynamics of the silverleaf whitefly from simulation on the Imperial Valley, CA. Average whitefly density in the system has been scaled to the carrying capacity in a quarter section (one cell) in the spatial grid. (a) result of a five year simulation comparing whitefly dynamics in the entire system with their dynamics when no alfalfa is grown; (b) adult whitefly dynamics in a single year. 226

6-9. Dynamics of the silverleaf whitefly from simulation on the Imperial Valley, CA. Average whitefly density in the system has been scaled to the carrying capacity in a quarter section (one cell) in the spatial grid. (a) result of a five year simulation comparing whitefly dynamics in the entire system with their dynamics when alfalfa has a dry down period (Late July to early October); (b) adult whitefly dynamics in a single year. 227

6-10. Dynamics of the silverleaf whitefly from simulation on the Imperial Valley, CA. Average whitefly density in the system has been scaled to the carrying capacity in a quarter section (one cell) in the spatial grid. (a) result of a five year simulation comparing whitefly

dynamics in the entire system with their dynamics when no cotton is grown; (b) adult whitefly dynamics in a single year. 228

6-11. Dynamics of the silverleaf whitefly from simulation on the Imperial Valley, CA. Average whitefly density in the system has been scaled to the carrying capacity in a quarter section (one cell) in the spatial grid. (a) result of a five year simulation comparing whitefly dynamics in the entire system with their dynamics when no spring melons are grown; (b) adult whitefly dynamics in a single year. 229

6-12. Dynamics of the silverleaf whitefly from simulation on the Imperial Valley, CA. Average whitefly density in the system has been scaled to the carrying capacity in a quarter section (one cell) in the spatial grid. (a) result of a five year simulation comparing whitefly dynamics in the entire system with their dynamics when no cole crops are grown; (b) adult whitefly dynamics in a single year. 230

6-13. Dynamics of the silverleaf whitefly from simulation on the Imperial Valley, CA. Y-axis values represent adult densities averaged over the total area planted in each crop and scaled to the carrying capacity in a quarter section (one cell) in the spatial grid. (a) adult whitefly dynamics on alfalfa in a single year; (b) adult whitefly dynamics on cotton in a single year. 231

Abstract of Dissertation Presented to the Graduate School
of the University of Florida in Partial Fulfillment of the
Requirements for the Degree of Doctor of Philosophy

SPATIOTEMPORAL DYNAMICS OF INSECTS IN LARGE-SCALE AGRICULTURAL SYSTEMS: METHODOLOGY AND ANALYSIS WITH THE SILVERLEAF WHITEFLY, *BEMISIA ARGENTIFOLII* (BELLOWS AND PERRING)

By

Carlyle Christopher Brewster

December 1996

Chairman: Dr. Jon C. Allen
Major Department: Entomology and Nematology

This study focused on the development of methods for studying and analyzing insect dynamics in agricultural systems. Emphasis was placed on the formulation of a spatiotemporal model as a tool for studying these dynamics. The utility of the model was demonstrated with the silverleaf whitefly (SLW), *Bemisia argentifolii*, in two contrasting spatial systems.

The model developed is a grid-based model that integrates ideas from spatially explicit population models, coupled map lattices and integrodifference equations (IDEs). It combines an age-structured prey-predator population model with a resource map that describes the structure of the insect's habitat. Spatial movement is accomplished with two-dimensional IDEs. One IDE is used to couple prey reproduction with their dispersal,

while another IDE redistributes adult natural enemies over the spatial region at each time step in the model. The couplings in these IDEs are convolutions that are solved efficiently with Fourier transforms.

The dynamics generated from simulations with the model on artificial systems were similar to those observed with other discrete-time models that used different dispersal rules. These dynamics included spiral waves of predator chasing prey, crystal lattice structures, and spatiotemporal chaos.

The utility of the model was first demonstrated with the SLW at a small-scale mixed-crop organic system on Pine Island, FL. After simulation results were matched with whitefly population trends from pan-sampling data, the model was used to explore several scenarios. Simulations with experimental resource maps created by altering the arrangement of crops in the original resource map showed that changes in the spatial structure of resources at the farm affected SLW dynamics.

SLW dynamics in a large-scale regional system, the Imperial Valley, CA were also explored with the model. Resource maps were constructed from Landsat thematic mapper data on the Valley. Qualitative whitefly trends from simulations were consistent with those observed for the insect in the Valley. Simulations also showed that among all SLW host plants, alfalfa had the greatest influence on whiteflies. Planting no alfalfa resulted in a 6.4-fold reduction in overall whitefly abundance. The importance of alfalfa in the management of whiteflies in the Valley was noted.

CHAPTER 1
INTRODUCTION AND LITERATURE REVIEW

The dynamics of polyphagous insect species such as whiteflies have been studied extensively at the farm or local scale but very little has been done to explore these dynamics at larger spatial scales such as in regional agricultural systems. Field experiments, the method most commonly used for studying animal species dynamics, are clearly inadequate, since only a narrow range of possible dynamics can be observed. Conducting a full set of large-scale ecological experiments in regional agricultural systems is logistically infeasible (Turner et al. 1995) and is therefore likely to generate results that are inconsistent with those observed locally (Levin 1992). Tools are needed for exploring species dynamics at the landscape or regional scale. These tools must consider both the animal species and its interaction with its habitat in time and space. This study was initiated in response to the need to develop a tool that could be used to explore the implications of events that are likely to impact insect species dynamics, and that are also very difficult to test with large-scale experiments. The tool is tested on the silverleaf whitefly, *Bemisia argentifolii* Bellows & Perring, an insect that has recently become a problem in regional agricultural systems.

Whiteflies are common insect pests of tropical and subtropical agricultural systems, but are also found on the fringes of some temperate areas (Mound and Halsey 1978, Byrne et al. 1990). One of the most important whiteflies in agricultural systems is

the sweetpotato whitefly (SPW), *Bemisia tabaci* (Gennadius), also commonly known as the tobacco or cotton whitefly (Byrne et al. 1990). This insect has been present in the United States since 1894 (Quaintance 1900) but before 1981 was considered a sporadic pest (Horowitz 1986, Byrne & Draeger 1989, Brown et al. 1995). By the mid-1980s, the status of this whitefly changed dramatically and the insect became a primary pest. Today, SPW is a worldwide problem in both indoor and outdoor agricultural production systems and is responsible for multimillion dollar losses each year (Perring et al. 1993a, Bellows et al. 1994).

The rise to pest status of SPW was attributed mainly to the intensification of agricultural production and greater use of production inputs such as pesticides, fertilizers, and irrigation (Ahmed et al. 1987, Gill 1992). Many believed that these events resulted in the evolution of a more pestilent strain of SPW, strain B (or poinsettia strain) that was responsible for the increased damage (Price et al. 1987, Byrne & Miller 1990, Perring et al. 1991,1992). Other studies however have suggested that strain B is in fact a new species of *Bemisia* rather than a strain of *B. tabaci*. Silverleaf whitefly (SLW) was proposed as the common name for this new whitefly because of its ability to induce a silvering disorder on squash foliage upon feeding (Perring et al. 1993a). Later, the insect was described by Bellows et al. (1994) as *Bemisia argentifolii* Bellows & Perring.

There is still some debate on the true taxonomic nature of this new whitefly. Regardless of the final verdict on this matter however, one thing is clear--much is still unknown about the biology and ecology of the SPW. In this study, the taxonomic question is avoided and left to more qualified individuals. Therefore, unless otherwise

stated, SPW and SLW will be used interchangeably to refer to both whiteflies with the knowledge that these insects are either different strains of *B. tabaci* or part of a species complex in the genus *Bemisia* (Brown et al. 1995).

SPW and SLW have the ability to move extensively within regional crop systems (Perring et al. 1992, Brown et al. 1995), and therefore their dynamics are expected to be closely tied to regional crop patterns in time and space. Dynamics observed at the local scale are often inadequate for making predictions on species dynamics at larger spatial scales (Levin 1992). Since it is extremely difficult to manipulate and control large-scale experiments, tools such as simulation models must be considered. Whitefly models have in the past been used mainly to explore the local dynamics of this insect. Recently however, a model on a regional (multi-crop) system, the Imperial Valley, CA, was described (Wilhoit et al. 1994). No evidence of other models of this type was found and therefore more effort is needed in this area.

The rapid rise in pest status and other recent events have resulted in a rejuvenation of interest in the biology and dynamics of these whiteflies (Brown et al. 1995). This encouraged USDA/ARS, university and state scientists in 1992 to initiate a 5-year national research and action plan for whitefly management with the major goal "to provide the necessary research and team effort that will continue to yield environmentally and publicly acceptable, safe technologies for area-wide management and suppression of the SPW" (Faust 1992 p. i).

This present study was undertaken partly in an effort to fulfil some of the objectives in the whitefly management research and action plan. The more specific

objective was to develop general methodology for studying insect-habitat interactions in large-scale agricultural systems. A nonspecific insect interaction model was therefore formulated, and theoretical as well as practical facets of this model explored. Construction and integration of the insect's spatial environment into the model are also described in detail for real and experimental systems. The model was applied specifically to studying whitefly dynamics in a small- and a large-scale agricultural system. The study begins with an extensive review of the literature on the sweetpotato and silverleaf whiteflies.

Origin, Distribution and Taxonomic History of Whiteflies

Like aphids, whiteflies are in the insect order Homoptera and can cause similar types of damage to their host plants (Byrne et al. 1990). They have often been referred to as the aphids of the tropics (Mound & Halsey 1978). The majority of the 1,200 or more described species of whiteflies are of tropical or subtropical origin (Mound & Halsey 1978), with about 724 species described from the tropics, and only 420 species from temperate regions (Strong et al. 1984).

Among the homopterans, the whitefly superfamily Aleyrodoidea bears close relation to the three other superfamilies, Psylloidea (psyllids), Aphidoidea (aphids), and Coccoidea (scales) that make up the suborder Sternorrhyncha (Borror et al. 1989, Evans 1993). The single whitefly family, Aleyrodidae, consists of two subfamilies, Aleurodicinae and Aleyrodinae that contain 126 genera. Aleurodicinae, the more primitive of the two subfamilies, is made up of 17 genera and about 100 mainly Neotropical species, while

Aleyrodinae, which contains all other species, is cosmopolitan in distribution (Evans 1993).

Byrne et al. (1990) pointed out that among all the species of whiteflies, very few have actually been characterized as pests. Of these, only two species appear to be important in protected agricultural systems, four species are considered serious pests in annual cropping systems, and about twelve species reoccur as pests in perennial systems. They also noted that only three species vector plant pathogens--the SPW, *Bemisia tabaci* (Gennadius), the greenhouse whitefly, *Trialeurodes vaporariorum* (Westwood), and the bandedwinged whitefly, *T. abutilonea* (Haldeman).

The SPW is by far the most important whitefly found in annual cropping systems (Byrne et al. 1990). This insect was first described as *Aleyrodes tabaci* in Greece in 1889 as a pest of tobacco (Gennadius 1889) and is believed to have originated from either the Orient, Africa, or the Middle East (Mound 1963, Brown et al. 1995). Strong evidence suggests that this insect is in fact a native of Pakistan or India since areas within these geographical regions contain the greatest diversity of whitefly parasitoids which often indicates a genus epicenter (R. Gill pers.comm. cited in Brown et al. 1995). This evidence is overwhelming in spite of the fact that the insect was first observed in India in 1905 (Misra & Lambda 1929, Reddy & Rao 1989) and in Pakistan in 1919 (Immaraju 1989).

The first New World specimen was collected in 1897 in the United States on sweet potato, and was identified as *B. inconspicua* (Quaintance 1900). Interestingly, species determinations in whiteflies are normally based on characteristics of the pupal cases and not on adult morphology (Russell 1957, Bink-Moenen & Mound 1990). Pupal

characteristics however are polymorphic and are influenced by the hosts on which the insect develops (Mound 1963, Lopez-Avila 1986, Brown et al. 1995). As such, it is very difficult to accurately characterize individual whitefly species from pupal cases. Therefore, by a reexamination of the group, *B. inconspicua* was synonymized along with 18 other species into the single taxon, *B. tabaci* (Russell 1957, Mound & Halsey 1978, see Gill 1992 for a list of synonyms). There may now be more than the 22 synonyms of *B. tabaci* (Mound & Halsey 1978), but again, difficulties with accurate characterization may mean that many of these could go unnoticed (Bellows et al. 1994). As it stands, the genus *Bemisia* contains 37 recognized species (Mound & Halsey 1978) that were all typed from *B. tabaci* (Bellows et al. 1994).

Until quite recently *B. tabaci* was considered a sporadic pest in US agriculture (Horowitz 1986, Byrne & Draeger 1989, Brown et al. 1995). Subsequent heavy damage as a result of whitefly attacks has led to a reevaluation of the status of this pest (Perring et al. 1993a). Early indications were that a new strain of *B. tabaci* (strain B or poinsettia strain) was responsible for the increasing attacks (Price et al. 1987, Byrne & Miller 1990). Entomologists now believe that the change to more intensive systems of agriculture led to the evolution of this new and more pestilent strain that is responsible for the increasing attacks (Price et al. 1987, Byrne & Miller 1990, Perring et al. 1991,1992).

Strain B is morphologically similar to the strain A (Bethke et al. 1991, Bergh et al. 1995), but it is more fecund (Bethke et al. 1991), has a wider host range, greater feeding ability, slightly different oviposition preferences (Byrne & Miller 1990, Blua et al. 1995), an enhanced ability to transmit plant viruses (Brown & Nelson, 1984, Duffus et al. 1986,

Costa & Brown, 1990, 1991), and appears to be reproductively incompatible with strain A (Perring et al. 1993a,b). It is also reported to be more cold tolerant (Gill 1992) and was observed overwintering on tomato foliage in southern Ontario, Canada (Broadbent et al. 1989, Bergh et al. 1995). Gill (1992) suggested that these two "strains" were in fact distinct species. Shortly thereafter, Perring et al. (1993a,b) proposed the common name silverleaf whitefly (SLW) for this insect because it had the ability to cause a silvering effect of plant foliage upon feeding. In the following year, SLW was described as *Bemisia argentifolii* Bellows & Perring (Bellows et al. 1994).

The two whiteflies are highly polyphagous insects that have spread extensively throughout their ranges (Perring et al. 1992, Brown et al. 1995), although it now appears that *B. argentifolii* or *B. tabaci* strain B is displacing SPW in many regions (Perring et al. 1994, Brown et al. 1995). However, in spite of the many differences between the two whiteflies, continuing debate among entomologists suggests that the strain/species questions have not been completely resolved (Brown et al. 1995).

Whitefly Biology and Host Preferences

Life Stages

Biological studies conducted on whiteflies often yield inconsistent results primarily because these studies are conducted under varying environmental conditions and also because tests done on a particular host plant often use insects that have been reared on a number of different host plants (Lopez-Avila 1986).

There are some discrepancies over the number of nymphal stages for the SPW and therefore it is not entirely clear whether the insect develops through five or six life stages before it emerges as an adult. Those who recognize five life stages before the adult stage list these as egg, crawler (1st nymphal instar), 2nd and 3rd instars (which are sessile), and a pupa (Azab et al. 1970, El-Helaly et al. 1971, Gill 1990). Those who accept six life stages before the adult stage have included a 4th nymphal instar before a so-called "pupal" stage (Husain 1931, Lopez-Avila 1986). This 4th nymphal instar is very often lumped with the pupal stage in developmental studies (Bethke et al. 1991, Salas & Mendoza 1995) since it is very difficult to distinguish between the two stages. The transition from 4th instar to pupa simply involves morphological changes rather than shedding of nymphal skin as occurs with earlier stages and that is indicative of molting (Salas & Mendoza 1995).

Eggs of SPW and SLW are elongate-oval in shape. The 1st instar or crawler is mobile and can move over leaf surfaces looking for suitable feeding sites. The 2nd and 3rd instars unlike the 1st instar are sessile. The 4th instar is elliptical in shape and yellowish or clear in color. Transition of this instar to the pupal stage is marked by the appearance of large red eyes and a color change from green to yellow (Lopez-Avila 1986). This stage has therefore been commonly referred to as the red-eyed nymphal stage. It is on the morphological characteristics of the pupal stage that taxonomic determinations are normally made (Bink-Moenen & Mound 1990, Brown et al. 1995). Adults are winged, with yellow bodies and white wings, and exhibit sexual dimorphism. Females are usually larger than males.

The size of individuals in the immature stages is an important criterion for distinguishing between SPW and SLW. Although immatures of whitefly species vary morphologically and morphometrically on different host plants (Mound 1963), immatures of SPW tend to be larger than those of the SLW even when both whiteflies are reared on the same hosts (Bethke et al. 1991).

Development

Temperature, relative humidity, rainfall and host plant are the primary factors that influence whitefly life processes such as development, fecundity, longevity and mortality. Whiteflies usually favor areas with high temperature, low humidity, and periods of no or low rainfall and mild winters (Jagdev & Butter 1988, Gill 1992). Table 1-1 shows the variability in development times for the insect and the influence of temperature and host plants.

Development is positively correlated with temperature (Butler et al. 1983). However, below and above certain temperature limits little or no development occurs. Zalom et al. (1985) estimated the lower and upper threshold temperatures for development as 10.0 and 32.2 °C, respectively, although Powell and Bellows (1992a) later observed lower thresholds of 14.65 °C on cotton and 16.71 °C on cucumber. Discrepancies in estimating these thresholds generally arise when it is assumed that the relationship between development and temperature is linear instead of curvilinear as was observed in some studies (Powell & Bellows 1992a). Development appears to be optimal at 28.0 °C (van Lenteren & Noldus 1990).

Development time has also been determined in physiological time or degree-days. Zalom et al. (1985) observed from field studies on *B. tabaci* in the Imperial Valley, California, that it took between 316.0 and 316.3 degree-days for development from egg to adult.

Table 1-1 also shows the effects of host plants on development. Host plant factors such as plant varieties (Ozgur & Sekerogh 1986), leaf shape, and surface characteristics are important. Host plant influences are most striking when development is assessed on hosts that are different from the insect's original host. For example, Bethke et al. (1991) observed that a cotton strain and a poinsettia strain of whitefly developed faster on cotton and poinsettia, respectively than on the other host plant. Finally, from the data presented in Table 1-1 and other sources, it appears that under favorable conditions, SPW is expected to complete eleven to fifteen generations per year (Brown & Bird 1992).

Survival and Mortality

In addition to abiotic factors (temperature, humidity, rainfall) that affect whitefly development, other (biotic) factors also influence whitefly survival and mortality. Included in the list of biotic factors are parasitoids, predators, pathogens, and host plant nutrition.

The effects of temperature and host plants on mortality were studied by Powell and Bellows (1992a) who observed the insect on two plants (cotton and cucumber) at four temperatures–20.0, 25.5, 29.0 and 32.0 °C. On cotton, egg mortality was lowest at 29.0°C but varied from 15.5% at 20.0 °C to 5.1% at 32.0 °C. On cucumber, egg mortality was lowest at 25.5 °C and varied from 26.7% at 20.0 °C to 7.2% at 32.0 °C.

When overall mortality within the immature stage was considered, mortality was highest at the lowest temperature (20.0 °C). On cotton, 29.0 °C seemed to be the most favorable temperature while 25.5 °C was the most favorable for the insect reared on cucumber. Several studies suggest that first instar nymphs suffer most from climatic factors such as humidity, temperature and rainfall (Gerling et al. 1986, Horowitz 1986). Parasitization on the other hand seems to be the most important mortality factor acting on whiteflies during the advanced nymphal stages (Horowitz et al. 1984).

The effects of different host plants on survival and mortality were also studied by Costa et al. (1991) who compared whitefly survival from egg to adult on healthy and virus-infected plants. They observed significant differences in survival among the healthy plants tested. The results from survival tests on healthy versus virus infected plants were inconsistent. When Byrne and Draeger (1989) studied survival on lettuce plants they found that percentage survival of 1st instar *B. tabaci* was greater on plants at the 3-leaf stage than on plants that had more than 25 leaves. This suggested that whitefly mortality was related to plant nutrition.

Fecundity and Longevity

Changes in animal population levels are directly related to two major processes--births and deaths. Whitefly population sizes are a function of female fecundity and the survival of eggs to the adult stage. Fecundity like other life processes is highly variable and is influenced by environmental conditions and the quality and quantity of host. Females have been known to produce over 300 eggs in their lifetime (Powell & Bellows, 1992b). Ovipositional rate is age-dependent, gradually increasing during the first days of

adult life and reaching a plateau shortly before females die. Ovipositional behavior is affected by factors such as sunlight, leafshape and color, and the growth habit of the host plants (Mound 1962, Ohnesorge et al. 1980, El-Helaly et al. 1981a,b, Simmons 1994).

Powell and Bellows (1992b) observed females at four temperatures (20.0, 25.5, 29.0 and 32.0 °C) on cotton and cucumber. They found that the number of eggs a female laid during her lifetime on cotton was greatest at 20.0 °C and lowest at 32.0 °C, but that oviposition rate was higher at 25.5 °C. This was in contrast to cucumber where fertility and oviposition rate were highest at 29.0 °C. They also found that at the same temperatures, *B. tabaci* was more fertile on cucumber than on cotton.

In addition to varying with temperature and host plant, adult longevity also differs between the sexes. On the same host, adults live longer at lower than at the higher temperatures and females live longer than males (Butler et al. 1983; von Arx et al. 1983; Powell & Bellows, 1992b).

Sex Ratio

The SPW is not unlike other whiteflies in that females are arrhenotokous and can regulate the sex of their progeny in the presence of sufficient supply of sperm by selective fertilization (Horowitz & Gerling 1992). Mated females therefore can lay both haploid (male) or diploid (female) eggs, whereas unmated females lay only haploid (male) eggs.

Although a sex ratio of 1:1 was reported for the SPW on cotton (Gameel, 1974) , it is difficult to generalize since this ratio can be quite variable (Butler et al. 1986, Gerling et al. 1986). Horowitz and Gerling (1992) found that on cotton in Israel, SPW had a sex ratio that ranged from a female-biased condition early in the season to male-biased by the

end of summer. In addition, females reared at low temperatures, young females, and females that had access to males throughout their lives, tended to lay proportionately more female-producing eggs (Sharaf & Batta 1985, Horowitz & Gerling 1992).

Host Plant Specificity, Suitability and Preferences

B. tabaci has been recorded on over 506 crop and weed hosts from 74 plant families (Greathead 1986). The actual number of hosts for *B. argentifolii* is not known but appears to be considerably greater than that of *B. tabaci* (Byrne & Miller 1990, Perring et al. 1992).

It is uncertain whether these insects develop successfully on all host plants on which they were recorded. Here, a distinction must be made between a "preferred" host and a "suitable" host as these relate to whiteflies. Preference is essentially an adult phenomenon related to feeding and oviposition success on host plants, while suitability relates to the adequacy of host plants for immature development. Preference is therefore associated with adult behavior and because immature whiteflies develop from egg to adult on single hosts, adult preference is often used as an indicator of host suitability (although it may not always be the best indicator). Nevertheless, experiments conducted by Blua et al. (1995) clearly showed that oviposition preference is an adequate indicator of the extent of host use by whiteflies and that SPW and SLW have distinct ovipositional preferences. In general, females are known to deposit more eggs, have higher fecundity rates and greater longevity, and immatures usually have shorter development times and lower mortality on preferred hosts.

Host preference and suitability are influenced by host plant characteristics such as leaf color (Van Lenteren & Noldus 1990), hairiness (McAuslane 1996) and shape (Mound 1965), leaf age and nutritional status (Rote & Puri 1992, Simmons 1994, Bentz et al. 1995a,b,c), and the presence of insecticide residues (Liu & Stansly 1995). Whiteflies are strongly attracted to certain wavelengths of light, particularly those that produce yellow/green color. Plant odors have not been shown to be important in this attraction (Mound 1962, Berlinger 1986). Pubescent leaf and closed-canopy cotton varieties were reported to be much more heavily infested with whiteflies than glabrous, smaller-leaf, open-canopy varieties (Ozgur & Sekeroglu 1986). After examining 20 commercial cultivars and 7 wild relatives of tomato, Heinz and Zalom (1995) observed higher whitefly ovipositon rates on leaves with dense trichomes and especially on those positioned close to the stem terminus. Low trichome densities were less preferable. Pubescence seems to provide a physical barrier to natural enemies and a favorable microclimate for immature whiteflies (Mound 1965).

Differences in the quality of host plants affect ovipositional behavior. After examining oviposition behavior of *B. tabaci* strain B, Simmons (1994) observed that feeding and oviposition started on the cotyledon stages (which are more nutritious), and that 90 to 95% of eggs were deposited on the lower leaf surfaces. Bentz et al. (1995a,b) also related host preference to nutritional status and found that by increasing the level of nitrogen applied to poinsettia more eggs were deposited by females.

The nutrient status of the host plant determines its suitability. The levels and type of nitrogen in the plant are very important determinants of host suitability (Byrne &

Draeger 1989, Bentz et al 1995b,c). Poinsettia plants that received ammonium nitrate fertilizer were more likely to be infested with whiteflies than plants that were fertilized with calcium nitrate or unfertilized plants. In addition, although a greater number of 1st instars were produced on nonfertilized plants, they also suffered higher mortality (Bentz et al. 1995b,c).

Economic Importance

Whitefly Induced Host Injury

The sweetpotato whitefly, *B. tabaci* has been recognized as a very important pest in annual cropping systems (Byrne et al. 1990). This recognition is due primarily to the damage that results from SPW infestations.

Feeding and oviposition by SPW result in both direct and indirect plant damage. Adults and immatures feed on host plants and extract phloem sap causing changes in the plant's physiological processes and a weakening and reduction of growth (Pollard 1955, Lopez-Avila & Cook 1986, Buntin et al. 1993). Such effects are particularly devastating to ornamental producers who rely on the aesthetic appeal of the crop to obtain good prices (Price et al. 1990).

Indirect damage results from exposure of plants to excretions of undigested sugars and water (honeydew). Honeydew deposited on plant leaves provides an excellent medium for sooty mold development which in turn reduces plant photosynthesis and the quality of the final plant product (Blua &Toscano 1994). The undesirable effects of sooty mold have been observed in cotton where contamination results in "sticky cotton" that is

difficult to process (Cheung & Roberts 1980, Nuessly & Henneberry 1989, Davidson et al. 1994).

The greatest threat posed by whiteflies is in their ability to transmit viruses and induce phytotoxic or physiological disorders (Table 1-2). *B. tabaci* and *B. argentifolii* are very important whitefly vectors (Mound & Halsey 1978, Duffus 1987, Brown & Bird 1992), vectoring over 25 viral diseases (Costa 1976) and having the ability to transmit more than one virus simultaneously (Varma 1963, Brown & Bird 1992). They are also the only whitefly vectors of geminiviruses (Duffus 1987, Harrison 1985). Diseases transmitted by infectious whiteflies can be placed into three basic groups depending on their symptoms. The first group includes those diseases that induce color changes in infected plant parts mainly leaves (diseases of the mosaic type); the second causes leaf-curl-type effects (diseases of the leaf-curl type); the third group (diseases of the yellowing type) causes symptoms such as yellowing and vein clearing (Costa 1976, Duffus & Flock 1982). Regardless however of the type of symptoms observed on infested plants, it is the economic impact of these diseases that is important.

Economic Losses

Estimates of the economic impact of whitefly infestations include both direct dollar losses due to yield losses as well as indirect dollar losses that result from undesirable events such as unemployment. Losses from whitefly infestations in California and Arizona in 1982 were estimated at $100 million (Duffus & Flock 1982). In the 1991-92 cropping season, the Imperial County Agricultural Commissioner's Office estimated that whitefly damage to fall and winter crops cost the county approximately $111 million (Gonzales et

al. 1992). It was estimated that from November 1991 to January 1992, there was a 21% increase over the same period in 1990-91 in the number of unemployment insurance weeks claimed because of the whitefly problem. Farmers were forced to cease planting crops such as cantaloupes altogether or to delay planting until conditions were more favorable. As a result, fewer farm jobs were available.

Perring et al. (1993a) listed losses incurred by various states in 1991 because of whitefly attacks. Losses to Florida's tomato industry during 1990-91 were estimated at $125 million (Schuster 1995), while total state losses were put at $141.1 million. Losses in Texas were $250 million and 6460 jobs, and in Arizonia approximately $37 million. Total US losses were estimated at over $500 million.

Population Dynamics

Factors Affecting Whitefly Dynamics

Whitefly population dynamics are influenced by environmental factors such as temperature, rainfall and relative humidity, by cultural, chemical and other control practices, and by biotic factors such as host plant nutritional status and physical characteristics, availability of alternate hosts, and natural enemies (predators, parasitoids and pathogens) (Baumgärtner & Yano 1990).

The study of whitefly dynamics is often restricted to studies on the insect's temporal dynamics in a particular system. These studies are used mainly to investigate relationships between temperature and the population dynamics of the insect under field or greenhouse conditions. Temperature is one of the most important factors known to

influence whitefly population dynamics and in agroecosystems unaffected by management practices and environmental factors such as excessive rainfall and humidity, whitefly population growth is usually exponential (Gerling et al. 1980, Zalom et al. 1985). Spatiotemporal host plant factors such as quality and availability, and whitefly dispersal (migration) serve to modify these population responses (Hirano et al. 1993).

Recently researchers have attempted to understand the spatiotemporal dynamics of this insect. These dynamical studies can be broken down into studies that describe the spatial distribution of the insect within host plants, studies that examine population monitoring tools, studies that try to understand mechanisms behind dispersal and migration, and studies that use simulation models to understand the insect's infestation patterns in large (homogeneous and heterogeneous) systems.

Spatial Distribution of Whiteflies

Consistent patterns in spatial distribution have been observed for whiteflies on different host plants. Naranjo and Flint (1994) for example studied the spatial distribution of *B. tabaci* in cotton and observed that all four sectors of a leaf contained an equal distribution of eggs and nymphs and that this pattern did not depend on nodal location of the leaf, cotton cultivar or sampling date. They also noticed that both eggs and nymphs were clustered at the proximal end of each sector. Like von Arx et al. (1984), they proposed a sequential sampling plan for whiteflies in cotton and determined the most efficient sampling unit to be a single 3.88 cm^2 disk taken from the base of the second sector of the fifth mainstem node leaf. Tonhasca et al. (1994) observed similar distribution patterns in cantaloupe and found that adults were more abundant on terminal leaves and

that no differences existed between leaf sectors for any immature stages. However, eggs appeared to be more abundant on terminal leaves while red-eyed nymphs were more abundant on crown leaves.

Monitoring Whitefly Population

Several techniques and tools are available for sampling and monitoring whitefly populations. Sampling and monitoring of insect populations are essential components in the development and implementation of action thresholds and other pest management strategies. Two of the most important considerations in any sampling program are the precision and efficiency with which samples are taken. These are particularly important when sampling small insects with large population densities such as whiteflies (Naranjo & Flint 1994). Understanding the insect's biology, ecology and spatial distribution is therefore a prerequisite to establishing the most cost effective and efficient sampling programs (Morris 1960, Ekbom & Xu 1990).

The adult whitefly is usually sampled with yellow sticky traps (Berlinger 1980, Gerling & Horowitz 1984, Byrne et al. 1986, Ohnesorge & Rapp 1986) since, like a number of other insects, whiteflies are strongly attracted to yellow (Mound 1962). Sticky trap efficiency can be affected by temperature, rainfall, photophase, trap characteristics, surrounding vegetation, and field size (Gerling & Horowitz 1984, Ohnesorge & Rapp 1986, Byrne & von Bretzel 1987, Ekbom & Xu 1990, Palumbo et al. 1995, Naranjo et al. 1995).

Gerling and Horowitz (1984) compared yellow traps placed horizontally and vertically with visual counts and D-vac samples and found that adult population trends for

visual counts and D-vac samples were similar. Traps placed horizontally however caught more adults than those placed vertically. Later Byrne et al. (1986) observed that cylindrical traps caught more adults than upward-facing horizontal traps, vertical traps and downward-facing horizontal traps. The number of insects caught on traps placed ground level correlated better with visual counts than higher traps. Some caution must be exercised in transferring sampling methods tested in an experimental plot to commercial fields. When Palumbo et al. (1995) examined the effect of field size on three sampling techniques (yellow sticky trap, visual [Leafturn] and modified vacuum [Handvac])) in experimental plots with cantaloupe, they observed that these methods all indicated similar whitefly population trends that were highly correlated with immature densities. In commercial fields however data collected by the sticky trap method differed significantly from those of the other two methods.

Other less common adult whitefly sampling methods include the visual or scouting method (Musuna 1986, Palumbo et al. 1995), a black pan method that is a modification of a technique described by Butler and Wilson (1986), vacuum sampling (Palumbo et al. 1995), and rating of adult swarms from disturbed plants (Butler et al. 1986).

Immature densities are usually established from counts on leaves at certain positions within the plant canopy and from defined units within these leaves. This technique has been used for estimating population sizes and designing sampling plans for whiteflies on crops such as cassava (Abishold & Fishpool 1990), cotton (Melamed-Madjar et al. 1982, von Arx et al. 1984, Ohnesorge & Rapp 1986, Naranjo & Flint 1994), cantaloupe (Tonhasca et al. 1994), and peanuts (Lynch & Simmons 1993). Results from

immature sampling would of course depend on leaf characteristics such as age and position, the presence of similar structures such as dead larvae, and immatures of other whiteflies (Ohnesorge & Rapp, 1986).

Dispersal and Migration

In the absence of natural enemy influences, whitefly population changes become a function of adult fecundity, within-stage mortality, and immigration and emigration of adults. Effective and ecologically-sound management of any insect depends not only on knowledge of their reproductive and survival potentials, but also on their dispersal capacity. This knowledge can be used to predict when and where the insect is likely to become a problem.

The dispersal ability of whiteflies is the least understood amongst all factors affecting its distribution and abundance. Their ability and propensity to disperse depend on light, temperature, precipitation, humidity, wind, the quality and age of host plants, and sex. Berlinger (1986) and Byrne and Houck (1990) have suggested that SPW adults have two distinct flight morphs--a trivial flying morph and a migratory morph. Trivial fliers engage in short-distance flight under the plant canopy (Ohnesorge et al. 1980), while individuals in the migratory morph engage in relatively long-distance dispersal. Recently emerged adults move from the lower leaf canopy to the upper leaves to feed and oviposit. In response to deteriorating environmental conditions, some of these adults may move to ground level within fields and tumble along at this level assisted by wind. Others take off from their host plant, get caught in an air current and drift passively sometimes for several kilometers not unlike aerial plankton (Byrne & Bellows 1991).

Attempts are being made to derive models that describe whitefly dispersal. Although these insects weigh only 33 μg (Byrne et al. 1988) and can easily be taken up in wind currents, Byrne et al. (1995) observed that localized movement was not consistent with models for passive transport. They detected patchy dispersal patterns with an underlying bimodal distribution in whiteflies captured after a source release. They explained these patterns as a result of two distinct flight morphs. Insects caught near the source field were trivial fliers, while those caught further downwind were most likely migratory. Very few insects were caught between the two extremes in the study.

Time of day, temperature and wind patterns also affect the number of SPW adults taking flight. Blackmer and Byrne (1993a) found that whiteflies initiated flight activity during all hours of the photoperiod but most often exhibited long phototactic flights from 06.00 to 10.00 hours. This response was correlated with temperature in that at higher temperatures there appeared to be a distinct switch in phototactic response (Byrne & von Bretzel 1987, Bellows et al. 1988, Blackmer & Byrne 1993b). In Arizona for example, the periodicity of whitefly flight activity was found to be unimodal. In October, this activity was observed to be at maximum during midmorning hours, while in late November, when temperatures were declining, activity shifted to mid-afternoon (Byrne & von Bretzel 1987). By restricting flight activity to certain times the insect restricts its activity to cooler temperatures and hence is able to reduce its chances of desiccation, predation, and the harmful effects of radiation. In addition, and particularly for the trivial fliers, this period of flight activity corresponds to time of low wind speeds. Like many

other insects (Johnson 1969), this insect can exercise greater control over the direction of flight when flight is initiated during this period.

One day old whiteflies showed no flight activity but once they had attained flight age, the quality of the host plant dictated how soon they flew (Blackmer & Byrne 1993a). In addition, individuals reared on low quality hosts responded earlier than individuals reared on high quality host. It was suggested that because of poor host quality the insect initiated obligatory dispersal in search of high quality material to replenish nutritional reserves. Correlated with age is the fact that a large proportion of females that engage in migratory flights possess mature functional reproductive systems (Blackmer & Byrne 1993b).

Male and female whiteflies have different flight periodicities over the course of the day. Females usually engage in long-duration flights restricted to early morning whereas males fly throughout the day. This is explained by the fact that males are shorter lived than females and therefore need to locate a mate as quickly as possible (Byrne & Bellows 1991). They therefore tend to fly for longer periods throughout the day (Blackmer & Byrne 1993a).

Whitefly Population Models

Baumgärtner and Yano (1990) recognized three major approaches used for analyzing population dynamics of whiteflies. These are the evaluation of ecological factors in controlled experiments, field and greenhouse studies where population densities and age structures are related to environmental factors, and population modeling.

Whereas population models have been widely used for studying the dynamics of the greenhouse whitefly, *Trialeurodes vaporariorum* (Xu et al. 1981, Xu 1987,1991a,b, Hulspas-Jordaan & van Lenteren 1988, Yano et al. 1988a,b), less effort has been placed on the development of population models for *B. tabaci*. This is probably because it is much simpler to develop models for closed systems such as greenhouses than it is to develop models for field populations that are affected by changing weather and plant conditions, immigration and emigration. Models of *B. tabaci* have generally been used to describe the insect's dynamics in homogeneous systems such as in cotton fields (von Arx et al. 1983, Baumgärtner et al. 1986, Berlinger & Nir 1989, Baumgärtner & Yano 1990), to study the relationship between transient vector (whitefly) densities and disease incidence (Bellows & Arakawa 1986), or to evaluate germplasm for antibiotic resistance (Van Giessen et al. 1995).

A demographic approach has been used to model whiteflies on cotton (von Arx et al. 1983, Baumgärtner et al. 1986, Baumgärtner & Yano 1990). The distribution of developmental times was described with a time-varying distributed delay as outlined in Manetsch (1976) and Vansickle (1977). These models examined the effects of temperature, host plant, natural enemies, and migration. Simulation results indicated that temperature and plant quality were the most important factors affecting whitefly life systems followed by migration, and that an initially slow whitefly population growth was usually followed by rapid exponential growth as temperatures increased. Populations usually peaked when temperatures were changing and thereafter decreased as cooler temperatures set in. The extent of population growth also seemed to be more affected by

the initial numbers of whiteflies in the system and was therefore very sensitive to initial populations than to continuing migration.

Van Giessen et al. (1995) on the other hand used a deterministic simulation model, SARAH (**S**oftware for the **A**ssessment of antibiotic **R**esistance to **A**leyrodidae in **H**ost plants) to evaluate antibiotic resistance of single plants. Resistance was determined by the relationship between simulated intrinsic population growth rate and the growth rate determined on a susceptible control genotype.

Only one study was found where an attempt was made to model whitefly dynamics in a spatially heterogeneous system (Wilhoit et al. 1994). In this system, the Imperial Valley, California, the spatial and temporal dynamics of adult whiteflies were studied in 19 crops. The valley was subdivided into one-square-mile sections and crop dynamics and whitefly densities were followed in each section. The model included environmental forcing by temperature and wind which, along with crop type, influenced whitefly population densities. Natural enemies were however excluded from the system.

Management of Whitefly Populations

Chemical Control

The most widely used method for managing whitefly populations has been chemical application. Cock (1993) gave a comprehensive list of insecticides that have been tested against *B. tabaci*. In many cases, insecticides have been used as a prophylactic measure. The increasing use of insecticides is highly correlated with the rapid development of different types of pesticide groups such as organophosphates (OPs),

pyrethroids, insect growth regulators (IGRs), and biorationals. Intensification in pesticide applications has led to high selection pressures on whitefly populations and is thought to be responsible for the development of resistance and exacerbation of the whitefly problem (Prahaker et al. 1985, Ahmed et al. 1987, Dittrich et al. 1990).

Attempts have been made to manage whitefly resistance. For successful management however it is necessary that some of the requirements listed by Dittrich et al. (1990) for any resistance management program should be included. These are a definition of resistance and cross-resistance patterns in the field, the development of suitable insecticide rotation, development of effective insecticide mixtures, and the detection and development of new insecticides that are unaffected by the current resistance mechanisms. Horowitz and Ishaaya (1994) found that insecticide resistance to the IGRs, buprofezin and pyriproxyfen, could be prevented by restricting application to once per crop season during the period of peak crop activity. Liu and Stansly (1995) pointed out that there was a tendency for spray systems to concentrate chemicals on the upward facing adaxial leaf surfaces which tended to reinforce strong whitefly preferences for the downward-facing abaxial surfaces. They insisted that chemical coverage of abaxial leaf surfaces or bottom leaves of plants should be increased.

Spray scheduling should be based on action thresholds in managing resistance in the pest. Riley and Palumbo (1995) for example found that by using action thresholds established for SLW on melons they were able to reduce the number of calendar insecticide treatments by half.

Biological Control

Whitefly natural enemies (pathogens, predators, and parasitoids) are not found in equal abundance throughout the range of this pest and therefore their effects on whitefly populations are not always the same for all regions. In agricultural areas in Florida for example, a wide range of natural enemies has been observed (Evans 1993, Dean 1994). Evans (1993) reared 15 parasitoids from SPW; Dean (1994) observed at least 19 species of arthropods attacking this insect, and in noninsecticide-treated peanut fields, McAuslane et al. (1993, 1994) observed very high levels of mortality (up to 100% by the end of the crop cycle) due to parasitism. In agricultural areas in southern California, natural enemy populations are often very low (Meyerdirk et al. 1986, Bellows & Arakawa 1988) and their impact on whitefly populations is often minimal (Meyerdirk et al. 1986, Gill 1992).

The inadequacy of natural enemies to effectively control SLW to below economic levels in some situations has been noted (Parrella et al. 1992). One possible reason for this may be differences in the growth rates of the natural enemy agent and the whitefly. Powell and Bellows (1992c) for example studied two populations of *Eretmocerus* species, a California and an Hawaiian species. Both species had lower intrinsic rates of increase than *B. tabaci* on cotton when parasitism was examined at 20 °C. At 29 °C however, the Hawaiian population had higher intrinsic rates of increase than the whitefly. They indicated that the Hawaiian species was the more adequate species for biocontrol.

Very few natural enemy agents can or have been integrated into biological control programs against whiteflies (Onillon 1990). Presently, biocontrol has only been effective in managing SLW infesting greenhouse crops (Breene et al. 1992, Heinz & Parrella 1994).

Biocontrol has been justified based partly on lower production costs and increased returns that are to be expected from this strategy. Cherkasov (1986) observed that using *Encarsia formosa* Gahan or *Verticillium* on *B. tabaci* in glasshouse cucumber resulted in increased yields and reduced costs over standard insecticide control. There are however instances where biocontrol has been associated with higher production cost. On poinsettia, the parasitoid *E. formosa* gave little control of *B. argentifolii* even at low densities, and although releases of the parasitoid reduced the number of insecticide applications by 75%, on a m^2 basis the cost of using the parasitoid was 9.5 times that of using the insecticides alone (Hoddle & VanDriesche 1996). These results imply that both the crop and whitefly species should be equally considered in any biocontrol program, and that biocontrol packages are crop specific.

Cultural and Other Control Strategies

Alteration of planting date, destruction of alternate hosts, trap cropping , close cropping seasons, and barriers are some of the more common cultural methods used to manage whitefly populations (Cook 1986b). A number of workers have tested various cover types as barriers against whitefly infestation (Al-Musa et al. 1985, Abbass et al. 1988, Berlinger et al. 1988). Polyethylene row covers were compared with pesticide-treated and untreated zucchini plots for management of whiteflies (Costa et al. 1994). Yields from row-cover treated plots were significantly greater, and plants showed less silvering than in the two other treatments.

Removal of alternate hosts such as weeds and changes in seasonal cropping patterns seem to prevent the build-up of SPW populations and whitefly transmitted

diseases such as lettuce infectious yellows (Woods 1988, Blua et al. 1994). Breeding host plants for whitefly resistance has also been investigated (Berlinger 1986, De Ponti et al. 1990). Plant resistance to insects involves two basic mechanisms--antixenosis which elicits a behavioral response from the target insect and antibiosis that acts on the developmental processes of the insect. Both mechanisms of resistance have been observed for whiteflies although antixenosis appears to be the more common mechanism of resistance. In cotton for example plants with glabrous, okra-leaf shape and open canopy are less susceptible to SPW infestations (De Ponti et al. 1990).

Integrated Control

It appears now that no one method can be effective in managing whitefly populations so that an integrated pest management (IPM) approach is required. This strategy involves the simultaneous manipulation of the whitefly's environment, its host plants and the whitefly itself. An example of an IPM package for cotton in India was suggested by Natarajan et al. (1986). This package included growing cotton once a year and rotating with cereals, limiting the use of fertilizers and irrigation, removal of alternative hosts, monitoring SPW populations and applying pesticides based on different thresholds, and avoiding the use of certain pesticides.

Table 1-1. Mean duration of development for *Bemisia tabaci* and *Bemsia argentifolii* at various temperatures and on various host plants.

Life Stage(s)	Temp(°C) (R.H.%) [a]	Host Plants	Development Time (days)	Reference
EGG				
	28.4	Sweet potato	3.0	Azab et al. (1972)
	14.3		29.0	
	16.7	Cotton	22.5	Butler et al. (1983)
	20.0		11.5	
	22.5		9.9	
	25.0		7.6	
	27.5		6.1	
	30.0		5.4	
	32.5		5.0	
	36.0		No Hatch	
	14.0	Tomato	16.5	Sharaf & Batta (1985)
	25.0		6.4	
	25.0 (75%)	Bean	6.14	Lopez-Avila (1986)
	25.0 (75%)	Tobacco	6.37	
	25.0 (75%)	Lantana	6.9	
	25.0 (75%)	Tomato	7.3	
	25.0 (75%)	Cotton	7.67	
	20.0 (>50%)	Cotton	8.75	Powell & Bellows (1992a)
	25.5 (>50%)		4.81	
	29.0 (>50%)		4.17	
	32.0 (>50%)		3.92	
	20.0 (>50%)	Cucumber	12.4	Powell & Bellows (1992a)
	25.5 (>50%)		5.82	
	29.0 (>50%)		4.11	
	32.0 (>50%)		4.1	
	25.0 (65%)	Tomato	7.3	Salas & Mendoza (1995)

Table 1-1--continued

Life Stage(s)	Temp(°C) (R.H.%) [a]	Host Plants	Development Time (days)	Reference
	15.41	Cotton	21.9	Wagner (1995)
	20.01		11.4	
	24.81		6.2	
	26.02		6.3	
	28.00		5.4	
	34.66		5.0	
	25.0 (80-90%)	Eggplant	5.96	Tsai & Wang (1996)
	25.0 (80-90%)	Tomato	6.21	
	25.0 (80-90%)	Sweet potato	6.14	
	25.0 (80-90%)	Cucumber	6.37	
	25.0 (80-90%)	Garden Bean	6.0	
	27.0 (67%)	Alfalfa	7.4	Yee & Toscano (1996)
	27.0 (67%)	Broccoli	7.5	
	27.0 (67%)	Cantaloupe	7.3	
	27.0 (67%)	Cotton	7.1	
	27.0 (67%)	Zucchini	7.3	
	15.0 (70-90%)	Eggplant	25.8	Wang & Tsai (1996)
	20.0 (70-90%)		10.3	
	25.0 (70-90%)		5.9	
	27.0 (70-90%)		4.9	
	30.0 (70-90%)		4.2	
	35.0 (70-90%)		4.9	
1st INSTAR				
	14.3	Sweet potato	6.0	Azab et al. (1972)
	28.4		2.0	
	14.0	Tomato	9.0	Sharaf & Batta (1985)
	25.0		2.8	
	26.7 (91.7%)	Cotton	2.9	Bethke et al. (1991)
	26.7 (91.7%)	Poinsettia	4.9	

Table 1-1--continued

Life Stage(s)	Temp(°C) (R.H.%) [a]	Host Plants	Development Time (days)	Reference
	20.0 (>50%)	Cotton	4.92	Powell & Bellows (1992a)
	25.5 (>50%)		3.40	
	29.0 (>50%)		5.17	
	32.0 (>50%)		3.92	
	20.0 (>50%)	Cucumber	6.60	Powell & Bellows (1992a)
	25.5 (>50%)		4.08	
	29.0 (>50%)		3.47	
	32.0 (>50%)		3.68	
	25.0 (65%)	Tomato	4.0	Salas & Mendoza (1995)
	25.0 (80-90%)	Eggplant	1.99	Tsai & Wang (1996)
	25.0 (80-90%)	Tomato	2.21	
	25.0 (80-90%)	Sweet potato	2.39	
	25.0 (80-90%)	Cucumber	2.34	
	25.0 (80-90%)	Garden Bean	3.05	
	27.0 (67%)	Alfalfa	4.0	Yee & Toscano (1996)
	27.0 (67%)	Broccoli	3.8	
	27.0 (67%)	Cantaloupe	4.7	
	27.0 (67%)	Cotton	4.1	
	27.0 (67%)	Zucchini	5.1	
	15.0 (70-90%)	Eggplant	15.0	Wang & Tsai (1996)
	20.0 (70-90%)		4.1	
	25.0 (70-90%)		2.0	
	27.0 (70-90%)		1.7	
	30.0 (70-90%)		1.7	
	35.0 (70-90%)		3.0	

Table 1-1--continued

Life Stage(s)	Temp(°C) (R.H.%) [a]	Host Plants	Development Time (days)	Reference
2nd INSTAR				
	14.3	Sweet potato	5.0	Azab et al. (1972)
	28.4		1.0	
	14.0	Tomato	7.0	Sharaf & Batta (1985)
	25.0		2.4	
	26.7 (91.7%)	Cotton	2.1	Bethke et al. (1991)
	26.7 (91.7%)	Poinsettia	2.5	
	20.0 (>50%)	Cotton	3.25	Powell & Bellows (1992a)
	25.5 (>50%)		1.74	
	29.0 (>50%)		2.26	
	32.0 (>50%)		2.14	
	20.0 (>50%)	Cucumber	4.40	Powell & Bellows (1992a)
	25.5 (>50%)		2.14	
	29.0 (>50%)		2.32	
	32.0 (>50%)		2.15	
	25.0 (65%)	Tomato	2.7	Salas & Mendoza (1995)
	25.0 (80-90%)	Eggplant	2.35	Tsai & Wang (1996)
	25.0 (80-90%)	Tomato	2.23	
	25.0 (80-90%)	Sweet potato	2.11	
	25.0 (80-90%)	Cucumber	2.43	
	25.0 (80-90%)	Garden Bean	3.10	
	15.0 (70-90%)	Eggplant	13.1	Wang & Tsai (1996)
	20.0 (70-90%		3.6	
	25.0 (70-90%)		2.3	
	27.0 (70-90%)		2.0	
	30.0 (70-90%)		1.7	
	35.0 (70-90%)		2.3	

Table 1-1--continued

Life Stage(s)	Temp(°C) (R.H.%) [a]	Host Plants	Development Time (days)	Reference
3rd INSTAR				
	14.3	Sweet potato	7.0	Azab et al. (1972)
	28.4		2.0	
	14.0	Tomato	9.5	Sharaf & Batta (1985)
	25.0		3.0	
	26.7 (91.7%)	Cotton	3.0	Bethke et al. (1991)
	26.7 (91.7%)	Poinsettia	3.3	
	20.0 (>50%)	Cotton	3.38	Powell & Bellows (1992a)
	25.5 (>50%)		2.38	
	29.0 (>50%)		2.29	
	32.0 (>50%)		2.21	
	20.0 (>50%)	Cucumber	4.00	Powell & Bellows (1992a)
	25.5 (>50%)		2.42	
	29.0 (>50%)		2.34	
	32.0 (>50%)		2.03	
	25.0 (65%)	Tomato	4.0	Salas & Mendoza (1995)
	25.0 (80-90%)	Eggplant	1.92	Tsai & Wang (1996)
	25.0 (80-90%)	Tomato	2.23	
	25.0 (80-90%)	Sweet potato	2.36	
	25.0 (80-90%)	Cucumber	2.31	
	25.0 (80-90%)	Garden Bean	2.87	
	15.0 (70-90%)	Eggplant	15.0	Wang & Tsai (1996)
	20.0 (70-90%)		3.2	
	25.0 (70-90%)		2.3	
	27.0 (70-90%)		2.1	
	30.0 (70-90%)		1.6	
	35.0 (70-90%)		2.8	

Table 1-1--continued

Life Stage(s)	Temp(°C) (R.H.%) [a]	Host Plants	Development Time (days)	Reference
4th INSTAR				
	25 (75%)	Bean	3.4	Lopez-Avila (1986)
	25 (75%)	Tobacco	2.2	
	25 (75%)	Lantana	3.8	
	25 (75%)	Tomato	2.0	
	25 (75%)	Cotton	2.1	
	14.0	Tomato	27.5	Sharaf & Batta (1985)
	25.0		4.7	
	25.0 (80-90%)	Eggplant	5.09	Tsai & Wang (1996)
	25.0 (80-90%)	Tomato	5.11	
	25.0 (80-90%)	Sweet potato	5.14	
	25.0 (80-90%)	Cucumber	5.89	
	25.0 (80-90%)	Garden Bean	5.92	
	27.0 (67%)	Alfalfa	6.4	Yee & Toscano (1996)
	27.0 (67%)	Broccoli	6.0	
	27.0 (67%)	Cantaloupe	5.0	
	27.0 (67%)	Cotton	5.6	
	27.0 (67%)	Zucchini	6.1	
	15.0 (70-90%)	Eggplant	36.0	Wang & Tsai (1996)
	20.0 (70-90%)		8.5	
	25.0 (70-90%)		5.1	
	27.0 (70-90%)		4.8	
	30.0 (70-90%)		4.1	
	35.0 (70-90%)		5.8	
PUPA				
	25.0 (75%)	Bean	4.4	Lopez-Avila (1986)
	25.0 (75%)	Tobacco	4.5	
	25.0 (75%)	Lantana	2.3	
	25.0 (75%)	Tomato	2.4	
	25.0 (75%)	Cotton	1.7	

Table 1-1--continued

Life Stage(s)	Temp(°C) (R.H.%) [a]	Host Plants	Development Time (days)	Reference
	27.0(67%)	Alfalfa	3.2	Yee & Toscano (1996)
	27.0(67%)	Broccoli	3.0	
	27.0(67%)	Cantaloupe	3.0	
	27.0(67%)	Cotton	2.8	
	27.0(67%)	Zucchini	2.9	
4th & PUPA				
	14.3	Sweet potato	23.0	Azab et al. (1972)
	28.4		4.0	
	26.7 (91.7%)	Cotton	5.3	Bethke et al. (1991)
	26.7 (91.7%)	Poinsettia	4.4	
	20.0 (>50%)	Cotton	8.33	Powell & Bellows (1992a)
	25.5 (>50%)		5.34	
	29.0 (>50%)		5.23	
	32.0 (>50%)		5.39	
	20.0 (>50%)	Cucumber	10.8	Powell & Bellows (1992a)
	25.5 (>50%)		5.76	
	29.0 (>50%)		5.11	
	32.0 (>50%)		5.47	
	25.0 (65%)	Tomato	5.8	Salas & Mendoza (1995)
EGG to ADULT				
	14.9	Cotton	65.1	Butler et al. (1983)
	16.7		48.7	
	20.0		34.7	
	22.5		27.8	
	25.0		23.6	
	27.5		17.8	
	30.0		16.6	

Table 1-1--continued

Life Stage(s)	Temp(°C) (R.H.%) [a]	Host Plants	Development Time (days)	Reference
	26.7 (40-60%)	Carrot	29.8	Coudriet et al. (1985)
	26.7 (40-60%)	Broccoli	29.7	
	26.7 (40-60%)	Tomato	27.3	
	26.7 (40-60%)	Pepper	23.0	
	26.7 (40-60%)	Cantaloupe	22.3	
	26.7 (40-60%)	Watermelon	22.3	
	26.7 (40-60%)	Cotton	21.7	
	26.7 (40-60%)	Alfalfa	21.4	
	26.7 (40-60%)	Squash	21.3	
	26.7 (40-60%)	Eggplant	20.9	
	26.7 (40-60%)	Cucumber	20.6	
	26.7 (40-60%)	Lettuce	19.4	
	26.7 (40-60%)	Sweet potato	18.6	
	25.0 (75%)	Bean	21.4	Lopez-Avila (1986)
	25.0 (75%)	Tobacco	22.4	
	25.0 (75%)	Lantana	25.4	
	25.0 (75%)	Tomato	23.5	
	25.0 (75%)	Cotton	23.0	
	26.7 (91.7%)	Cotton	23.3	Bethke et al. (1991)
	26.7 (91.7%)	Poinsettia	23.2	
	25.0 (60%)	Tomato	21.0	Van Giessen et al. (1995)
	25.0 (60%)	Collard	21.2	
	25.0 (60%)	Eggplant	18.5	
	25.0 (60%)	Pepper	19.2	
	17.39	Cotton	51.9	Wagner (1995)
	20.01		32.2	
	24.81		18.3	
	26.02		18.7	
	28.00		17.3	
	34.66		29.3	

Table 1-1--continued

Life Stage(s)	Temp(°C) (R.H.%) [a]	Host Plants	Development Time (days)	Reference
	25.0 (80-90%)	Eggplant	17.30	Tsai & Wang (1996)
	25.0 (80-90%)	Tomato	17.96	
	25.0 (80-90%)	Sweet potato	18.14	
	25.0 (80-90%)	Cucumber	19.34	
	25.0 (80-90%)	Garden Bean	20.95	
	27.0 (67%)	Alfalfa	22.4	Yee & Toscano (1996)
	27.0 (67%)	Broccoli	22.2	
	27.0 (67%)	Cantaloupe	21.7	
	27.0 (67%)	Cotton	21.3	
	27.0 (67%)	Zucchini	23.0	
	15.0 (70-90%)	Eggplant	104.9	Wang & Tsai (1996)
	20.0 (70-90%)		29.8	
	25.0 (70-90%)		27.6	
	27.0 (70-90%)		16.0	
	30.0 (70-90%)		13.6	
	35.0 (70-90%)		18.8	

[a] Temperture and Relative Humidity

Table 1-2. Economically important viruses and phytotoxic disease disorders resulting from feeding by *Bemisia tabaci* and *Bemisia argentifolii* on agricultural crops.

Virus or Disease (Acronym)	Disease Type[a]	Major Host	Reference
African cassava mosaic (ACMV)	GM	Cassava	Bock et al. (1978)
Bean golden mosaic (BGMV)	GM	Bean	Goodman et al. (1977)
Chino del tomate (CdTV)	GM	Solanaceae	Brown & Nelson (1988)
Cowpea mild mosaic (CMMV)	CM	Cowpea	Brunt & Kenten (1973)
Cotton leaf crumple (CLCV)	GM	Cotton	Brown & Nelson (1984)
Cucumber vein yellowing (CVYV)	RS	Cucurbits	Sela et al. (1980)
Lettuce infectious yellow (LIYV)	ClV	Lettuce	Duffus & Flock (1982)
Mung bean yellow (MBYMV)	GM	Mung bean	Honda et al. (1983)
Pepper streak	P	Pepper	Summers & Estrada (1996)
Soybean crinkle leaf (SCLV)	GM	Soybean	Iwaki et al. (1983)
Squash leaf curl (SLCV)	GM	Cucurbits	Cohen et al. (1983)
Squash silverleaf (SSL)	P	Cucurbits	Maynard & Cantliffe (1989)
Tobacco leaf curl (TLCV)	GM	Tobacco	Osaki & Inouyi (1981)
Tomato golden mosaic (TGMV)	GM	Tomato	Hamilton et al. (1981)
Tomato mottle (ToMoV)	GM	Tomato	Kring et al. (1991)
Tomato yellow leaf curl (TYLCV)	GM	Tomato	Czosnek et al. (1988)
Tomato irregular ripening (TIR)	P	Tomato	Maynard & Cantliffe (1989)
Watermelon curly mottle (WCMoV)	GM	Cucurbits	Brown & Nelson (1986)
White stem (WS)	P	Pumpkin	Costa & Brown (1990)

adapted from Byrne et al. (1990)

[a] GM, Geminivirus; CV, Carlavirus; ClV, Closterovirus; RS, Rod shaped; P, Phytotoxic effect

CHAPTER 2
A SPATIOTEMPORAL INSECT SPECIES INTERACTION MODEL FOR LARGE-SCALE DYNAMICS

Introduction

The intractable nature of large-scale ecological experiments presents a problem to population ecologists trying to understand the dynamics of plant and animal species, and the effects of important ecological processes, over large spatial extents (Turner et al. 1995). When such large-scale experiments are conceived, it is often logistically impossible to replicate these efforts. Data taken from Kareiva and Anderson (1988), and summarized in Levin (1992), clearly indicate that as the size of the experimental unit is increased, there is generally a corresponding decrease in the number of experimental replicates that are conducted. Replication and randomization are two basic requirements in any good experiment (Mead & Curnow 1983). Ecologists have therefore been searching for tools to complement field experimentation and replication in studying species population dynamics in large spatial systems and have found simulation models to be quite useful (Levin 1992).

Simulation models are already being used by landscape managers and population ecologists to investigate animal species dynamics in large heterogeneous habitats. These models have generally been formulated as spatially explicit population models (SEPMs) that combine a population simulation model with a habitat or landscape map that describes

the spatial distribution of species resources in the region. SEPMs have therefore captured the attention of population ecologists and conservation biologists, and are now being applied in a number of situations (Dunning et al. 1995, Turner et al. 1995, Conroy et al. 1995, Holt et al. 1995). Insect ecologists have been slow to adopt these types of models, and have done very little to incorporate habitat complexity of the real world into their models.

In insect ecology, models have been used mainly to investigate insect-habitat and/or insect-insect relationships in homogeneous (real and artificial) systems (e.g. von Arx et al. 1983, Liebhold & McManus 1991, DeGrandi-Hoffman et al. 1994), and to examine questions pertaining to the effects of spatial variability and species dispersal on population stability and persistence (Reeve 1990, Hastings 1990, Taylor 1990, Hassell et al. 1991, Alder 1993). For examining theoretical questions, the insect system in these models is generally formulated as Coupled Map Lattices (CML) (Allen 1975, Allen et al.1993, Hassell et al. 1991,1994, Bascompte & Solé 1994). CMLs represent dynamical systems with discrete time and space, and continuous state (Kaneko 1989, 1990, 1992) in which the degree of coupling between subpopulations is clearly defined by dispersal or migration rules.

Two different ways have generally been used to incorporate spatial movement into ecological models, and these depend on several factors including the type of system being considered–continuous (in time and space) or discrete (in time). For continuous systems, spatial movement is commonly incorporated through reaction-diffusion equations (Okubo 1980, Rudd & Gabdour 1985, Banks et al. 1988, Corbett & Plant 1993), but the

mathematics involved in the solution of these equations can be quite difficult (Stinner et al. 1983, Barclay 1992, Allen et al. 1995). Reaction-diffusion equations are not appropriate for describing spatial movement in discrete systems (Kot 1989, Andersen 1991) and instead patch models are developed where each patch is occupied by a subpopulation, and population processes are unique to that patch. Spatial movement in this case is modeled with dispersal rules that specify neighborhood (local) or global connection between subpopulations. Examples of local movement rules include rook's (orthogonal), bishop's (diagonal), and queen's (orthogonal and diagonal) moves (Sokal & Oden 1978). Integrodifference equations (IDEs) have recently emerged as alternatives to reaction-diffusion equations in discrete-time ecological systems (Kot & Schaffer 1986, Kot 1989, Andersen 1991). Rules for species movement in continuous as well as discrete spatial systems can be applied.

In this chapter, the framework for a discrete-time spatiotemporal insect population model is developed and described. This model integrates ideas from SEPMs, CMLs and IDEs and is developed primarily as a tool for studying insect dynamics in regional crop systems. It combines a population simulation submodel with landscape or resource maps that describe the heterogeneous habitat of the insect, and spatial movement is explicitly incorporated. The merits and limitations of this modeling approach as it relates to the study of insect dynamics in regional agricultural systems are discussed.

Model Formulation, Development and Description

Ideas from SEPMs, CMLs and IDEs are integrated in formulating the framework for the spatiotemporal model. The model is an age-structured form of the Nicholson-Bailey (Nicholson & Bailey 1935) model in which prey and natural enemy populations inhabit a two-dimensional spatially heterogeneous environment that is characterized with a spatial matrix of resource types. Spatial movement is accomplished by summing the dispersal of individuals into each point from all other points in the spatial system, and is coupled with reproduction using a two-dimensional discrete space counterpart of an IDE model. The discussion begins with some background on SEPMs, CMLs, IDEs, and Nicholson-Bailey (NB) model.

Spatially Explicit Population Models

Dunning et al. (1995 p. 3) define SEPMs as models that "combine a population simulator with a landscape map that describes the spatial distribution of landscape features". These models have the ability to include some degree of spatial realism by capturing important features of the habitat in which a species exists, and therefore can be used to test hypotheses on the effects of explicit resource distributions on species dynamics (Dunning et al. 1995, Turner et al. 1995, Conroy et al. 1995, Holt et al. 1995). SEPMs therefore can be used for studying animal species dynamics and ecological processes across spatial scales ranging from local to regional to global. The capability to do so is only limited by the ability to adequately describe the species habitat, and to identify and estimate model parameters at the relevant spatial scales.

Many SEPMs are mobile animal population (MAP) models (Dunning et al. 1995) that incorporate information about the dispersal behavior of the animal under study. These can be used to examine the influences that selective dispersal rules have on population dynamics.

According to Dunning et al. (1995), SEPMs can also be classified as "individual-based" or "population-based" models. Individual-based SEPMs have been used mainly for studying the dynamics of large animals such as wolves, *Canus lupus* (Lewis & Murray 1993). Population-based SEPMs on the other hand are particularly useful for smaller organisms such as insects. Fahrig and Paloheimo (1988) for example used a population-based SEPM to examine the effect of spatial arrangement of habitat patches on the abundance of the cabbage butterfly (*Pieris rapae*), while Hassell et al. (1991) and Comins et al. (1992) used this type of model to study the types of spatial dynamics that could arise through insect interaction in a two-dimensional spatially subdivided environment where species movement was localized.

Coupled Map Lattices

The coupling of subpopulations in CML models is achieved with clearly defined redistribution rules. Some overlap exist between SEPMs and CMLs in that both model spatial populations and rules for coupling subpopulations are clearly stated. Unlike SEPMs however, characteristics relevant to each habitat unit, and as such to each subpopulation in some CMLs, may not always be explicitly known.

Two types of CMLs are important--locally coupled maps (LCMs) and globally coupled maps (GCMs). The models of Hassell et al. (1991) and Comins et al. (1992)

mentioned previously as examples of a population-based SEPMs, and a modified Hassell (1975) model (Bascompte & Solé 1994) can all be considered LCMs since the locations of subpopulations in the spatial systems are explicitly stated, and only neighboring subpopulations are linked through dispersal. A one species two-dimensional LCM model may be represented mathematically by

$$Y_{t+1}(i,j) = f(Y_t(i,j)) + D\nabla^2 Y_t(r)$$
$$\textit{where} \qquad (2.1),$$
$$D\nabla^2 Y_t(r) = D[Y_t(i-1,j) + Y_t(i+1,j) + Y_t(i,j-1) + Y_t(i,j+1) - 4Y_t(i,j)]$$

Y_{t+1} represents the population in the following generation at the i,j location in the spatial system, $f(Y_t(i,j))$ is the species growth function at time t at the same location, and D is the movement rate or fraction of individuals that move between each location per unit time. Bascompte and Solé (1994) replaced $f(Y_t(i,j))$ with the Hassell (1975) model and used their model to study the effects of spatial system size on species dynamics. In eqn (2.1), dispersal is local and follows rook's movement rule (connection to the four nearest row and column cells only).

In GCMs, subpopulation locations are not always specified, and more importantly coupling is achieved through global mixing of dispersing individuals from each subpopulation. So for example, a GCM version of eqn (2.1) is

$$Y_{t+1}(i,j) = (1-D)f(Y_t(i,j)) + D\frac{\sum_x \sum_y f(Y_t(x,y))}{n^2}, \quad x=y=1,2,\ldots,n \qquad (2.2),$$

In this case, a fraction (D) of the individuals from each subpopulation enters a migrant pool to be redistributed evenly amongst all subpopulations. The system in eqn (2.2) was formulated by considering the explicit arrangement of subpopulations in the system on a square grid with equal size cells (patches). More commonly, GCMs are formulated without giving consideration to any explicit spatial arrangement but instead by simply indexing all subpopulations in the system (Reeve 1990, Hastings 1990, Taylor 1990, Alder 1993, Allen et al.1993). Therefore, eqn (2.2) becomes

$$Y_{t+1}(i) = (1-D)f(Y_t(i)) + D\frac{\sum_j f(Y_t(j))}{n} \quad , (j = 1, 2, ..., n = subpopulations) \tag{2.3}.$$

In this case, there is no explicit spatial arrangement for subpopulations in the system.

Integrodifference Equations and Discrete Space Counterparts

These models have found applications in population genetics (Slatkin 1973, Lui 1989a,b), ecology (Kot & Schaffer 1986, Kot 1989, Andersen 1991), and even in studying nerve transmission and mollusc shell pattern formation (Murray 1989). Some very interesting dynamics have also been observed in one-dimensional systems modeled with IDEs (Kot & Schaffer 1986, Kot 1989, Hastings & Higgins 1994, Neubert et al. 1995). IDEs can be considered as discrete-time analogues of reaction-diffusion equations, and are generally used to model populations having distinct growth and dispersal phases and inhabiting continuous habitats (Kot 1989, Andersen 1991).

Consider a population (Y_t) existing in one-dimensional continuous space, where individuals in the following generation (Y_{t+1}) come directly from individuals produced

during the sedentary stage of the previous generation and redistributed during the dispersal stage. Mathematically, the result is an IDE of the form,

$$Y_{t+1}(l) = \int_x K(l-x) f(Y_t(x)) dx \qquad (2.4),$$

where *f(Y)* is the reproductive function, and *K*, the dispersal or redistribution kernel. *K(l - x)dx* is the probability density function for individuals dispersing from the point *x*. IDEs can be modified for simulating spatial systems that are discrete (a spatial grid) by replacing the integral with a summation. Therefore, in the discrete case for a one-dimensional space of *n* locations, eqn (2.4) becomes

$$Y_{t+1}(l) = \sum_{x=1}^{n} K(l-x) f(Y_t(x)) \qquad (2.5),$$

with *K(l - x)* now the probability that an individual will move during dispersal from point *x* to point *l*. For two-dimensional systems, eqns (2.4) and (2.5) are rewritten as

$$\begin{aligned} Y_{t+1}(l,m) &= \int_x \int_y K(l-x, m-y) f(Y_t(x,y))\, dx dy && (a)\ \textit{continuous space} \\ Y_{t+1}(l,m) &= \sum_{x=1}^{n} \sum_{y=1}^{n} K(l-x, m-y) f(Y_t(x,y)) && (b)\ \textit{discrete space} \end{aligned} \qquad (2.6)$$

K(l - m,x - y) is the probability of moving from *x,y* to *l,m* across two-dimensional space. The couplings in eqns (2.6a) and (2.6b) are in fact mathematical convolutions that calculate all of the dispersal (and reproduction) by integrating or summing over the whole

space into each point *l,m*. If this is done for all *l,m* points in the spatial system, a density surface (eqn 2.6a) or a matrix of densities (eqn 2.6b) is obtained.

Nicholson-Bailey Model Examined

A nonspatial discrete-time predator-prey or host-parasitoid model can be represented by

$$\begin{aligned} Y_{t+1} &= H(Y_t, Z_t) \\ Z_{t+1} &= G(Y_t, Z_t) \end{aligned} \tag{2.7}$$

where Y is the prey (host) , Z the predator (parasitoid), and t is time. In the Nicholsonian type models three assumptions are made (Edelstein-Keshet 1988); 1) parasitized hosts will give rise to the next generation of parasitoids, 2) unparasitized hosts will give rise to their own progeny, and 3) the rate of encounter of the two species will determine the fraction of hosts that are parasitized. With these assumptions eqn (2.7) becomes

$$\begin{aligned} Y_{t+1} &= rY_t f(Y_t, Z_t) \\ Z_{t+1} &= cY_t(1 - f(Y_t, Z_t)) \end{aligned} \tag{2.8},$$

where Y_t and Z_t are host and parasitoid densities in generation t, respectively, r is host reproductive rate, $f(Y_t, Z_t)$ is the fraction of hosts not parasitized, and c is the conversion rate of parasitized hosts into parasitoids or the average number of viable eggs laid per parasitized host (Hassell 1978).

Nicholson-Bailey (1935) also assumed that in the absence of the parasitoid, host population increase is geometric by a factor of r (i.e., host population is limited solely by

the parasitoid), and that parasitoids search independently of each other and encounter hosts at random. In continuous time, the rate of change in the host population, dY/dt, is proportional to the product of host and parasitoid densities. Mathematically, $dY/dt = -aYZ$ where a is *area of discovery* which is a species-specific parameter representing the searching efficiency or effective area of search of the parasitoid. The number of encounters of the parasitoid with hosts per time interval, $Ne = aY_tZ_t$, appears to differ between parasitoids and predators. Parasitoids can usually encounter a single host several times and therefore Ne is the total number of encounters with hosts (whether or not an egg is laid on each encounter). Predators on the other hand, usually remove their prey as they are eaten and so prevent re-encounter (Hassell 1978).

Since the numbers of encounters was assumed to be random, then the probability of a particular host not being attacked was assumed to be the zero term of the Poisson distribution that describes the occurrence of discrete random events. In the Poisson distribution, the probability of k events occurring is

$$p(k) = \frac{e^{-\mu}\mu^k}{k!} \qquad (2.9)$$

where μ is the average number of events per time interval and in this case is equivalent to Ne/Y_t, the average number of encounters per host per unit time. Since $Ne = aY_tZ_t$ then μ can be replaced by aY_tZ_t/Y_t which is equal to aZ_t. The probability of escaping parasitism is the same as the probability of zero encounters during the host lifetime, i.e., $p(0)$ is equal

to $exp(-aZ_t)$. This represents $f(N_t,P_t)$ in eqn (2.8). The Nicholson-Bailey model can now be written as

$$\begin{aligned} Y_{t+1} &= rY_t \exp(-aZ_t) \\ Z_{t+1} &= cY_t(1 - \exp(-aZ_t) \end{aligned} \tag{2.10}$$

Analysis of this model indicates that the equilibrium states are never stable and that any deviation from steady state in prey or natural enemy leads to diverging oscillations and ultimate extinction in the system. These observations will be explored in a subsequent study.

The Spatiotemporal Insect Model

If the model in eqn (2.10) is modified and now takes on a form similar to that of eqn (2.6b), it becomes

$$\begin{aligned} Y_{t+1}(l,m) &= \sum_{x=1}^{n} \sum_{y=1}^{n} K_Y(l-x,m-y)\ rY_t(x,y)\exp(-aZ_t(x,y)) \\ Z_{t+1}(l,m) &= \sum_{x=1}^{n} \sum_{y=1}^{n} K_Z(l-x,m-y)\ cY_t(x,y)(1 - \exp(-aZ_t(x,y))) \end{aligned} \tag{2.11}.$$

This model can be further modified to include population age-structure with individuals in each age-class having distinct survival and development probabilities at each time step. If for example, the population for each species is divided into three age-classes (egg, immature and adult), individuals in each age-class undergo partial development at each time step, and the natural enemy can attack only immature prey, eqn (2.11) becomes

$$
\begin{aligned}
Y1_{t+1} &= R_t + S_{Y1}(1-D_{Y1})\,Y1_t \\
Y2_{t+1} &= S_{Y1}D_{Y1}\,Y1_t + S_{Y2}(1-D_{Y2})\,Y2_t \exp(-aP_t) \\
Y3_{t+1} &= S_{Y2}D_{Y2}\,Y2_t \exp(-aP_t) + S_{Y3}Y3_t \\
\\
Z1_{t+1} &= Y2_t\,(1-\exp(-aP_t)) + S_{Z1}(1-D_{Z1})\,Z1_t \\
Z2_{t+1} &= S_{Z1}D_{Z1}\,Z1_t + S_{Z2}(1-D_{Z2})\,Z2_t \\
Z3_{t+1} &= S_{Z2}D_{Z2}\,Z2_t + S_{Z3}Z3_t
\end{aligned}
\qquad (2.12).
$$

where

$$
R_t(l,m) = \sum_{x=1}^{n}\sum_{y=1}^{n} K_Y(l-x,m-y)f(Y3_t(x,y))
$$

(*redistributed host reproduction*)

$$
P_t(l,m) = \sum_{x=1}^{n}\sum_{y=1}^{n} K_Z(l-x,m-y)\,Z3_t(x,y))
$$

(*redistributed natural enemy*)

Y1, *Y2*, and *Y3* are spatial matrices of egg, immature and adult prey densities, while *Z1*, *Z2*, and *Z3* are (overlaid) matrices of natural enemy egg, immature and adult densities. S_{Y1}, S_{Y2}, S_{Y3}, S_{Z1}, S_{Z2} and S_{Z3} are proportions representing survival of each age-class during a timestep, while D_{Y1}, D_{Y2}, D_{Z1}, and D_{Z2} are proportions representing development out of each age-class during a timestep. The proportion of individuals not developing is $1 - D$. Survival, development, and natural enemy attack (a) could of course be functions of climate and biotic factors (time-varying), and may vary with location (i.e., become spatial matrices).

Prey reproduction

The function *f(Y3)* is a general function for prey reproduction that can be substituted with a number of specific reproductive functions (see for example, Cohen 1995). It can as in eqn (2.10) be linear where r is constant and $f(Y3) = rY3$. However, if

reproduction is density-dependent (non-linear), then *f(Y3)* may be represented by a function such as the Ricker function (Ricker 1954) which at each *l,m* location is equal to

$$f(Y3_t) = Y3_t \exp\left(r\left(1 - \frac{Y3_t}{k}\right)\right) \qquad (2.13)$$

where *exp(r)* is the egg production per female per time period, *k* is the carrying capacity of the host resource, and *Y3* the adult prey density. In a heterogeneous environment, the extent of reproduction may be specific to each patch and therefore *r* and *k* in eqn (2.13) would also be site-specific. These parameters could therefore become spatial matrices with or without the inclusion of environmental forcing.

Natural enemy attack function

Recall that in the Nicholson-Bailey model, the probability of prey escaping parasitism is given by $exp(-aP_t)$, with *a* the *per capita* searching efficiency of a natural enemy that searches independently and randomly within each patch. Hassell and Varley (1969) and Hassell and May (1973) showed that *a* depends on factors such as the density of the predator. The relationship between this parameter and the predator density was described as inverse linear by Hassell and Varley (1969) and curvilinear by Beddington (1975). If the inverse linear relationship is adopted, $a = QP^{-m}$ with *Q* the searching efficiency of one individual and *m* ($0 \leq m < 1$) the *mutual interference* constant. Estimates of *m* in laboratory and field studies are given in Hassell and May (1973). Notice that $exp(-aP_t)$ can be replaced with a general function, $g(P_t, Y2_t)$ that represents a number of parasitism survival functions. A list of these is given in Hassell and May (1973). Like *r*

and k, parameter a may also be a spatial matrix representing the searching efficiencies of the natural enemy in a heterogeneous environment.

Dispersal or redistribution kernels

In eqn (2.12), K_Y and K_Z are the dispersal or redistribution kernels for the prey and natural enemy, respectively. The kernels characterize the frequency distributions of dispersal distances for each species and their form can be determined from observed data. Methods for doing so have been discussed by several authors including Southwood (1978) and Silverman (1986). One major strength of IDE models is the fact that the redistribution function is very general and therefore experiments can be done to test different hypotheses concerning dispersal behavior.

Neubert et al. (1995) give a review of redistribution kernels in one-dimensional predator-prey systems. In a two-dimensional map with a local coupling, the degree of coupling drops off with distance, i.e. the probability of dispersing to patches closer to the source patch is greater than for distant patches. It is possible to achieve this type of "local" coupling with a number of redistribution kernels. Kot et al. (1996) for example, have found that much of the data on dispersal patterns suggest leptokurtic dispersal with more individuals near the source and in the tails than would be expected with a normal distribution of equal mean and variance. Normal redistribution kernels they noted also tended to underestimate rates of spread. The normal redistribution kernel is however a good starting assumption for many invading organisms especially if one assumes that insect dispersal is a random process (Rudd & Gandour 1985, Johnson & Milne 1992). If

normal dispersal patterns are considered these may be described by two-dimensional normal density functions such as

$$K(l,m,x,y) = \frac{1}{2\pi\sigma^2} exp\left(-\left(\frac{(l-x)^2+(m-y)^2}{2\sigma^2}\right)\right) \qquad (a)$$

$$K(l,m,x,y) = \frac{1}{2\pi\sigma_x\sigma_y} exp\left(-\frac{1}{2}\left(\frac{(l-x)^2}{\sigma_x^2}+\frac{(m-y)^2}{\sigma_y^2}\right)\right) \qquad (b)$$

$$with \quad \sigma_x \neq \sigma_y \qquad (2.14)$$

$$K_t(l,m,x,y) = \frac{1}{2\pi\sigma^2} exp\left(-\left(\frac{(l-\hat{x})^2+(m-\hat{y})^2}{2\sigma^2}\right)\right) \qquad (c)$$

$$where \quad \hat{x} = (v_x t - x) \; and \; \hat{y} = (v_y t - y)$$

A symmetrical redistribution pattern (Fig. 2-1a) is generated with eqn (2.14a), while biased redistribution patterns in the x and/or y directions can be obtained with eqn (2.14b) (Figs. 2-1b,c). If $\sigma_x = \sigma_y$, eqn (2.14b) essentially becomes eqn (2.14a). In eqn (2.14c), $\hat{x}$ and $\hat{y}$ are the wind-shifted coordinates at each time step (t) that result from a shift ($v_x t$) in the x-direction, and a shift ($v_y t$) in the y-direction due to wind, where v_x and v_y are the x and y components of wind velocity (Fig. 2-1d). The standard deviation of dispersal per time step, σ, depends on the insect, the habitat's extent and grain (Wiens 1989), and characteristics of the host resource in each patch. A highly mobile insect may have a time-varying σ that reaches a maximum near host-plant senescence.

Other types of two-dimensional dispersal patterns have been considered. These were developed specifically to describe the dispersal patterns of *B. tabaci* and *B. argentifolii*, but can be adapted and applied to other insects. Since adult whitefly

populations consist of two distinct dispersal morphs--a trivial flying morph that moves only within source fields and a migratory morph that takes long flights(Byrne & Houck 1990, Blackmer & Byrne 1993a,b, Byrne et al. 1996), a bimodal proportional mix of two dispersal density functions can be used to model this phenomenon, that is

$$K_{total} = p\,K_{trivial} + (1-p)\,K_{migrator} \qquad (2.15)$$

where p is the proportion of trivial fliers in the source field. $K_{trivial}$ and $K_{migrator}$ are then dispersal density functions for the trivial flyers and migrators, respectively. K_{total} is the bimodal proportional sum which still integrates to one as a probability density (Allen et al.1996) (Fig. 2-2a).

There is also what can be called a "ripple" function (Fig. 2-2b) that generates a repulsive dispersal pattern analogous to a ripple spreading out across a water surface (Allen et al. 1996). Biologically, this function implies some sort of repulsion from a source patch resulting from some undesirable condition there (e.g., high density or deteriorating resources). This pattern has been observed for at least one insect in a natural system. *Cales noacki*, a parasitoid of the wooly whitefly, *Aleurothrixus floccosus* (Maskell), exhibited this type of dispersal pattern in citrus orchards (Onillon & Onillon 1974). The ripple density function is written as

$$K_{ripple}(x,y) = \frac{1}{v}\exp\left(-\frac{\left(\sqrt{x^2+y^2}-\bar{r}\right)^2}{2\sigma^2}\right) \qquad (2.16)$$

where

$$v = \pi\sqrt{2}\,\sigma\left[\bar{r}\sqrt{\pi}\left(1 + erf\left(\frac{\bar{r}}{\sqrt{2}\,\sigma}\right)\right) + \sqrt{2}\,\sigma\exp\left(-\left(\frac{\bar{r}}{\sqrt{2}\,\sigma}\right)^2\right)\right] \quad (2.17)$$

is the total volume under the distribution that forces eqn (2.16) to integrate to one when summed over its entire range thus making it a probability density. The error function given by

$$erf(x) = \frac{2}{\sqrt{\pi}}\int_0^x e^{-t^2}\,dt \quad (2.18),$$

is commonly available in many simulation packages such as MATLAB® (MathWorks 1994). In K_{ripple}, $\bar{r}$ is the distance from the center (origin) of the ripple to the peak, and σ^2 is the variance of the corresponding normal density cross-section through the peak. These parameters allow control over the diameter and "spread" of the ripple density function.

Solving the convolutions

Directly solving the double summations in R_t and P_t (eqn 2.10) for each location in the spatial system is numerically intensive. These couplings (convolutions) may instead be solved in a single operation using the Fourier transforms as described by Andersen (1991) for a one-dimensional model. Using the simulation package, MATLAB® (MathWorks 1994), the convolution of K_{Y3} with *f(Y3)* at every location in the two-dimensional system can be solved in one step, as follows:

$$R_t = \sum_{x=1}^{n} \sum_{y=1}^{n} K_{Y3}(l,m,x,y) f(Y3_t(x,y)) = IFFT2\left[FFT2(K_{Y3})\ FFT2(f(Y3_t))\right] \quad (2.19)$$

That is, the two-dimensional discrete fast Fourier transforms (FFT2) of K_{Y3} and *f(Y3)* are multiplied together (element-by-element) where *K* and *f(Y3)* are matrices, and inverted with IFFT2 back to the spatial domain. The result, R_t, is a single matrix of dispersed host egg densities. Similarly for P_t, the result is a single matrix of dispersed natural enemy adults (*Z3*).

Certain peculiarities of the Fourier transform must be pointed out. The transform is most efficient on systems that are powers of two. It is best therefore to construct the system as a spatial matrix with 2^h x 2^h spatial locations. In addition, the Fourier transform "wraps" on itself (is periodic) (Andersen 1991) as if insects leaving one side of the grid reentered on the other. To avoid this unrealistic scenario, the spatial (n x n) matrix can be embedded in the center of a $2n$ x $2n$ matrix of zeros before doing the transforms, thereby producing an absorbing boundary from which insects do not return.

The Fourier transform also assumes that parameters are spatially invariant which is not true in a spatially-varying resource system. To circumvent this problem in the heterogenous system, the transforms can be applied one-at-a-time for each resource and the results summed. Implicit in this is that the insects in one resource are not influenced by another. An efficient alternative is to construct an emigration probability matrix (EPM) for each species in the system based on the probability of leaving each resource. During each time step, the EPM is applied to the insect's spatial density matrix to create an

emigrant density matrix (EDM). Since the EDM is now considered to be constant within each time step, a single dispersal kernel may be applied to redistribute individuals in this matrix over the entire spatial system. Therefore, if the system contained N resources, then instead of having to apply the Fourier transform pair N times within each timestep, these are now be applied once. This results in significant savings in computation time. Notice that the EPM can be a matrix of probabilities forced by the environment with the degree and type of forcing dependent on the state of the resource at each location.

The Resource Map

Although the insect's habitat and the resources therein are not shown explicitly in eqn (2.12), they are characterized by a similar spatial matrix, X, whose entries are integers representing the resources at every l,m location in a region. This resource matrix or map can be used by the model in two basic ways. Each integer (i) in the resource map can serve as the index to model parameters so that if $X(l,m) = i$, then i is an index to prey and natural enemy parameters on resource i at location l,m. Parameter values relevant to each resource are then stored in a parameter look-up table with row numbers corresponding to resources and columns to paramters. Alternatively, the resource matrix can be used to create individual parameter matrices for each parameter (survival, reproduction, development, natural enemy attack) in eqn (2.12). Methods for constructing resource maps will vary and depend on the size of the system. Discussion on the construction of these maps will be given later.

Discussion

The scale at which studies are conducted can have a significant effect on dynamical patterns that are observed (Weins 1989). There is no natural scale at which to study ecological phenomenon (Levin 1992) and therefore having the ability to study spatial systems efficiently at any scale is important. In the past, ecologists, and in particular insect ecologists, have focused on small-scale questions amenable to experimental studies and have largely ignored large-scale processes which many feel are likely to be responsible for the patterns observed at larger spatial scales (Dayton & Tegner 1984). Field experiments observe the environment at a limited range of scales and therefore only provide what Levin (1992 p.1945) saw as a "low-dimensional slice through a high-dimensional cake". Modeling can make up for some of the deficiencies in field experimentation and can play a powerful role in suggesting possible mechanisms and experiments, in exploring the possible consequences of individual factors that cannot be separated easily experimentally, and by allowing us to observe dynamical patterns in a system at a various spatial scales..

The model that was described is quite general and can be adapted for studying the spatiotemporal dynamics of a number of insects. The number of age-classes can be increased by adding a pre-oviposition adult age-class, natural enemy could be made to attack more than one prey age-class, and multi-stage dispersal can be included. Since the redistribution kernel, K, is general, it can represent any dispersal process and this gives us the ability to test hypotheses about how dispersal impacts spatial dynamics.

Characteristics of an organism's habitat are known to influence its dynamics (Fahrig 1988, Levin 1992). In the insect model in eqn (2.12), these characteristics are

defined with the resource map and therefore changes to the map will result in changes in population dynamics of the insect. This map can be altered simply by changing resource types altogether or by changing the arrangement of resources in time and space. Some realism can therefore be included into the model and experiments can be done with different spatiotemporal habitat arrangements. This type of experimentation has proven very useful in improving the understanding and knowledge of species-habitat interactions (Dunning et al. 1995, Turner et al. 1995, Conroy et al. 1995, Holt et al. 1995).

Models for examining the effects of spatial arrangement of habitat patches on an organism's dynamics were categorized by Fahrig (1988) into three basic types–grid, dispersal-pool and dispersal-corridor models. Grid models were criticized because Fahrig (1988 p.56) felt that it would be "expensive and time-consuming" to examine the wide range of spatial arrangements possible with these models. The rapid growth of cheap fast computer hardware, and the sophistication of simulation software has already reduced this argument considerably. Large grid systems (greater than 100 x 100 cells) can now be simulated quite easily using an IBM compatible Pentium PC and simulation package like MATLAB® (Mathworks 1994). Additionally, faster simulation times are obtained with the model by implementing some of the time-saving strategies that were discussed (i.e., IDEs and Fourier transforms). Spatial movement in an n^2 discrete system can be solved efficiently in one calculation rather than doing n^2 x n^2 individual calculations by using IDEs to couple this process with reproduction and by applying Fourier transforms. In a multi-crop system, the EPM formulation along with a single dispersal kernel can further improve the computational efficiency of the model.

Finally, the need to visualize the spatiotemporal model output was emphasized by Turner et al. (1995), and this problem is not a trivial one due to the shear complexity of the data. In MATLAB® (Mathworks 1994), the spatiotemporal model output of the system can be visualized as a time-varying color-coded density matrix that is simply displayed as an iterative screen image during simulations. In addition, to better visualize these spatial dynamics, spatiotemporal "movies" made during simulation can be played back later at high speed.

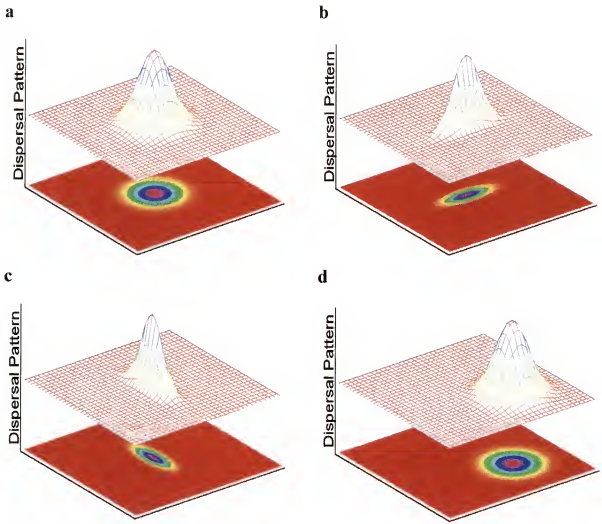

Fig. 2-1. Redistribution kernels generated from two-dimensional normal density functions. (a) symmetric redistribution; (b) and (c), direction-biased redistribution; (d), wind blown redistribution kernel from (a)

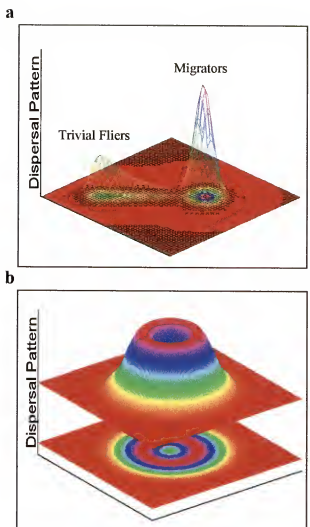

Fig. 2-2. Dispersal patterns for whiteflies. (a) bimodal redistribution showing the dispersal patterns for trivial fliers and migrators (b) a repulsive dispersal pattern or ripple density function.

CHAPTER 3
EQUILIBRIUM, STABILITY AND CHAOS IN DISCRETE-TIME MODELS OF INSECT SPECIES INTERACTIONS

Introduction

Equilibrium and stability are important in many biological systems. Organisms usually attempt to maintain their external and internal environments at or near steady-state or equilibrium levels necessary for their survival. The temperature regulating mechanism for example, restricts the animal's body temperature within some optimum temperature range required for many physiological processes. Operating within the realm of unique equilibrium states therefore is extremely important for the system's continued existence.

Not all steady-state conditions are necessarily good for a system. Death for example, is one steady-state from which it is impossible for organisms to recover, and is not unlike zero population or extinction for a species. Such zero equilibrium states are considered uninteresting or trivial in dynamical studies. Greater emphasis is placed on nonzero equilibrium since knowledge of factors that could drive a system to and away from these conditions is important in gaining complete understanding of the system's behavior.

Although disputed, it is the belief of some that the size of most natural populations generally remains constant through time or fluctuates around some equilibrium state or average level of abundance (Maynard Smith 1968, Hassell & Waage 1984). If this is true,

then it is the stability of these equilibrium states that determines this. Steady-states can either be stable (if neighboring states are attracted to them) or unstable (if neighboring states are not attracted to them) (Edelstein-Keshet 1988). Steady-state stability however does not necessarily imply population stability, and this distinction must be made. The stability of steady-states (mathematical stability) pertains to the ability of a system to return to its steady-states after being perturbed. Population stability (dynamical stability or persistence) on the other hand reflects on the ability of a system to persist. A system can have unstable steady-states but under certain conditions is able to persist.

Mathematical stability and persistence over time and space have been the focus of investigation by theoretical and experimental ecologists particularly those interested in the dynamics of interacting species (Hassell & May 1973, Allen 1975, Hassell et al. 1991, Alder 1993, Dennis et al. 1995). It has been argued for instance that isolated host-natural enemy systems that are locally unstable cannot always be stabilized by coupling identical populations since these essentially acted like a single-patch system (Allen 1975, Reeve 1988,1990). In fact, such couplings through dispersal have been shown to have either no effect or a detrimental effect on population stability (Reeve 1990). For persistence it was suggested that asynchrony among subpopulations in the system needed to be maintained in a manner that could buffer external perturbations. Mechanisms have been proposed for maintaining asynchrony and these included the creation of temporal and spatial heterogeneity in the system (Taylor 1988). Spatial heterogeneity however is not a prerequisite for persistence as was clearly demonstrated by Hassell et al. (1991) and Comins et al. (1992).

The discussion above focused on stability and persistence in systems of insect species interaction where spatial movement was carried out with local coupling rules such as queen's move. This chapter carries the discussion further. First, equilibrium, stability, and persistence in discrete systems are re-examined and the criteria for stability of the steady-states for some systems are presented. Next, the effects of dispersal on stability and persistence in integrodifference equation (IDE) systems are developed and discussed. In this discussion, the Jury conditions for stability in these systems are restated and is newly developed for one particular system. The dynamics of species interaction in system that use IDEs are then compared with those that use more traditional types of local coupling procedures to model dispersal. To this end, dynamical studies are conducted on two-dimensional systems to highlight the range of dynamics possible with IDE systems.

Equilibrium and Stability in Nonspatial Discrete-Time Systems

Single Species First-Order Difference Equations

A first-order discrete-time population system can in general be represented by

$$Y_{t+1} = f(Y_t) \tag{3.1}$$

Equilibrium in eqn (3.1) requires that no change occurs in the population during the time period t and $t+1$, so that

$$Y_{t+1} = Y_t = \hat{Y} = f(\hat{Y})$$

where (3.2)

$$\hat{Y} = \textit{steady-state (equilibrium) population}$$

Stability of the steady-state can be assessed by considering a small perturbation (y_t) close to $\hat{Y}$, and determining if this quantity moves towards or away from $\hat{Y}$. That is, it is important to consider whether y_t gets bigger or smaller. To do this, the system is linearized about its steady-state by approximating the value of the perturbed population $f(\hat{Y} + y_t)$ using Taylor series expansion (Edelstein-Keshet 1988). The linearization precess leads to the following expansion,

$$Y_{t+1} = f(\hat{Y}) + \left(\frac{df}{dY}\bigg|_{\hat{Y}} \right) Y_t - \hat{Y} + (\textit{very small terms})$$

or

$$Y_{t+1} = \hat{Y} + \left(\frac{df}{dY}\bigg|_{\hat{Y}} \right) Y_t - \hat{Y} \tag{3.3}$$

so that

$$Y_{t+1} - \hat{Y} = \left(\frac{df}{dY}\bigg|_{\hat{Y}} \right) Y_t - \hat{Y}$$

Letting $\hat{y}_t = Y_t - \hat{Y}$, eqn (3.3) can be rewritten as

$$\tilde{y}_{t+1} = \left(\frac{df}{dY}\bigg|_{\hat{Y}} \right) \tilde{y}_t$$

$$or$$

$$\tilde{y}_{t+1} = \lambda \tilde{y}_t \qquad (3.4)$$

$$where \quad \lambda = \left(\frac{df}{dY}\bigg|_{\hat{Y}} \right)$$

The necessary and sufficient condition for $\hat{Y}$ to be a stable steady-state of this system is that the modulus or absolute value of λ be less than one ($|\lambda| < 1$) which would indicate that the solution in eqn (3.4) (the deviation from equilibrium with time) is becoming smaller.

Systems of Two and Three First-Order Difference Equations

In discrete time, two interacting populations may be related in some nonlinear manner by a system of two first-order difference equations such as

$$\begin{aligned} Y_{t+1} &= f(Y_t, Z_t) \\ Z_{t+1} &= g(Y_t, Z_t) \end{aligned} \qquad (3.5)$$

with the steady-state values given by

$$\begin{aligned} Y_{t+1} &= \hat{Y} = f(\hat{Y}, \hat{Z}) \\ Z_{t+1} &= \hat{Z} = g(\hat{Y}, \hat{Z}) \end{aligned} \qquad (3.6)$$

Again, if small perturbations $(\tilde{y}_t, \tilde{z}_t)$ from the steady states are considered, the Taylor series expansion results in

$$\begin{aligned} Y_{t+1} &= \hat{Y} + \left(\frac{\partial f}{\partial Y}\bigg|_{\hat{Y},\hat{Z}}\right) Y_t - \hat{Y} + \left(\frac{\partial f}{\partial Z}\bigg|_{\hat{Y},\hat{Z}}\right) Z_t - \hat{Z} + \cdots \\ Z_{t+1} &= \hat{Z} + \left(\frac{\partial g}{\partial Y}\bigg|_{\hat{Y},\hat{Z}}\right) Y_t - \hat{Y} + \left(\frac{\partial g}{\partial Z}\bigg|_{\hat{Y},\hat{Z}}\right) Z_t - \hat{Z} + \cdots \end{aligned} \tag{3.7}$$

Eqn (3.7) can be rewritten to correspond to eqn (3.4), and therefore

$$\begin{aligned} \tilde{y}_{t+1} &= a_{11}\tilde{y}_t + a_{12}\tilde{z}_t \\ \tilde{z}_{t+1} &= a_{21}\tilde{y}_t + a_{22}\tilde{z}_t \end{aligned} \tag{3.8}$$

where

$$\begin{aligned} a_{11} &= \left(\frac{\partial f}{\partial Y}\bigg|_{\hat{Y},\hat{Z}}\right), \qquad a_{12} = \left(\frac{\partial f}{\partial Z}\bigg|_{\hat{Y},\hat{Z}}\right) \\ a_{21} &= \left(\frac{\partial g}{\partial Y}\bigg|_{\hat{Y},\hat{Z}}\right), \qquad a_{22} = \left(\frac{\partial g}{\partial Z}\bigg|_{\hat{Y},\hat{Z}}\right) \end{aligned} \tag{3.9}$$

The connection between eqns (3.8) and (3.9), and eqn (3.4) becomes clearer by using matrix notation, i.e.,

$$\begin{aligned} &\tilde{v}_{t+1} = \boldsymbol{A}\,\tilde{v}_t \\ &\textit{and} \\ &\boldsymbol{A} = \begin{pmatrix} a_{11} & a_{12} \\ a_{21} & a_{22} \end{pmatrix}, \quad \tilde{v}_t = \begin{pmatrix} \tilde{y}_t \\ \tilde{z}_t \end{pmatrix} \end{aligned} \tag{3.10}$$

A is the Jacobian or community matrix of the system. The characteristic equation of **A** can be derived by setting **det(A** - λ**I)** = 0, where **det** is the determinant, **I** is an identity matrix, and λ_n the roots or eigenvalues of **A**. For an *n*th-order system there are *n* roots. The characteristic equation for the system in eqn (3.5) turns out to be

$$
\begin{aligned}
&C(\lambda) = \lambda^2 - \beta\lambda + \gamma = 0 \\
&\textit{where} \\
&\qquad \beta = a_{11} + a_{22} \qquad (\textit{trace of } A) \\
&\qquad \gamma = a_{11}a_{22} - a_{12}a_{21} \qquad (\textit{determinant of } A)
\end{aligned}
\tag{3.11}
$$

Again, the necessary and sufficient condition for stability are for the roots of C(λ) to be of modulus less than unity or to lie inside the unit circle.

In second- and third-order systems, explicit computation of the eigenvalues are not always required since one may employ the criteria of Schur-Cohen that have been simplified and restated by May (1974). For a second-order system it is only necessary (and sufficient) that

$$2 > 1 + \gamma > |\beta| \tag{3.12}$$

for the roots of the system to lie within the unit circle. As an example, consider the Nicholson-Bailey (NB) model used as the basis for the spatiotemporal model described in eqn (2.12). For convenience, this model is restated here as

$$
\begin{aligned}
Y_{t+1} &= rY_t \exp(-aZ_t) \\
Z_{t+1} &= cY_t(1 - \exp(-aZ_t))
\end{aligned}
\tag{3.13}
$$

The stability of the steady-states in eqn (3.13) was determined using the symbolic mathematical software, Maple V (Waterloo Maple Inc., Canada), and is presented in Appendix (1.1a). Examination of the non-zero equilibrium reveal that r cannot be one since this would lead to the equilibrium states $\dot{Y} = \dot{Z} = 0$. In fact, to satisfy the stability conditions given in eqn (3.12), $1 > r > 1$, which is clearly impossible. The steady-states in this model are therefore never stable. Small deviations of any species from equilibrium leads to diverging oscillations in the system.

Similar rules have been discussed by May (1974) for third-order systems having characteristic equations,

$$\lambda^3 + a\lambda^2 + b\lambda + c \qquad (3.14).$$

The necessary and sufficient conditions for $|\lambda| < 1$ in these systems are

$$1 - c^2 > |ac - b| \quad and \quad |1 + b| > |a + c| \qquad (3.15).$$

Systems of Order Greater than Three

Determination of stability of steady-states in systems of order greater than three is slightly more involved than has been described for lower-order systems. Like lower-order systems however, stability in higher-order systems depends on whether or not the roots of the characteristic equation of the system lie inside the unit circle.

The characteristic equation for any linear system is generally given as

$$C(\lambda_n) = \sum_{k=0}^{n} a_k \lambda^k, \quad a_n > 0 \qquad (3.16).$$

Thus, the characteristic equations for a second- and third-order systems already discussed may be rewritten

$$C(\lambda_2) = a_2\lambda^2 + a_1\lambda + a_0, \quad a_2>0 \qquad (a)$$
$$C(\lambda_3) = a_3\lambda^3 + a_2\lambda^2 + a_1\lambda + a_0, \quad a_3>0 \qquad (b) \qquad (3.17).$$

Similarities between eqn (3.11) and eqn (3.17a) are clear. In eqn (3.11), $a_2 = 1$, $a_1 = -\beta$, and $a_0 = \gamma$.

Several methods are available for determining whether the roots of $C(\lambda_n)$ for higher-order systems lie inside the unit circle (the necessary and sufficient condition for stablity). Two of the more common and related approches that are frequently referred to as the *Jury Tests* (Jury 1964, 1971, 1974) are the *Inners* or *Determinant* approach and the *Table* approach. In the *Inners* approach, successive simple matrices are constructed from the coefficients of $C(\lambda_n)$, and the determinants of these matrices evaluated. In the *Table* approach, a simple table of the coefficients of $C(\lambda_n)$ is constructed, and the relative magnitudes of the entries in this table evaluated. Only the *Inners* approach is described here since this approach will be used throughout the remainder of this study for determining the stability of steady-states. Much broader treatment with examples using both approaches are given in Jury (1964, 1971, 1974), Lewis (1977) and Edelstein-Keshet (1988).

To demonstrate the use of this approach, a fourth-order system is considered. The characteristic equation for this system is the fourth-degree polynomial,

$$C(\lambda_4) = a_4\lambda^4 + a_3\lambda^3 + a_2\lambda^2 + a_1\lambda + a_0, \quad a_4>0 \tag{3.18}$$

The first step in developing the criteria for stability of steady-states for this system is to construct two matrices ($\mathbf{W_n}$, a right upper triangular, and $\mathbf{X_n}$, a left upper triangular) from the coefficients in $C(\lambda_n)$. For the system in eqn (3.18) these matrices are

$$W_n = \begin{bmatrix} a_4 & a_3 & a_2 & a_1 & a_0 \\ 0 & a_4 & a_3 & a_2 & a_1 \\ 0 & 0 & a_4 & a_3 & a_2 \\ 0 & 0 & 0 & a_4 & a_3 \\ 0 & 0 & 0 & 0 & a_4 \end{bmatrix}, \qquad X_n = \begin{bmatrix} a_4 & a_3 & a_2 & a_1 & a_0 \\ a_3 & a_2 & a_1 & a_0 & 0 \\ a_2 & a_1 & a_0 & 0 & 0 \\ a_1 & a_0 & 0 & 0 & 0 \\ a_0 & 0 & 0 & 0 & 0 \end{bmatrix} \tag{3.19}$$

Next, two matrices based on ($\mathbf{W_n} \pm \mathbf{X_n}$) are constructed. For convenience, these are presented here as a single matrix,

$$W_n \pm X_n = \begin{bmatrix} a_4 \pm a_4 & a_3 \pm a_3 & a_2 \pm a_2 & a_1 \pm a_1 & a_0 \pm a_0 \\ \pm a_3 & a_4 \pm a_2 & a_3 \pm a_1 & a_2 \pm a_0 & a_1 \pm \\ \pm a_2 & \pm a_1 & a_4 \pm a_0 & a_3 \pm & a_2 \pm \\ \pm a_1 & \pm a_0 & 0 & a_4 \pm & a_3 \pm \\ \pm a_0 & 0 & 0 & 0 & a_4 \pm \end{bmatrix} \tag{3.20}$$

Properties of the determinants of the inners of ($\mathbf{W_n} \pm \mathbf{X_n}$) determine the stability of the steady-states in this system. For *n*-even matrices, the number of inners is $n/2$ so that from eqn (3.20) both the 'positive' and 'negative' matrices contain two inners. These are

designated $\mathbf{I}_k$ with $k = 1,3,5,\ldots, n\text{-}1$ being the dimension of successive inners. In the above case the inners are

$$I^{\pm}_{k=1} = \left[\, a_4 \pm a_0 \,\right], \qquad I^{\pm}_{k=3} = \begin{bmatrix} a_4 \pm a_2 & a_3 \pm a_1 & a_2 \pm a_0 \\ \pm a_1 & a_4 \pm a_0 & a_3 \pm \\ \pm a_0 & 0 & a_4 \pm \end{bmatrix} \tag{3.21}$$

The number of inners in n-odd systems larger than or equal to three is $(n - 1)/2$ with $k = 2,4,6,\ldots, n\text{-}1$. The necessary and sufficient conditions for the roots of the characteristic equation $C(\lambda_n)$ to lie inside the unit circle therefore depend on whether the system is n-even or n-odd. These conditions are summarized from Jury (1974) and are

$$\begin{aligned} &n\text{-}even \\ &\qquad C(1) > 0, \quad C(-1) > 0 \\ &\qquad \det(W_k \pm X_k) \text{ are positive innerwise}, \quad k = 1,3,5,\ldots,n-1 \\ &n\text{-}odd \\ &\qquad C(1) > 0, \quad C(-1) < 0 \\ &\qquad \det(W_k \pm X_k) \text{ are positive innerwise}, \quad k = 2,4,6,\ldots,n-1 \end{aligned} \tag{3.22}$$

A matrix is positive innerwise if the determinants of all its inners as well as of the matrix itself are positive. Complete analysis on the stability for the system in eqn (3.18) is given in Appendix (1.2). Specifically, the necessary and sufficient conditions for the roots of this system to lie inside the unit circle are

$$
\begin{aligned}
&a_4 + a_3 + a_2 + a_1 + a_0 > 0 \\
&a_4 - a_3 + a_2 - a_1 + a_0 > 0 \\
&a_4 + a_0 > 0 \\
&a_4 - a_0 > 0 \\
&a_4^3 + a_0 a_4^2 + a_2 a_4^2 - a_1 a_4 a_3 - a_1^2 a_4 + a_0 a_3^2 + a_0 a_3 a_1 \cdots \\
&\qquad - a_2 a_0^2 - a_0^2 a_4 - a_0^3 > 0 \\
&a_4^3 - a_0 a_4^2 - a_2 a_4^2 + 2a_4 a_2 a_0 + a_1 a_4 a_3 - a_1^2 a_4 - a_0 a_3^2 \cdots \\
&\qquad + a_0 a_3 a_1 - a_2 a_0^2 - a_0^2 a_4 + a_0^3 > 0
\end{aligned}
\tag{3.23}
$$

Two worked examples are also given (Appendix 1.3a,b) using the *Inners* approach on systems having fourth-degree polynomials,

$$
\begin{aligned}
C(\lambda_4) &= \lambda^4 - \lambda^3 + 9\lambda^2 - 7\lambda + 2 \qquad (a) \\
C(\lambda_4) &= \lambda^4 + 0.8\lambda^3 + 0.55\lambda^2 + 0.4\lambda + 0.12 \qquad (b)
\end{aligned}
\tag{3.24}
$$

to demonstrate this approach on an unstable (eqn 3.24a) and stable (eqn 3.24b) system. It may be noted that it is not always necessary to apply the *Inners* method in attempting to evaluate the stability of systems of this type. The coefficients in eqn (3.24a,b) were deliberately chosen to indicate the ease with which stability of some systems may be determined by simply examining the relative magnitudes of the coefficients in the characteristic equation. If the coefficients satisfy the conditions that

$$
a_n > a_{n-1} > a_{n-2} > a_{n-3} \cdots a_1 > a_0 > 0 \tag{3.25}
$$

then all the roots of this system lie within the unit circle, and the system is stable (Jury, 1964). Since in eqn (3.24b) $1 > 0.8 > 0.55 > 0.4 > 0.12 > 0$, the steady-states for this system are determined to be stable without resorting to the *Inners* test. Note however that these are sufficient but not necessary conditions for stability since in cases where eqn (3.25) does not hold, the steady-states of a system may still be stable.

A connection can now be made between the criteria for stability in a second-order system stated in eqn (3.12) and the criteria established by the *Inners* approach for the same system. The stability criteria established by the *Inners* approach for a second-order system are

$$\begin{aligned} &C(1) > 0, \quad C(-1) > 0 \\ &a_0 - a_2 < 0 \end{aligned} \tag{3.26}$$

The criterion $a_0 - a_2 < 0$ is equivalent to $(2 > 1 + \gamma)$ in eqn (3.12) where $a_2 = 1$ and $a_0 = \gamma$. The criteria given in eqn (3.26) can also be stated directly in terms of the determinant and trace of the Jacobian as was done by Kot (1989) and Neubert et al. (1995), i.e.,

$$\begin{aligned} 1 - trA + \det A > 0, \\ 1 + trA + \det A > 0, \\ 1 - \det A > 0 \end{aligned} \tag{3.27}$$

where **tr** is the trace of the Jacobian **A,** and **det** the determinant.

Nonspatial Age-Structured Systems of Interacting Species

A nonspatial form of the age-structured prey-natural enemy model described in eqn (2.12) is now considered, and the stability of its steady states determined using the *Inners* approach just described. The characteristic equation for this system is a sixth-degree polynomial, and therefore the stability criteria for a general sixth-order system were first derived and are presented in Appendix (1.4). Although the criteria are rather long and messy, considerable reduction can take place after substituting actual values for the coefficients.

Attempts to obtain closed-form equilibrium solutions for a non-spatial version of the model in eqn (2.12) proved difficult since the solutions were rather awkward and quite difficult to interpret. This was not surprising because of the strong nonlinearities in the system introduced through the reproductive and predation survival functions. To obtain a complete analytical description for equilibrium and stability for this type of system, simplification by removal of some nonlinearities was necessary. After some manipulation, the simplest non-spatial model that retained many of the original ideas in the non-spatial form of the model in eqn (2.12) was

$$\begin{aligned} Y1_{t+1} &= rY3_t \\ Y2_{t+1} &= S_{Y1}Y1_t \\ Y3_{t+1} &= S_{Y2}Y2_t \exp(-aZ3_t) \\ Z1_{t+1} &= Y2_t\,(1-\exp(-aZ3_t)) \\ Z2_{t+1} &= S_{Z1}Z1_t \\ Z3_{t+1} &= S_{Z2}Z2_t \end{aligned} \tag{3.28}$$

In this simplified system, an exponential or geometric reproductive function replaces the density-dependent Ricker type function from eqn (2.12), and survival and development are given by a single parameter, *S*. Exponential population growth is not an unreasonable starting assumption for insects such as whiteflies that have been known to exhibit this type of growth under certain field conditions (Zalom et al. 1985). Closer examination would indicate that eqn (3.28) is simply a non-spatial age-structured form of the Nicholson-Bailey model in eqn (3.13).

Analysis of the model in eqn (3.28), showed that the system possessed several closed-form non-negative equilibrium solutions and had a characteristic polynomial,

$$\lambda^6 + \frac{\left(1 + \ln\left(\frac{1}{r S_{Y1} S_{Y2}}\right) - r S_{Y1} S_{Y2}\right)}{r S_{Y1} S_{Y2} - 1} \lambda^3 - \frac{\ln\left(\frac{1}{r S_{Y1} S_{Y2}}\right) r S_{Y1} S_{Y2}}{r S_{Y1} S_{Y2} - 1} \qquad (3.29)$$

(see Appendix 1.5a,b). Several things were immediately clear from these analyses. The combined parameters ($r\, S_{Y1}\, S_{Y2}$) cannot be less than or equal to 1 since this would result in zero or negative equilibrium states (Appendix 1.5). This is not unlike the non age-structured NB model where stability depends on the prey's reproductive capacity, *r*. Also, if the stability criteria stated in eqn (3.25) are applied to eqn (3.29), then it is strongly suspected that the steady-states of this system will be unstable. Since ($r\, S_{Y1}\, S_{Y2}$) had to be greater than 1, and S_{Y1} and S_{Y2} between 0 and 1, these limits were used in evaluating the stablity of the system using the *Inners* criteria. Based on this, the steady-states in this system were determined to be unstable.

Instability of steady-states were also confirmed by substituting actual values for r, S_{Y1}, and S_{Y2}, and other parameters in the model. If Y in eqn (3.28) is assumed to be the greenhouse whitefly, *Trialeurodes vaporariorum*, and Z one of its natural enemies, say, *Encarsia formosa*, then parameter values obtained from the literature for these insects on tomato could be incorporated into eqn (3.28) and the stability of steady-states determined based on these parameters. These insects were chosen because biological parameters on both species could conveniently be obtained from a single source (i.e. van Roermund & van Lenteren 1992). Table 3-1 gives parameter values used in the system in eqn (3.28) for these two insects. Stability analysis on the model with these values indicated that the system is unstable. Inclusion of age-structure in the basic Nicholson-Bailey model therefore does not seem to affect the stability of the steady-states of that system.

Stabilizing an Unstable System: Model Modification

The NB model in eqn (3.13) is both mathematically and dynamically unstable since populations never return to their steady-states after even the slightest perturbation. The result is always diverging oscillations in the populations and eventual extinctions. Several modifications have been made to this model that improve the stablity of its steady-states. If the environment can only support a limited density of prey (or has a specific carrying capacity, k), then in the absence of natural enemies, prey population growth will be restricted. Environmental carrying capacity can be included by replacing the exponential growth function with a Ricker type function (Beddington et al. 1975). The difference

equations that now describe the changes in prey and natural enemy densities from one generation to the next are then

$$\begin{aligned} Y_{t+1} &= Y_t \exp\left(r\left(1 - \frac{Y_t}{k}\right) - aZ_t\right) \\ Z_{t+1} &= cY_t(1 - \exp(-aZ_t)) \end{aligned} \tag{3.30}$$

Beddington et al. (1975) performed a local stability analysis on this model and found that stability could be characterized in terms of r, and also by $q = \hat{Y}/k$. The parameter q measures the extent to which the natural enemy depresses the density of the host below k; low values reflect high natural enemy efficiency.

Stability can also be improved by directly adjusting the searching efficiency of the parasitoid (a) to account for large natural enemy populations. Since a is constant in the NB model, there is no compensation for large natural enemy densities although it has been shown that efficiency tends to generally decrease as the natural enemy population becomes very large (Hassell & Varley 1969). The model described by Hassell and Varley (1969) to account for the variation in a with increasing natural enemy numbers is

$$\begin{aligned} Y_{t+1} &= rY_t \exp(-(QZ_t^{1-m}) \\ Z_{t+1} &= cY_t(1 - \exp(-(QZ_t^{1-m}) \end{aligned} \tag{3.31}$$

where $Q = aZ^m$ is the "quest" constant and m, the "mutual interference" constant that relate to the natural enemy. By creating a situation where there is mutual interference among natural enemies at high density, stability can be achieved. Steady-states are

however only stable for $0 < m < 1$ for as $m \to 0$, the model in eqn (3.31) approaches the NB model. These stabilizing influences should also apply to the non-spatial age structured model.

Equilibrium, Persistence and Dynamics in Spatial Systems

In the Nicholson-Bailey system species interaction occurs at a single location. In defense of the model's instability, Nicholson pointed out that populations in nature generally existed in spatially defined areas each of which is unstable enough to lead to extinction. However, not all subpopulations were likely to become extinct at the same time, and the whole system would then persist because of spatial linkages. Spatial movement of individuals between patches was therefore considered important for maintaining the whole system.

What effect therefore is dispersal likely to have on steady-state stability in systems of species interaction? This question was examined using the familiar but unstable NB model given in eqn (3.13), and a model developed by Kot (1989) that is stable within certain parameter ranges. Kot's model is similar to the NB and is simply,

$$\begin{aligned} Y_{t+1} &= Y_t \exp(r(1 - Y_t - Z_t)) \\ Z_{t+1} &= c Y_t Z_t \end{aligned} \tag{3.32}$$

The steady-states of this model are asymptotically stable for

$$1 < c < 2$$
$$0 < r < \frac{4c}{3 - c} \qquad (3.33)$$

Stability of the steady-states in spatial and non-spatial versions of these models were explored.

Mathematical stability in the NB model has already been explored (Appendix 1.1a). Assuming now that the populations in this model occupy infinite one-dimensional continuous space, then the model in integrodifference (IDE) form becomes

$$\begin{aligned} Y_{t+1}(l) &= \int_{-\infty}^{+\infty} K_Y(l-x)\, rY_t(x) \exp(-aZ_t(x))dx \\ Z_{t+1}(l) &= \int_{-\infty}^{+\infty} K_Z(l-x)\, cY_t(x)(1-\exp(-aZ_t(x)))dx \end{aligned} \qquad (3.34)$$

Kot and Schaffer (1986), Kot (1989) and Neubert et al. (1995) showed that for systems like that in eqn (3.34), stability criteria similar to those given in eqn (3.27) for the non-spatial model can be applied if Fourier transformed perturbations are considered. The criteria for stability in this one dimensional second-order spatial model are

$$\begin{aligned} 1 - tr(\boldsymbol{KA}) + \det(\boldsymbol{KA}) > 0 \qquad & (a) \\ 1 + tr(\boldsymbol{KA}) + \det(\boldsymbol{KA}) > 0 \qquad & (b) \\ 1 - \det(\boldsymbol{KA}) > 0 \qquad & (c) \end{aligned} \qquad (3.35)$$

where **A** is the Jacobian of the non-spatial model, while **K** is

$$\boldsymbol{K} = \begin{bmatrix} k_y(\omega) & 0 \\ 0 & k_z(\omega) \end{bmatrix}$$

with (3.36)

$$k_{y(or\ z)}(\omega) = \int_{-\infty}^{+\infty} k_{y(or\ z)}(x)\, e^{-j\omega x} dx \ , \qquad 0 \le k_y(\omega), k_z(\omega) \le 1$$

the Fourier transforms of the dispersal kernels K_Y and K_Z from eqn (3.34), respectively. Stability analyses of this system are given in Appendix (1.1b). The characteristic equation is similar in form to that of the model without dispersal. The Jury criterion in eqn (3.35c), is violated however since

$$\lim_{r \to \infty} \ 1 - \frac{e^{(-\omega^2)} \ln(r) r}{(r - 1)} < 0 \tag{3.37}$$

and therefore the steady-states of the spatial 1-D model are still unstable. Therefore with equal prey and predator dispersal the unstable NB model is still unstable. It has been shown elsewhere that adding equal prey and predator dispersals does not affect the stability of previously stable steady-states. However, stability of stable systems can be affected by having unequal prey and predator dispersals. These ideas were tested with the Kot model. Analysis of this model is given in Appendix (1.6). Steady-state stability was maintained in one- and two-dimensional systems where prey and predator dispersals were the same. However, when predator dispersal was greater (in either one- or two-dimensional space), some of the Jury conditions were violated and the steady-states became unstable. Predator overdispersal in stable systems often results in what has been

called *diffusive instability* (Segel & Jackson 1972, Kot 1989, Neubert et al. 1995), where the predator disperses so rapidly that its stabilizing influence on the prey is lost. This type of dynamics is common in continuous-time diffusion system but is now also known to occur in discrete systems.

Dynamics of Interacting Species in 2-D Systems

The use of IDE models to study the dynamics of interacting species in two-dimensional habitats is lacking. Therefore studies were undertaken using an IDE Nicholson-Bailey (1935) model to compare the dynamics with traditional spatial NB models with local coupling procedures such as queen's moves. The effects of dispersal on the dynamics in this model have been widely studied and thus provide a good basis for comparsion. The model with no age-structure was chosen in favor of the age-structured model because of the much simplier parameter space. Also preliminary studies indicated that under comparable conditions, the overall dynamics in both models were similar although the period of oscillations in the age-structured model tended to be less. This resulted mainly because of the trickling of individuals through the age classes which according to Oster (1978 p. 436) causes a shift in the prey and predator waves and forces the predator "to live off the tails of the host wave".

Study 1: Spatially Varying Initial Populations: Homogeneous System

In this first study, a two-dimensional IDE form of the NB system in eqn. 3.30 was simulated on a 64 x 64 spatial grid with each cell seeded with random numbers of prey and natural enemy. Parameters ($r = 2.0$, $a = 0.5$) were held spatially constant and identical for

all locations in the system, and the dispersal kernel for both species was Gaussian with an initial standard deviation (SD) of dispersal of one grid cell. Results for this study are not shown since for all simulations, one (usually the predator) or both populations went extinct. These results were insensitive to the extent of dispersal of both species. Starting therefore with spatially random varying initial populations and spatially invariant parameters did not lead to persistence in this unstable model probably because the whole system acted like a single location under these conditions. The qualitative dynamics are therefore no different to those of an isolated single population.

Study 2: Initial Populations at a Single Location: Homogeneous system

A single cell in a 64 x 64 grid was randomly chosen and random numbers of prey and natural enemy individuals placed into this cell. All other cells on the grid were empty. The same cell (row 43, column 28) and population assignment were used in all simulations although other combinations were also tested. Parameters were assigned to all locations and were identical to those in Study 1. The dispersal kernels were also Gaussian with SD of dispersal measured in grid cells. Some very interesting dynamics were observed and these depended mainly on the relationship between prey and predator dispersal. When predator extinctions occurred, these appeared to depend strongly on the relationship between initial cell seeded and the SD of dispersal. As the SDs were increased the choice of initial cell became more critical.

The most interesting patterns observed were *spiral waves* of predator chasing prey (Fig. 3-1a). These patterns usually arose when the SD of dispersal in the kernels were the same for both species and equal to 1 grid cell, and parameters were spatially invariant.

For equal SD of the dispersal kernels greater than 1 grid cell, the spiral waves disappeared and persistence of the interaction depended mainly on the choice of initial location and species density in that cell. Also when the SD of the dispersal kernels were 1 grid cell for both species but either *a* or *r* varied spatially, the spiral waves again disappeared although the interaction persisted.

When prey dispersal was greater than that of the predator, the predator population usually went extinct. For greater SD of predator dispersal (predator overdispersal) however the spiral waves disappeared and the dynamics were primarily determined by the extent of overdispersal. Very high levels of predator overdispersal caused the predator population to go extinct, while for moderate to low levels of overdispersal, the system persisted but no underlying patterns could be distinguished by looking at the color-coded density maps (Figs. 3-2, 3-3).

Clues to a description of these patterns were obtained by observing the Lyapunov exponents (Lichtenberg & Lieberman 1992 ch. 5). Positive Lyapunov exponents indicate the presence of chaos, and for greater predator overdispersal this exponent was "more positive" (Figs, 3.1d, 3.2d, 3.3d). Generally, the greater the disparity between prey and predator dispersals in favor of the predator, the more chaotic were the dynamics. These dynamical patterns (Figs. 3-2 and 3.3) are indicative of *spatiotemporal chaos* (Hassell et al. 1991,Comins et al. 1992, Pearson 1993, Cross & Hohenberg 1994, Braiman et al 1995, Dennin et al. 1996). Notice that the dynamics underlying the apparently regular spiral wave patterns are also chaotic since the Lyapunov exponents are positive (Fig. 3-1d).

Study 3: Spatially Varying Initial Populations: Heterogeneous System

Environmental heterogeneity may be introduced into the system in a number of ways. Here, it was included by spatially varying the reproductive rate of the prey (r) and/or the searching efficiency of the predator (a). The spiral waves observed in Study 2 disappeared when r or a were varied spatially and all other conditions were the same.

When the initial populations of prey and predator, and also r were spatially varying, the system persisted unlike in the case with the homogeneous environment (Study 1). The types of dynamics observed were again dependent on the relationship between prey and predator dispersal (Figs. 3.4, 3.5. 3.6, 3.7). Generally however, these dynamics were less chaotic than those in Study 2, as indicated by the Lyapunov exponents near zero (Figs 3.4d & 3.5d). Where there was predator overdispersal, the dynamics became increasingly *quasi-periodic* (Oster 1978, Bergé et al. 1984) and the Lyapunov exponents dropped to zero (Figs. 3.6c,d & 3.7c,d).

Study 4: Prey Refuge

Prey refuges in the environment was simulated by excluding the predator from some locations through manipulation of its searching efficiency (a). The value of the predator's searching efficiency at any location in the grid was determined by having

$$\begin{aligned} \hat{a} &= \bar{a} * ((1 + \Delta) * U(0,1) - \Delta) \\ a &= \begin{cases} 0 & \hat{a} < 0 \\ \hat{a} & \hat{a} > 0 \end{cases} \end{aligned} \tag{3.38}$$

Delta (Δ) determines the amount of refuge available to the prey (Fig. 3.8), U(0,1) is a uniform random distribution, and $\bar{a}$ is the average searching efficiency of the predator. Cells in the grid with $a = 0.0$ are host refuge sites. For $\Delta = 0.0$, there are therefore no refuges in the system, while for $\Delta = 1.0$, approximately half of the environment is considered as refuge. The dynamics for the system where $\Delta = 0.0$ (Fig. 3.9) is therefore similar to those in Study 3 where environmental heterogeneity was introduced through spatially varying a values but no refuge was present. As Δ was increased, the color-coded density maps showed little changes during the simulations.. The maps observed after 2000 time steps given in Figs 3.10a, 3.11a, and 3.12a looked exactly like those of the previous 1500 time steps. These conditions generated what are known as *crystal lattices* where the dynamics appear to lock onto a particular pattern. These patterns are generally devoid of spatiotemporal chaos and the only clue as to the underlying dynamics comes again from the phase-plane plots and Lyapunov exponents. Fig. 3.10c for example indicates that when approximately 9-10% of the environment consisted of refuges, an invariant circle was generated and the dynamics were quasi-periodic. On the other hand, as the amount of refuges rose above $\approx$12% (Fig. 3.11 & 3.12), the system approached a stable point, and the Lyapunov exponents were negative.

For convenience, the types of spatial dynamics observed in these studies and that are likely to appear in dynamical systems with species interaction are summarized in Table 3-2.

Discussion

Equilibrium, stability and persistence of interacting species in discrete-time spatial and non-spatial systems were the main focus of this study. Stability of steady-states in systems of different orders were discussed along with the development of stability criteria for specific systems. Little or no work has been done on the stability in systems with polynomials of degree greater than five. May (1974 p. 196) in explaining the Routh-Hurwitz stability criterion for differential systems remarked that "no one in their right mind" would attempt to use that criterion to determine the stability of any system with a characteristic polynomial of degree greater than five. Advances in computer hardware and mathematical software have made it possible to perform stability analysis on systems with sixth-degree polynomials and higher.

Equilibrium and stability conditions in any system are prerequisites for exploring the dynamics of that system. It is clear from the studies undertaken here that systems of interacting species having unstable steady-states cannot be stabilized by adding symmetric dispersals (Allen 1975, Kot 1989, Neubert et al. 1995). Allen (1975 p. 331) concluded that "when the dispersal rates of the host and parasite are identical, stability or instability near equilibrium in the simple time model implies stability or instability in the space-time model ... ." These restrictions seem to apply only to cases where dispersal is symmetric and equal. For unequal dispersal, and in particular, in the case of predator overdispersal, the stability of steady-states in initially stable systems can be altered. Predator overdispersal has been shown to lead to diffusive instability in one-dimensional IDE systems, and is generated under much broader conditions than are possible with

continuous-time diffusive systems (Kot & Schaffer 1986, Kot 1989, Neubert et al. 1995). The loss of stability in one-dimensional IDE systems with predator overdispersal was reconfirmed. In addition, it was shown for the first time that stability in a two-dimensional IDE system is also lost with predator overdispersal.

Although a system may be mathematically unstable, when extended into space and under certain conditions, the interaction can persist. Persistence is enhanced by having asynchrony among subpopulations in the system. Taylor (1988a) proposed three mechanisms for maintaining asynchrony; spatial and temporal heterogeneity among patches, low but nonzero migration rates, and large numbers of patches or subpopulations. Reeve (1990) showed that where there is spatial subdivision and environmental variability, only mathematically stable systems are able to persist at high migration rates, while at low rates both unstable and stable systems persisted. In general Reeve (1990) noted that the persistence of mathematically unstable systems could only be maintained in the presence of environmental variability, spatial subdivision, and species migration.

In many studies that examined the effects of environmental heterogeneity, coupling through dispersal was global rather than local. Hassell et al. (1991) and Comins et al. (1992) however found that persistence of interacting species in homogeneous environments was possible with local or neighborhood dispersal. They pointed out that heterogeneity and density dependence were likely to be less important under local coupling conditions. The dynamical studies in this paper support this view (Figs. 3.1, 3.2, 3.3). What is interesting is that the results appear to be independent of the type of local dispersal model used. Hassell et al. (1991) and Comins et al. (1992) used queen's

(orthogonal and diagonal) local dispersal rule where in each time step movement was to the 8 neighboring cells. Gaussian dispersal kernels and the IDE models maintain the local coupling idea. It is not surprising therefore that they also observed similar dynamical patterns (spiral waves, crystal lattices, chaos) although the conditions under which these appeared were quite different. Hassell et al. (1991) and Comins et al. (1992) also made a distinction between spiral waves and spatiotemporal chaos and made no mention of how chaos was determined. From this study, it appears that the spiral waves are just another type of spatiotemporal chaos based on the positive Lyapunov exponents observed.

There are many ways to include environmental heterogeneity in species interaction systems. These include creation of host refugia (Hassell 1978), biased dispersal between the species (Comins and Blatt 1974), having uncorrelated stochasticity in parameters (Reeve 1988), differences in initial conditions (Alder 1993), and varying the connectivity within the habitat (Molofsky 1994, With & Crist 1995). The effect of initial population on *B. tabaci* dynamics was demonstrated by von Arx et al. (1983) and Baumgärtner et al. (1986) for the whitefly cotton system who observed that whitefly population growth was highly affected by the initial numbers of insects in the field.

All the methods for adding environmental heterogeneity given above result in the creation of prey refuges and therefore studies on the effects of host refuges on system dynamics were conducted. In discussing approaches to biological control of whiteflies Gerling (1992) discussed three forms of refuges. The first is *natural enemy stage preference* refuge where some host stages are invulnerable to attack because of natural enemy preference for other stages. This may not be an important type of refuge for

whiteflies since all stages except adults are usually taken by one natural enemy or another. However, variations in the development between the age-classes of whitefly and some of its natural enemies may create what has been called a temporal niche (Oster 1978), a period where an insect is relatively free from the effects of predation. Powell and Bellows (1992c) observed these effects when they compared a California and an Hawaiian *Eretmocerus* species. The Hawaiian species was more effective at controlling the whitefly because its intrinsic rate of increase was higher than that of the whitefly. *Temporal* refuge, the second type of refuge results from the more rapid establishment of whiteflies in new areas in relation to their natural enemies. A classic example of this is the establishment of the insect in the San Joaquin Valley, California. The SLW was discovered in the southern part of the valley in the summer of 1992, and by fall had spread approximately 100 miles north. The foci of infestation were suspected to be greenhouses, and 1993 surveys found no parasitoids in the valley (Summers pers. comm.). Thirdly, there is *spatial* refuge created because of differences in host plant architecture, climatic characteristics and host density in specific areas. Plant architecture for example is known to limit natural enemy performance as has been shown by the reduced effectiveness of *Encarsia formosa* on Gerbera plants infested with the greenhouse whitefly (van Lenteren pers. comm. cited in Gerling 1992). The results of Study 4 indicate that varying host refugia can have a dramatic effect on the dynamics in predator-prey systems. Refuges create a distinct advantage for the prey and therefore their elimination is essential for maintaining low pest population and enhancing the effects of its natural enemies (Murdoch 1990).

Table 3-1. Parameter values for *Trialeurodes vaporariorum* and *Encarsia formosa* in the simplifed non-spatial age-structured model.

Model Parameters	Mean Parameter Values[a]
r	6.000
S_{Y1}	0.144
S_{Y2}	0.058
a	0.750
S_{Z1}	0.250
S_{Z2}	0.045

[a] per day at an average temperature of 25 °C.

Table 3-2. Spatiotemporal patterns observed in discrete-time coupled systems with species interaction.

Dynamical Patterns		Lyapunov Exponent[a]
Spatial	Temporal	
Uniform	Constant	negative
Crystal Lattice		
Non-Uniform	Constant	negative
Crystal Lattice		
Non-Uniform	Varying	
Periodic		0
Quasi-periodic		0
Chaotic		positive
Spiral Waves		
Spatiotemporal Chaos		positive

[a] A positive Lyapunov exponent indicates chaos.

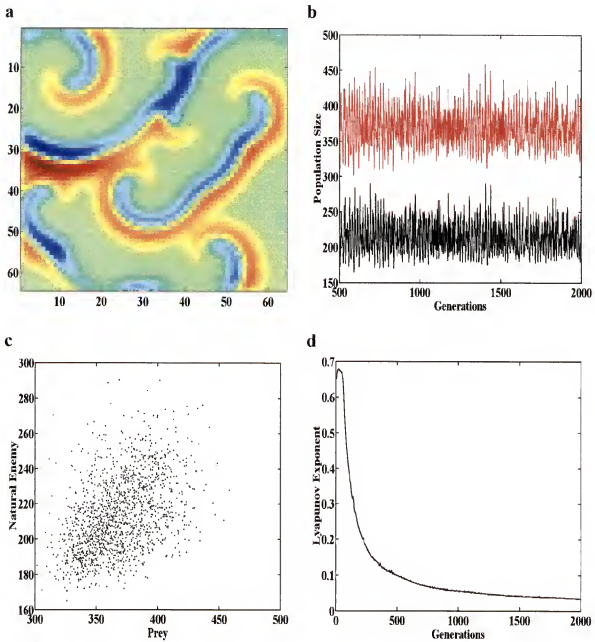

Fig. 3-1. Spatiotemporal dynamics on a 64 x 64 grid with a 2-D integrodifference equation Nicholson-Bailey model. One cell initially seeded and prey and predator dispersal is Gaussian with equal standard deviations (1:1 grid cell); $r = 2.0$, $a = 0.5$. (a) prey and predator interaction--high prey density (red), high predator density (dark-blue); (b) simulation time plot--prey (red), predator (black); (c) phase-plane plot; (d) Lyapunov exponent.

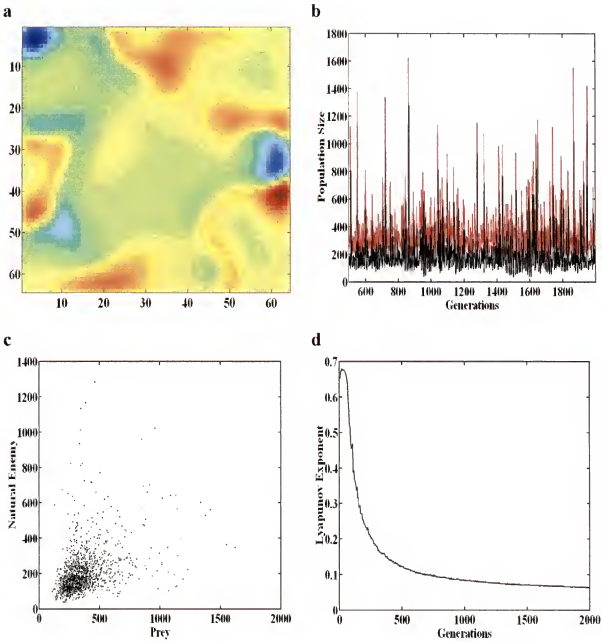

Fig. 3-2. Spatiotemporal dynamics on a 64 x 64 grid with a 2-D integrodifference equation Nicholson-Bailey model. One cell initially seeded, and prey and predator dispersal is Gaussian with the standard deviation of predator dispersal twice that of prey (2:1 grid cells); $r = 2.0$, $a = 0.5$.(a) prey and predator interaction--high prey density (red), high predator density (dark-blue), (b) simulation time plot--prey (red), predator (black), (c) phase-plane plot,; (d) Lyapunov exponent.

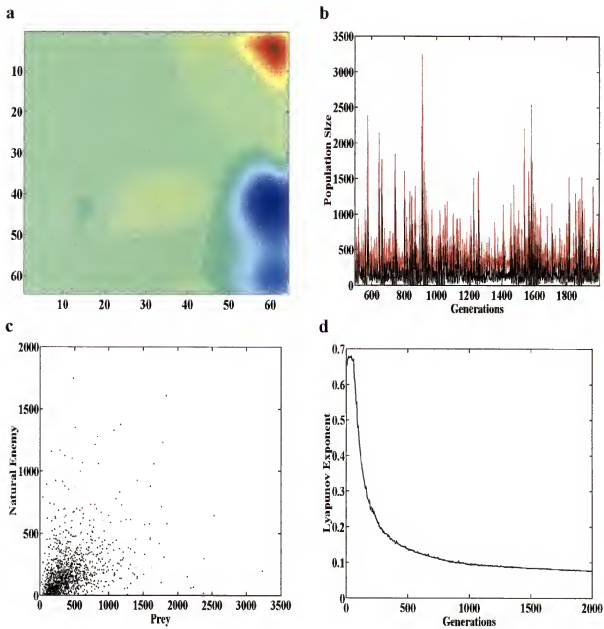

Fig. 3-3. Spatiotemporal dynamics on a 64 x 64 grid with a 2-D integrodifference equation Nicholson-Bailey model. One cell initially seeded, and prey and predator dispersal is Gaussian with the standard deviation of predator dispersal four times that of prey (4:1 grid cells); $r = 2.0$, $a = 0.5$ (a) prey and predator interaction--high prey density (red), high predator density (dark-blue); (b) simulation time plot--prey (red), predator (black); (c) phase-plane plot; (d) Lyapunov exponent.

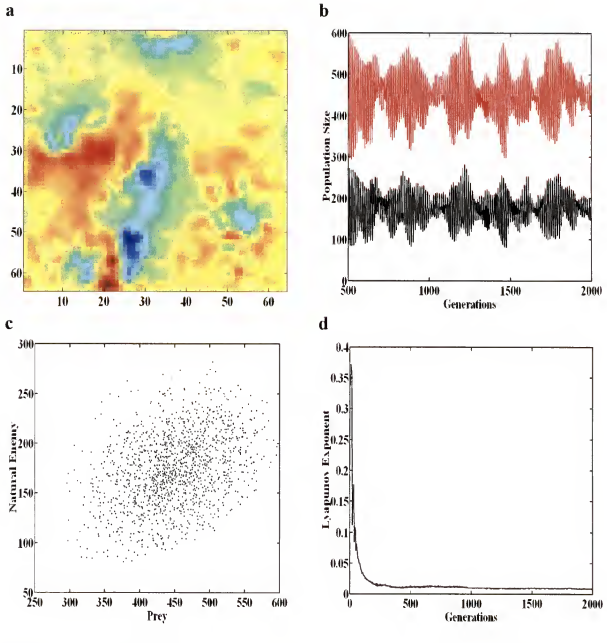

Fig. 3-4. Spatiotemporal dynamics on a 64 x 64 grid with a 2-D integrodifference equation Nicholson-Bailey model. All cells initially seeded, and prey and predator dispersal is Gaussian with equal standard deviations (1:1 grid cell); r varies spatially with Uniform distribution as $1 < r < 2.0$, $a = 0.5$. (a) prey and predator interaction--high prey density (red), high predator density (dark-blue); (b) simulation time plot--prey (red), predator (black); (c) phase-plane plot; (d) Lyapunov exponent.

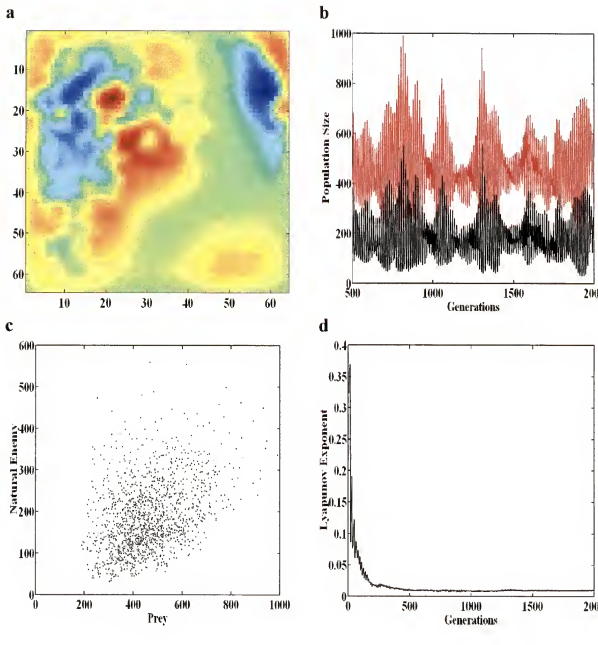

Fig. 3-5. Spatiotemporal dynamics on a 64 x 64 grid with a 2-D integrodifference equation Nicholson-Bailey model. All cells initially seeded, and prey and predator dispersal is Gaussian with the standard deviation of prey dispersal twice that of predator (2:1 grid cells); r varies spatially with Uniform distribution as $1 < r < 2.0$, and $a = 0.5$. (a) prey and predator interaction--high prey density (red), high predator density (dark-blue); (b) simulation time plot--prey (red), predator (black); (c) phase-plane plot; (d) Lyapunov exponent.

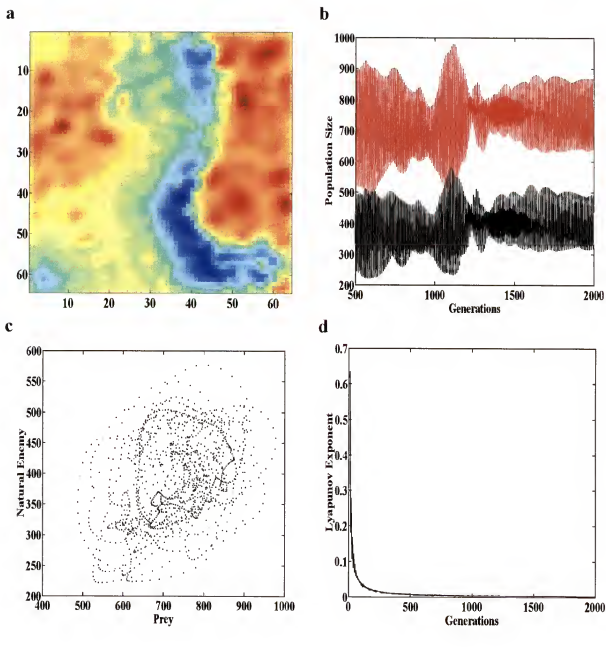

Fig. 3-6. Spatiotemporal dynamics on a 64 x 64 grid with a 2-D integrodifference equation Nicholson-Bailey model. All cells initial seeded, and prey and predator dispersal is Gaussian with the standard deviation of predator dispersal twice that of prey (2:1 grid cells), $r = 2.0$, a varies spatially with Uniform distribution as $0 < a < 0.5$. (a) prey and predator interaction--high prey density (red), high predator density (dark-blue); (b) simulation time plot--prey (red), predator (black); (c) phase-plane plot; (d) Lyapunov exponent.

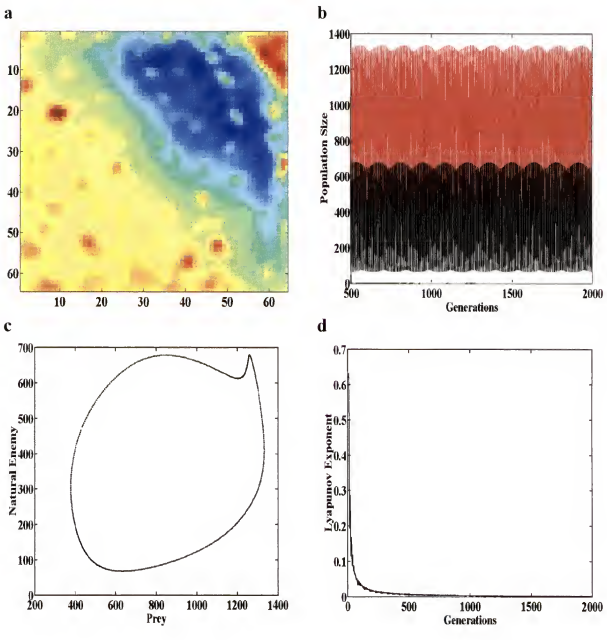

Fig. 3-7. Spatiotemporal dynamics on a 64 x 64 grid with a 2-D integrodifference equation Nicholson-Bailey model. All cells initially seeded, and prey and predator dispersal is Gaussian with the standard deviation of predator dispersal four times that of prey (4:1 grid cells) ; r =2, a varies spatially with Uniform distribution as $0 < a < 0.5$. (a) prey and predator interaction--high prey density (red), high predator density (dark-blue); (b) simulation time plot--prey (red), predator (black); (c) phase-plane plot, (d) Lyapunov exponent.

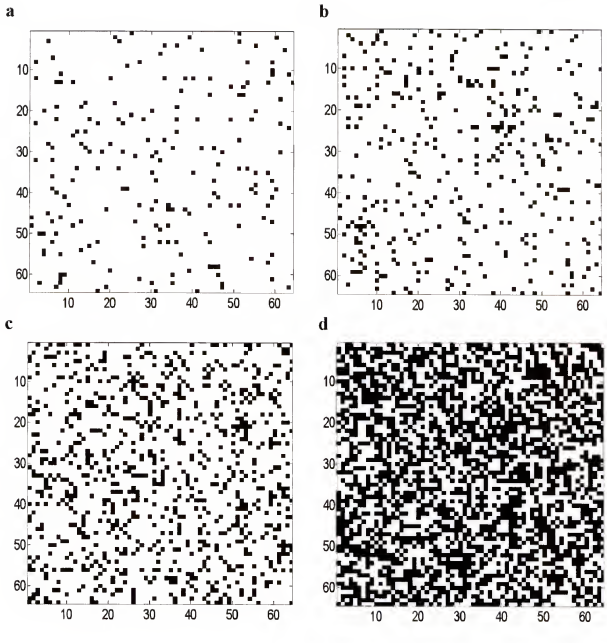

Fig. 3-8. Varying prey refuge in a 64 x 64 spatial grid. Black areas represent refuge cells with predator searching efficiency $a = 0.0$; White areas are non-refuge cells with $a > 0$. The amount of refuge is obtained from the equation, $a = \bar{a}\ [(1 + \Delta)*U(0,1) - \Delta]$. Negative a values are reassigned to 0.0. In the refuge maps shown (a) $\Delta = 0.05$, (b) $\Delta = 0.10$, (c) $\Delta = 0.25$, and (d) $\Delta = 1.00$.

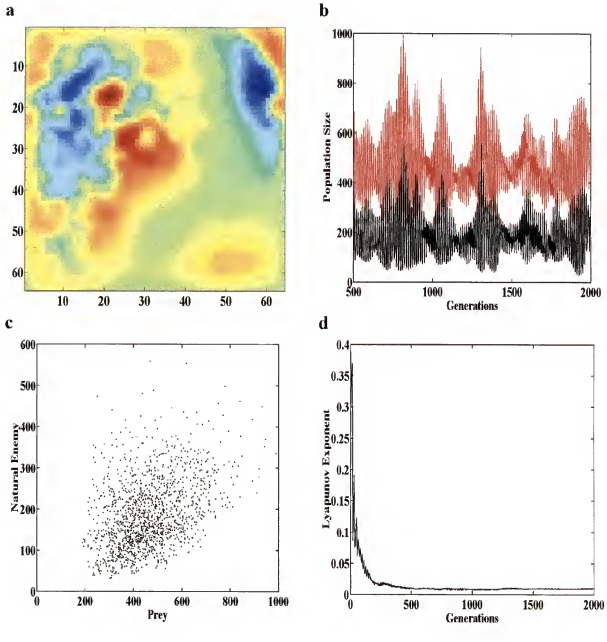

Fig. 3-9. Spatiotemporal dynamics on a 64 x 64 grid with a 2-D integrodifference equation Nicholson-Bailey model. No prey refuge ($\Delta = 0.00$). Prey and predator dispersal is Gaussian with the standard deviation of prey dispersal twice that of predator (2:1 grid cells); r and a vary spatially with Uniform distribution as $1 < r < 2.0$, $0 < a < 1$. (a) prey and predator interaction--high prey density (red), high predator density (dark-blue); (b) simulation time plot--prey (red), predator (black); (c) phase-plane plot; (d) Lyapunov exponent.

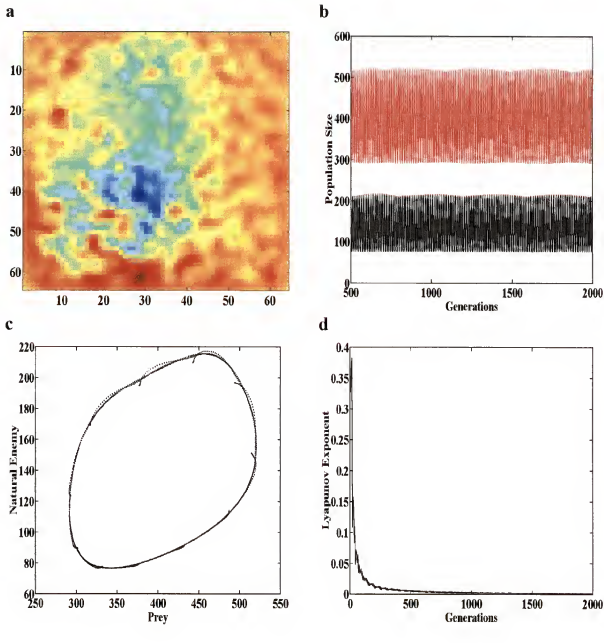

Fig. 3-10. Spatiotemporal dynamics on a 64 x 64 grid with a 2-D integrodifference equation Nicholson-Bailey model. Approximately 9% of cells are prey refuge ($\Delta = 0.10$). Prey and predator dispersal is Gaussian with the standard deviation of prey dispersal twice that of predator (2.1 grid cells); r and a vary spatially with Uniform distribution as $1 < r < 2.0$, $0 < a < 1$; (a) prey and predator interaction--high prey density (red), high predator density (dark-blue);(b) simulation time plot--prey (red), predator (black); (c) phase-plane plot; (d) Lyapunov exponent.

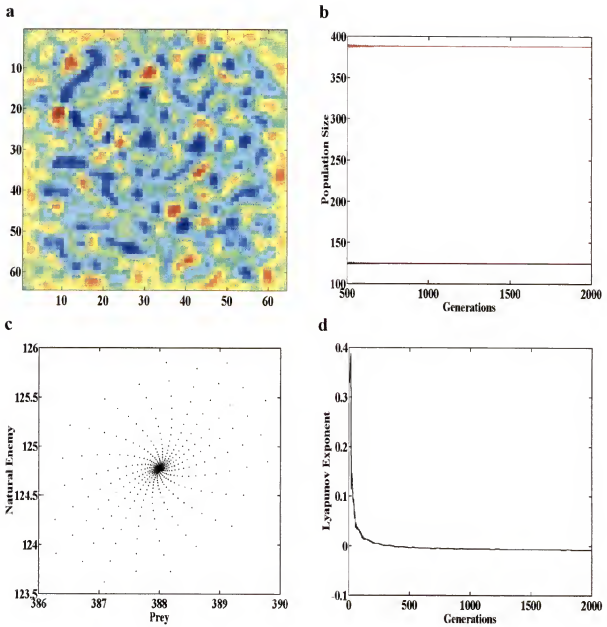

Fig. 3-11. Spatiotemporal dynamics on a 64 x 64 grid with a 2-D integrodifference equation Nicholson-Bailey model. Approximately 12 % of cells are prey refuge ($\Delta = 0.15$). Prey and predator dispersal is Gaussian with the standard deviation of prey dispersal twice that of predator (2:1 grid cells); r varies spatially with Uniform distribution as $1 < r < 2.0$ and average $a = 0.5$.(a) prey and predator interaction--high prey density (red), high predator density (dark-blue); (b) simulation time plot--prey (red), predator (black); (c) phase-plane plot; (d) Lyapunov exponent.

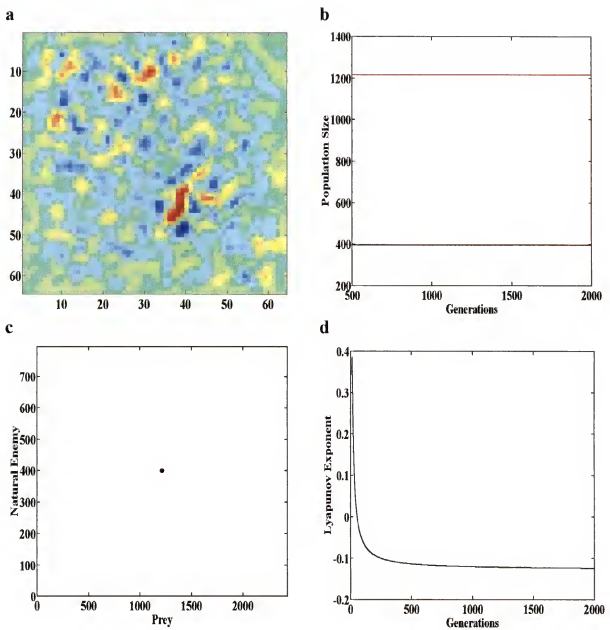

Fig. 3-12. Spatiotemporal dynamics on a 64 x 64 grid with a 2-D integrodifference equation Nicholson-Bailey model. Approximately 50% of cells are prey refuge ($\Delta = 1.0$). Prey and predator dispersal is Gaussian with the standard deviation of prey dispersal twice that of predator (2:1 grid cells); r varies spatially with Uniform distribution as $1 < r < 2.0$ and average $a = 0.5$. (a) prey and predator interaction--high prey density (red), high predator density (dark-blue); (b) simulation time plot--prey (red), predator (black); (c) phase-plane plot; (d) Lyapunov exponent.

CHAPTER 4
CONSTRUCTION AND ANALYSIS OF RESOURCE MAPS FOR HERBIVOROUS INSECTS

Introduction

The spatiotemporal dynamics of animal species are directly affected by characteristics of their environment such as those defined by habitat structure. It is important therefore to determine how habitat structure affects ecological processes such as dispersal that operate at spatial and temporal scales relevant to the organism. Measures of habitat structure are varied but can be categorized into two groups: measures of habitat composition that determine the relative extent of species resources within the habitat, and measures of habitat physiognomy or the spatial arrangement of these resources (Dunning et al. 1992). Spatially explicit population models (SEPMs) include resource or habitat maps that provide clear and accurate descriptions of both habitat composition and physiognomy. These models can be used to examine the impact of changes in habitat structure on the animal's population dynamics (Dunning et al. 1995).

The form of the resource map in SEPMs may differ depending on the system being studied. For example, in some special types of SEPMs such as dispersal-corridor models, the animal's habitat is made up of explicit patches or nodes that may or may not be connected through dispersal corridors, and nonpatch habitat locations are not always explicitly considered (Fahrig 1988, Fahrig & Paloheimo 1988). More commonly however,

the animal's habitat in SEPMs is represented by a grid of interconnecting squares or cells each of which is homogeneous in some habitat feature. Heterogeneity is introduced into the system by assigning different habitat characteristics to different cells (Dunning et al. 1995).

The purpose of this chapter is to discuss the construction of grid-based insect resource maps for use with spatially explicit population models. Resource maps for the silverleaf whitefly (SLW), *Bemisia argentifolii* are developed for spatial systems of two different extents. The first resource map is constructed from a relatively small and isolated farm system, while resource maps for the insect in large-scale agricultural systems are developed later using remotely sensed data. Finally, some discussion on experimental resource maps is given.

Farm-Level Whitefly Resource Maps

A silverleaf whitefly resource map is developed on a mixed-crop organic farm, Pine Island Organics, on Pine Island, Florida. Pine Island is fairly isolated from the Florida mainland, and is the largest island (27.2 km x 3.2 km) of its kind on the west coast of Florida (Fig. 4-1).

The first step in setting up the SLW resource map was to gather information on features within the farm. Measurements were taken on the cropping area and the spatial arrangement of SLW resources within fields was recorded. This information was used to create a scaled-map of the farm as seen Fig. 4-2a. The cropping area consisted of two fields (1 and 2) that were divided into 14 and 12 blocks, respectively. Each block

contained a single crop type and was separated from other blocks by a sugarcane windbreak. Blocks were also divided into plots to facilitate insect population sampling on the farm.

The next step was to superimpose a grid consisting of 128 cells x 128 cells onto the scaled-map and to index SLW resources in each cell in that grid. The final resource map shown as a color-coded image in Fig. 4-2b has an extent of ≈31 hectares with each patch or grid cell ≈18.92 m^2 (4.35 m x 4.35 m).

Resources were assigned to their respective spatial locations in the grid in the following manner. It can be observed in Fig. 4-2b that six main crops or resource types were grown. These are tomato, eggplant, cucumber, zucchini, pepper and sugarcane. Resident vegetation was added as the seventh resource to cover areas unoccupied by the six other resources. If a crop was planted in different blocks on the same date the same resource index was assigned to these blocks and to the respective cells in the resource spatial matrix. However, if a crop was planted in different blocks on different dates, these were given different resource indices. The final map therefore contains sixteen rather than seven resource indices (Fig. 4-2b). Tomato for example, was assigned resource indices 4, 5, 8 and 11 because of different planting dates. Similarly, eggplant was assigned resource indices 6 and 12, cucumber, 3, 9 and 16, zucchini, 13, 14 and 15, and pepper, resource indices 7 and 10. Sugarcane and resident vegetation were assigned resource indices 1 and 2, respectively. The matrix of resource types was saved in ASCII file format so that it could be read by the simulation package, MATLAB® (MathWorks 1994) into the spatial resource matrix, X, at the start of simulations.

Remote Sensing and Large-scale Resource Maps

The methodology described in the Pine Island example for constructing resource maps is clearly inadequate for animal habitats that extend into regional agricultural systems. For such systems, habitat feature information can be captured using remote sensing technology such as satellite imagery.

Remote Sensing Data

Remote sensing is defined as "the technique of obtaining information about objects through the analysis of data collected by special instruments that are not in physical contact with the objects of investigation" (Avery & Berlin 1992 p. 1). This technology has been widely used in agriculture and ecology. It has for example been used to determine crop stress due to plant pathogens (Hatfield 1990), to quantify organic matter degradation in agricultural fields (Schreier et al. 1988), to detect salinity and nutrient deficiencies in soils (Rahman et al. 1994) and nonpoint-source pollution in waterways (Jakubauskas et al. 1992), and to assess the effects of water stress in crops (Mahey et al. 1991). Ecological applications have included the identification of broad ecological land classes in particular regions. Information of this type is often required for the proper analysis and management of large-scale landscapes, and for planning, design and development of nature reserves (Talbot & Talbot 1994, Rey-Benayas & Pope 1995, Host et al. 1996). In large heterogeneous agricultural landscapes, remote sensing technology has generally been restricted to identifying and determining production levels of major crops such as wheat, cotton and corn. Little emphasis has been placed on the relationship between habitat structure and insect spatiotemporal dynamics.

Data Acquisition and Display

Remotely sensed data can be acquired by two major methods--airphotography and earth observation satellite (EOS) imagery. Although emphasis here is placed on data collected by EOSs, the techniques for manipulating these data can also be applied to data collected by airphotography.

Land satellite (Landsat) is the first international satellite program designed specifically for the collection of data on the earth's surface (Jensen 1986, Avery & Berlin 1992). In 1985, the Land Remote Sensing Act transferred the Landsat program to the Earth Observation Satellite Corporation (EOSAT; 4300 Forbes Blvd. Lanham, MD 20706-9954) which now has responsibility for managing EOS data in the US.

Today, the most widely used Landsat sensor for collecting ground data is the Landsat Thematic Mapper (TM) system. The orbits of the current Landsats (4 and 5) carrying these sensors are near-polar (passes within 8° of the North and South Poles), sun synchronous (passes over all places on earth having the same latitude at approximately the same local time), with a nominal altitude of 705 km. This low orbit allows these Landsats to revisit the same location every 16 days (233 orbits) at approximately the same local time, 9:45 a.m., and to achieve a ground resolution of approximately 28.5 m to 30 m (Jensen 1986, Avery & Berlin 1992, Richards 1993).

Landsat TM sensors simultaneously collect electromagnetic data in seven narrow spectral bands between 0.45 and 12.5 μm (Table 4-1) (Quattrochi & Pelletier 1991, Avery & Berlin 1992). The data are converted to numerical form, positive integers or digital numbers, and are supplied by EOSAT as full scenes or sub scenes on magnetic tape or

CD-ROM. Full scenes are 105 miles x 115 miles (170 km x 185 km) and consist of approximately 5965 rows and 6967 columns of data, while subscenes are 62 miles x 62 miles (100 km x 100 km) and consist of 3510 rows and columns. Knowledge of a scene's center is required for purchasing the whole or any part of that scene since scene centers are located along specific Landsat rows and paths. The locations of all scene centers can be found in the Index to Landsat Worldwide Reference Systems distributed by EOSAT (Fig. 4-3).

Each TM band generally detects specific ground features (Table 4-1). Many vegetation indices rely on band 3 (Red) and band 4 (NIR). An example is the Normalized Difference Vegetation Index (NDVI) defined by

$$NDVI = ((IR - Red) / (IR + Red))*scale \quad (4.1),$$

that provides a useful indicator of biomass vigor. Fig 4-4a. shows the NDVI image for July 30, 1986 satellite data on Crow Butte, Nebraska. Another index that is a variation of NDVI, is the Transformed Vegetation Index (TVI) given by

$$TVI = 100*sqrt((IR - Red) / (IR + RED)) \quad (4.2).$$

The Crow Butte image after this transformation is given in Fig. 4-4b. Other useful indices are the Graham-Schmidt™ Orthogonalization Index that delineates bare soil from vegetation, and Tasseled Cap (or Kauth's Tasseled Cap) that is used to compute greenness, brightness, and wetness indices. Unlike other indices however, Tesseled Cap uses six TM bands. The Graham-Schmidt™ Orthogonalization index will be used later on and will therefore be described in more detail at that time.

TM data can be displayed as color images but these data must first be converted to raster format and quantized to 4-, 8- or 16-bit scales before this can be done. Raster data files consist of grids of uniform cells with each cell coded with a data value that represents the average reflectance of all features within that area on the ground. Rasters are displayed as images on the computer screen where cells become color-coded screen pixels having a range of 16 (2^4) colors if the data were quantized on the 4-bit scale, and 256 and 65536 colors if the data were quantized on the 8- and 16-bit scales, respectively.

Human color perception is limited to the three primary colors, red, green and blue. Therefore, the seven spectral bands of TM data can only be displayed in combinations of these three colors. For displaying the data, three bands are usually chosen and assigned to Red, Green, and Blue (RGB) with the choice of bands depending on the information required. For example, if Landsat TM bands 3 (red), 2 (green) and 1 (blue) were assigned to RGB, a natural color image is obtained (Fig. 4-4c). In this image, vegetated areas appear as dark intensity pixels and in shades of green and unvegetated areas and soils in grey, brown or tan. If bands 5 (Mid IR), 4 (NIR) and 3 (red) were assigned to RGB, vegetated areas now appear bright green and unvegetated areas in shades of red or purple (Fig. 4-4d).

The indices and the RGB color assignments are useful for distinguishing broad landscape features but generally cannot be used to distinguish between vegetation types. The indices simply help to highlight vegetated areas within the landscape and to separate these from other landscape features such as bare soil and water bodies. To distinguish between different land cover objects feature classification is required.

Feature Classification

In feature classification, an analysis of the spectral properties of multiband data and the sorting of these data into spectrally similar categories based on predefined decision rules is undertaken. Two general approaches are available, unsupervised and supervised classification. In unsupervised classification, the decision on whether a feature belongs to one spectral class or another is determined by the classification algorithm (classifier). The analyst simply specifies the number of classes into which he wishes the data to be grouped based on his knowledge of the area. If complete knowledge is lacking, a larger number of classes than are actually thought to be present in the data are specified. The classifier uses statistical and mathematical rules to decide how many of the requested classes should be retained. After classification, similar classes are aggregated using ancillary information from ground truthing, crop growth characteristics, and local expert knowledge. In some cases an initial classification may provide useful information that could be used to reclassify the data using other clustering and statistical procedures such as centroid clustering and discriminant analysis (Rey-Benayas & Pope 1995).

Two of the more widely used unsupervised classification algorithms are K-Means and Isoclass or ISODATA (**I**terative **S**elf-**O**rganization **D**ata **A**nalysis **T**echniques **A**). These cluster seeking algorithms determine classes or clusters by calculating the Euclidean distance between data elements and cluster means (Tou & Gonzalez 1974).

Supervised classification requires some prior information on cover types and features within the area. This information is used to create features or training sets that "train" the classifier to recognize other features in the image having similar spectral

characteristics. A common classifier under this category uses the Gaussian Maximum Likelihood algorithm.

Data Preparation for Classification

Quite often, preprocessing of the Landsat TM data is required before classification is undertaken to ensure that the best possible data are used for analysis. This activity that mainly involves image rectification and restoration, helps to remove noise introduced into the signals when they are recorded by the TM sensors, to replace missing data, and to correct for radiometric problems caused by differences in sun angle, and the presence of atmospheric haze. Obtaining data that are completely free from atmospheric effects due to clouds, dust and smoke is not always possible. Several algorithms are available for the removal of haze and smoke from Landsat TM data (Lavreau 1991). Removal of clouds appears to be somewhat more difficult (J. Paris, pers. comm.).

Remotely sensed data from multiple dates that are to be used in multi-temporal feature classification often have to be normalized to correct for variation in reflectance due to differences in sun angle on the different dates. One way of making this correction is to divide each pixel or raster value in the image by the cosine of the sun's illumination angle (Avery and Berlin 1992). In addition, although multi-temporal data are collected by the same Landsat TM sensors, slight variation will often occur in the size of each data set. Data collected on multiple dates may have to be resampled to conform to a standard size before being used in feature classification.

Georeferencing is yet another preprocessing exercise that ensures that the data are all in alignment with the same common geographic coordinate system and therefore with

points on the earth. The Latitude-Longitude and the Universal Transverse Mercator systems are the most commonly used projection systems (Jensen 1986).

Feature Classification: The San Joaquin Valley Agricultural System

Data Acquisition

Three Landsat TM subscenes on the San Joaquin Valley, California were purchased from EOSAT. These data were collected by Landsat on April 27, June 30, and October 20, 1993, and were taken from scenes that had their centers located at Path 42: :Row 35 in the Index shown in Fig. 4-3. Each subscene was imported, converted to raster format and prepared for display and analysis with the map and image processing system, TNTmips™ (MicroImages, Inc., Lincoln, Nebraska 68508). Three TM bands (5,4,3) from each date coded in RGB are presented in Fig. 4-5. Changes in vegetation intensity across the three dates are evident from the amount of green present in these images. Also, the orientation of each image indicates the natural angular path of the satellite. Resource maps created from these data may have to be rotated 10° counterclockwise (north to top) before they are used in simulations.

Preprocessing and Supporting Data

Preprocessing included georeferencing, and normalization of the April and October reflectances to match the June data. Differences in the size (number of rows and columns) of the data sets were corrected by resampling the April and October data to conform to the size of the June data since only equal size data can be used together in classification (Avery & Berlin 1992).

Supporting information was obtained to assist in recognition and aggregation of feature classes. First, changes in greenness and soil brightness across the three periods were determined using the Graham-Schmidt™ Orthogonalization. Greenness and Soil Brightness rasters were generated for each date using sample values from dark soil, bright soil, and green soil. Sample values were obtained from raster correlation between the Red band (X axis), and the NIR band (Y axis) for each data set (Table 4-2). Green Vegetation Coefficients (C_1 and C_2) were computed from sample values entered for Red and NIR dark soil and green soil values, respectively, while Bright Soil Coefficients (C_3 and C_4) were calculated from sample values entered for the Red and NIR dark and bright soils, respectively. These coefficients were then used in the equations

$$\begin{aligned} &\textit{Greenness} = 0.5 + (C_1 * \textit{Red cell value}) + (C_2 * \textit{NIR cell value}) \quad (a) \\ &\textit{Brightness} = 0.5 + (C_3 * \textit{Red cell value}) + (C_4 * \textit{NIR cell value}) \quad (b) \end{aligned} \tag{4.3},$$

to perform the Graham-Schmidt™ transformations on each data value for each date. The rasters that resulted from these transformations are shown in Fig. 4-6.

Ground Truth data were also collected as supporting data. Figure 4-7a for example shows data obtained from Air-Ways Farm Inc. The boundaries of each ranch were vectorized and overlaid on the June image (Fig. 4-7b). Crop types within these ranches were used to identify similar crop types throughout the data.

Classification Procedure: K-Means and ISODATA

Eighteen bands (bands 1 to 5, and band 7 for each date) were used simultaneously in classifying crop types in the San Joaquin Valley. Band 6 was eliminated because of its

lower spatial resolution, and the lack of useful information for the type of crop feature identification required. Classification was performed using the unsupervised ISODATA algorithm in TNTmips™.

The ISODATA algorithm is an enhanced form of the much simpler K-Means algorithm. K-Means seeks to minimize the square distance from all data elements in a cluster domain to the cluster center, and involves the following basic steps (Tou & Gonzalez 1974);

Step 1: K initial cluster centers are arbitrarily chosen from the data.

Step 2: Data elements are distributed amongst the K cluster domains using the minimum Euclidean distance between each data element and the cluster centers. If the K cluster centers chosen are $\mathbf{c}_1, \mathbf{c}_2, \ldots, \mathbf{c}_K$, then the data elements $\boldsymbol{x} = (x_1, x_2, \ldots, x_n)$ are assigned to cluster $\mathbf{c}_j$, $j = 1$ to K based on the relation

$$\boldsymbol{x} \in S_j \quad \text{if } \|\boldsymbol{x} - \boldsymbol{c}_j\| < \|\boldsymbol{x} - \boldsymbol{c}_m\| \qquad \forall\ j, m = 1, 2, \ldots, K;\ \ m \neq j \tag{4.4}$$

S_j is the set of samples whose cluster center is $\mathbf{c}_j$. Ties resulting from eqn (4.1) are resolved arbitrarily.

Step 3: New cluster centers are calculated from the mean of each S_j.

Step 4: Steps 2 and 3 are repeated until the algorithm converges on K clusters.

In the ISODATA algorithm, cluster centers are also iteratively determined from sample means. Additional parameters are however required. The following general steps are involved in this procedure (Tou & Gonzalez 1974);

Step 1: A set N of initial cluster centers $\mathbf{c}_1, \mathbf{c}_2, \ldots, \mathbf{c}_N$ are chosen and the following processing parameters specified;

K = number of cluster centers desired;

P = comparison parameter or the parameter against which the size of a cluster domain (S) is compared;

SD = standard deviation parameter;

L = lumping parameter;

M = maximum number of pairs of clusters which can be lumped;

I = number of iterations allowed.

Step 2: The n data elements or samples $\boldsymbol{x} = (x_1, x_2, \ldots, x_n)$ are distributed among the cluster centers using

$$\boldsymbol{x} \in S_j \quad \text{if } \|\boldsymbol{x} - \boldsymbol{c}_j\| < \|\boldsymbol{x} - \boldsymbol{c}_m\| \qquad \forall \; j, m = 1, 2, \ldots, N; \quad m \neq j \tag{4.5}$$

Again S_j represents the set of samples whose cluster center is $\mathbf{c}_j$.

Step 3: Any S with fewer than P members are discarded and N is reduced by 1.

Step 4: Cluster centers $\mathbf{c}_j$, j = 1,2, ..., N, are updated using the new mean of the sample sets S_j.

Step 5: The average distance $\bar{D}_j$ of elements in S_j are computed from the cluster center $\mathbf{c}_j$ using

$$\bar{D}_j = \frac{1}{n_j} \sum_{x \in S_j} \| x - c_j \|, \quad j = 1,2,...,N \tag{4.6}$$

where n_j is the number of samples in S_j

Step 6: The overall average distance $\bar{D}$ of the elements from their respective cluster centers are computed by

$$\bar{D} = \frac{1}{N} \sum_{j=1}^{N} n_j \bar{D}_j \tag{4.7}$$

Step 7:

(a) If this is the last iteration, i.e., if I is reached, then set $L = 0$ and go to Step 11.

(b) If $N \leq K/2$, go to Step 8

(c) If an even-numbered iteration is reached, or $N \geq 2K$, go to Step 11; otherwise continue.

Step 8: The standard deviation vector $\boldsymbol{\sigma}_j = (\sigma_{1j}, \sigma_{2j}, ..., \sigma_{nj})$ for each sample set S_j is derived

Step 9: The maximum component ($\sigma_{j\,max}$) of each $\boldsymbol{\sigma}_j$, $j = 1, 2, ..., N$, is determined.

Step 10: If for any j, ($j = 1,2,..., N$), $\sigma_{j\,max} > SD$ and

(a) $\bar{D}_j > \bar{D}$ and $N_j > 2(P + 1)$

or

(b) $N \leq K/2$,

then $\mathbf{c}_j$ is split into two new cluster centers ($\mathbf{c}_j^+$ and $\mathbf{c}_j^-$), $\mathbf{c}_j$ is deleted, and N is increased by 1. Cluster center $\mathbf{c}_j^+$ is formed by adding a fraction of $\sigma_{j\,\max}$ to $\mathbf{c}_j$, while $\mathbf{c}_j^-$ is formed by subtracting that quantity from $\mathbf{c}_j$. If splitting took place in this step, then go to Step 2; otherwise continue:

Step 11: The pairwise distances D_{ij} between the cluster centers are computed;

$$D_{ij} = \| \boldsymbol{c}_i - \boldsymbol{c}_j \|, \quad i = 1,2,...,(N-1); \quad j = (i+1),...,N \tag{4.8}$$

Step 12: The distances D_{ij} are compared against L, the lumping parameter, and the M smallest distances which are less than L are arranged in ascending order.

Step 13: Since for each distance there is associated a pair of clusters, a pairwise lumping operation is performed starting with the smallest distance.

Step 14: The algorithm is terminated if this is the last iteration. Otherwise go to Step 1 or Step 2 depending on whether parameters are to be changed.

Parameter values used in the ISODATA classification are given in Fig. 4-8. These correspond to parameters outlined above as follows; $K = 100$, $P = 30$, $SD = 3.0$, $L = 3.2$, and $I = 20$. The parameter that specifies the maximum number of pairs of cluster centers that can be lumped, M, is not entered directly but is calculated from the value entered for 'Minimum Distance for Chaining.' Output from classification included a classified raster, a distance raster, and statistical report.

Classification Results and Interpretation

Classification of the eighteen TM bands (3 dates, 6 bands each) of San Joaquin Valley data was completed in approximately 80 hours using a 486-66 MHz IBM PC with 16 MB of RAM. The 100 requested classes were all returned. Output included the classified and distance rasters shown in Fig. 4-9. In the distance raster, the closeness of each data element to its respective class center is indicated by the grey-level intensity of the pixel. The closer the data element is to its class center the darker the pixel and therefore pixels that fell close to the mean of their classes were black. Pixels in the location of the Sierras at the top right corner of the image and the coastal mountains at the bottom left corner are the darkest indicating a high proportion of "good" fits within these classes.

Clues to the identity of most of the features classes (i.e., crop, natural vegetation, soil, water) were obtained using the ground truth information and from an analysis of the statistical report generated by the classifier. The statistical report contained the mean radiance for each band in each class for all three dates, the average distance between classes, and the percentage area occupied by each class. Table 4-3 shows a portion of the statistical report along with feature characteristics and identities for most of the 100 classes. Radiance trends for each class across the three dates were used to make these determinations. Changes in features across dates were discerned by plotting mean radiance for TM band 3 against mean radiance for TM band 4. Sometimes, mean radiance is converted to percent reflectance before plotting. In these radiance or reflectance plots, one can imagine a line running diagonally across the data that delineates certain

characteristic zones (Fig 4-10) and that can assist in interpreting temporal trends in the data (Engvall et al. 1977, Richardson & Weigand 1977, Curran 1983, Jensen 1986). Trends in radiance for the 100 classes from the San Joaquin Valley classification are given in groups of ten in Fig. 4-11.

The final step of the classification involved the aggregation of similar classes based on the supporting data gathered. This process was carried out manually using the color editing procedure in TNTmips™ . The raster that resulted is presented in Fig 4-12a. The following examples are given as illustration of the procedures involved:

Cotton. Ground truth data was used to identify cotton areas in the classified raster shown in Fig 4-9a. Class numbers of features in these areas were noted and their spectral patterns checked in Fig. 4-11. Radiance trends for most cotton classes, e.g., classes 18, 19, 26, 66 and 86, were very similar. In April, mean radiance for cotton was close to soil indicating the presence of bare soil in these fields since plants had not yet covered the ground. The June pattern suggested an increase in greenness and very little soil since plants by this time had almost completely covered the ground. In October, there was a shift away from green matter toward dry vegetation and soil. This probably resulted from the defoliation of cotton.

Natural areas, resident vegetation and classes in soil. The hilly terrains in the top right-hand and lower left-hand corners of the image in Fig. 4-5 make it fairly easy to identify and group all natural vegetation and resident vegetation classes, and classes near soil. Another look at Fig. 4-5 shows that these areas were green in April, purple in June, and contained a mixture of green and purple in October. These color changes suggested a

shift away from green matter in April toward bare soil in June and a mixture of both features in October. These observations were confirmed by the radiance plots that showed unique trends for natural and resident vegetation. For example, from April to June, the curves for classes 11, 13, 15, 16, 59, and 63 were almost flat (horizontal) in the direction of the soil line. The flat nature indicated the presence of some green matter on the ground in April and an increase in soil brightness as summer approached. In October, a gentle shift away from soil toward green matter was observed probably because conditions became cooler and wetter. There were very few cases of pure soil classes (e.g., classes 60, 64, 70). Other classes were placed in an "In Soil" group since their radiance plots indicated bare soil on two of the three dates (e.g., classes 31 and 32).

Classes in or near water. Water bodies and wet areas are unique and can usually be identified before the data are classified. Water absorbs all light and therefore is the darkest feature on an unclassified image in which TM bands 5, 4, 3 are coded in RGB. In Fig. 4-5, water bodies can be seen at the top of the image near the left corner and at the bottom near the right corner. In April, mean radiance for most water classes was on or close to the origin of the radiance plots. A shift away from the wetness zone occurred between June and October as these curves ran parallel to the soil line but on the green side. This suggested an increase in vegetative matter (weeds in water etc.) in the signature. Deviations where they occurred were due mainly to the interaction of water with soil.

Overlapping and undetermined classes. In Table 4-3, several classes were undetermined and some classes overlapped. This highlights one of the problems with

unsupervised classification in that it is very difficult to distinguish between features in heterogeneous agricultural systems that have very similar spectral characteristics. Unsupervised classification has proven to be most useful for distinguishing broad landscape features such as between agriculture, water, urban and different types of forest cover types.

San Joaquin Valley Resource Map

Limitations on computer software and hardware make it unlikely that resource maps consisting of 3510 by 3510 pixels can be used efficiently in SEPMs. One solution to this problem is to decrease the size of the map while retaining much of the information contained therein. To do this, the classified raster can be resampled to a coarser grain (i.e., resolution is decreased). The San Joaquin Valley raster obtained after class aggregation (Fig. 4-12a) was therefore filtered using a 3 x 3 majority filter to smooth the data, and resampled to 128 x 128 pixels (Fig. 4-12b). The approximate new cell size of the map is 822.8 m x 822.8 m as apposed to the original cell size of 28.5 m x 28.5 m. Cell size is important because the insect's standard deviation of dispersal in the dispersal kernels depend on this value.

Feature Classification: The Imperial Valley Agricultural System

Data Acquisition

Four Landsat TM subscenes on the Imperial Valley, California, were purchased from EOSAT. These data were collected by Landsat on August 31, 1994, December 21, 1994, February 23, 1995, and May 30, 1995, and were taken from scenes that had their

centers located at Path 39:Row 37 in the Index shown in Fig. 4-3. Each subscene was imported, converted to raster format, and prepared for display and analysis with the map and image processing software, TNTmips™. Three TM bands (5,4,3) from each date were coded in RGB and presented in Fig. 4-13. Changes in vegetation intensity across the four dates are evident from the amount of green in these images. Unlike the San Joaquin data however, each Imperial Valley raster was rotated counterclockwise 10° (top to north) so that the Landsat's path is not evident.

The choice of subscenes was influenced by several factors. First, the data had to cover the yearly crop cycle in the valley. Secondly, ground truth data in the valley were collected on September 1, 1994, December 10-11, 1994, February 1-2, 1995, and May 13-14, 1995. Subscene dates had to therefore be within approximately two weeks of the respective ground truth data collection date for these data to be useful. Finally, subscene acquisition dates were influenced by the 16-day cycle of Landsat and by cloud cover considerations on those days. Based on cloud cover information from EOSAT and the ground truth dates, the four representative subscenes were chosen.

Preprocessing and Supporting Data

The size of each data set was checked for consistency before georeferencing was carried out with TigerLine reference data. TigerLine data are prepared by the Bureau of the Census in cooperation with the U.S. Geological Survey (USGS). The match between the TigerLine data and the Landsat TM data after georeferencing is observed in Fig. 4-14.

Ground truth information was used to create training sets for the supervised classification process. The central position at each sample site was recorded using a

GARMIN GPS 50 Personal Navigator™ (Garmin International, Lenexa, KS 66219) so that these sites could be located on the relevant subscene (Fig 4-15). Each point in the images in Fig. 4-15 identifies a field or road intersection and therefore records four or more crop types.

The training sets created with the ground truth data were rasters prepared with the feature mapping procedure in TNTmips™. Representative sample pixels for each feature identified by the ground truth data were chosen in the image and assigned to that feature class (Fig 4-16a), until all observed features were recorded. An image of a training raster created with the feature mapping process shown in Fig. 4-16a is given in Fig 4-16b.

The "purity" of samples chosen in each training class is important for accurate classification. This was checked by running the training data through a few preliminary classifications and making revisions to the samples where needed. Since this process was expected to be rather time consuming because it had to be done individually for each date using six TM bands at every revision, data requiring shorter processing time were needed. This reduction in processing time could be achieved if the dimension of the original TM could be reduced without loss of information. Principal Components Analysis (PCA) was used to achieve this reduction by transforming the six highly correlated TM bands for each date into six uncorrelated PC bands that had most of the variability in the original data contained within the first PC band (Byrne et al. 1980, Richards 1984, Manly 1986, Fung et al. 1987, Dunteman 1989). Analysis of the four Imperial Valley TM data sets indicated that more than 98% of the total variability in each data set was contained in the first three PC bands (Table 4-4) and therefore these bands were used to prepare the training data

before final classifications were undertaken. RGB rasters of PC1, PC2, and PC3 for each data set are shown in Fig. 4-17.

Classification Procedure: Maximum Likelihood

Classification of each data set was performed separately using the supervised Gaussian Maximum Likelihood classification algorithm along with the respective training rasters. The Maximum Likelihood algorithm assumes that the distribution of sample values for each class in the training set is Gaussian. The algorithm computes the probabilities of data elements belonging to defined feature training classes and assigns them to the class that has the highest probability (Tou & Gonzalez 1974, Strahler 1980, Jensen 1986). For example, for $k = 1...6$ TM bands, the pixel location in each of s training classes can be represented by a vector of raster values, RV_m, such that

$$RV_m = [V_{ij,1}, V_{ij,2}, V_{ij,3}, \ldots, V_{ij,k}]^T \qquad m = 1,2,3,\ldots,s \tag{4.9}$$

where $V_{i,j,k}$ is the raster value for the (i,j)th cell in band k. A mean vector, M_m, can also be determined for each class with

$$M_m = [\mu_{m,1}, \mu_{m,2}, \mu_{m,3}, \ldots, \mu_{m,k}]^T \qquad m = 1,2,3,\ldots,s \tag{4.10}$$

where $\mu_{m,k}$ is the mean raster value for class m in band k (Jensen 1986). In addition, a covariance matrix for each class m can be calculated:

$$CV_m = \begin{bmatrix} C_{m11} & C_{m12} & \cdots & C_{m1k} \\ C_{m21} & C_{m22} & \cdots & C_{m2k} \\ \vdots & & & \vdots \\ C_{mn1} & C_{mn2} & \cdots & C_{mnk} \end{bmatrix} \tag{4.11}$$

Unknown data elements in the vector of raster values, X, are placed into class m if, and only if

$$p_m \geq p_q, \quad where\ q = 1,2,3,\ldots,s$$
$$and \tag{4.12}$$
$$p_m = [-0.5 \ln(\det(CV_m))] - [0.5(X - M_m)^T (CV_m^{-1}) (X - M_m)]$$

The classifier therefore computes the probabilities, p_m, of an unknown data vector, X, belonging to each training set class, and assigns these to the class having the largest probability (Jensen 1986).

Classification Results and Interpretation

Each Imperial Valley classification took approximately three hours to complete on a Pentium-90 MHz IBM PC with 64 MB of RAM. Output included a classified raster and dendrogram (Fig. 4-18), a distance raster, and statistical reports consisting of data on class means and standard deviations, co-occurrence matrices, class distances between means, covariance matrices and confusion or error matrices.

Dendrograms provide a relative measure of the distance at which two classes are no longer statistically separable and as those in Fig. 4-18 indicate, that with the exception

of water, most classes were generally only separable by relatively short distances. This reflects strongly on the similar reflectance characteristics of agricultural crops as a result of their common growth patterns and also on the difficulties in separating agricultural features using remote sensing.

The accuracy of the classification must be assessed before confidence can be attached to the results. Several methods are available for determining classification accuracy (Hord & Broone 1976, Van Genderen et al. 1978, Rosenfield et al. 1982, Hudson & Ramm, 1987, Congalton 1991, Richards 1993), but the most common rely on the data given in the confusion or error matrix.

Congalton (1991 p. 36) defines a confusion matrix as "a square array of numbers set out in rows and columns which express the number of sample units (i.e., pixels, clusters of pixels, or polygons) assigned to a particular category relative to the actual category as verified on the ground." The confusion matrix from the classification of the February 23, 1995 data is given in Table 4-5 to demonstrate some of the characteristics of these matrices. Although not the case for all such matrices, rows in Table 4-5 represent the ground truth data, while columns report the classification of these data in each class. The probability that ground truth pixels in a class are correctly classified (*omission error*) is obtained by dividing the number of correctly classified pixels in that class by the total number of ground truth pixels selected for that class. This accuracy estimate is called the *producer's accuracy* and it indicates to the producer of the classification how well the classification was for each class with the ground truth data provided. On the other hand, the probability that ground truth pixels classified in the map actually represents that class

on the ground (*commission error*) is determined by dividing the total number of correct pixels in that class by the total number of pixels that were classified in that class. This accuracy estimate is known as *user's accuracy* since it provides an estimate of the reliability users should have in the classification. Finally, by dividing the sum of the major diagonal elements of the matrix (total correct pixels) by the total number of pixels, an estimate of *overall accuracy* of the classification is obtained.

Another measure of accuracy that is derived from the confusion matrix is the Kappa statistic (κ) (Hudson & Ramm 1987, Congalton 1991, Richards 1993). This estimate is calculated as

$$\kappa = \frac{N\sum_{k} x_{kk} - \sum_{k}\left(\sum_{j} x_{kj}\right)\left(\sum_{i} x_{ik}\right)}{N^2 - \sum_{k}\left(\sum_{j} x_{kj}\right)\left(\sum_{i} x_{ik}\right)} \qquad (4\text{-}12),$$

where k is the length of the error matrix, i and j are row and column indices, x is an element in the matrix, and N is the total number of pixels. Unlike *overall accuracy* that considers only the elements of the major diagonal, κ indirectly incorporates the off-diagonal elements and hence often does not agree with the *overall accuracy* estimate. Accuracy estimates for the four Imperial Valley classifications are given in Table 4-6.

Imperial Valley Resource Maps

The large sizes of the classified rasters prohibit their use directly in the SEPMs. The Imperial Valley maps were therefore clipped to exclude most of Mexico, filtered with a 3 x 3 majority filter, and resampled to 100 x 100 raster cells. The cell size of the final

resource maps in Fig. 4-19 was 778 m x 778 m (≈ 0.5 mi x 0.5 mi = quarter section). One disadvantage of clipping, filtering and resampling is that some low frequency classes are removed from the final map. For example, Watermelon (Early) and Oats (Harv.) were removed from the May 30, 1995 classified raster after the above processes were performed (Fig. 4-18g & Fig. 4-19d).

Experimental Resource Maps

The ability to experiment with various habitat structures is one of the major advantages of SEPMs. Changes can easily be made to the farm-level resource map for whiteflies at Pine Island Organics. Such changes might for example include the removal of the sugarcane barriers or the grouping of similar crop types within fields. Changes in structure can similarly be made to the maps generated from remotely sensed data. The following MATLAB™ code for example removes resource *i* from the resource matrix X and replaces it with resource *j*;

$$X = X.*(X \sim= i) + j*(X == i) \qquad (4.13).$$

The structure of the resource map can therefore be altered by replacing or rearranging the resources, and the effects of these changes on insect dynamics can then be tested within the spatially explicit model framework.

Discussion

The dynamics of insects are directly affected by the structure of their habitat and therefore by the resource map that represents this habitat. It is important that these maps

accurately represent features on the ground. Direct information on farm structure and resource types for Pine Island Organics were used to create the SLW resource map and therefore this map's accuracy was expected to be very good. On the other hand, for the San Joaquin Valley and Imperial Valley, data were collected by remote sensing that is often subject to environmental and technical problems. These data are therefore likely to be less accurate and so would be the resource maps created from them. In addition, reliance on mathematical software algorithms to categorize ground features could also create problems in the identification of ground features as was observed in the San Joaquin classification.

The more *a priori* information that is available, the greater confidence there will be in the results obtained from feature classification. If for example remotely sensed data on an area were available for each day, and extensive ground truth data collection was undertaken, classification accuracy should approach 100%. Although this was not the case in the Imperial Valley classifications, Overall accuracies were 96-98% (Table 4-6). It should be pointed out that these accuracy figures are based on the assumption that the ground truth data were correct (Congalton 1991). One could obtain high accuracies using incorrect data.

Data collection is generally an expensive exercise, especially if data are to be collected in large agricultural areas. Also, the cost of Landsat TM data may be prohibitive to many potential users. Today, full-scenes (170 km x 185 km) and subscenes (100 km x 100 km) purchased from EOSAT cost US $4400 and $3100 respectively, with half- price

offered for any other two data sets on the same site ordered at the same time. The four Imperial Valley subscenes cost $9300.

The timeliness of remotely sensed satellite data is affected by Landsat's revisit period of 16 days and atmospheric occurrences such as heavy cloud cover. The revisit period problem may be corrected in the near future with faster access to less expensive high quality real-time data. This fact was emphasized at a conference entitled, Land Satellite Information in the Next Decade, held in Vienna, Virginia, in September 1995 that was sponsored by the American Society for Photogrammetry and Remote Sensing (ASPRS), and co-sponsored by the National Aeronautics and Space Administration (NASA), United States Geological Suvey (USGS), and the National Oceanic and Atmospheric Administration (NOAA). At that conference, a list of land data satellites planned for the next decade was presented (Table 4-7). In all, twenty-three land data satellites are planned for the next decade, and funding for ten of these will most likely come from the US government.

Table 4-1. Characteristics of remotely sensed Landsat Thematic Mapper data.

TM Band	Wavelength Range (μm)	Spectral Location	Resolution (m)	General Description of Uses
1	0.45 - 0.52	Blue-green	30	Good penetration of water. Useful for discriminating soil from vegetation. Sensitive to atmospheric haze and smoke.
2	0.52 - 0.60	Green	30	Corresponds to green reflectance of healthy vegetation. Can be used to discriminate broad classes of vegetation. Sensitive to water turbidity differences.
3	0.63 - 0.69	Red	30	Senses strong chlorophyll absorption region. Useful for vegetation discrimination. Has a strong reflectance for most soils.
4	0.76 - 0.90	Near Infrared	30	Distinguishes vegetation varieties and conditions. Water is a strong absorber of NIR, so this band is useful for locating and delineating water bodies and soil moisture conditions.
5	1.55 - 1.75	Mid Infrared	30	Responsive to changes in plant water content and vigor. Also useful for discriminating different plant species and soil moisture content.
6	10.40 - 12.50	Thermal	120	Good for thermal mapping applications, and vegeation stress analysis.
7	2.08 - 2.35	Mid Infrared	30	Sensitive to moisture variations in both vegetation and soils. Good for discriminating minerals and soils types.

Sources: Jensen (1986), Quattrochi & Pelletier (1991), Avery & Berlin (1992).

Table 4-2. Green Soil, Bright Soil and Dark Soil sample values obtained from raster correlation, that were used in the Graham-Schmidt™ Orthogonalization transformations of the San Joaquin Valley Landsat TM subscenes.

Subscene Acquisition Date	Parameter	X axis (Red band) sample values	Y axis (NIR band) sample values
April 27, 1993	Green Soil	16	208
	Bright Soil	122	130
	Dark Soil	19	16
June 30, 1993	Green Soil	17	224
	Bright Soil	158	176
	Dark Soil	23	12
October 20, 1993	Green Soil	20	241
	Bright Soil	155	168
	Dark Soil	14	10

Table 4-3. Mean radiance for TM bands 3 and 4, and feature class characteristics from the ISODATA classification of Landsat TM data on the San Joaquin Valley.

Class	Average Distance	April 27 Mean TM3	April 27 Mean TM4	June 30 Mean TM3	June 30 Mean TM4	October 20 Mean TM3	October 20 Mean TM4	Class Feature Name or Characteristics [a]
1	0	0	0	0	0	0	0	Image background
2	142	36	49	37	73	38	76	In soil to green vegetation
3	173	36	77	29	81	51	79	Resident vegetation
4	139	38	89	42	144	69	80	Safflower
5	191	21	19	24	28	26	32	In or near wet soil
6	110	27	94	30	111	18	93	Natural
7	117	2	9	1	2	77	105	In water to dry soil
8	187	48	100	43	124	88	109	Tomato
9	125	14	82	43	78	35	71	Natural
10	131	1	1	59	111	1	2	In water to green vegetation
11	110	40	84	61	83	63	86	Natural
12	135	45	108	82	106	74	98	Natural
13	122	21	83	51	80	54	85	Natural
14	225	9	13	58	100	61	98	In water to green vegetation
15	123	28	94	63	89	83	111	Natural
16	195	25	123	93	116	125	145	Natural
17	139	49	98	67	115	50	102	Natural
18	109	53	59	56	100	67	105	Cotton
19	123	66	74	46	124	67	110	Cotton
20	163	69	94	32	100	34	94	Watermelon
21	180	51	81	34	148	31	19	Alfalfa/Safflower
22	144	59	75	28	110	62	94	Safflower
23	148	50	71	16	139	75	97	Safflower
24	155	85	98	42	117	56	106	Cotton
25	126	62	76	26	121	45	92	Cotton
26	118	55	61	28	92	57	103	Cotton
27	152	65	85	55	108	74	102	Soil
28	129	65	81	66	100	62	100	In Urban
29	106	54	58	43	105	46	94	Cotton
30	136	71	88	90	102	90	103	Urban
31	125	63	78	47	118	51	98	Soil
32	163	70	92	70	113	37	106	In Soil
33	120	9	70	28	76	17	54	Natural (wet)
34	123	19	102	23	109	29	97	???
35	151	14	116	53	83	59	86	Natural

Table 4-3--continued

Class	Average Distance	April 27 Mean TM3	April 27 Mean TM4	June 30 Mean TM3	June 30 Mean TM4	October 20 Mean TM3	October 20 Mean TM4	Class Feature Name or Characteristics [a]
36	164	18	139	83	113	83	98	Safflower/Garbanzo
37	24	31	92	37	108	38	94	Natural
38	107	16	107	17	121	13	100	Alfalfa
39	213	20	132	42	124	108	123	Safflower to soil
40	135	16	162	17	165	40	120	Cotton
41	158	20	131	82	104	57	68	Wheat/Garbanzo
42	167	19	136	122	148	65	75	Wheat
43	165	21	126	75	95	75	94	???
44	199	26	128	125	146	106	123	Wheat
45	173	18	122	63	87	24	106	???
46	124	37	95	46	118	26	91	Resident vegetation
47	126	43	104	82	105	101	128	Natural
48	181	60	111	109	125	109	127	In or near soil
49	5	254	254	0	0	0	0	Dry soil to water
50	125	45	83	33	118	32	88	Natural
51	140	49	78	64	88	65	90	Natural
52	133	60	71	30	164	74	85	Tomato
53	185	49	93	4	5	4	5	In green soil to water
54	131	42	94	24	137	20	92	Apples
55	182	75	92	23	132	88	110	Cotton
56	141	46	107	48	119	57	106	Resident vegetation
57	132	44	81	51	101	37	85	???
58	147	54	90	74	101	0	1	Dry green soil to water
59	94	48	90	70	92	83	107	Natural
60	141	64	98	77	112	67	103	In Soil
61	178	96	111	95	134	62	114	Grape
62	109	64	104	58	131	45	101	Grape
63	121	57	103	85	107	93	117	Natural
64	238	104	120	119	130	119	133	In dry soil
65	125	47	59	56	80	51	67	In Urban
66	125	46	62	39	107	52	90	Cotton
67	129	80	106	68	133	57	108	Almonds/Apples
68	120	53	63	28	157	57	65	Tomato
69	114	54	58	29	114	40	109	Tomato
70	157	70	94	89	107	93	113	Soil
71	114	43	45	36	89	60	98	Cotton

Table 4-3--continued

Class	Average Distance	April 27 Mean TM3	April 27 Mean TM4	June 30 Mean TM3	June 30 Mean TM4	October 20 Mean TM3	October 20 Mean TM4	Class Feature Name or Characteristics[a]
72	94	54	57	38	120	64	114	Cotton/Watermelon
73	126	56	68	68	80	63	75	Urban
74	128	44	94	59	105	52	95	Near Soil/Urban
75	135	64	79	80	92	78	91	In Soil/Pistachios
76	167	90	108	91	116	88	113	???
77	127	57	63	61	98	41	112	Soil to Cotton
78	185	23	100	66	97	6	4	Green to soil to water
79	153	33	66	27	153	42	61	Beet
80	153	37	113	26	138	16	195	???
81	210	22	131	99	120	30	119	Spring/Fall crop
82	153	14	164	55	111	18	189	Spring/Fall crop
83	162	24	140	46	126	40	131	???
84	193	69	94	25	148	24	159	Summer crop
85	127	5	160	16	166	17	187	Raisin grape
86	133	42	58	19	118	43	78	Cotton
87	192	43	53	49	51	46	49	Urban
88	119	59	101	48	134	29	91	Grape
89	164	72	110	78	93	32	176	In soil to green vegetation
90	147	57	62	55	89	26	154	In soil to green vegetation
91	95	0	2	1	2	39	93	In water to green vegetation
92	200	25	96	2	3	40	95	In water to green vegetation
93	205	82	103	52	123	104	123	In green soil
94	217	16	9	31	21	85	130	In water to green vegetation
95	236	60	88	7	9	60	99	In green wet soil and water
96	154	38	115	23	148	39	120	Alfalfa
97	153	42	111	54	112	19	184	???
98	166	15	152	37	156	60	70	Beet/ Safflower
99	187	20	128	25	138	77	98	Beet
100	368	23	18	43	41	174	179	In water to dry soil

[a] ??? - features or characteristics are undetermined.

Table 4-4. Factor loadings and correlation between Landsat TM bands and Principal Component axes for Landsat TM data on the Imperial Valley, California.

Subscene Date	TM Band	PC1	PC2	PC3	PC4	PC5	PC6
Aug. 31, 1994	1	0.9033	0.3202	0.2583	-0.1009	-0.0657	-0.0170
	2	0.9512	0.2337	-0.1832	0.0205	0.0089	0.0803
	3	0.9608	0.2257	-0.0861	0.0965	0.0940	-0.0173
	4	0.7775	-0.5207	-0.3457	0.0578	-0.0374	-0.0036
	5	0.9776	-0.1459	0.1333	-0.0624	0.0355	0.0011
	7	0.9580	0.0659	0.2496	0.0788	-0.0964	-0.0018
Factor Loading (%)		88.10	6.54	4.32	0.57	0.42	0.05
Dec. 21, 1994	1	0.9052	0.1340	-0.3842	-0.0730	-0.0961	-0.0207
	2	0.9535	0.0844	-0.2696	0.0206	0.0222	0.1004
	3	0.9664	0.1281	-0.1806	0.0602	0.1138	-0.0238
	4	0.7511	-0.6540	-0.0770	0.0447	-0.0135	-0.0038
	5	0.9837	-0.0041	0.1645	-0.0716	0.0130	0.0012
	7	0.9618	0.1634	0.1671	0.1260	-0.0663	-0.0017
Factor Loading (%)		88.36	6.36	4.21	0.61	0.38	0.07
Feb. 23, 1995	1	0.8908	0.1778	0.3982	0.0950	-0.0844	-0.0158
	2	0.9418	0.1295	0.2969	-0.0084	0.0302	0.0845
	3	0.9518	0.1834	0.2149	-0.0791	0.0869	-0.0212
	4	0.4435	-0.8870	0.1237	-0.0331	-0.0106	-0.0017
	5	0.9791	-0.0514	-0.1856	0.0616	0.0211	-0.0005
	7	0.9659	0.1430	-0.1688	-0.1111	-0.0756	0.0018
Factor Loading (%)		81.55	12.56	4.97	0.56	0.31	0.05
May 30, 1995	1	0.8906	0.2525	0.3567	0.1039	-0.0691	0.0151
	2	0.9445	0.1821	0.2603	-0.0235	0.0264	-0.0756
	3	0.9590	0.1846	0.1396	-0.1482	0.0669	0.0173
	4	0.5897	-0.7782	0.2091	0.0278	0.0461	0.0029
	5	0.9751	-0.1029	-0.1833	-0.0261	-0.0664	-0.0017
	7	0.9512	0.1472	-0.2261	0.1089	0.1024	0.0022
Factor Loading (%)		83.50	10.13	5.11	0.73	0.49	0.04

Table 4-5. Confusion matrix and accuracy estimates from classification of the February 23, 1995 Landsat TM data on the Imperial Valley, CA.

	Classified Pixels in Each Class																	
Class[a]	A	B	C	D	E	F	G	H	I	J	K	L	M	N	O	P	Total	Prod. %[b]
A	1077	254	0	15	35	0	11	337	143	0	0	0	0	0	0	77	1949	55
B	144	800	0	0	41	2	12	78	27	0	0	0	0	0	0	134	1238	65
C	1	0	591	0	0	0	0	0	0	0	0	0	38	0	0	0	630	94
D	0	0	0	906	0	0	0	0	0	0	0	0	0	0	0	0	906	100
E	1	34	19	0	766	0	0	2	0	0	0	0	3	0	0	0	825	93
F	0	0	0	0	0	45	0	0	0	0	0	0	0	0	0	0	45	100
G	0	0	0	0	0	0	41	0	0	3	0	0	0	0	0	0	44	93
H	15	25	0	0	0	0	0	372	80	0	0	0	0	0	0	0	492	76
I	1	0	0	0	0	0	0	6	80	0	0	0	0	0	0	0	87	92
J	0	0	0	0	0	0	0	0	0	79	0	0	0	0	0	0	79	100
K	0	0	0	0	0	0	0	0	0	0	115	0	0	0	0	0	115	100
L	0	0	0	0	0	0	0	0	0	0	0	52	0	0	4	1	57	91
M	1	0	19	0	0	0	0	0	0	0	0	0	316	0	0	0	336	94
N	0	3	52	0	0	0	0	0	0	6	0	0	16	126869	0	0	126946	100
O	0	0	0	0	0	0	0	0	0	0	0	16	0	0	241	10	267	90
P	26	1	0	0	0	15	0	63	0	0	0	146	0	0	260	1354	1865	73
Total	1266	1117	681	921	842	62	64	858	330	88	115	214	373	126869	505	1576	135881	
User %[c]	85	72	87	98	91	73	64	43	24	90	100	24	85	100	48	86		98.40[d]

[a] Letters represent classes assigned in the training set; A = Alfalfa (Late), B = Alfalfa(Mid), C= Bare Soil, D = Beet (Late), E = Bermuda (Early), F = Broccoli, G = Cabbage, H = Carrots (Late), I = Carrots (Mid), J = Lettuce, K = Onions, L = Rye, M = Urban etc., N = Water, O = Wheat (Late), P = Wheat (Mid).

[b] Prod. % is Producers accuracy for each class (percentages were rounded)

[c] User % is Users accuracy for each class (percentages were rounded)

[d] Overall accuracy.

Table 4-6. Classification accuracy estimates for Landsat TM data on the Imperial Valley, California.

Subscene Date	Feature Classes	% Accuracy			
		Producers	Users	Overall	Kappa
August 31 1994					
	Alfalfa (Cut)	20.63	22.54	98.15	91.49
	Alfalfa (Early)	76.88	67.77		
	Alfalfa (Late)	100.00	100.00		
	Alfalfa (Mid)	47.30	91.92		
	Asparagus	93.48	26.14		
	Bare Soil	94.42	99.47		
	Bare Soil (Wet)	96.77	24.39		
	Bermuda (Early)	90.83	72.98		
	Bermuda (Late)	100.00	45.88		
	Bermuda (Mid)	80.43	83.87		
	Cotton (Harv)	99.07	89.17		
	Cotton (Late)	93.72	86.21		
	Sorghum	100.00	100.00		
	Sudan (Cut)	91.64	75.98		
	Sudan (Early)	63.38	57.94		
	Sudan (Mid)	64.25	82.48		
	Tomato	100.00	100.00		
	Urban etc.	99.38	98.59		
	Water	99.97	100.00		
December 21 1994					
	Alfalfa (Cut)	87.85	50.95	96.06	83.75
	Alfalfa (Early)	53.20	63.28		
	Alfalfa (Grazed)	95.64	89.06		
	Alfalfa (Late)	51.24	50.96		
	Alfalfa (Mid)	38.01	67.75		
	Artichokes	100.00	92.86		
	Asparagus	100.00	77.27		
	Bare Soil (Dry)	72.46	84.30		
	Bare Soil (Wet)	53.53	42.52		
	Beet (Mid)	85.03	96.75		

Table 4-6--continued

Subscene Date	Feature Classes	% Accuracy			
		Producers	Users	Overall	Kappa
	Bermuda	99.14	99.83		
	Brocolli (Harv)	100.00	32.94		
	Broccoli (Mid)	87.95	74.57		
	Burnt Field	100.00	93.60		
	Cabbage (Mid)	92.56	58.64		
	Carrots (Early)	61.11	53.66		
	Carrots (Mid)	69.52	27.06		
	Cauliflower (Late)	100.00	62.50		
	Lettuce (Early)	75.84	44.41		
	Lettuce (Late)	100.00	44.44		
	Lettuce (Mid)	84.45	88.47		
	Lettuce (Mix)	80.56	38.93		
	Onions (Early)	57.42	25.36		
	Rye (Mature)	100.00	58.33		
	Sudan	100.00	94.59		
	Sudan (Early)	100.00	46.15		
	Urban etc.	67.31	96.52		
	Dry Vegetation	85.86	60.28		
	Water	99.99	100.00		
February 23 1995					
	Alfalfa (Late)	55.26	85.07	98.40	87.40
	Alfalfa (Mid)	64.62	71.62		
	Bare Soil	93.81	86.78		
	Beets (Late)	100.00	98.37		
	Bermuda (Early)	92.85	90.97		
	Broccoli	100.00	72.58		
	Cabbage	93.18	64.06		
	Carrots (Late)	75.61	43.36		
	Carrots (Mid)	91.95	24.24		
	Lettuce	100.00	89.77		
	Onions	100.00	100.00		
	Rye	91.23	24.30		
	Urban etc.	94.05	84.72		

Table 4-6--continued.

Subscene Date	Feature Classes	% Accuracy			
		Producers	Users	Overall	Kappa
	Water	99.94	100.00		
	Wheat (Late)	90.26	47.72		
	Wheat (Mid)	72.60	85.91		
May 30 1995					
	Alfalfa (Late)	44.73	88.26	98.07	91.03
	Alfalfa (Cut)	74.25	26.78		
	Alfalfa (Mid)	51.06	59.36		
	Asparagus	95.57	40.76		
	Bare Soil	86.10	74.88		
	Beet	99.84	100.00		
	Bermuda (Late)	95.30	77.60		
	Bermuda (Mid)	100.00	94.37		
	Cantaloupe (Late)	100.00	58.82		
	Cantaloupe (Mid)	73.85	78.80		
	Carrot (Late)	92.11	67.31		
	Corn	98.98	98.98		
	Corn (Dry)	96.67	93.55		
	Corn (Late)	100.00	94.12		
	Cotton (Early)	86.30	87.07		
	Watermelon (Early)	100.00	94.12		
	Watermelon (Late)	6.47	64.57		
	Oats (Harv)	92.90	87.27		
	Onions	96.97	90.14		
	Sorghum	83.06	91.96		
	Sudan (Early)	100.00	67.86		
	Sudan (Late)	87.46	49.05		
	Sudan (Mid)	59.22	94.21		
	Urban etc.	92.46	90.39		
	Resident Vegetation	99.99	100.00		
	Dry Vegetation	88.67	60.59		
	Water	100.00	100.00		
	Wheat (Late)	90.64	95.58		

Table 4-7. Earth observation satellites planned for the next decade.

Country	Owner[a]	Program	Date	Resolution (m)[b]			Color Bands	Type[c]
				P	M	R		
France	G/O	Spot 5B	2004	5	10	—	4	F/A
U.S.	G/O	EOS AM-2 / L-8	2004	10	30	—	7	—
France	G/O	Spot 5A	1999	5	10	—	4	F/A
India	G/O	IRS-1 D	1999	10	20	—	4	C/T
U.S.	C/O	Space Imaging	1998	1	4	—	4	F/A
Korea	G/O	KOMSAT	1998	10	10	—	3	F/A
U.S./Japan	G/O	EOS AM-1	1998	15	15	—	14	F/A
U.S.	G/O	Landsat-7	1998	15	30	—	7	—
ESA	G/O	ENVISAT	1998	—	—	30	0	—
U.S.	C/O	Space Imaging	1997	1	4	—	4	F/A
U.S.	C/O	Eyeglass	1997	1	—	—	—	F/A
France	G/O	Spot 4	1997	10	20	—	4	C/T
U.S.	C/O	EarthWatch	1997	1	4	—	4	F/A
U.S.	C/O	EarthWatch	1996	3	15	—	3	F/A
U.S.	G/E	CTA Clark	1996	3	15	—	3	F/A
U.S.	G/E	TRW Lewis	1996	5	30	—	384	—
Russia	G/O	Almaz 2	1996	—	—	5	—	—
Japan	G/O	ADEOS	1996	8	16	—	4	C/T
China/Brazil	G/O	CBERS	1996	20	20	—	7	C/T
Canada	G/O	Radarsat	1995	—	—	9	—	—
India	G/O	IRS-1 C	1995	10	20	—	4	C/T
China/Brazil	G/O	CBERS	1995	20	20	—	7	C/T
Russia	G/O	Resours-02	1995	—	27	—	3	—

Source: Conference on Land Satellite Information in the Next Decade, Vienna, Virginia. September 1995.

[a] G- Government Funded; C - Commercially Funded; 0 - Operational; E - Experimental;

[b] M - Multispectral; R - Radar; P - Panchromatic;

[c] F/A - Fore and Aft Stereo; C/T - Cross Track Stereo.

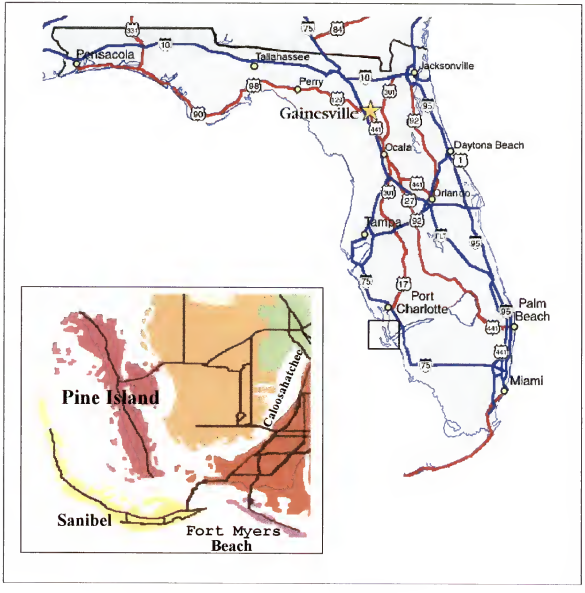

Fig. 4-1. Map of Florida showing Pine Island on the west coast near Fort Myers.

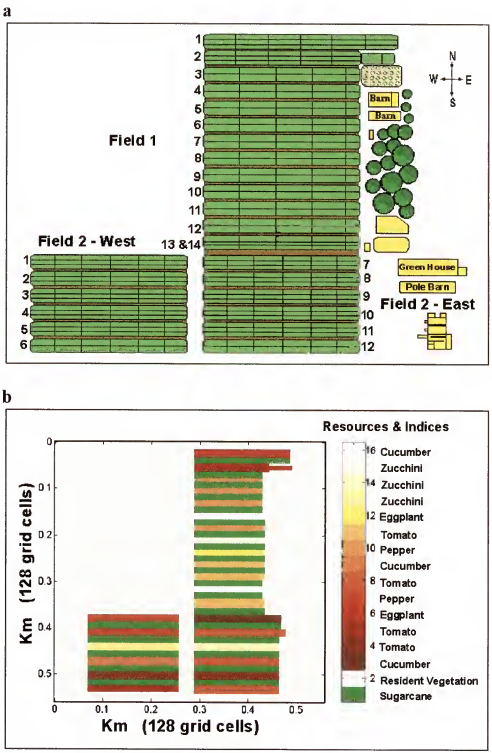

Fig. 4-2. Maps of Pine Island Organics, Pine Island, FL. (a) scaled map; (b) color-coded whitefly resource map created from the scaled-map.

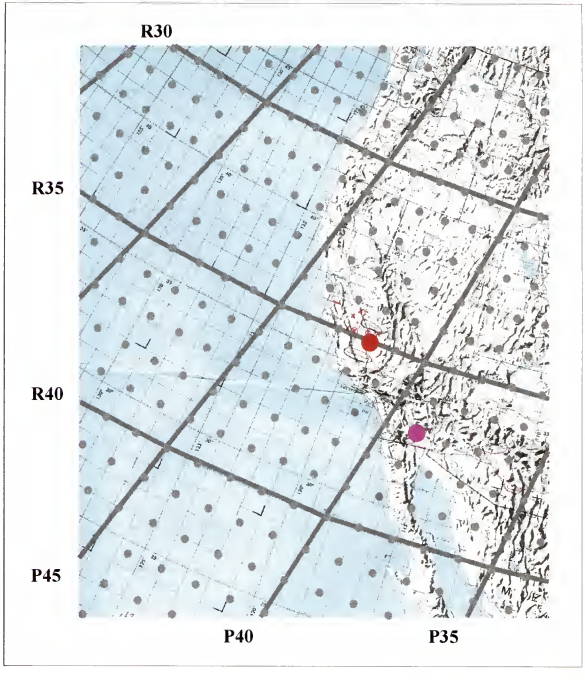

Fig. 4-3. Index to Landsat Worldwide Reference Systems showing the United States west coast and part of Mexico. Gray dots are Landsat scene centers located along specific rows (R) and paths (P). The red dot is the scene center (P42:R35) for the San Joaquin Valley, CA. The magenta dot is the scene center (P39:R37) for the Imperial Valley, CA.

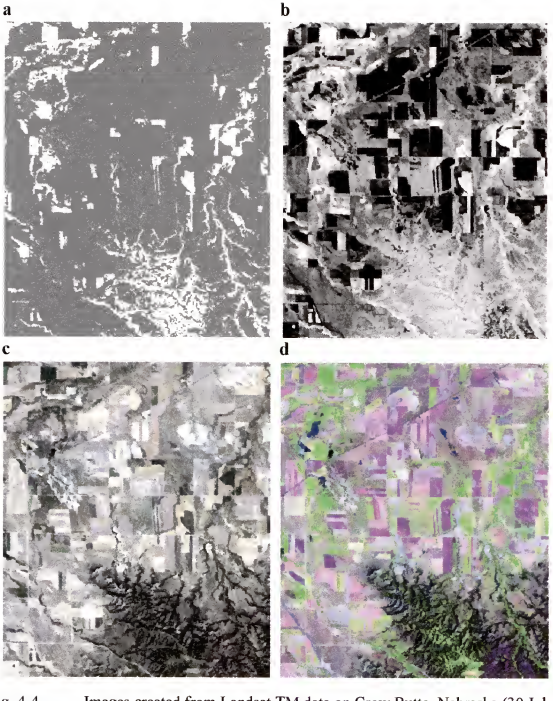

Fig. 4-4. Images created from Landsat TM data on Crow Butte, Nebraska (30 July, 1986). Original data supplied by MicroImages, Inc., Lincoln, Nebraska. (a) Normalized Difference Vegetation Index raster with scale equal 2; (b) Transformed Vegetation Index raster; (c) natural color image with band 3 (red), band 2 (green), and band 1 (blue) assigned to RGB; (d) enhanced vegetation color image with band 5 (Mid IR), band 4 (Near IR) and band3 (red) assigned to RGB.

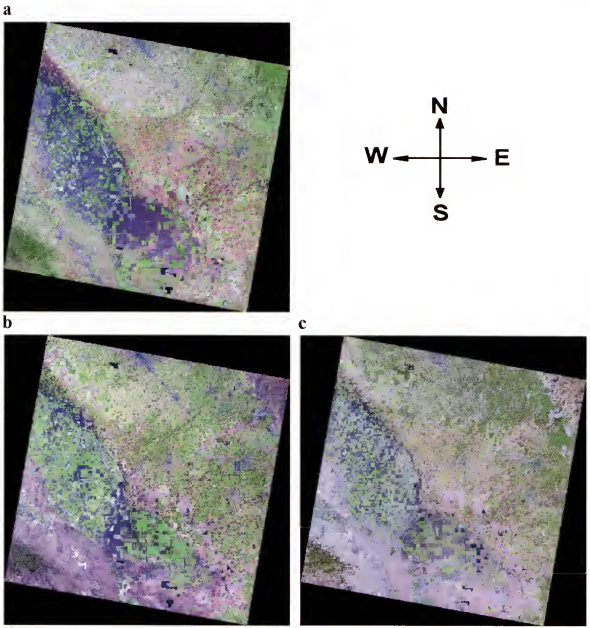

Fig. 4-5. Landsat TM subscenes of the San Joaquin Valley, CA. Bands 5, 4 and 3 were assigned to Red, Green and Blue (RGB). Each image covers approximately 100 km x 100 km (62 mi x 62 mi) and consists of 3510 by 3510 pixels (cells). Vegetated areas appear in green, non-vegetated areas in shades of red and purple, and water bodies in black. Image dates are (a) April 27, 1993; (b) June 30, 1993; (c) October 20, 1993.

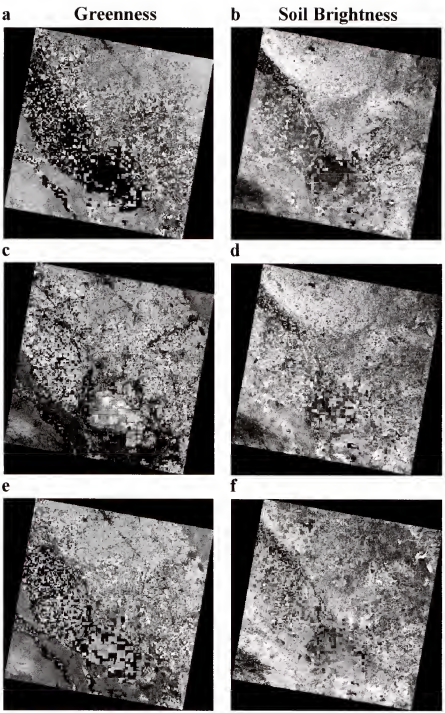

Fig. 4-6. Results of the Graham-Schmidt™ Orthogonalization of TM data on the San Joaquin Valley, CA. (a), (c), (e) Greenness rasters for April 27, June 30, and October 20, 1993, respectively. Areas with active vegetative growth are whiter. (b), (d), (f) Soil brightness rasters for April 27, June 30, and October 20, 1993, respectively. High intensity white indicates bare soil.

a

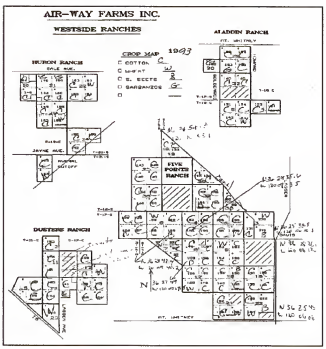

b

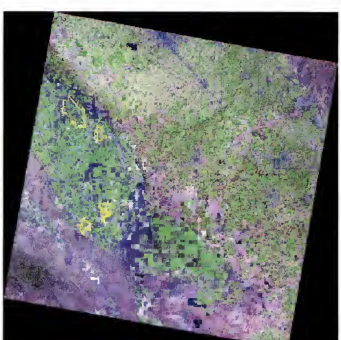

Fig. 4-7. Ground truth data in the San Joaquin Valley, CA. (a) Air-Ways Farms Inc. ranches and crop types; (b) ranches overlaid on June 30, 1993 satellite image of the valley (yellow vector objects).

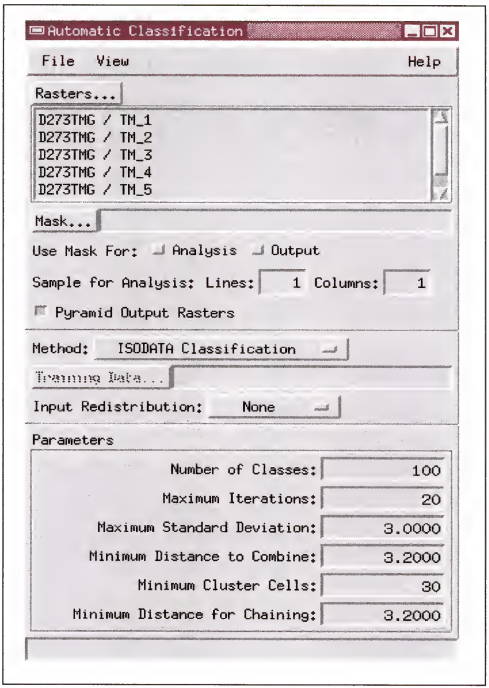

Fig. 4-8. MicroImages Inc. TNTmips™ automatic classification window with parameters used in the ISODATA classification of 18 TM bands of Landsat data on the San Joaquin Valley, CA.

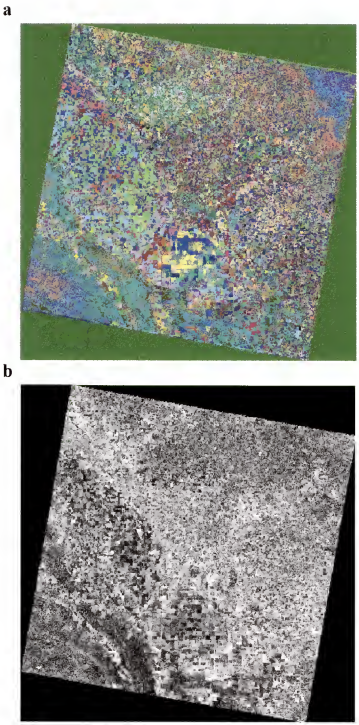

Fig. 4-9. ISODATA classification rasters for the San Joaquin Valley, CA. (a) classified raster with 100 classes assigned to different colors; (b) distance raster. Darker pixels are closer to their class mean than lighter pixels.

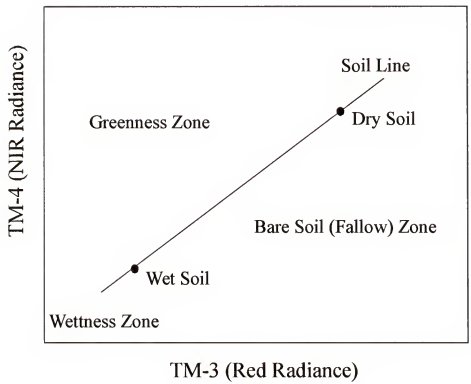

Fig. 4-10. Characteristic zones in a TM 3 (Red) and TM 4 (Near Infrared) radiance plot.

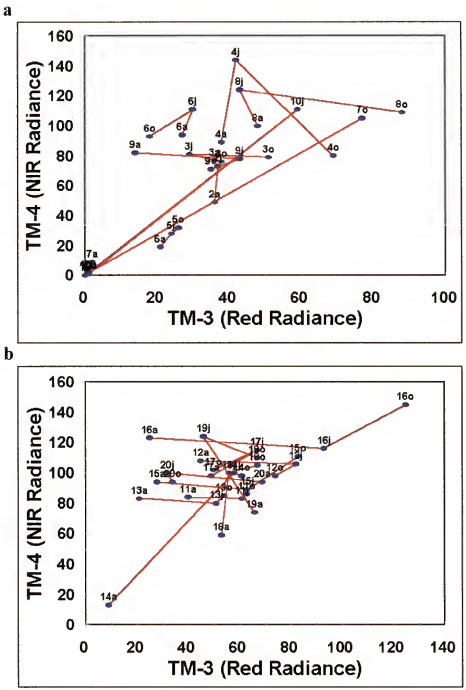

Fig. 4.11. TM band 3 and band 4 radiance plots from the ISODATA classification of Landsat data on the San Joaquin Valley, CA. Letters a, j and o in plot labels represent April 27, June 30 and October 20, 1993, respectively. Numbers next to letters represent classes 1 to 100; Classes are plotted in groups of 10 as (a) 1-10; (b) 11-20; (c) 21-30; (d) 31-40; (e) 41-50; (f) 51-60; (g) 61-70; (h) 71-80; (i) 81-90; (j) 91-100.

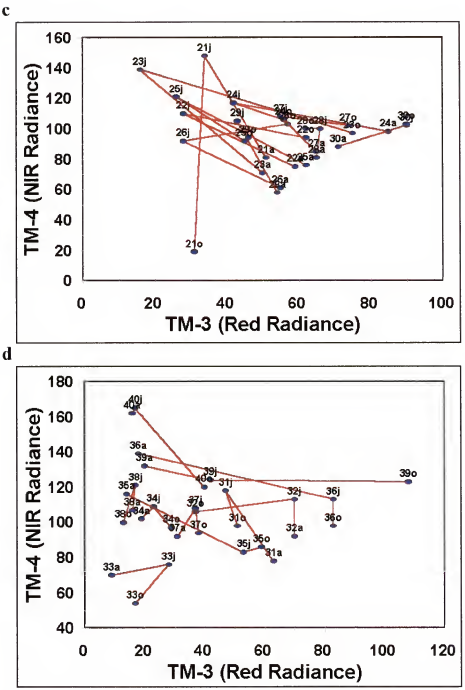

Fig. 4-11--continued.

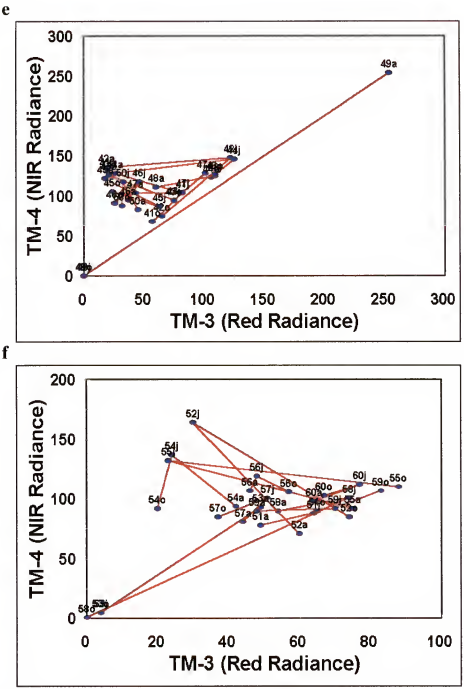

Fig. 4-11--continued.

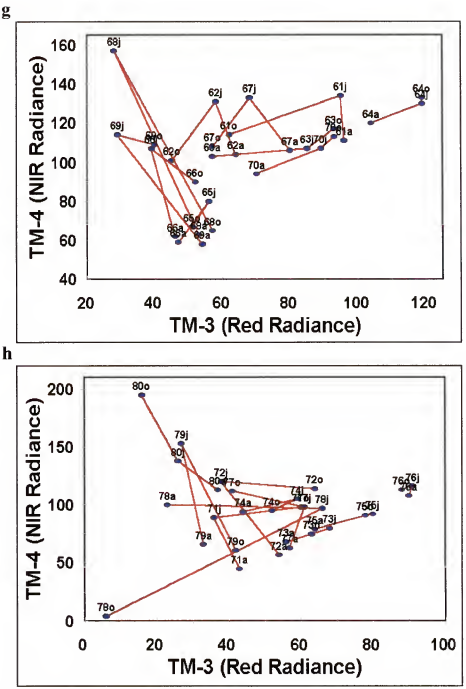

Fig. 4-11--continued.

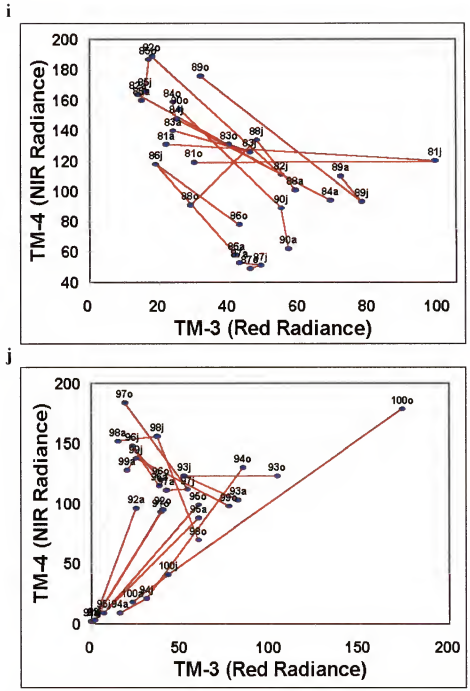

Fig. 4-11--continued.

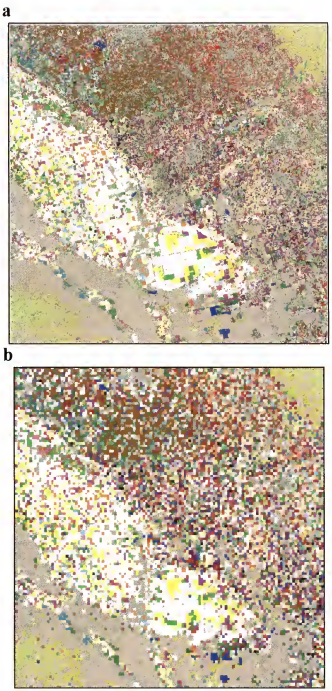

Fig. 4-12. Result of class aggregation on the classified raster of the San Joaquin Valley, CA. (a) classified raster after merging similar classes. Major classes include cotton (white), soil (tan), grapes (brown & purple), water (blue), safflower (yellow), natural vegetation (light green); (b) the final resource map created by filtering the raster in (a) with a 3 x 3 majority filter and nearest neighbor resampling to 128 x 128 raster cells.

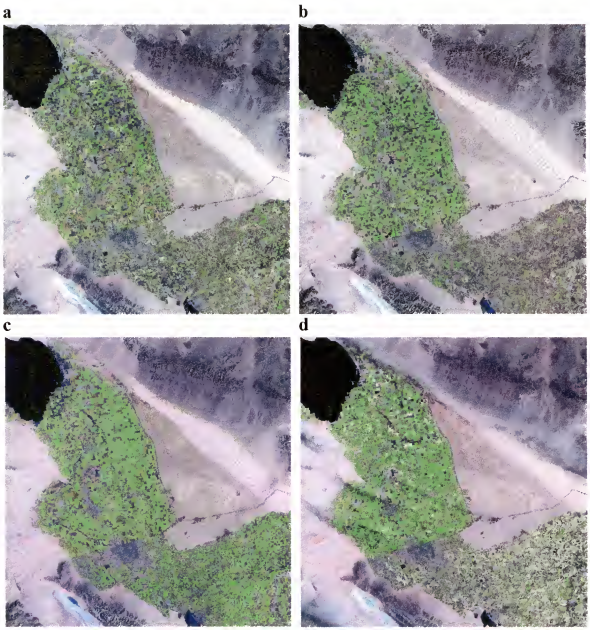

Fig. 4-13. Landsat TM subscenes of the Imperial Valley, CA. TM bands 5, 4 and 3 displayed in RGB. Each image is ≈100 km x 100 km (62 mi x 62 mi) and consist of close to 3510 x 3510 pixels (cells). Green indicates active plant growth; unvegetated areas are in shades of purple. The Salton Sea (black area) is located at the top left corner, and Mexico in the lower portion of each image. Images are from satellite data taken on (a) August 31, 1994; (b) December 21, 1994; (c) February 23, 1995; (d) May 30, 1995.

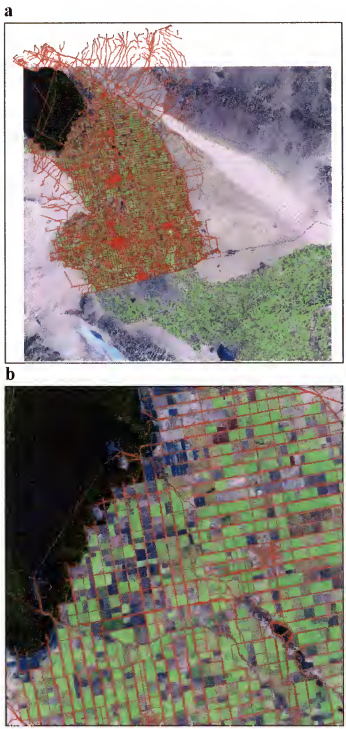

Fig. 4-14. Georeferencing of the Imperial Valley satellite data using TigerLine vector data. (a) TigerLine overlaid on a subscene; (b) close up of an area near the Salton Sea showing the agreement between the TigerLine vector, roads and field boundaries in the image.

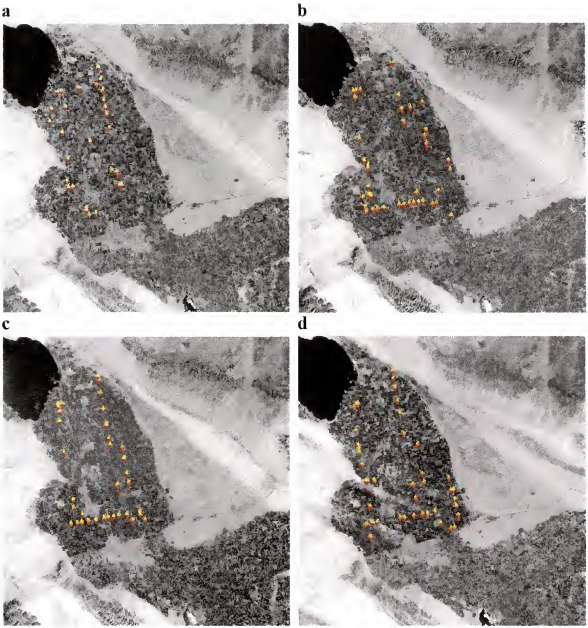

Fig. 4-15. Location of ground truth sample points in the Imperial Valley, CA. Only TM band 1 from Landsat subscenes on each date is shown.
(a) August 31, 1994 image--samples taken on September 1, 1994;
(b) December 21, 1994 image--samples taken on December 10-11, 1994;
(c) February 23, 1995 image--samples taken on February 1-2, 1995;
(d) May 30, 1995 image--samples taken on May 13-14, 1995.

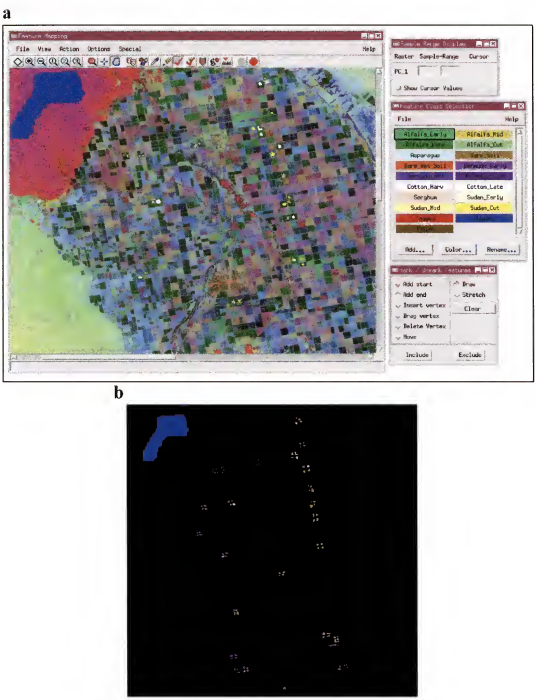

Fig. 4-16. Training rasters in MicroImages Inc. TNTmips™. (a) using feature mapping to create training sets (rasters). A portion of August 31, 1994 principal component RGB image with feature samples shown as small colored specks. (b) training raster image. The position of each colored feature sample gives the location of feature cells in the TM data.

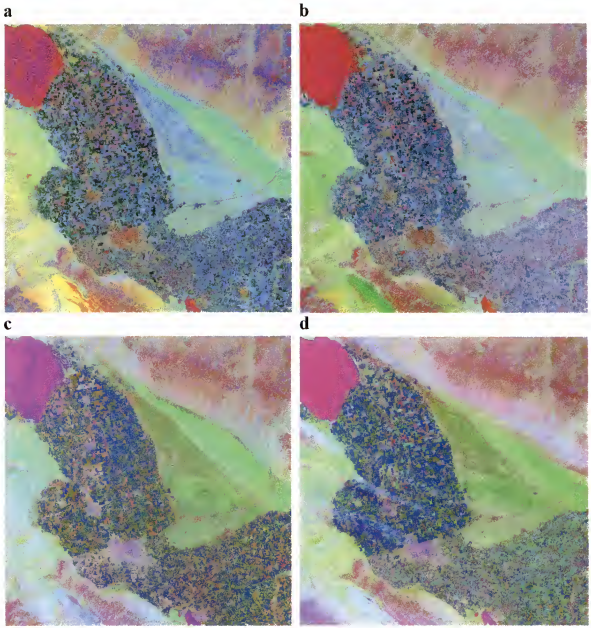

Fig 4-17. Principal component rasters from four Landsat subscenes on the Imperial Valley, CA. PC bands 2, 1 and 3 assigned to RGB. (a) August 31, 1994; (b) December 21, 1994; (c) February 23, 1995; (d) May 30, 1995.

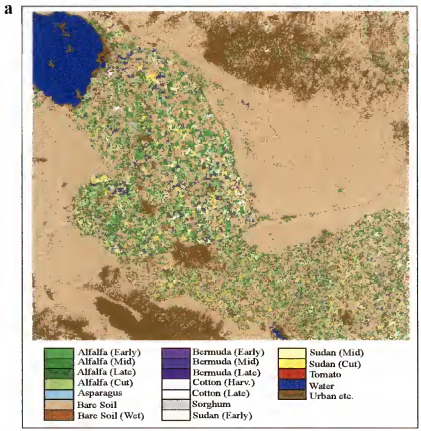

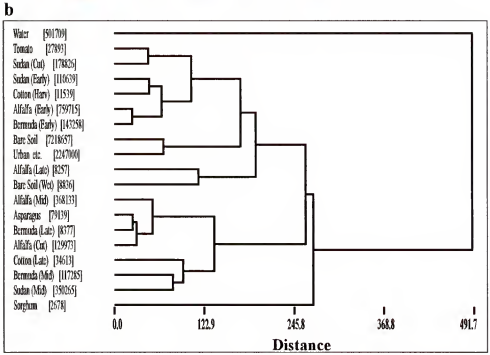

Fig. 4-18. Classified rasters and dendrograms from maximum likelihood classification of Landsat TM data on the Imperial Valley, CA. Number of cells in each class is in square brackets. Data are for (a & b) August 31, 1994; (c & d) December 21, 1994; (e & f) February 23, 1995;(g & h) May 30, 1995.

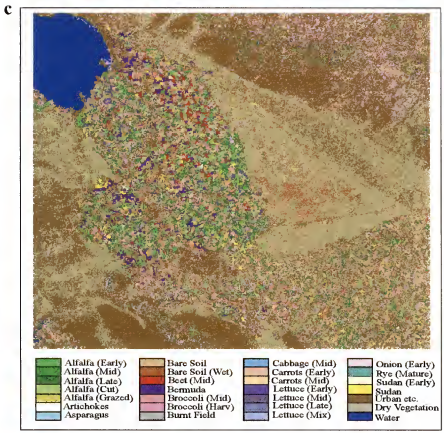

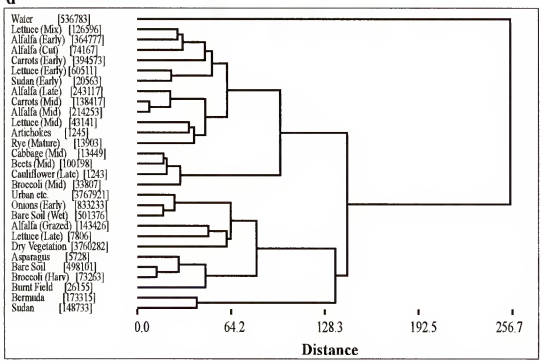

Fig. 4-18--continued

e

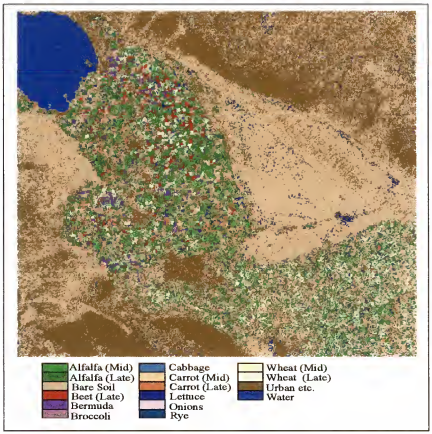

f

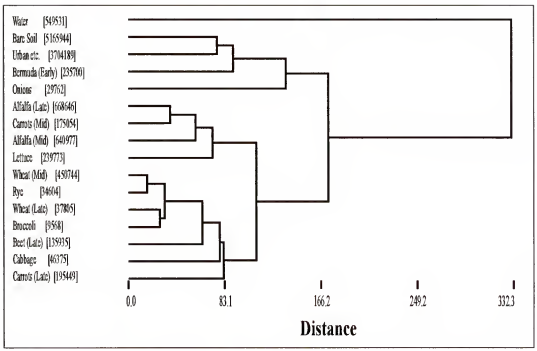

Fig. 4-18--continued

g

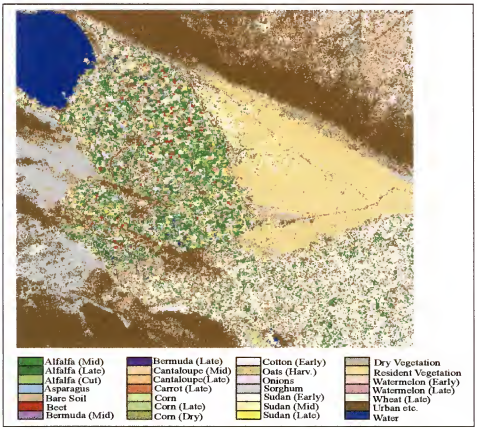

h

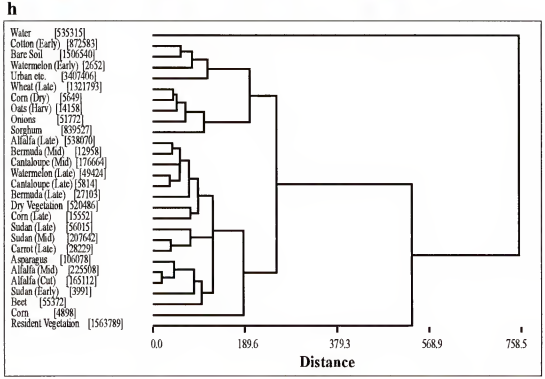

Fig. 4-18--continued

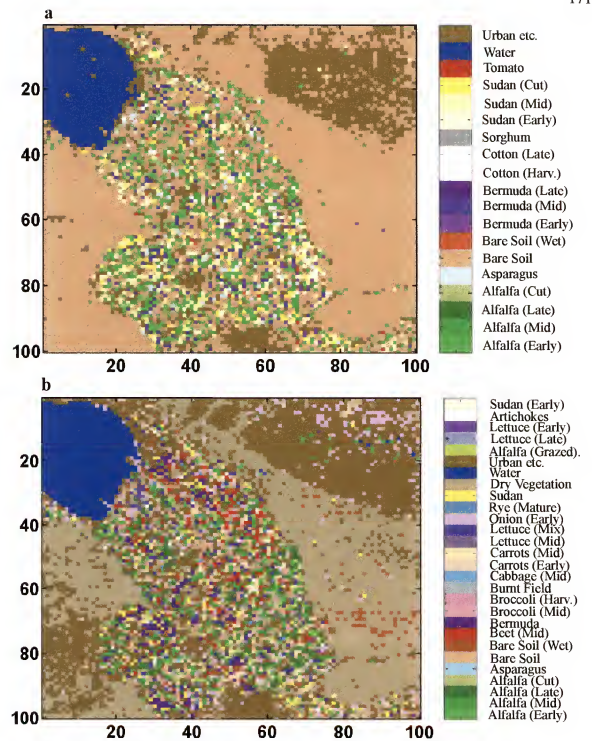

Fig. 4-19. Whitefly resource maps. Classified rasters for the Imperial Valley, CA. were clipped close to the Mexican border, filtered with a 3 x 3 majority filter and resampled (nearest neighbor) to 100 x 100 cells. Map dates are (a) August 31, 1994; (b) December 21, 1994; (c) February 23, 1995; (d) May 30, 1995.

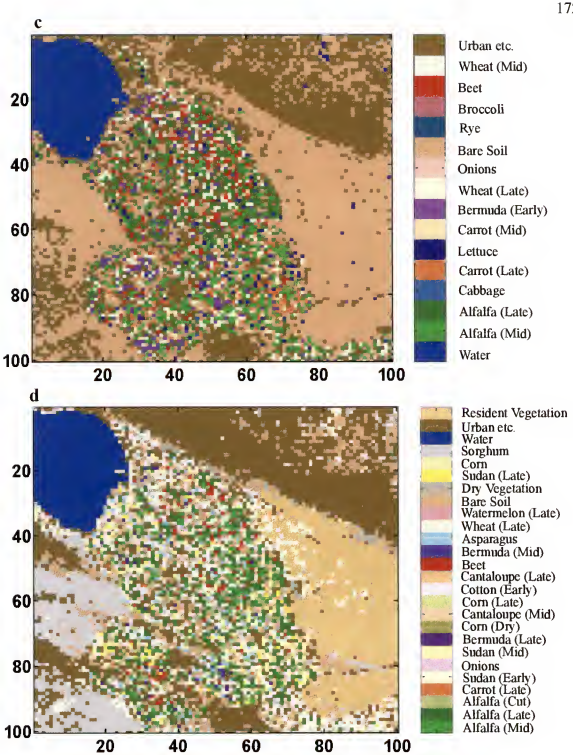

Fig. 4-19--continued

CHAPTER 5
SIMULATING THE DYNAMICS OF THE SILVERLEAF WHITEFLY IN AN ORGANIC CROPPING SYSTEM

Introduction

The dynamics of the sweetpotato whitefly, *Bemisia tabaci* (Gennadius), and to a lesser extent, the silverleaf whitefly, *Bemisia argentifolii* Bellows & Perring, in small- to medium-size cropping systems have been studied (Schuster et al. 1992, Hirano et al. 1993, Zalom et al. 1995). Many of these studies were done in monocultural cropping systems with field experiments (e.g., Dean 1994) or with field experiments combined with nonspatial simulation models to explore the insects' dynamics (von Arx et al. 1983, Baumgärtner et al. 1986, Baumgärtner & Yano 1990). Although these studies provided useful insights into the dynamics of these pests, the results could not usually be used to predict the insects' dynamics in similar size systems in which host plants varied temporally and spatially. Field experimentation combined with spatially explicit population models give us the ability to study and compare the dynamics of these insects in such varied systems.

The objectives of this chapter are two-fold. First, a field study of the dynamics of the silverleaf whitefly (SLW), *B. argentifolii* in a relatively small-scale heterogeneous cropping system with spatiotemporal variation in host plants is described. Next, the appropriateness of the spatially explicit age-structured model (eqn 2.12 in chapter 2) as a

tool for studying insect dynamics is demonstrated on this system. It must be emphasized that this is not a validation exercise per se, but one that serves to illustrate the utility of the SEPM for studying insect dynamics in temporally and spatially varying crop systems.

Materials and Methods

Study Site and Farm Layout

The study was conducted at a mixed-crop organic farm, Pine Island Organics, located on Pine Island, Florida (Fig. 4-1). The cropping area at the farm was divided into two fields with 14 and 12 blocks, respectively. Each block was planted with one of five main crops--tomato, eggplant, pepper, cucumber or zucchini. Blocks were separated from each other by a sugarcane windbreak.

Insect Population Sampling and Field Data

To facilitate insect population sampling and data collection, each block was divided into several plots. During the period September 1992 to January 1993, adult insect samples were collected weekly from each plot by beat-pan sampling. No samples were taken from sugarcane or resident vegetation. The beat-pan sampling method involved vigorously shaking the upper foliage of five plants from each plot over a black pan containing a thin layer of vegetable oil. Dislodged insects were identified and counted. Also at two week intervals, visual counts of insects were taken independently by commercial scouts on the same areas covered by the beat-pan sampling. Parasitism on whiteflies was determined by taking five leaves from tomato and eggplant plots every two weeks, placing them in paper cartons in the laboratory and observing for emergence of

whiteflies and their parasitoids. Percentage parasitism was then calculated by dividing the number of emerged parasitoids (x 100) by the number of emerged parasitoids and whiteflies (McAuslane et al. 1994, Simmons & Minkenberg 1994).

The Spatially Explicit Whitefly Model

A spatially explicit population model (SEPM) was used to simulate the dynamics of the silverleaf whitefly at Pine Island Organics. This model is described in detail in another chapter 2, but for convenience, some important characteristics of the model are briefly restated.

The model is a spatiotemporal age-structured Nicholson-Bailey model (Nicholson & Bailey 1935) that uses intergrodifference equations (IDEs) to simultaneously model insect dispersal and reproduction or growth (Kot & Schaffer 1986, Kot 1989, Murray 1989, Andersen 1991, Hasting & Higgins 1994, Neubert et al. 1995). Unlike many previous IDE models however, the spatial system in this study is two-dimensional. The IDEs for a prey-predator system with no age-structure in a two-dimensional environment can be written as

$$\begin{aligned} Y_{t+1}(l,m) &= \int_y \int_x K_Y(l-x, m-y)\, f(Y_t(x,y), Z_t(x,y))\, dx\, dy \\ Z_{t+1}(l,m) &= \int_y \int_x K_Z(l-x, m-y)\, g(Y_t(x,y)\, Z_t(x,y))\, dx\, dy \end{aligned} \qquad (5.1),$$

where Y_t and Z_t are the prey and predator in generation t, and f and g are their respective interaction functions. K_Y and K_Z are redistribution (dispersal) functions for prey and predator so that $K(l - x, m - y)$ gives the probability of insects moving from point x,y to

point *l,m* in the spatial system. Within each time step, each *K* is convolved separately with its respective interaction function over space thereby creating a density surface of redistributed individuals for each species. These convolutions are carried out efficiently by taking 2-dimensional Fourier transforms of the dispersal and interaction functions separately, multiplying them, and inverting the results back to the spatial domain with the inverse Fourier transforms. For simulations in discrete space, the double integrals in eqn (5.1) are replaced with double sums so that the *Ys* and *Zs* become matrices of prey and predator densities. The convolutions in this case are carried out using discrete Fast Fourier transforms and the results are instead spatial density matrices.

In the case of the Pine Island system, the model in eqn (5.1) was reformulated so that the SLW and natural enemy both have three age-classes with survival and partial development of individuals within each age-class. The spatially explicit nature of this model arises because the Pine Island system is represented by a grid (map) of whitefly resources, and although it is not explicitly included in the model, it is a spatial matrix that defines the structure of SLW resources at Pine Island Organics. State variables, parameters and functions in the model (eqn 2.12 in chapter 2) are given in Table 5-1 for the whitefly and natural enemy.

Reproductive and attack functions

The whitefly's reproductive function was a density-dependent Ricker function (Ricker 1954) with *exp(r)* representing the reproductive egg production per female per time period. The model assumes that a generic natural enemy could be used to represent the natural enemy complex of the whitefly. The searching efficiency (*a*) of this natural

enemy was a function of its density and was given by $a = Qp_i^{-m}$. (Hassell & Varley 1969, Hassell & May 1973). The importance of the mutual interference constant (m) in natural enemy interactions was alluded to by Hassell and May (1973) who reported m values between 0.28 and 0.69 from laboratory studies, and between 0.48 and 0.96 from field studies. These ranges were used to estimate starting values for m in the simulations.

Whitefly resource map

The construction of the SLW resource map at Pine Island Organics was previously described in chapter 4. A color-coded version of this map is given in Fig. 5-1a. The map is a spatial matrix, X, consisting of 128 x 128 cells that each represents an area of ≈ 18.92 m^2. This map contains consecutive integers starting at one that represent the resources at Pine Island Organics. Each integer (i) in this spatial resource map serves as an index to a row in a lookup table that contains SLW and natural enemy parameters. Since there are sixteen whitefly resource indices in the Pine Island system, the lookup table has sixteen rows of parameters.

Insect dispersal

Dispersal of both the whitefly and natural enemy was assumed to be local and random with no long-range migration during the study period. The effects of wind on insect movement were therefore ignored. Except in the simulations that used one type of experimental map (described later) where the sugarcane barriers were removed, it was assumed that a greater degree of spatial movement occurred in the east-west direction (x-direction) than in the north-south direction (y-direction). The above assumptions seemed reasonable considering the relative isolation of the farm on the island, the greater

dimension of the field blocks in the east-west direction, and the sugarcane barriers to movement in the north-south direction. Therefore, unless otherwise stated, a direction-biased normal density function such as

$$K(l,m,x,y) = \frac{1}{2\pi\sigma_x\sigma_y} exp\left(-\frac{1}{2}\left(\frac{(l-x)^2}{\sigma_x^2} + \frac{(m-y)^2}{\sigma_y^2} \right) \right) \qquad (5.2),$$

$$with \quad \sigma_x \neq \sigma_y$$

was chosen as the dispersal or redistribution function, K. In this function, σ_x and σ_y are the standard deviations of dispersal in the x- and y-directions, respectively. An unbiased 2-dimensional normal density function was used only in those simulations with the experimental map with no sugarcane barriers. The standard deviation of dispersal (σ) in all cases depended on the insect species and the host resource at each location. This parameter was therefore expected to be time-varying and to be at a maximum near host-plants senescence.

Model parameters

Estimates for most whitefly parameters came from the literature and were mainly for adult longevity, egg production, and egg and immature survival and development. Data on carrying capacity and spatial movement probabilities were lacking and where available were not crop specific. Based on host plant preference information and the levels of infestation observed, crops were ranked, and this ranking used to derive estimates for unknown parameters. Although the independently collected visual count data taken by commercial scouts were not statistically independent from the other sampling data since

they were collected during the same periods, these data were nevertheless used to derive estimates for natural enemy parameters.

Temperature and crop growth were the only driving or forcing variables on parameters. Temperature thresholds close to 10 °C (lower) and 32.2 °C (upper) have been quoted for whiteflies (Butler et al. 1983, Zalom et al. 1985, Powell & Bellows 1992a). Within these limits, rate processes tend to vary linearly with temperature (Worner 1992). Since average weekly temperature at Pine Island Organics for the period of study fell well within these established thresholds (Fig. 5-2a), rates were assumed to vary linear with temperature.

The forcing of parameters with crop growth was achieved by multiplying each parameter by a scaling factor, β_t, that was calculated from a cosine wave

$$\beta_t = 1 + \delta \cos\left(\frac{2\pi(ST - PT)}{CP} \right) \qquad (5.3),$$

that represented the crop's growth cycle (Fig. 5-2b). In eqn (5.3), δ ($0 < \delta > 1$) is the amplitude of the crop's cycle, ST is simulation time, PT is time at peak crop growth and CP, the crop's growth period. Since dispersal was expected to be maximum near crop senescence, the standard deviation of dispersal parameters (σ) were forced by a cycle that was approximately 180° out-of-phase with the crop cycle and that was also shifted to account for any lag in response time for dispersal as crop growth began to decline (Fig. 5-2b). Standard values for parameters used in the model are given in Table 5-2.

Simulations

The Pine Island Organics whitefly system was simulated using the simulation package, MATLAB® (MathWorks 1994). Simulations ran for 25 weeks on a weekly time step. Initial population densities are always very difficult to determine but because only the qualitative behavior of the model was important and not its ability to predict absolute whitefly densities, it was not critical that simulations be started with actual initial densities. Therefore each cell in the spatial grid was seeded with low random (0–1) densities of individuals in all whitefly age-class spatial matrices (*Y1*, *Y2*, *Y3*). An examination of the sampling data revealed that natural enemy densities were much lower than that of the whitefly. Therefore cells in the natural enemy age-class spatial matrices (*Z1*, *Z2*, *Z3*) were also seeded randomly as was done for the whitefly but the densities were lowered to account for differences in initial densities. These density matrices were saved and reused to initialize populations at the start of all simulations. In addition, a three week initialization period was used to allow the whitefly population to build before the natural enemy was introduced. During this period the resource map contained resources 1 and 2 (sugarcane and resident vegetation) only and the natural enemy was excluded. The full resource map and the natural enemy were introduced into the simulation after this three-week initialization period. Table 5-2 gives the parameter values used to generate the simulation output that qualitatively matched the adult SLW dynamics observed from the sampling data.

Comparing model output and sampling data

The sampling data were used to standardize the model's output so that the model could be used to explore SLW dynamics at Pine Island Organics. To determine the degree to which the sampling data and simulation results agreed, visual comparisons were made between the field sampling data and the simulation data for each resource after similar resources were lumped, scaled to 0–1, and plotted on the same graphs. Correlation analysis were used to quantify the visual comparisons and to compare simulated whitefly adult density maps with the observed density maps. These analysis were performed using the XCORR and CORR2 functions available in the signal processing and image processing toolboxes in MATLAB®. XCORR estimates the cross-correlation between two equal length n data sequences and returns a correlation coefficient sequence of length equal to the sum of the original sequences minus one. The nth element of this output sequence represents the correlation coefficient at zero lag, and is equivalent to the standard Pearson's correlation coefficient between the two data sequences. This procedure therefore estimate the correlation coefficients between two sequences at various lags (Krauss et al. 1993, Stearns & David 1996). CORR2 computes the two-dimensional correlation coefficient between two matrices (Thompson & Shure 1995). In the case of two n length vectors, the output is a single value equivalent to the value returned by XCORR at zero lag. Correlations and significant levels were verified in SigmaStat™ (Kuo et al. 1992).

Simulation experiments

One of the major advantages of spatially explicit population models is that it gives us the ability to experiment with different spatial arrangements in the resource map. To explore this possibility in the Pine Island system, a series of simulation experiments were conducted to explore SLW dynamics at Pine Island Organics. In the first experimental map similar crop types were grouped together. All solanaceous resources (tomato, eggplant and peppers) were grouped as much as possible within the same fields, as also were the cucurbits (cucumber and zucchini) (Fig. 5-1b). In the second experimental map, the sugarcane barriers between blocks were removed and replaced by resident vegetation (resource 2). This second map contained fifteen rather than sixteen resources (Fig. 5-1c). In both experimental maps, planting and harvesting dates for the crops were the same as in the original map.

The effects that changes in the resource map had on insect dynamics were determined by comparing simulations with the original Pine Island map with those using experimental SLW resource maps. Comparisons were made by estimating the relative differences (RDs) in adult densities in simulations with these maps. During simulations, the norm of adult densities in the adult spatial matrices for both the SLW and natural enemy were calculated using the NORM procedure in MATLAB® (MathWorks 1994). RDs between adult densities in simulations with the original and experimental maps were calculated as the differences between the Frobenius norms in both maps at each timestep, so that

$$RD_{Y3_t} = \|OM_{Y3_t}\| - \|EM_{Y3_t}\|$$

$$RD_{Z3_t} = \|OM_{Z3_t}\| - \|EM_{Z3_t}\| \qquad (5.4),$$

with OM = *original map*,
EM = *experimental map*

where $Y3_t$ and $Z3_t$ are whitefly and natural enemy adults at time t, and $\|.\|$ is the Frobenius norm (a measure of distance from zero). RDs of zero indicated no differences in adult densities between the maps. Positive RDs meant that the original map produced relatively higher densities compared with the experimental map, while negative RDs meant relatively higher lower densities compared with the experimental map. All simulations in the study were started with identical parameters and initial densities, but because the removal of the sugarcane barrier in the second experimental map (Fig. 5-1c) allowed for freer movement of both insects across blocks, an unbiased normal density dispersal function (eqn 2.14a) was used in these simulations as apposed to the function in eqn. 5.2..

Results and Discussion

Analysis of the beat-pan sampling data taken at Pine Island Organics suggested that tomato and eggplant were the most attractive host plants for whiteflies followed by cucumber and zucchini, and then pepper (Fig. 5-3). Whitefly numbers reached 529 adults/pan sample on tomato and 317 adults/pan sample on eggplant. Maxima of 160 and 35 adults/pan sample were obtained on cucumber and zucchini, respectively. On pepper, the highest number of whiteflies observed was 41 adults. Pepper was considered to be a poorer host than zucchini since overall whitefly numbers were generally lower. Sugarcane

and resident vegetation were not sampled but sugarcane was not expected to be a very good host for whiteflies. Resident vegetation on the other hand is known to harbor whiteflies and natural enemies (Evans 1992). Schuster et al. (1992) for example observed in west-central Florida that although low numbers of adult whiteflies were normally found on weeds, this resource acted as a reservoir for these insects after surrounding crops were harvested.

The host preference ranking in this study differs somewhat from observations made in studies done under controlled conditions with high quality hosts (Coudriet et al. 1985, Costa et al. 199, Wilholt et al. 1994). In the field, conditions are continuously changing especially with the succession of different host types and the variability in the quality of these hosts.

Time series data on beat-pan sampling and simulation data are given in Fig. 5-4. Each graph represents the collective data (after scaling) for a resource from one or more blocks. Fig. 5-4a for example shows data obtained from all blocks containing resource 4, tomato. Two distinct peaks in adult whitefly numbers were observed on tomato planted before late September (Figs. 5-4a,b). The first peak occurred in mid October while the second peak occurred in mid to late November. On tomato planted in late October however, adult numbers were generally lower and only one peak, in mid to late December, was observed (Fig. 5-4c). Whitefly populations on eggplant showed the same general trends (Fig. 5-4d,e). These trends most likely resulted from the interaction of planting date and temperature. Similar trends were observed by Dean (1994) in Florida where

whitefly numbers increased exponentially on spring tomatoes but fluctuated on fall tomatoes in a manner similar to that observed in this study.

Environmental temperature has always been considered an important determinant of whitefly population dynamics (Zalom et al. 1985, Byrne & Bellows 1991, Powell & Bellows 1992a,b). In simulations of whitefly populations on cotton, von Arx et al. (1983) concluded that temperature and the quality of host plants were more than likely the most important factors controlling whitefly dynamics. At Pine Island Organics, whiteflies infesting crops planted in September or early October were exposed to higher average temperatures (Fig. 5-2a) that resulted in shorter generation times and increased female fecundity. On the other hand, whiteflies infesting crops planted in late October were exposed to lower average temperatures and therefore had longer generation times and lower female fecundity.

Natural enemies were the main agent of whitefly control at the farm. Florida is renowned for its large fauna of whitefly natural enemies (Evans 1992, Dean 1994), and under situations of limited pesticide use, parasitism plays a very important role in limiting whitefly population increases. For example, in noninsecticide treated peanut fields in north-central Florida, up to 100% parasitism of whiteflies was observed (McAuslane et al. 1993, McAuslane et al. 1994). In this study, percentage parasitism on tomato and eggplant reached 80% during the season (Fig. 5-5).

Comparisons made between the beat-pan sampling data and the simulation results indicated that the qualitative dynamics from the simulations were similar to those observed in the field (Fig. 5-4). These comparisons yielded correlation coefficients greater than

0.65. The observed whitefly adult density maps also compared reasonably with the simulated adult density maps (Fig. 5-6). Cross-correlation analysis on the time series data in Fig. 5-4 however indicated that in some cases these data lagged each other by as much as two weeks (e.g. Figs. 5-4a,c). This may have resulted from the manner in which crop growth was represented (eqn 5.3, Fig. 5-2b) and from the estimates of natural enemy parameters. It was important to have good agreement between the model's output and field data (at least qualitatively) so that the model could be used to examine other scenarios that were likely to impact whitefly dynamics.

The simulation results were sensitive to natural enemy parameters. In particular, the initial densities of the natural enemy relative to the whitefly, the level of mutual interference (m) between natural enemy individuals, and the attack parameter (Q), affected the final whitefly dynamics in the system. Although there was a general increasing trend in parasitism in both field and simulated data, simulated percentage parasitism fluctuated during the season compared with the observed parasitism (Fig. 5-5). Differences between the two were likely due to the many unknown aspects of natural enemy behavior and the fact that one generic natural enemy was used to represent what is actually a group of several species in the field.

The simulations with the experimental whitefly resource maps showed the effects of changes in resource structure on SLW dynamics. The simulations also demonstrated an inherent advantage of spatially explicit models as tools for quickly exploring alternative habitat compositions and arrangements. Planting similar crop types within the same location generally lowered the densities of insects relative to the original arrangement

where crops were more dispersed (RDs were positive) (Fig. 5-7a). The dispersed spatial arrangement provided the whitefly with different types of resources that were in close proximity. The grouping of crops left gaps in the spatial resources at harvest and along with the sugarcane barriers prevented movement of the whitefly to other resources. On the other hand, removal of the sugarcane barriers improved the ability of both insects to move freely between blocks and provided the whitefly with additional hosts (RDs were negative). The result was relatively higher adult densities with this experimental map compared with the original map (Fig. 5-7b).

Concluding Remarks

The need for a better understanding of the relationships between insect population dynamics and host plant spatiotemporal variations in heterogeneous systems was highlighted with the silverleaf whitefly, *B. argentifolii* at Pine Island Organics. Spatiotemporal variations of host plants affects SLW dynamics, and some authors have suggested that such variation may be more important than climatic factors such as temperature in determining whitefly population fluctuations (Hirano et al. 1993). These authors believe that continuous cultivation of suitable host plants in time and space results in serious damage by these insects to crops that are planted later and that because these late season crops experience heavier whitefly damage earlier in their growth, they tend to support fewer whiteflies compared with earlier planted crops. Therefore, under the same conditions, differences in host plant spatiotemporal patterns are likely to result in differences in insects population infestation levels.

In a relatively small system like Pine Island Organics, it is fairly easy to test the effects of host plant arrangements on SLW dynamics with field experiments. However, spatiotemporal models like the one used in this study open the door to simulations of crop systems of much larger extent and suggests that we could design whole crop regions to minimize pest populations.

Table 5-1. State variables, parameters and functions in the spatiotemporal model for *Bemisia argentifolii* at Pine Island Organics.

Variable, Parameters and Functions	Description and functions
$Y1$, $Y2$, $Y3$	spatial matrices of whitefly egg, immature and adult densities
S_{Y1}, S_{Y2}, S_{Y3}	whitefly egg, immature and adult survival probabilities
D_{Y1}, D_{Y2}	whitefly egg, and immature development probabilities
$f(Y3)$	whitefly reproductive function (density-dependent Ricker function)
exp(r)	reproductive egg production per female per time period
K_Y	whitefly dispersal function or redistribution kernel
R_t	spatial matrix of redistributed whitefly reproduction
a	searching efficiency of natural enemy
Q	quest constant for natural enemy
m	mutual interference constant for natural enemy
$Z1$, $Z2$, $Z3$	spatial matrices of natural enemy egg, immature and adult densities
S_{Z1}, S_{Z2}, S_{Z3}	natural enemy egg, immature and adult survival probabilities
D_{Z1}, D_{Z2}	natural enemy egg, and immature development probabilities
K_Z	natural enemy dispersal or redistribution kernel
P_t	spatial matrix of redistributed natural enemy
σ_x,σ_y	standard deviation of dispersal in the *x*- and *y*-directions
X	spatial matrix of whitefly resources (resource or crop map)

Table 5-2. Standard parameter values used for *Bemisia argentifolii* and the natural enemy in the Pine Island simulations.

Resources	Model Parameters [a]											
	r	S_{Y1}	S_{Y2}	S_{Y3}	D_{Y1}	D_{Y2}	Q	m	S_Zs	D_Zs	σ_x [b]	σy [b]
Tomato	4.4	0.90	0.60	0.30	1.0	0.60	0.08	0.35	0.50	0.50	2.0	1.0
Eggplant	4.4	0.90	0.88	0.30	1.0	0.60	0.08	0.35	0.50	0.50	2.0	1.0
Cucumber	3.8	0.90	0.50	0.30	1.0	0.54	0.08	0.35	0.50	0.50	2.0	1.0
Zucchini	3.8	0.90	0.50	0.30	1.0	0.54	0.08	0.35	0.50	0.50	2.0	1.0
Pepper	3.3	0.90	0.10	0.30	1.0	0.10	0.08	0.35	0.50	0.50	3.0	1.5
R.V.[c]	4.0	0.90	0.80	0.30	1.0	0.40	0.25	0.35	0.50	0.50	6.0	3.0
Sugarcane	1.0	0.20	0.01	0.30	1.0	0.01	0.02	0.35	0.50	0.50	6.0	3.0

[a] Standard values are based on a weekly time step and average temperature of 25 °C
Y and *Z* in parameter subscript represent whitefly and natural enemy, respectively.
Sources for whitefly parameters include–Costa et al. 1991; Powell & Bellows 1992a,b; Wilhoit et al. 1994; Salas & Mendoza 1995; van Giessen et al. 1995; Yee & Toscano 1996; Tsai & Wang 1996.
Average values were used for most natural enemy parameters.

[b] Values are in units of grid cells. x and y represent east-west and north-south directions, respectively. The standard deviation of dispersal for the natural enemy was half that of the whitefly.

[c] RV. = Resident Vegetation.

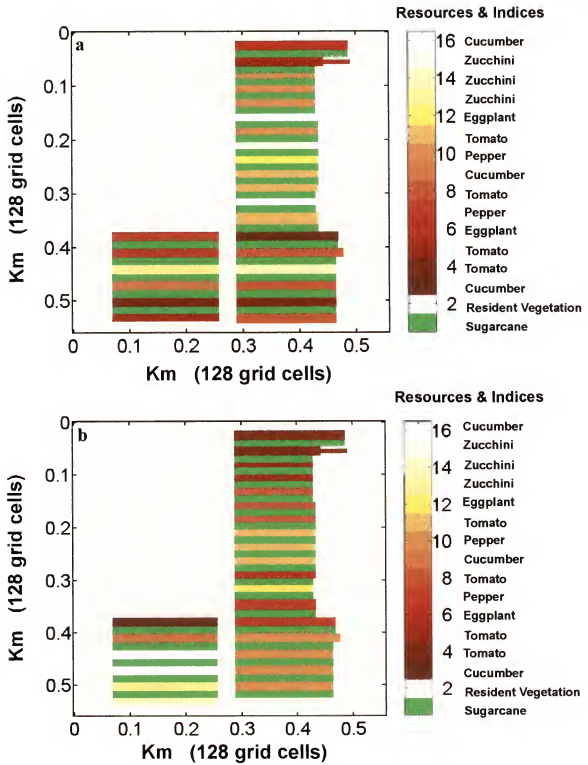

Fig. 5-1. Color-coded whitefly resource maps at Pine Island Organics, Pine Island, FL. (a) original resource map; (b) experimental resource map with resources grouped by plant Family; (c) experimental resource map with sugarcane barriers removed.

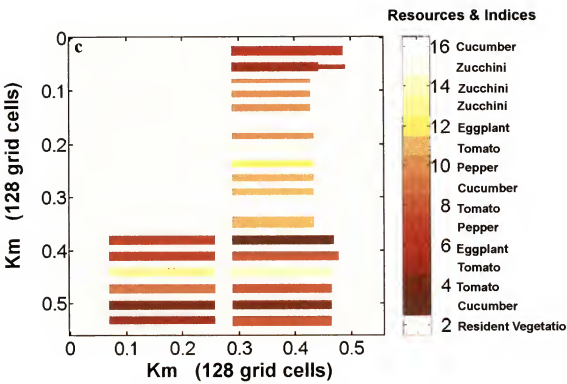

Fig. 5-1--continued

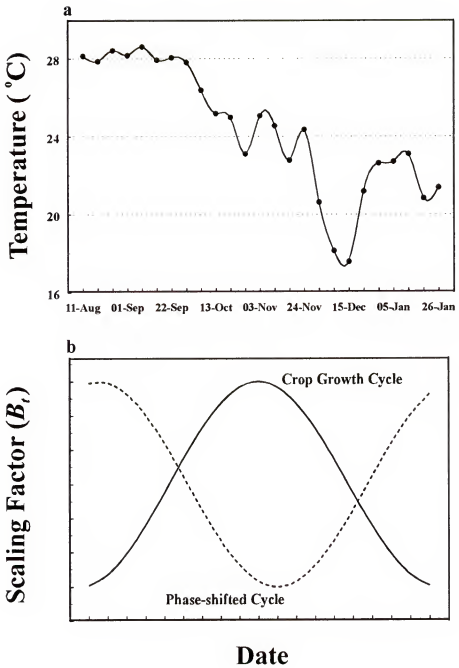

Fig. 5-2. Forcing or driving variables for parameters in the spatiotemporal model on whiteflies at Pine Island Organics, Pine Island, FL. (a) weekly average temperature; (b) an example of a crop growth cycle and that cycle 180° out-of-phase and shifted. The phase-shifted cycle forces dispersal.

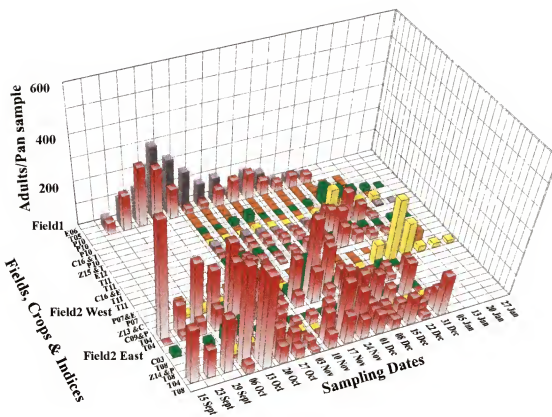

Fig. 5-3. Number of adult whiteflies collected by beat-pan sampling on the various crops at Pine Island Organics. Letters and numbers in the Field, Crops & Indices axis represent the crops and their resource indices, respectively. C16&T for example is cucumber, resource 16 followed by tomato; E06 is eggplant, resource 6; Z is zucchini, and P is pepper.

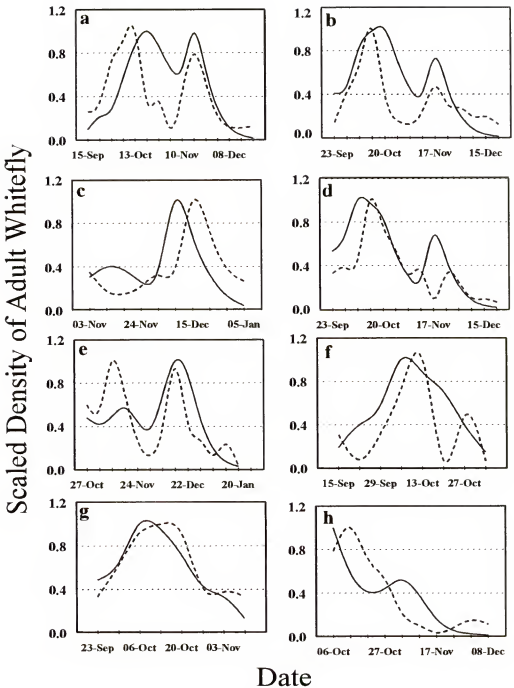

Fig. 5-4. Comparison of scaled beat-pan sampling data (---) with simulation results (—) for adult whiteflies at Pine Island Organics. (a) tomato, resource 4 ($r = 0.85$, $P < 0.001$); (b) tomato, resource 5 ($r = 0.90$, $P < 0.001$); (c) tomato, resource 11 ($r = 0.82$, $P < 0.01$; (d) eggplant, resource 6 ($r = 0.92$, $P < 0.001$); (e) eggplant, resource 12 ($r = 0.89$, $P < 0.001$); (f) cucumber, resource 3($r = 0.88$, $P < 0.005$); (g) zucchini, resource 13 ($r = 0.98$, $P < 0.001$); (h) pepper, resource 7 ($r = 0.88$, $P < 0.001$)

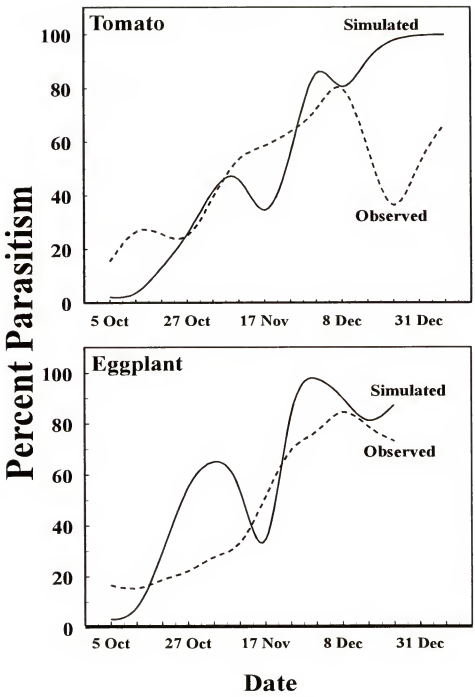

Fig. 5-5. Parasitism of whiteflies on tomato and eggplant at Pine Island Organics.

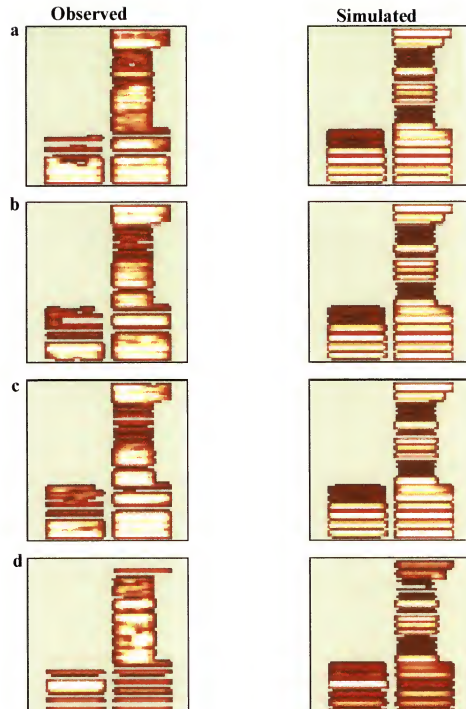

Fig. 5-6. Examples of comparisons of observed with simulated adult whitefly density maps at Pine Island Organics. Two-dimensional correlation coefficients for all comparisons were greater than 0.70. Highest densities are white. Map dates are (a) 17 November, 1992; (b) 24 November, 1992; (c) 1 December, 1992; (d) 7 January, 1993

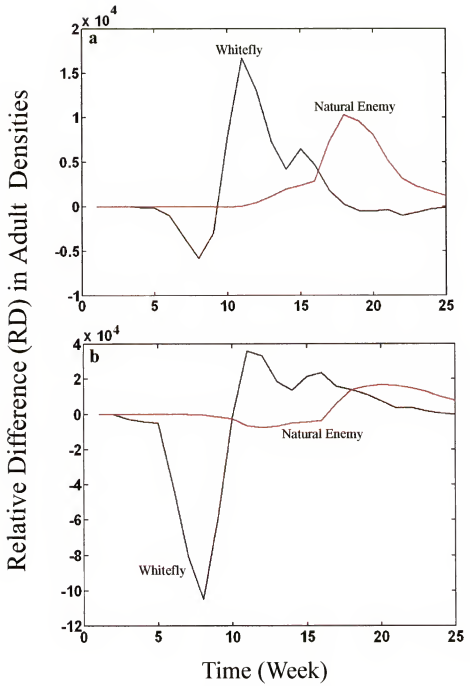

Fig. 5-7. Relative differences in whitefly and natural enemy densities at Pine Island Organics in simualtions with the original and experimental resource maps. RDs = 0 indicate no differences in densities with the original versus the experimental maps; positive RDs indicate that densities with the original map were higher; negative RDs indicate that densites with the experimental maps were higher. (a) RDs between the original map and an experimental map where resources were grouped by plant Family; (b) RDs between the original map and an experimental map with no sugarcane barriers.

CHAPTER 6
SIMULATING THE DYNAMICS OF THE SILVERLEAF WHITEFLY IN THE IMPERIAL VALLEY AGRICULTURAL SYSTEM

Introduction

The heavy economic losses suffered by farmers in agricultural regions throughout the southern United States as a result of attacks by the sweetpotato whitefly, *Bemisia tabaci*, and the silverleaf whitefly, *Bemisia argentifolii* (Duffus & Flock 1982, Gonzales 1992, Perring et al. 1993a, Schuster 1995) are ample evidence of the ability of these insects to invade regional agricultural cropping systems. The nomadic nature of these whiteflies is enhanced by their ability to exist as two dispersal morphs, trivial fliers and migrators (Berlinger 1986, Byrne & Houck 1990, Byrne et al. 1996), and by the large number of host plants that they can attack (Byrne & Miller 1990, Perring et al. 1992, Brown et al. 1995). The dynamics of both whiteflies are likely to be closely tied to crop patterns and natural environment factors in these systems and therefore must be studied under these conditions. Conducting a full set of field experiments to study these dynamics in large-scale systems would require tremendous effort. One feasible alternative is simulation modeling, but so far only one study has applied this methodology in exploring the dynamics of whiteflies in large-scale heterogeneous systems. Wilhoit et al. (1994) used a spatiotemporal model to evaluate various management strategies for the silverleaf whitefly in the Imperial Valley agricultural system.

In contrast to the previous study where the utility of the spatially explicit model (eqn. 2.12) as a tool for studying the dynamics of insects in spatiotemporal systems was demonstrated with the silverleaf whitefly, *Bemisia argentifolii*, in a relatively small system, this chapter highlights the model as a tool for exploring insect dynamics in large regional agricultural systems. In this case, the model is used to explore the dynamics of the SLW in the Imperial Valley agricultural system. The intention here is to show that the model can be used to study insect dynamics in spatial systems of varying sizes and scales.

Materials and Methods

Study Site: The Imperial Valley

The Imperial Valley is located in the extreme south of California on the Mexican Border and is bordered to the north by the Salton Sea. The supply of water from the All American canal has helped this desert region to become one of the major agricultural areas in the US.

The Spatially Explicit Whitefly Model

The spatially explicit population model (eqn 2.12) was modified slightly and used to simulate silverleaf whitefly (SLW) dynamics in the Imperial Valley. In the revised model

$$
\begin{aligned}
YI_{t+1} &= f(\hat{Y}3_t) + S_{Y1}(1-D_{Y1})\,YI_t \\
Y2_{t+1} &= S_{Y1}D_{Y1}\,YI_t + S_{Y2}(1-D_{Y2})\,Y2_t \exp(-aP_t) \\
Y3_{t+1} &= S_{Y2}D_{Y2}\,Y2_t \exp(-aP_t) + S_{Y3}\hat{Y}3_t \\
\\
Z1_{t+1} &= Y2_t\,(1-\exp(-aP_t)) + S_{Z1}(1-D_{Z1})\,ZI_t \\
Z2_{t+1} &= S_{Z1}D_{Z1}\,Z1_t + S_{Z2}(1-D_{Z2})\,Z2_t \\
Z3_{t+1} &= S_{Z2}D_{Z2}\,Z2_t + S_{Z3}\,Z3_t
\end{aligned}
\qquad (6.1),
$$

where

$$
\hat{Y}3_t(l,m) = \sum_{x=1}^{n}\sum_{y=1}^{n} K_Y(l-x,m-y)\,Y3_t(x,y))
$$

(*redistributed adult whiteflies*)

$$
P_t(l,m) = \sum_{x=1}^{n}\sum_{y=1}^{n} K_Z(l-x,m-y)\,Z3_t(x,y))
$$

(*redistributed adult natural enemy*)

adult whiteflies are redistributed directly instead of through their reproduction as was previously done (eqn 2.12). The reasons for making this change will be made clearer shortly.

Like the unmodified version of the model, the revised model combines a population model with resource maps that define the structure of the insect's resources in the Valley. The population model is a discrete-space age-structured Nicholson-Bailey (Nicholson & Bailey 1935) model with individuals in each age-class having distinct survival probabilities and partial development in each time step. State variables, parameters, and functions in this new model are given in Table 6-1.

A density-dependent Ricker function (Ricker 1954) was used as the whitefly's reproductive function so that at each location in the spatial system whitefly egg production was calculated by

$$f(\hat{Y}3_t) = \hat{Y}3_t \exp\left(r\left(1 - \frac{\hat{Y}3_t}{k}\right)\right) \qquad (6.2)$$

where $\hat{Y}3_t$ is a density matrix of redistributed adult female whiteflies, *exp(r)* is the egg production per female time period and k, the carrying capacity on the host resource. The reproductive parameter, r (natural log of eggs/female/week), and other parameters such as survival and development are matrices similar to the resource map. These spatial parameter maps are generated by assigning parameter values to the resources in the system. Therefore, the resource map and parameter look-up table idea were not applied directly as was done in the previous study on the Pine Island system. Using direct spatial parameter maps was much faster than looking up parameters from the index map.

Dispersal density functions or redistribution kernels determined the pattern of spatial movement for the insects. Movement was modeled with integrodifference equations (IDEs) and was accomplished by summing the dispersal of individuals into each point from all other points in the spatial system. In this case however, the dispersal density functions for both the whitefly and its natural enemy were coupled directly with the respective adult density matrices and solved using Fourier transforms. Previously, the problem of a spatiotemporal varying crop system was handled by applying the transforms one-at-a-time for each resource within a time step and summing the results. A different

approach was used here that allowed the transforms to be applied only once for the entire system at each time step. The revised model in eqn (6.1) takes advantage of this approach. In this alternative approach, an emigration probability matrix (EPM) for each insect is constructed and applied at each time step to the spatial density matrix to create an emigrant density matrix (EDM) of adults 'in flight.' The dispersal function is then convolved with this EDM thereby moving individuals in the air throughout the spatial system. In the whitefly's case, it is the redistributed adults ($\hat{Y}3$) that produce the next generation of offspring. The probabilities of individuals leaving and falling may be constants as in this case or could be made to vary with the state of resources on the ground.

The existence of separate dispersal morphs in whiteflies (Byrne & Houck 1990, Blackmer & Byrne 1993a,b, Byrne et al. 1996) and the openness of the Imperial Valley system encouraged the use of a dispersal function made up of a bimodal proportional mix of two dispersal functions, so that

$$K_{total} = pK_{trivial} + (1-p)K_{migrator} \qquad (6.3),$$

where p is the proportion of adult whiteflies in a source field that are trivial fliers and $K_{trivial}$ and $K_{migrator}$ are the dispersal density functions for the trivial fliers and migrators, respectively. K_{total} is then the bimodal proportional sum that integrates to one as a probability density (Allen et al. 1996). The dispersal function for the trivial fliers, $K_{trivial}$, was a symmetric two-dimensional normal density function

$$K_{trivial}(l,m,x,y) = \frac{1}{2\pi\sigma^2} exp\left(-\left(\frac{(l-x)^2 + (m-y)^2}{2\sigma^2}\right)\right) \quad (6.4),$$

while the dispersal function for the migrators, $K_{migrator}$, was

$$K_t(l,m,x,y) = \frac{1}{2\pi\sigma^2} exp\left(-\left(\frac{(l-\hat{x})^2 + (m-\hat{y})^2}{2\sigma^2}\right)\right) \quad (6.5),$$

$$where\ \hat{x} = (v_x t - x)\ and\ \hat{y} = (v_y t - y)$$

which is a time-dependent dispersal function that includes the effects of wind on migration. The standard deviation of dispersal per time step, σ, in both dispersal functions depended mainly on the insect species and to a lesser extent on the host resource at each location. In addition, dispersal, as in the model by Wilhoit et al.'s (1994), was assumed to be unaffected by temperature. Unlike their model however, dispersal was not restricted only to crop harvest.

Natural enemies are known to have a very limited impact upon whitefly populations in the Imperial Valley (Meyerdirk et al. 1986, Bellows & Arakawa 1988, Gill 1992). For this reason, Wilhoit et al. (1994) excluded natural enemies completely from their study. Therefore, although a natural enemy component that represented the natural enemy complex of whiteflies in the Valley was included in this present study, its ability to affect whitefly populations levels in the standard simulations was restricted.

Model Parameters and Parameter Maps

Life history data on whiteflies indicated that very little variability exists in whitefly egg development and survival, and adult longevity within the range of environmental conditions and host plants experienced by these insects in natural systems. Egg development times on different host plants were not usually significantly different and generally take between 6 to 8 days (Lopez-Avila 1986, Butler et al. 1983, Salas & Mendoza 1995, Yee & Toscano 1996, Tsai & Wang 1996). Under similar conditions, the proportion of eggs that survive is usually greater than 0.90 (Powell & Bellows 1992a, Salas & Mendoza 1995, Wagner 1995, Tsai & Wang 1996). On the other hand, fecundity and nymphal survival and development tend to be more variable (Powell & Bellows 1992a, Wagner 1995, Tsai & Wang 1996). Several studies also indicated that first instars suffer the most from climatic factors compared with other stages (Gerling et al. 1986, Horowitz 1986). Therefore, except at locations where there was not expected to be any stage development or survival (e.g., in water), egg development and survival were the same for all resources. Emphasis was placed on estimating parameters for immature survival (*SY2*), immature development (*DY2*), and fecundity.

The biology of whiteflies has not been studied on many of the crops identified in the Imperial Valley system. Parameter values were therefore estimated from the insect's biology on other crops and the attractiveness of these crops to the insect. Wilhoit et al. (1994) devised a rating system for the host plants in their simulations in which cotton was given a rating of 1.0 (Table 6-1). A similar rating system was implemented for this study

based partly on the system used by Wilhoit et al. (1994) and additional information obtained from the literature (Table 6-2).

Primary parameter maps corresponding to each whitefly resource map were generated for whitefly reproduction, immature survival and development (Figs. 6-1, 6-2, 6-3). At each weekly time step during simulations with the model, intermediate parameter maps were generated from the primary parameter maps by simple linear interpolation. For example, in the simulation package MATLAB® (MathWorks 1994), fifteen weekly immature survival parameter maps (M_t) were generated during the period August 31 to December 21, 1994. These were generated using the primary parameter maps for August (M_{Aug}) and December (M_{Dec}) in the equation

$$M_t = M_{Aug} + t\left(\frac{M_{Dec} - M_{Aug}}{t_{Dec} - t_{Aug}}\right), \quad 2 \le t \le 16 \tag{6.6}.$$

In the above example, t_{Aug} =1 and t_{Dec} =17 are the values that correspond to the M_{Aug} and M_{Dec} maps, respectively, since these maps were separated by fifteen weeks. In the first week of simulation the M_{Aug} parameter map (matrix) was used directly. In the second week of simulation a new map was constructed using eqn (6.6) with $t = 2$. This process was repeated for each week of simulation up to week sixteen where $t = 16$, and at $t = 17$, the M_{Dec} map was used directly as the parameter map. In the following period, the M_{Dec} map from the previous period was used with the February map (M_{Feb}) with $t_{Dec} = 1$ and $t_{Feb} = 10$. This procedure was repeated for generating weekly parameter maps for other periods.

The value for carrying capacity, k, in eqn (6.2) was based on Wilhoit et al.'s (1994) estimate that was computed from data given in Riley & Wolfenbarger (1993). From these data, they estimated a carrying capacity of 4.5×10^7 whitefly adults per acre in cotton. They noted that this value may never be reached in the field since crops are usually harvested before this occurs. Their value was adopted for this study and was assumed to be constant at all spatial locations in the system.

Temperature was the main forcing variable on parameters in the model. Hourly temperature data for the period of the study were obtained from three weather stations in the Valley. These were the Calipatria weather station in the north, the Seeley station in the south-west and the Meloland station in the south-east of the Valley. The hourly temperature data were synthesized and used to derive daily average minimum and maximum temperatures at each site (Fig. 6-4a,b,c,). The daily pattern of temperature at the three sites was very similar (Fig. 6-4a,b,c,) and therefore these data were combined to derive average daily temperatures for the Valley (Fig. 6-4d). A cosine function of the form

$$T_t = T_{mean}\left(1 + \delta\cos\left(\frac{2\pi}{P}\left(t - peak\right)\right)\right) \qquad (6.7),$$

was fitted to these data that generated an overall average temperature cycle. T_{mean} is average temperature, δT_{mean} $(0 < \delta < 1)$ is the amplitude of the cycle, t is the present time, *peak* is time at peak temperature and P is the period of the temperature cycle (Fig 6-4d).

The annual cycle of average daily or weekly temperatures (Fig 6-4d) may be calculated by applying

$$T_{day} = 21.5\left(1 + 0.6 * \cos\left(\frac{2\pi}{365}\left(day - 192\right)\right)\right)$$
$$T_{week} = 21.5\left(1 + 0.6 * \cos\left(\frac{2\pi}{52}\left(week - 27\right)\right)\right) \quad (6.8)$$

The extent of whitefly dispersal in the model was influenced by the direction and speed of winds in the Valley. Since no data on wind flow patterns throughout the entire Valley were available, wind data from the weather stations at Calipatria, Meloland and Seeley were used to estimate wind directions and speed for the model. Hourly wind directions and speed recorded at each station for the period July 1, 1994 to June 30, 1995 were obtained, but because whitefly dispersal is usually restricted to the early morning hours between 6 a.m. and 10 a.m. when temperatures and wind speeds are generally low (Byrne & von Bretzel 1987, Bellows et al. 1988, Blackmer & Byrne 1993a, Blackmer & Byrne 1993b), only the data between these times were used. The average and standard deviation of wind direction for the selected data were determined by methods outlined in Zar (1984) for circular data and these were used to predict the pattern of wind flow in the Valley (Fig. 6-5).

The insects were dispersed within each weekly time step in the model. At each dispersal, a random component was added to both wind direction and speed based on the calculated standard deviations for these components. This was accomplished with

$$W = \hat{W} + \sigma_W * N(0,1) \tag{6.9}$$

where $\hat{W}$ is mean wind direction or speed, σ_W is the standard deviation of $\hat{W}$, and $N(0,1)$ is a standard normal deviate with mean zero and standard deviation one. Changes in the direction and distance of the whitefly's migrator dispersal patterns around a central trivial flier distribution in successive dispersal steps can be seen in the montage of images in Fig. 6-6. In Fig. 6-5d, it is observed that morning winds in the Valley rarely came from the north-east. During this period, winds come mainly from the south-east and south-west. This explains the distribution of the migrator dispersal patterns in the north-east, north-west, and south-east sections of the images in Fig. 6-6.

Simulating Whitefly Dynamics in the Imperial Valley System

Simulations examined the annual dynamical patterns of whiteflies in the Imperial Valley. It was assumed that little variation in the structure of the agricultural landscape in the Valley occurred between years and therefore the spatiotemporal arrangement of crops remained the same. This assumption allowed continuous simulations to be carried out for a number of years by recycling the parameter maps.

The spatial system consisted of a square 100 x 100 grid with each cell representing a quarter section (0.5 mi x 0.5 mi). Each cell therefore represented one quarter-square-mile or approximately 150 acres (61 ha). At the start of each simulation run all cells except those that were known to be free of whiteflies (e.g., cells in water) were seeded with a low random (0–1) density of individuals in each whitefly and natural enemy age-

class. For consistency, the initial population density matrices were saved and reused to initialize all simulations.

The qualitative dynamics were observed for whitefly adults in the whole system and separately for crops such as alfalfa, cotton, cole crops (cabbage and broccoli), and melons. The effects on dynamics from the removal of these crops from the system were also explored.

The Model by Wilhoit et al. (1994)

A brief review of the model by Wilhoit et al. (1994) and its results are given before proceeding to the results of the study in this paper. These authors developed their computer simulation model to "evaluate various regional strategies for managing the silverleaf whitefly in the Imperial Valley."(p. 1) In their model, the Valley was represented as a 36 x 42 rectangular grid with one-square-mile cells or sections. The model kept track of the dynamics of the whitefly on nineteen spatially and temporally varying crops. Only adult whiteflies were considered and natural enemies were excluded. Degree days were used to include temperature effects in the model. Wilhoit et al. (1994) assumed that whiteflies left the section only when the crop they were on was harvested and that they were passively redistributed by wind. This passive movement was achieved with a Gaussian plume function that generated a 35 x 35 two-dimensional grid of values representing the proportions of individuals that fell into cells around a central point.

They noted that simulations with their model gave qualitative dynamics that were consistent with their knowledge of whitefly dynamics in the Imperial Valley. Low whitefly

populations were observed during the early part of the year with large increases taking place in spring primarily because of the presence of spring melons. Harvesting of spring melons resulted in a drop in populations as adult whiteflies migrated to cotton. Harvesting of cotton caused a shift in populations back to melons and cole crops, and exponential population growth was again observed. In addition, removal of alfalfa had the largest effect on whitefly population levels resulting in a 67% reduction. Alfalfa was followed closely by melon, cotton, and the cole crops in the effect on whitefly population levels.

Results and Discussion

A five year simulation run with the standard parameter maps produced populations of adult whiteflies in the Imperial Valley system that peaked twice each year (Fig. 6-7a). There was an increase in regional populations in early- to mid-spring where growth was exponential. A decline in population levels occurred in late June but populations increased again in August and September before declining again near the end of the year (Fig. 6-7b). These trends were similar to those observed by Wilhoit et al.(1994). In their simulations and from their knowledge of the dynamics of whiteflies in the Imperial Valley they found that whitefly populations are generally low at the start of the calendar year. Large increases in population levels occurres in early spring on melons planted during this period. Population levels then decline because melons are harvested and whiteflies move to cotton and show an exponential increase in population. After cotton is harvested, another decrease in population takes place as populations move to cole crops and fall melons, and exponential growth is once again observed.

The results of simulations to test the effect of alfalfa removal from the Imperial Valley system is given in Fig. 6-8. Adult populations in the system where no alfalfa is grown are much lower indicating that alfalfa has a significant effect on the population levels of whiteflies in the Valley. The extent of the difference in the overall annual average of whitefly abundance with and without alfalfa was determined by taking the ratio of the sum of whitefly densities. From the simulation it appears that planting alfalfa results in a 6.4-fold increase in overall whitefly abundance in the Valley. This may be due to the fact that alfalfa is a perennial that makes up more than 35% of the agricultural acreage in the Valley (Imperial County Agricultural Commissioner's Office 1994). Wilhoit et al. (1994) reported a 67% reduction in whitefly population when no alfalfa was planted.

Wihoit et al. (1994) tested the effects of an alfalfa dry down period with their model. In the dry down period, farmers do not grow alfalfa for a period of six or more weeks. In their model, this period ran from 23 July to 8 October. A similar strategy was included in the scenarios tested with the model in this study. The results indicate that a dry down period also reduces overall whitefly populations but not to the same extent as the complete removal of alfalfa (Fig. 6-9). Overall whitefly abundance without the dry down period was 2.75 times higher than with the dry down period. Wilhoit et al. (1994) reported a 58% reduction in whitefly population with the dry down period and noted that periods of dry down shorter than 6 weeks had little effect on populations.

The effects on adult populations of the removal of cotton, spring melons and cole crops such as cabbages and broccoli were tested. Cotton was second to alfalfa in its effect on whitefly densities after removal (Fig. 6-10), followed by spring melons (Fig. 6-11) and

cole crops (Fig. 6-12). The presence of cotton, spring melons and cole crops increased whitefly abundance 1.25, 1.10 and 1.03 times, respectively. These observations were slightly different to those made by Wilhoit et al. (1994) who found that spring melons had a greater impact on whitefly population levels (57%) than did cotton (46%). Reasons for the reversal in these trends are not immediately obvious.

Finally, whitefly population trends on alfalfa and cotton were examined (Fig. 6-13). Whitefly population trends on alfalfa compared reasonably with trends reported in other studies. Meyerdirk and Coudriet (1986) presented data collected by yellow sticky cards that showed the flight activity of *B. tabaci* in alfalfa fields in the Imperial Valley. These data showed that whitefly activity was low in July but increased rapidly through late October after which there was a decline until March the following year. Activity also seemed to increase once more in March, April and May before declining again in June. Wilhoit et al. (1994) with their model observed that whitefly population levels in alfalfa began to increase in late June and continued this way until October when population levels declined. Cotton is probably the most widely studied whitefly host plant and therefore several sources of data were available for comparison with whitefly population trends on cotton generated by this model. Meyerdirk and Coudriet (1986) also presented data for whiteflies trapped with yellow sticky cards near cotton fields. They indicated that whitefly population levels generally increased from late June to September and that this increase continued until November under favorable weather conditions. Youngman et al. (1986) studied seasonal trap counts in several cotton fields in the Valley and also observed increases in whitefly activity from July to October. These trends were also later observed

by Blua et al. (1994) who found that whitefly abundance accelerated between July and September. Finally, Wihoit et al. (1994) in their simulations observed an increase in whitefly population between late June and September. These studies all indicate that whitefly population levels observed on cotton in the simulations conducted in this study peaked rather early. The reasons for this are not immediately clear but may have resulted from the time shift caused by ground truth data and satellite data asynchrony that causes the incorrect assignment of cotton during classification to fields that either contained other resources or an earlier stage of cotton.

Table 6-1. State variables, parameters and functions in the spatiotemporal model for the silverleaf whitefly, *Bemisia argentifolii* in the Imperial Valley, CA.

Variable, parameters and functions	Description
$Y1$, $Y2$, $Y3$	spatial matrices of whitefly egg, immature and adult densities
$\hat{Y}3$	spatial matrix of redistributed adult whitefly
S_{Y1}, S_{Y2}, S_{Y3}	whitefly egg, immature and adult weekly survival probabilities
D_{Y1}, D_{Y2}	whitefly egg, and immature weekly development probabilities
$f(\hat{Y}3)$	whitefly reproductive function (density-dependent Ricker function)
r	matrix of natural log of eggs/female/week
K_t	whitefly trivial flier dispersal function or redistribution kernel
K_m	whitefly migrator dispersal function or redistribution kernel
p	proportion of dispersing adults that are trivial fliers
σ_t,σ_m	standard deviation of dispersal for trivial fliers and migrators (in grid cell units).
$LY3$	emigration probability matrix for adult whiteflies
$FY3$	matrix of probabilities of falling for adult whiteflies
a	searching efficiency of the natural enemy
Q	quest constant for the natural enemy
m	mutual interference constant for natural enemy
$Z1$, $Z2$, $Z3$	spatial matrices of natural enemy egg, immature and adult densities
S_{Z1}, S_{Z2}, S_{Z3}	natural enemy egg, immature and adult weekly survival probability
D_{Z1}, D_{Z2}	natural enemy egg, and immature weekly development probabilities
K_Z	natural enemy dispersal or redistribution kernel
P_t	spatial matrix of redistributed natural enemy
σ_z	standard deviation of dispersal (in grid cell units)
$LZ3$	emigration probability matrix for adult natural enemy
$FZ3$	matrix of probabilities of falling for adult natural enemy

Table 6-2. Parameter values for *Bemisia argentifolii* reproduction, immature survival and development in the Imperial Valley whitefly simulation model.

Map Date	Resources	Scale		Parameters [a]		
		Wilhoit et al. (1994)	This Study	*r*	*SY2*	*DY2*
Aug 31, 1994	Alfalfa (Early)	0.385	0.656	3.15	0.89	0.47
	Alfalfa (Mid)	0.385	0.656	3.15	0.89	0.47
	Alfalfa (Late)	0.385	0.328	1.57	0.89	0.47
	Alfalfa (Cut)	0.385	0.164	0.79	0.29	0.47
	Asparagus	0.15	0.222	1.07	0.20	0.13
	Bare Soil	----	0.100	0.48	0.20	0.02
	Bare Soil (Wet)	----	0.100	0.48	0.20	0.02
	Bermuda (Early)	----	0.020	0.10	0.20	0.02
	Bermuda (Mid)	----	0.020	0.10	0.20	0.02
	Bermuda (Late)	----	0.020	0.10	0.20	0.02
	Cotton (Harv)	----	0.200	0.96	0.20	0.47
	Cotton (Late)	1.000	0.500	2.40	0.87	0.59
	Sorghum	0.015	0.025	0.12	0.20	0.02
	Sudan (Early)	----	0.020	0.10	0.20	0.02
	Sudan (Mid)	----	0.020	0.10	0.20	0.02
	Sudan (Cut)	----	0.020	0.10	0.20	0.02
	Tomato	0.39	0.786	3.77	0.40	0.46
	Water	----	0.000	0.00	0.00	0.00
	Urban etc.	----	0.300	1.44	0.40	0.46
Dec 21, 1994	Alfalfa (Early)	0.385	0.656	3.15	0.89	0.47
	Alfalfa (Mid)	0.385	0.656	3.15	0.89	0.47
	Alfalfa (Late)	0.385	0.328	1.57	0.89	0.47
	Alfalfa (Cut)	----	0.164	0.79	0.29	0.47
	Asparagus	0.150	0.222	1.07	0.20	0.13
	Bare Soil	----	0.100	0.48	0.20	0.47
	Bare Soil (Wet)	----	0.100	0.48	0.20	0.47
	Beets (Mid)	0.200	0.630	3.02	0.57	0.17
	Bermuda	----	0.020	0.10	0.20	0.02
	Broccoli (Mid)	1.080	1.080	5.18	0.97	0.48
	Broccoli (Harv)	----	0.500	2.40	0.97	0.48

Table 6-2--continued

Map Date	Resources	Scale		Parameters [a]		
		Wilhoit et al. (1994)	This Study	*r*	*SY2*	*DY2*
	Burnt Field	----	0.100	0.48	0.20	0.47
	Cabbage (Mid)	1.080	1.080	5.18	0.97	0.48
	Carrots (Early)	0.200	0.296	1.42	0.57	0.31
	Carrots (Mid)	0.200	0.296	1.42	0.57	0.31
	Lettuce (Mid)	0.200	0.802	3.85	0.57	0.56
	Lettuce (Mixed)	0.200	0.802	3.85	0.57	0.56
	Onions (Early)	0.015	0.025	0.12	0.20	0.02
	Rye (Mature)	----	0.020	0.10	0.20	0.02
	Sudan	----	0.020	0.10	0.20	0.02
	Dry Vegetation	----	0.200	0.96	0.20	0.02
	Water	----	0.000	0.00	0.00	0.00
	Urban	----	0.300	1.44	0.40	0.46
	Alfalfa (Grazed)	----	0.200	0.96	0.89	0.47
	Lettuce (Late)	0.200	0.508	2.44	0.57	0.56
	Lettuce (Early)	0.200	1.020	4.90	0.57	0.56
	Artichokes	----	0.222	1.07	0.20	0.13
	Sudan (Early)	----	0.020	0.10	0.20	0.02
Feb 23, 1995	Water	----	0.000	0.00	0.00	0.00
	Alfalfa (Mid)	0.385	0.656	3.15	0.57	0.47
	Alfalfa (Late)	0.385	0.328	1.57	0.57	0.47
	Cabbage	1.080	1.080	5.18	0.97	0.48
	Carrots (Late)	0.200	0.296	1.42	0.57	0.31
	Lettuce	0.200	0.802	3.85	0.57	0.56
	Carrots (Mid)	0.200	0.296	1.42	0.57	0.31
	Bermuda (Early)	----	0.020	0.10	0.20	0.02
	Wheat (Late)	0.015	0.025	0.12	0.20	0.02
	Onions	0.015	0.025	0.12	0.20	0.02
	Bare Soil	----	0.100	0.48	0.20	0.47
	Rye	----	0.020	0.10	0.20	0.02
	Broccoli	1.08	1.080	5.18	0.97	0.48
	Beets (Late)	0.20	0.630	3.02	0.57	0.17

Table 6-2--continued

Map Date	Resources	Scale		Parameters [a]		
		Wilhoit et al. (1994)	This Study	*r*	*SY2*	*DY2*
	Wheat (Mid)	0.015	0.025	0.12	0.20	0.02
	Urban (etc.)	----	0.300	1.44	0.40	0.46
May 30, 1995	Alfalfa (Mid)	0.385	0.656	3.15	0.57	0.47
	Alfalfa (Late)	0.385	0.328	1.57	0.57	0.47
	Alfalfa (Cut)	0.385	0.164	0.79	0.29	0.47
	Carrot (Late)	0.2	0.469	2.25	0.57	0.31
	Sudan (Early)	----	0.020	0.10	0.20	0.02
	Onions	0.015	0.025	0.12	0.20	0.02
	Sudan (Mid)	----	0.020	0.10	0.20	0.02
	Bermuda (Late)	----	0.020	0.10	0.20	0.02
	Corn (Dry)	0.015	0.025	0.12	0.20	0.02
	Cantaloupe (Mid)	1.540	0.948	4.55	0.94	0.49
	Corn (Late)	0.015	0.025	0.12	0.20	0.02
	Cotton (Early)	1.000	1.000	4.80	0.84	0.48
	Cantaloupe (Late)	1.540	0.948	4.55	0.94	0.49
	Beet	0.200	0.630	3.02	0.57	0.17
	Bermuda (Mid)	----	0.020	0.10	0.20	0.02
	Asparagus	0.150	0.222	1.07	0.20	0.13
	Wheat (Late)	0.015	0.025	0.12	0.20	0.02
	Watermelon (Late)	1.540	1.030	4.94	0.60	0.49
	Bare Soil	----	0.100	0.48	0.20	0.02
	Dry Vegetation	----	0.200	0.96	0.00	0.02
	Sudan (Late)	----	0.020	0.10	0.20	0.02
	Corn	0.015	0.025	0.12	0.20	0.02
	Sorghum	0.015	0.025	0.12	0.20	0.02
	Water	----	0.000	0.00	0.00	0.00
	Urban etc.	----	0.300	1.44	0.40	0.46
	Res. Veg.	----	0.020	0.10	0.20	0.02

[a] At 27 °C and a weekly time step. Data sources included: Butler & Henneberry (1983), Coudriet et al. (1985), Coudriet et al. (1986), Byrne et al. (1989), Costa et al. (1991a, b), Bethke et al. (1991), Powell &Bellows (1992a,b), Blua & Toscano (1994), Blua et. al. (1995), Salas & Mendoza (1995), Wagner (1995), Yee & Toscano (1996), Tsai & Wang (1996).

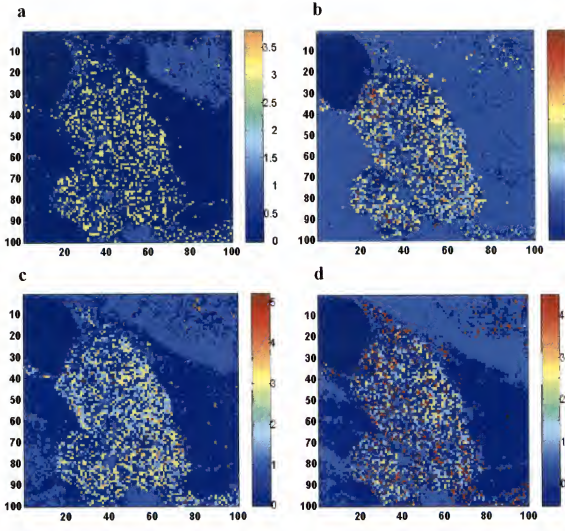

Fig. 6-1. Silverleaf whitefly reproduction parameter (r) maps for the Imperial Valley, CA. The colorbar next to each map shows the range of r values per week at 27 °C. Total weekly egg production per female on each resource is $exp(r)$. Map dates are (a) August 31, 1994; (b) December 21, 1994; (c) February 23, 1995; (d) May 30, 1995.

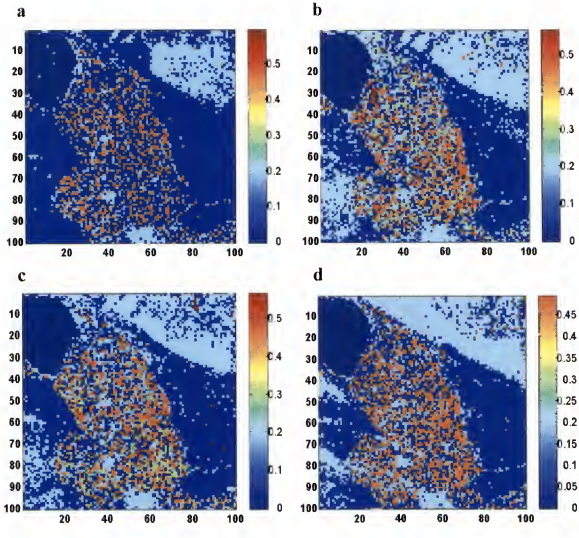

Fig. 6-2. Silverleaf whitefly immature stage development parameter (*DY2*) maps for the Imperial Valley, CA. The colorbar next to each map shows the proportion of immature whiteflies that develop each week on each resource at 27 °C. Map dates are (a) August 31, 1994; (b) December 21, 1994; (c) February 23, 1995; (d) May 30, 1995.

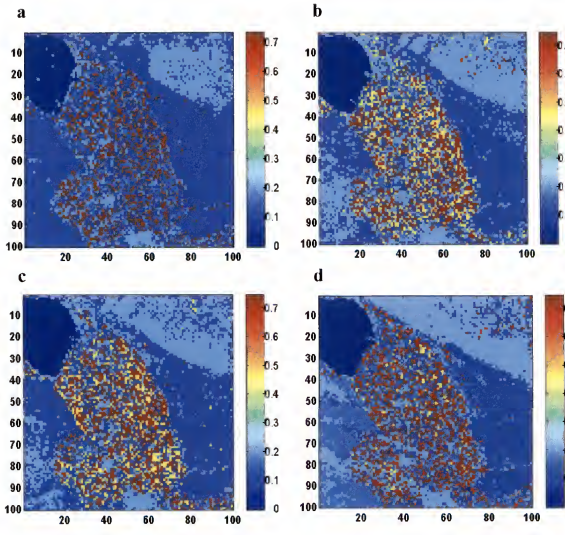

Fig. 6-3. Silverleaf whitefly immature stage survival parameter (*SY2*) maps for the Imperial Valley, CA. The colorbar next to each map shows the proportion of immature whiteflies that survive each week on each resource at 27 °C. Map dates are (a) August 31, 1994; (b) December 21, 1994; (c) February 23, 1995; (d) May 30, 1995.

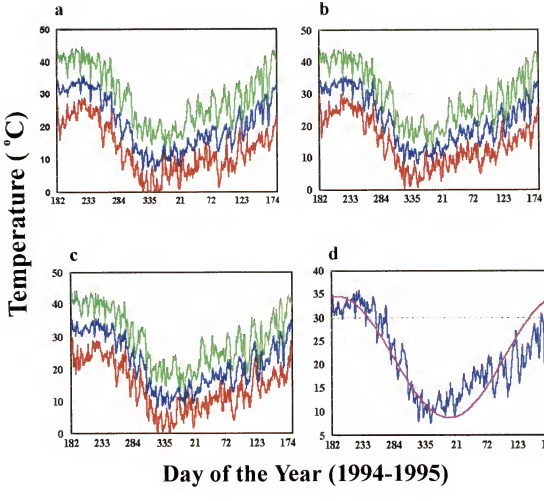

Fig. 6-4. Temperature at three weather stations in the Imperial Valley, CA for the period July 1994 to June 1995 . (a) minimum, maximum, and average temperature at Calipatria; (b) minimum, maximum, and average temperature at Meloland; (c) minimum, maximum, and average temperature at Seeley; (d) average temperature for all three sites, and a fitted temperature cycle. The fitted daily temperature cycle is given by 21.5(1 + 0.6 cos(((2*pi)/365)*(day - 192)), while 21.5(1 + 0.6 cos(((2*pi)/52)*(week - 27)) can be used to obtain a weekly temperature cycle.

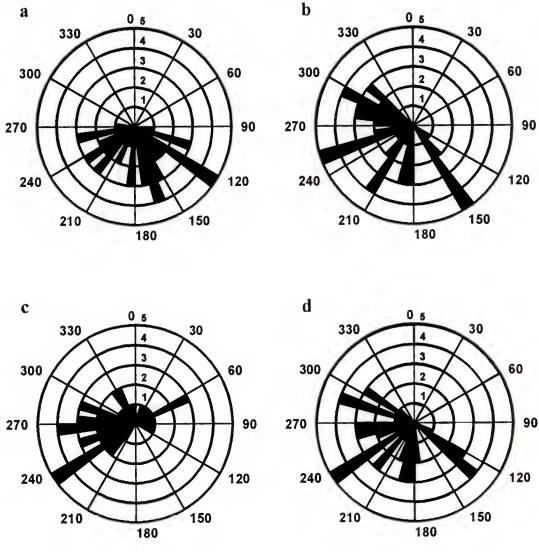

Fig. 6-5. Wind Rose diagrams for three weather stations in the Imperial valley, CA. Each plot presents wind data collected between 6 am–10 am for July 1, 1994 to June, 30 1995. Bars show the direction the wind is coming from, and their lengths indicate frequency. (a) Calipatria--mean 179° (± 46.33 SD), speed 2.4 m/s; (b) Meloland--mean 238.9° (± 51.47 SD), speed 2.4 m/s; (c) Seeley--mean 283° (± 61.53 SD), speed 2.3 m/s; (d) average of the three stations--mean 226.9° (± 52.44 SD), speed 2.3 m/s.

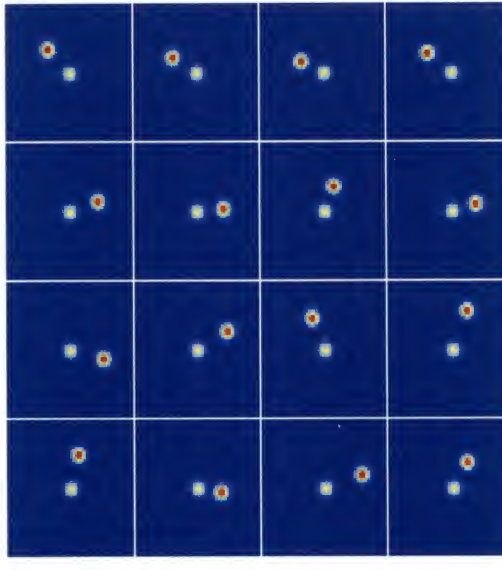

Fig. 6-6. Montage of images showing the effects of variability in wind direction and speed on the pattern of adult whitefly dispersal in a spatiotemporal model for the insect in the Imperial Valley, CA. Sixteen consecutive dispersal steps in the model are presented. The central distribution in each subimage represents the dispersal pattern of trivial fliers at the source, while the other distribution is the wind-shifted dispersal pattern of migrators.

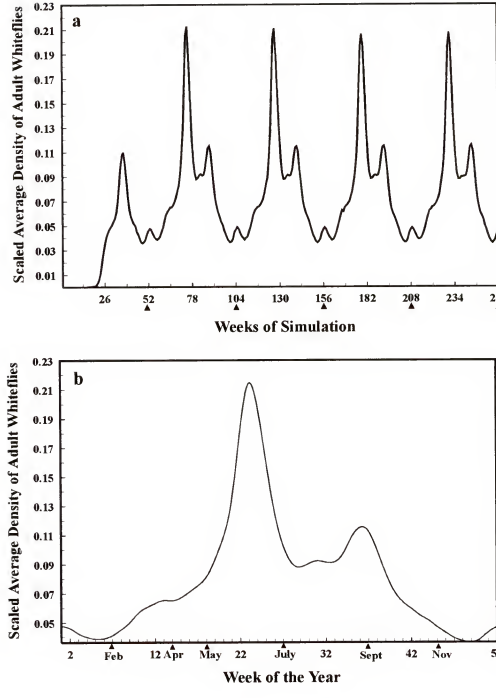

Fig. 6-7. Dynamics of silverleaf whitefly adults from simulations on the Imperial Valley, CA. Average whitefly density in the system have been scaled to the carrying capacity in a quarter section (one cell) in the spatial grid. (a) result of a five year simulation in the Valley; (b) adult whitefly dynamics in a single year.

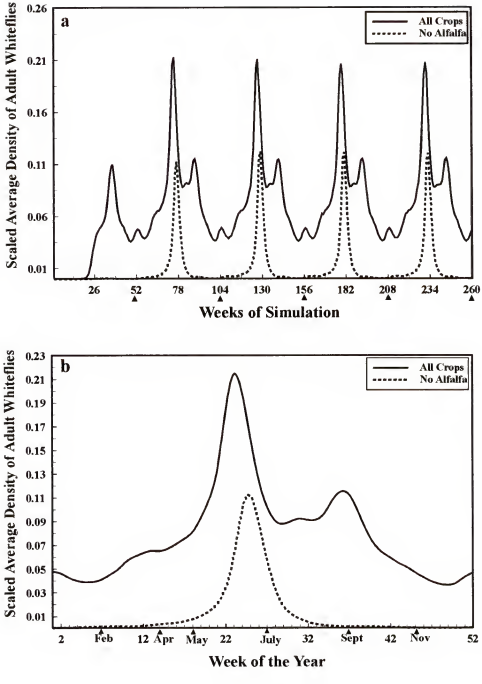

Fig. 6-8. Dynamics of silverleaf whitefly adults from simulations on the Imperial Valley, CA. Average whitefly density in the system have been scaled to the carrying capacity in a quarter section (one cell) in the spatial grid. (a) result of a five year simulation comparing whitefly dynamics in the entire system with their dynamics when no alfalfa is grown; (b) adult whitefly dynamics in a single year.

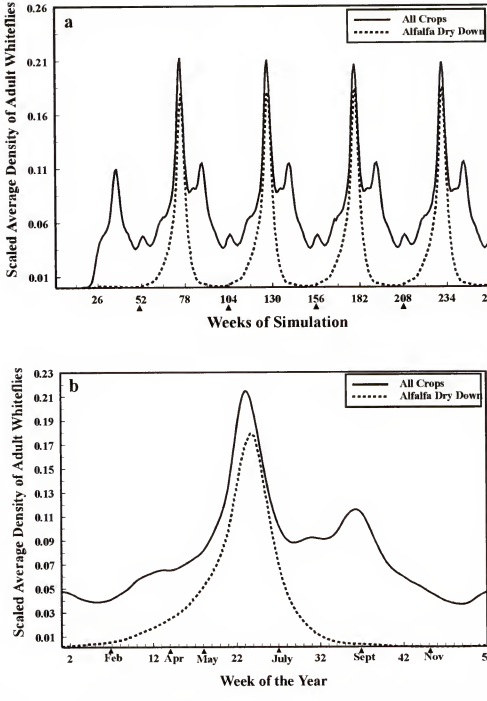

Fig. 6-9. Dynamics of silverleaf whitefly adults from simulations on the Imperial Valley, CA. Average whitefly density in the system have been scaled to the carrying capacity in a quarter section (one cell) in the spatial grid. (a) result of a five year simulation comparing whitefly dynamics in the entire system with their dynamics when alfalfa has a dry down period (Late July to Early October); (b) adult whitefly dynamics in a single.

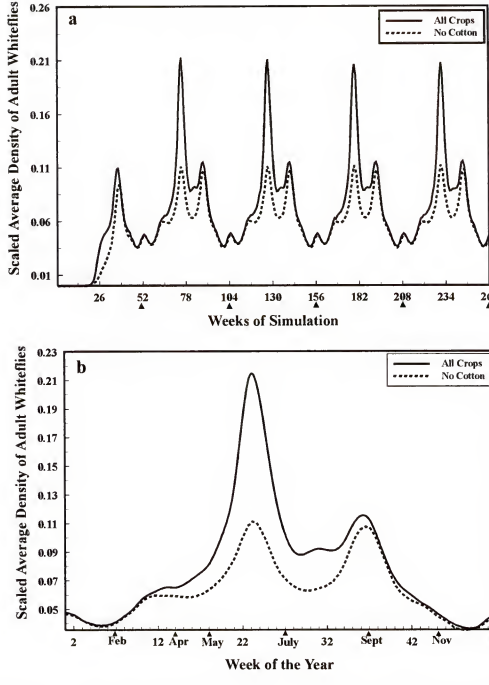

Fig. 6-10. Dynamics of silverleaf whitefly adults from simulations on the Imperial Valley, CA. Average whitefly density in the system have been scaled to the carrying capacity in a quarter section (one cell) in the spatial grid. (a) result of a five year simulation comparing whitefly dynamics in the entire system with their dynamics when no cotton is grown; (b) adult whitefly dynamics in a single year.

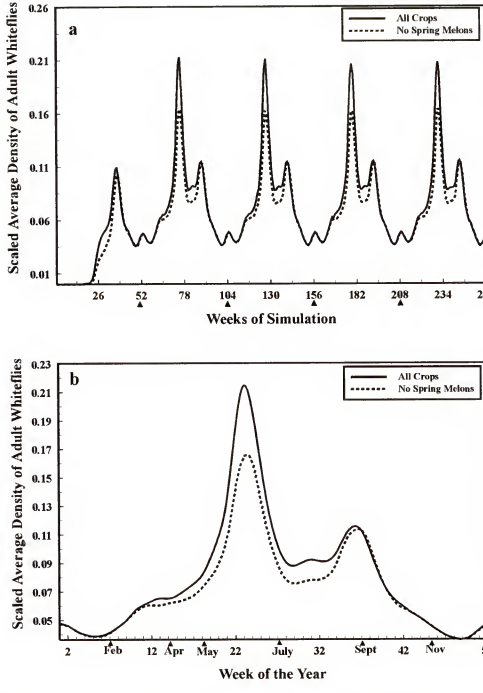

Fig. 6-11. Dynamics of silverleaf whitefly adults from simulations on the Imperial Valley, CA. Average whitefly density in the system have been scaled to the carrying capacity in a quarter section (one cell) in the spatial grid. (a) result of a five year simulation comparing whitefly dynamics in the entire system with their dynamics when no spring melons are grown; (b) adult whitefly dynamics in a single year.

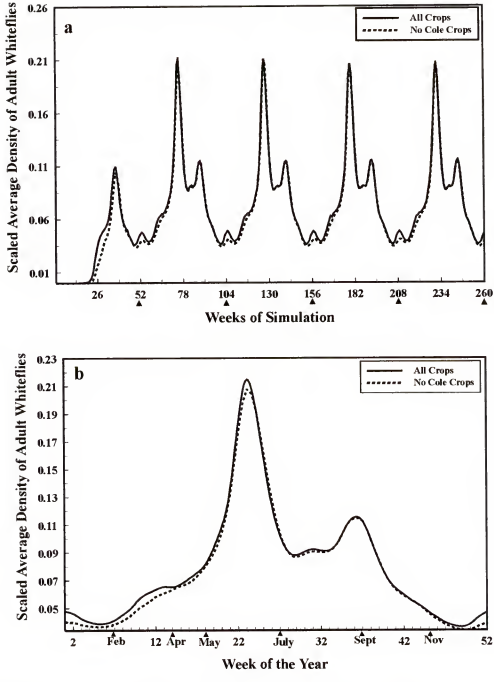

Fig. 6-12. Dynamics of silverleaf whitefly adults from simulations on the Imperial Valley, CA. Average whitefly density in the system has been scaled to the carrying capacity in a quarter section (one cell) in the spatial grid. (a) result of a five year simulation comparing whitefly dynamics in the entire system with their dynamics when no cole crops are grown; (b) adult whitefly dynamics in a single year.

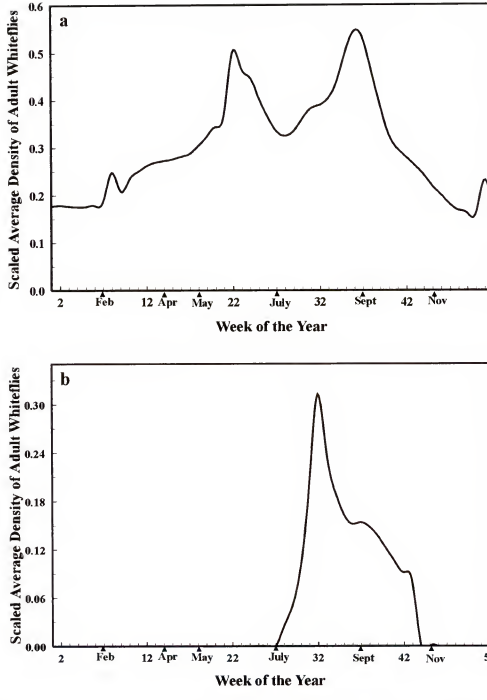

Fig. 6-13. Dynamics of silverleaf whitefly adults from simulations on the Imperial Valley, CA. Y-axis values represent adult densities averaged over the total area planted in each crop and scaled to the carrying capacity in a quarter section (one cell) in the spatial grid. (a) adult whitefly dynamics on alfalfa in a single year.; (b) adult whitefly dynamics on cotton in a single year

CHAPTER 7
SUMMARY AND DISCUSSION

An animal's habitat plays an important role in its dynamics, yet many studies that attempt to explore these dynamics do so without reference to the structure and scale of the animal's surroundings. Polyphagous insect species like the sweetpotato whitefly (SPW), *Bemisia tabaci* Gennadius, and the silverleaf whitefly (SLW), *Bemisia argentifolii* Bellows and Perring, have ranges that extend across large areas and into many agricultural regions. However, the dynamics of these insect are normally studied at the local or farm level with a combination of laboratory and field experiments. Although these local studies have allowed us to gather much information on the biology and dynamics of these insects on specific crops and under specific conditions, the results cannot always be extrapolated to larger spatial systems.

The preceding chapters outlined methodology for studying the spatiotemporal dynamics of insects in agricultural systems. The main focus was the development of a simulation model that could be used for this purpose. There is nothing unique in the use of models for studying insect dynamics. However, many past models were non-spatial and only accounted for the insect's temporal dynamics in systems that were assumed to be homogeneous, e.g., monocultures. In insect ecology, spatial models have been used mainly to address theoretical issues that many believe could have some practical implications, e.g. spatiotemporal chaos. Very little has been done with spatial models to

address more practical and immediate problems such as the whitefly management problem. The methodology emphasized in this study could prove useful for such endeavors, and as was demonstrated, the approach can be used for studying insect-habitat interactions in systems ranging in extent and scale from the farm-level to large-scale regional agricultural systems. This chapter summarizes some of the important concepts highlighted during these studies and also suggest some areas for future consideration. It begins with an overview of the insect that was studied.

The Silverleaf Whitefly Problem

One of the most important whiteflies in agricultural production systems is the sweetpotato whitefly (SPW), *Bemisia tabaci* (Gennadius), also commonly known as the tobacco or cotton whitefly (Byrne et al. 1990). Before 1981, this insect was considered a sporadic pest in the United Sates (Horowitz 1986, Byrne & Draeger 1989, Brown et al. 1995) but by the mid-1980s its status changed dramatically and it became a primary pest. The rise to pest status of the SPW was attributed mainly to the intensification of agricultural production and the greater use of production inputs such as pesticides, fertilizers, and irrigation (Ahmed et al. 1987, Gill 1992). It is believed that these events resulted in the evolution of a more pestilent strain of SPW, strain B (or poinsettia strain) that was responsible for the increased damage (Price et al. 1987, Byrne & Miller 1990, Perring et al. 1991,1992). Strain B was later described as a new species, the silverleaf whitefly (SLW), *Bemisia argentifolii* Bellows & Perring (Bellows et al. (1994). Although debate on the true nature of these whiteflies continues, it is clear that much is still

unknown about their biology and ecology. Today, both insects are a worldwide problem in both indoor and outdoor agricultural production systems and are responsible for multimillion dollar losses each year (Perring et al. 1993a, Bellows et al. 1994).

The rapid rise in pest status of these whiteflies lead to a rejuvenation of interest in their biology and dynamics (Brown et al. 1995). It is now known that these insects have the ability to move extensively within regional crop systems (Perring et al. 1992, Brown et al. 1995), and therefore their dynamics are expected to be closely tied to regional crop patterns in time and space. These observations and the heavy economic losses suffered by farmers encouraged USDA/ARS, university and state scientists in 1992 to initiate a 5-year national research and action plan for whitefly management with the major goal "to provide the necessary research and team effort that will continue to yield environmentally and publicly acceptable, safe technologies for area-wide management and suppression of the SPW" (Faust 1992 p. i). Section F (*Integrated Approaches and Techniques*) of this plan recognized that the whitefly problem could not be addressed in the scope of single fields or commodities and that a commodity management approach was inadequate. It was further recognized that local studies provided only a narrow view of the range of whitefly dynamics possible and that the approaches used in these studies were inadequate for large-scale studies primarily because of the costs and logistics involved. Ecosystem modeling and spatial analysis were suggested as good alternatives for conducting these types of studies. In these studies, a nonspecific insect interaction model was formulated, and theoretical as well as practical facets of this model explored. Construction and integration of the insect's spatial environment into the model was described in detail for real and

experimental systems. The model was specifically applied to the silverleaf whitefly in a small- and a large-scale agricultural system.

The Spatially Explicit Population Model

Levin (1992) noted that the dynamics observed for animal species at the local scale are often inadequate for making predictions on their dynamics at larger spatial scales. Since it is extremely difficult to manipulate and control large-scale experiments, tools such as simulation models must be considered. Recently, a model for the SLW in a regional (multi-crop) system, the Imperial Valley, CA, was described (Wilhoit et al. 1994). Evidence of other such models for this and many other insects is lacking.

The model formulated in these studies was a spatially explicit population model (SEPM). It included ideas from mobile animal population models (Dunning et al. 1995), coupled map lattices (CMLs) (Allen 1975, Allen et al.1993, Hassell et al. 1991,1994, Bascompte & Solé 1994) and integrodifference equations (IDEs) (Kot & Schaffer 1986, Kot 1989, Murray 1989, Andersen 1991 Hastings & Higgins 1994, Neubert et al. 1995, Kot et al. 1996). Researchers in landscape ecology and management studies have used SEPMs extensively and only recently have insect ecologists discovered the importance of these models for studying insect dynamics (Fahrig & Paloheimo 1988, Hassell et al. 1991, Comins et al. 1992). SEPMs combine a species population model with a habitat map that describes the structure (type and arrangement of resources) of the animal's habitat (Dunning et al. 1995, Turner et al. 1995, Conroy et al. 1995, Holt et al. 1995). These models can keep track of individuals or populations within defined locations or patches in

the animal's habitat. In this way, the effects of changes in habitat structure on the dynamics of the animal can be examined in less time than it would take to conduct the full set of studies on the actual system.

The specific model formulated was based on the familiar Nicholson-Bailey (NB) model (Nicholson &Bailey 1935) that is well known in ecology. Other prey-predator models such as that given in Kot (1989) can however be used in place of the NB model. This makes this approach quite robust. The robustness of the approach is enhanced by using IDEs to model species dispersal. The dispersal function (K) in the IDEs are very general and can be constructed directly from field data. The allow us to experiment with different hypotheses concerning dispersal behavior. A few examples of dispersal density functions for insects were discussed.

One may question whether the dynamics generated by models that use IDES to perform dispersal are any different from those generated using more traditional dispersal rules such as queen's, bishop's and rook's moves. The answer to this question is no. In simulations where IDEs were used to accomplish dispersal, the spatiotemporal dynamical patterns were similar to those observed with the types of dispersal. The patterns included spiral waves of predator chasing prey, crystal lattices, and spatiotemporal chaos (Hassell et al. 1991, Comins et al. 1992). It was also shown that mathematical stability of the already unstable model was not achieved by adding species dispersal, but that dispersal did affect the degree of persistence (dynamical stability) of the system.

The model also had the ability to include some information on the animal's habitat (although not explicitly). This information entered through the resource map that was

either used to index parameters for the animal in a lookup table or to create parameter maps for the animal for the resources in the system. This aspect of the model gives us the ability to manipulate the animal's habitat, and to experiment and study the effects of various resource structures on species dynamics. Construction of resource maps was therefore a major part of these studies.

Resource Maps

The construction of resource maps was shown for systems of two extreme extents. A farm-level resource map was created for the SLW at Pine Island Organics that had an extent of approximately 31 hectares. All that was required to create this map was for precise measurements of the farm and a record on all features that were relevant to the insect. The other SLW resource maps were constructed on large regional agricultural systems (San Joaquin Valley and Imperial Valley, California). Information on these systems were obtained through remote sensing with Lansat satellites. In addition, ground truth data was required to classify agricultural features in these maps. The resources maps from satellite data are obviously more difficult and costly to construct, required a greater amount planning, and were expected to be less accurate than the maps created from information taken directly. Although this technology is prohibitive to many potential users at this time, the future growth in the use of this technology is expected to be rapid especially with plans in place to launch several high quality satellites in the near future.

Applying the Model to Whiteflies in Two Spatial Systems

The appropriateness of the spatially explicit age-structured model as a tool for studying insect dynamics was demonstrated with respect to the SLW in two different size systems. These studies were not intended as validation exercises per se, but ones that served to illustrate the utility of the model for studying insect dynamics in temporally and spatially varying crop systems.

The first study in the Pine Island system combined field sampling with simulation modeling. The data generated by the model were first standardized with the field data, after which the model was used to examine the effects of changes in crop arrangements on the dynamics of whiteflies. The results indicated that changes in the spatial structure of resources at the farm did influence SLW dynamics.

The large-scale study looked at the insect and its interaction with host plants in the Imperial Valley, California. In this case, the dynamics generated by the model were compared with data available in the literature (Meyerdirk & Coudriet 1986, Youngman et al. 1986, Blua et al. 1994) and also with data generated by another simulation model for the insect in the Imperial Valley (Wilhoit et al. 1994). The results showed that alfalfa had the most significant effect on whitefly population levels in the Valley. Complete removal of alfalfa resulted in a 6.4-fold reduction of whiteflies, while summer removal (or alfalfa dry down) caused a 2.75-fold reduction. It was also clear that alfalfa is not a good overwintering host for whiteflies but seems to be an important host during the summer (Yee & Toscano 1996). Whitefly populations in the Valley could be controlled by

completely removing alfalfa from the system. Of course, this is not and probably will never be the politically or economically correct approach to adopt.

Final Considerations

The tool developed in these studies for studying insect dynamics in regional agricultural systems can become an important part of regional Integrated Pest Management programs. However for it to be widely accepted, its usefulness must be demonstrated under varying conditions. A number of gaps still exist in the approach as it was presented and these occur mainly because of the lack of available data. This exercise also pointed out areas where more research efforts are needed. The lack of data on the biology of whitefly natural enemies as a group is obvious. In the model, the natural enemy component was modeled as a natural enemy complex or a single generic species. While this may be adequate for the insect in the Imperial Valley system where natural enemy effects on whitefly populations are limited, one may question this approach for whiteflies in Florida. Another area of interest is in the dispersal of these natural enemies. Recently, efforts have been made to study whitefly dispersal (Byrne et al. 1996). The spatial movement of natural enemies within the same locations have not received the same attention. Finally, it is clear especially from the Imperial Valley study that data on environmental factors such as wind and temperature are very important for the success of this approach and therefore in designing and using models in these systems extensive data on environmental variables are required.

APPENDIX
EQUILIBRIUM AND STABILITY ANALYSIS

Maple V software (Waterloo Maple Inc. 450 Phillip St. Waterloo, ON N2L 5J2, Cananda) was used to derive equilibrium or steady-states, and stability conditions for the discete-time systems presented in Chapter 3. Stability conditions were based on several methods including the *Inners* or *Determinant* approach described by Jury (1964,1971,1974). The analyses were done on a 200 MHz. Pentium Pro IBM-compatible personal computer running under Windows NT4 operating system.

1.1 Equilibrium and Stability in the Nicholson-Bailey Predator-Prey Model

(a): The Non-Spatial Model:

Initialize linear algebra toolbox

```
> with(linalg):
```

f and g are the prey and predator at t+1, respectively

```
> f := r*Y*exp(-a*Z);
  g := c*Y*(1 - exp(-a*Z));
```

$$f := r\,Y\,\mathbf{e}^{(-a\,Z)}$$

$$g := c\,Y\,(1 - \mathbf{e}^{(-a\,Z)})$$

Equilibrium population levels

```
> sols := solve({f=Y,g=Z}, {Y,Z});
```

$$sols := \{Y = 0, Z = 0\}, \{Z = \frac{\ln(r)}{a}, Y = \frac{\ln(r)\, r}{c\, a\, (r-1)}\}$$

```
> solve({f=Y}, {r});
```

$$\{r = \frac{1}{e^{(-a\,Z)}}\}$$

Jacobian or community matrix

```
> A := subs(exp(-a*Z) = 1/r, sols[2]
  ,matrix(2,2,[[diff(f,Y),diff(f,Z)],[diff(g,Y),diff(g,
  Z)]]));
```

$$A := \begin{bmatrix} 1 & -\frac{\ln(r)\, r}{c\,(r-1)} \\ c\left(1-\frac{1}{r}\right) & \frac{\ln(r)}{r-1} \end{bmatrix}$$

Determinant and trace of A:

```
> DA := det(A); TA := trace(A);
```

$$DA := \frac{\ln(r)\, r}{r-1}$$

$$TA := 1 + \frac{\ln(r)}{r-1}$$

Characteristic equation (polynomial)

```
> CP := collect(charpoly(A,lambda), lambda);
```

$$CP := \lambda^2 + \frac{(1 - \ln(r) - r)\,\lambda}{r-1} + \frac{\ln(r)\, r}{r-1}$$

Stability of equilibrium states are determined by evaluating (2 > 1 + det > |trace|
).

```
> solve({2 > 1 + DA},{r}); solve({1 + DA >
  abs(TA)},{r});
```

$$\{r < 1\}$$

$$\{1 < r\}$$

Result: 1 > r > 1 cannot be true so equilibrium in this model are never stable

>

(b): Spatial IDE Model with 1-D Gaussian Dispersal (Mean = 0.0 , SD = 1.0):

```
> with(inttrans):
```

Dispersal kernels (prey dispersal is Kn, predator dispersal is Kp)

```
> Kn:=(1/sqrt(2*pi))*exp(-(x)^2/(2));
  Kp:=(1/sqrt(2*pi))*exp(-(x)^2/(2));
```

$$Kn := \frac{1}{2}\frac{\sqrt{2}\, e^{(-1/2x^2)}}{\sqrt{\pi}}$$

$$Kp := \frac{1}{2}\frac{\sqrt{2}\, e^{(-1/2x^2)}}{\sqrt{\pi}}$$

Fourier Transform (FFT) of 1-D dispersal kernels:

```
> kn:=fourier(Kn,x,omega);kp :=fourier(Kp,x,omega);
```

$$kn := \frac{\sqrt{\pi}\, e^{(-1/2\omega^2)}}{\sqrt{\pi}}$$

$$kp := \frac{\sqrt{\pi}\, e^{(-1/2\omega^2)}}{\sqrt{\pi}}$$

Dispersal matrix (K)

```
> K := matrix(2,2,[kn,0,0,kp]);
```

$$K := \begin{bmatrix} \frac{\sqrt{\pi}\, e^{(-1/2\omega^2)}}{\sqrt{\pi}} & 0 \\ 0 & \frac{\sqrt{\pi}\, e^{(-1/2\omega^2)}}{\sqrt{\pi}} \end{bmatrix}$$

Evaluate FFT of dispersal kernel and Jacobian.

```
> KA := evalm(K&*A);
```

$$KA := \begin{bmatrix} \frac{\sqrt{\pi}\,\%1}{\sqrt{\pi}} & -\frac{\sqrt{\pi}\,\%1\,\ln(r)\,r}{\sqrt{\pi}\,c\,(r-1)} \\ \frac{\sqrt{\pi}\,\%1\,c\left(1-\frac{1}{r}\right)}{\sqrt{\pi}} & \frac{\sqrt{\pi}\,\%1\,\ln(r)}{\sqrt{\pi}\,(r-1)} \end{bmatrix}$$

$$\%1 := e^{(-1/2\,\omega^2)}$$

Determinant and trace of KA:

```
> dA := simplify(det(KA)); beta := simplify(trace(KA));
```

$$dA := \frac{\pi\, e^{(-\omega^2)}\ln(r)\,r}{\pi\,(r-1)}$$

$$\beta := \frac{\sqrt{\pi}\, e^{(-1/2\,\omega^2)}\,(r-1+\ln(r))}{\sqrt{\pi}\,(r-1)}$$

Characteristic equation (polynomial) with 1-D dispersal:

```
> CP := collect(simplify(charpoly(KA,lambda)), lambda);
```

$$CP := \frac{(\pi\,r-\pi)\,\lambda^2}{\pi\,(r-1)} + \frac{(\sqrt{\pi}\, e^{(-1/2\,\omega^2)}\sqrt{\pi}-\sqrt{\pi}\sqrt{\pi}\, e^{(-1/2\,\omega^2)}\ln(r)-\sqrt{\pi}\, e^{(-1/2\,\omega^2)}\sqrt{\pi}\,r)\,\lambda}{\pi\,(r-1)} + \frac{\pi\, e^{(-\omega^2)}\ln(r)\,r}{\pi\,(r-1)}$$

Jury conditions (C1 - C3) for stability (Eqn 3.35) evaluated as r approaches infinity:

Criterion 1:

```
> C1 := (1 - beta + dA > 0);
```

$$C1 := 0 < 1 - \frac{\sqrt{\pi}\, e^{(-1/2\omega^2)}(r - 1 + \ln(r))}{\sqrt{\pi}\,(r-1)} + \frac{\pi\, e^{(-\omega^2)} \ln(r)\, r}{\pi\,(r-1)}$$

```
> limit(1 - beta + dA, r = infinity);
```

$$\frac{\infty}{\text{signum}(e^{(\omega^2)})\ \text{signum}(\pi)}$$

Criterion 2:

```
> C2 := (1 + beta + dA > 0);
```

$$C2 := 0 < 1 + \frac{\sqrt{\pi}\, e^{(-1/2\omega^2)}(r - 1 + \ln(r))}{\sqrt{\pi}\,(r-1)} + \frac{\pi\, e^{(-\omega^2)} \ln(r)\, r}{\pi\,(r-1)}$$

```
> limit(1 + beta + dA, r = infinity);
```

$$\frac{\infty}{\text{signum}(e^{(\omega^2)})\ \text{signum}(\pi)}$$

Criterion 3:

```
> C3 := (1 - dA > 0);
```

$$C3 := 0 < 1 - \frac{\pi\, e^{(-\omega^2)} \ln(r)\, r}{\pi\,(r-1)}$$

```
> limit(1 - dA, r=infinity);
```

$$-\frac{\infty}{\text{signum}(e^{(\omega^2)})\ \text{signum}(\pi)}$$

Result: C3 < 0. The system is unstable with 1-D dispersal.

1.2 Stability of a Discrete-Time 4th Order System .

```
> with(linalg):
```

4th-Degree characteristic polynomial:

```
> C[lambda]:=a[4]*lambda^4 + a[3]*lambda^3 +
  a[2]*lambda^2 + a[1]*lambda + a[0];
```

$$C_{\lambda} := a_4 \lambda^4 + a_3 \lambda^3 + a_2 \lambda^2 + a_1 \lambda + a_0$$

Stability Conditions 1: C(1) > 0 and C(-1) > 0

```
> C[[1]] := subs(lambda = 1, eval(C[lambda] > 0));
```

$$C_{[1]} := 0 < a_4 + a_3 + a_2 + a_1 + a_0$$

```
> C[[-1]] := subs(lambda = -1,eval(C[lambda] > 0));
```

$$C_{[-1]} := 0 < a_4 - a_3 + a_2 - a_1 + a_0$$

Form matrices (Wn and Xn) from coefficients the polynomial:

```
> W[n]:=matrix(5,5,[a[4],a[3],a[2],a[1],a[0],0,a[4],a[3
  ],a[2],a[1],0,0,a[4],a[3],a[2],0,0,0,a[4],a[3],0,0,0,
  0,a[4]]);
```

$$W_n := \begin{bmatrix} a_4 & a_3 & a_2 & a_1 & a_0 \\ 0 & a_4 & a_3 & a_2 & a_1 \\ 0 & 0 & a_4 & a_3 & a_2 \\ 0 & 0 & 0 & a_4 & a_3 \\ 0 & 0 & 0 & 0 & a_4 \end{bmatrix}$$

```
> X[n]:=matrix(5,5,[a[4],a[3],a[2],a[1],a[0],a[3],a[2],
  a[1],a[0],0,a[2],a[1],a[0],0,0,a[1],a[0],0,0,0,a[0],0
  ,0,0,0]);
```

$$X_n := \begin{bmatrix} a_4 & a_3 & a_2 & a_1 & a_0 \\ a_3 & a_2 & a_1 & a_0 & 0 \\ a_2 & a_1 & a_0 & 0 & 0 \\ a_1 & a_0 & 0 & 0 & 0 \\ a_0 & 0 & 0 & 0 & 0 \end{bmatrix}$$

Form (Wn + Xn) and (Wn - Xn) matrices:

```
> WXa := evalm(W[n]+X[n]);
```

$$WXa := \begin{bmatrix} 2a_4 & 2a_3 & 2a_2 & 2a_1 & 2a_0 \\ a_3 & a_4 + a_2 & a_3 + a_1 & a_2 + a_0 & a_1 \\ a_2 & a_1 & a_4 + a_0 & a_3 & a_2 \\ a_1 & a_0 & 0 & a_4 & a_3 \\ a_0 & 0 & 0 & 0 & a_4 \end{bmatrix}$$

```
> WXb := evalm(W[n]-X[n]);
```

$$WXb := \begin{bmatrix} 0 & 0 & 0 & 0 & 0 \\ -a_3 & a_4 - a_2 & a_3 - a_1 & a_2 - a_0 & a_1 \\ -a_2 & -a_1 & a_4 - a_0 & a_3 & a_2 \\ -a_1 & -a_0 & 0 & a_4 & a_3 \\ -a_0 & 0 & 0 & 0 & a_4 \end{bmatrix}$$

Stability Condition 2: Determinant of the inners (k = 1) > 0.

```
> eval(WXa[3,3] > 0); eval(WXb[3,3] > 0);
```

$$0 < a_4 + a_0$$

$$0 < a_4 - a_0$$

Inners (Wn + Xn) and (Wn - Xn) at k = 3:

```
> I3a:=array(1..3,1..3,[[WXa[2,2],WXa[2,3],WXa[2,4]],[W
  Xa[3,2],WXa[3,3],WXa[3,4]],[WXa[4,2],WXa[4,3],WXa[4,4
  ]]]);
```

$$I3a := \begin{bmatrix} a_4 + a_2 & a_3 + a_1 & a_2 + a_0 \\ a_1 & a_4 + a_0 & a_3 \\ a_0 & 0 & a_4 \end{bmatrix}$$

```
> I3b:=array(1..3,1..3,[[WXb[2,2],WXb[2,3],WXb[2,4]],[W
  Xb[3,2],WXb[3,3],WXb[3,4]],[WXb[4,2],WXb[4,3],WXb[4,4
  ]]]);
```

$$I3b := \begin{bmatrix} a_4 - a_2 & a_3 - a_1 & a_2 - a_0 \\ -a_1 & a_4 - a_0 & a_3 \\ -a_0 & 0 & a_4 \end{bmatrix}$$

Stability Condition 3: Determinant of the inners (k = 3) > 0:

```
> eval(det(I3a) > 0); eval(det(I3b) > 0);
```

$$0 < a_4^3 + a_0 a_4^2 + a_2 a_4^2 - a_1 a_4 a_3 - a_1^2 a_4 + a_0 a_3^2 + a_0 a_3 a_1 - a_2 a_0^2 - a_0^2 a_4 - a_0^3$$

$$0 < a_4^3 - a_0 a_4^2 - a_2 a_4^2 + 2 a_4 a_2 a_0 + a_1 a_4 a_3 - a_1^2 a_4 - a_0 a_3^2 + a_0 a_3 a_1 - a_2 a_0^2 - a_0^2 a_4 + a_0^3$$

1.3 Two Examples of Stability with 4th Degree Polynomials

(a): An Unstable System

```
> with(linalg):
> lambda := 'lambda';
```

$$\lambda := \lambda$$

Coefficients of the characteristic polynomial

```
> a[4] := 1; a[3] := -1; a[2] := 9; a[1] := -7; a[0] := 2;
```

$$a_4 := 1$$

$$a_3 := -1$$

$$a_2 := 9$$

$$a_1 := -7$$

$$a_0 := 2$$

Characteristic polynomial:

```
> C[lambda] := a[4]*lambda^4 + a[3]*lambda^3 +
  a[2]*lambda^2 + a[1]*lambda + a[0];
```

$$C_\lambda := \lambda^4 - \lambda^3 + 9\lambda^2 - 7\lambda + 2$$

Stability Conditions 1: C(1) > 0 and C(-1) > 0

```
> C[[1]] := subs(lambda = 1, eval(C[lambda]>0));
```

$$C_{[1]} := 0 < 4$$

```
> C[[-1]] := subs(lambda = -1,eval(C[lambda]>0));
```

$$C_{[-1]} := 0 < 20$$

```
> W[n]:=matrix(5,5,[a[4],a[3],a[2],a[1],a[0],0,a[4],a[3],a
  [2],a[1],0,0,a[4],a[3],a[2],0,0,0,a[4],a[3],0,0,0,0,a[4]
  ]);
```

$$W_n := \begin{bmatrix} 1 & -1 & 9 & -7 & 2 \\ 0 & 1 & -1 & 9 & -7 \\ 0 & 0 & 1 & -1 & 9 \\ 0 & 0 & 0 & 1 & -1 \\ 0 & 0 & 0 & 0 & 1 \end{bmatrix}$$

```
> X[n]:=matrix(5,5,[a[4],a[3],a[2],a[1],a[0],a[3],a[2],a[1
  ],a[0],0,a[2],a[1],a[0],0,0,a[1],a[0],0,0,0,a[0],0,0,0,0
  ]);
```

$$X_n := \begin{bmatrix} 1 & -1 & 9 & -7 & 2 \\ -1 & 9 & -7 & 2 & 0 \\ 9 & -7 & 2 & 0 & 0 \\ -7 & 2 & 0 & 0 & 0 \\ 2 & 0 & 0 & 0 & 0 \end{bmatrix}$$

```
> WXa := evalm(W[n]+X[n]);
```

$$WXa := \begin{bmatrix} 2 & -2 & 18 & -14 & 4 \\ -1 & 10 & -8 & 11 & -7 \\ 9 & -7 & 3 & -1 & 9 \\ -7 & 2 & 0 & 1 & -1 \\ 2 & 0 & 0 & 0 & 1 \end{bmatrix}$$

```
> WXb := evalm(W[n]-X[n]);
```

$$WXb := \begin{bmatrix} 0 & 0 & 0 & 0 & 0 \\ 1 & -8 & 6 & 7 & -7 \\ -9 & 7 & -1 & -1 & 9 \\ 7 & -2 & 0 & 1 & -1 \\ -2 & 0 & 0 & 0 & 1 \end{bmatrix}$$

Stability Conditions 2: Determinant of inners (k = 1) > 0

```
> eval(WXa[3,3]>0); eval(WXb[3,3]>0);
```

$$0 < 3$$

$$0 < -1$$

One condition is violated. Therefore the system is unstable

```
> I3a:=array(1..3,1..3,[[WXa[2,2],WXa[2,3],WXa[2,4]],[WXa[
  3,2],WXa[3,3],WXa[3,4]],[WXa[4,2],WXa[4,3],WXa[4,4]]]);
```

$$I3a := \begin{bmatrix} 10 & -8 & 11 \\ -7 & 3 & -1 \\ 2 & 0 & 1 \end{bmatrix}$$

```
> I3b:=array(1..3,1..3,[[WXb[2,2],WXb[2,3],WXb[2,4]],[WXb[
  3,2],WXb[3,3],WXb[3,4]],[WXb[4,2],WXb[4,3],WXb[4,4]]]);
```

$$I3b := \begin{bmatrix} -8 & 6 & 7 \\ 7 & -1 & -1 \\ -2 & 0 & 1 \end{bmatrix}$$

Stability Conditions 3: Determinant of inners (k = 3) > 0

```
> eval(det(I3a) > 0); eval(det(I3b) > 0);
```

$$0 < -76$$

$$0 < -36$$

These Conditions are also violated. The system is unstable

(b): A Stable System

Coefficients of the characteristic polynomial

```
> a[4] := 1; a[3] := 0.8; a[2] := 0.55; a[1] := 0.4; a[0]
  := 0.12;
```

$$a_4 := 1$$

$$a_3 := .8$$

$$a_2 := .55$$

$$a_1 := .4$$

$$a_0 := .12$$

Characteristic polynomial:

```
> C[lambda] := a[4]*lambda^4 + a[3]*lambda^3 +
  a[2]*lambda^2 + a[1]*lambda + a[0];
```

$$C_\lambda := \lambda^4 + .8\,\lambda^3 + .55\,\lambda^2 + .4\,\lambda + .12$$

Stability Conditions 1: C(1) > 0 and C(-1) > 0

```
> C[[1]] := subs(lambda = 1, eval(C[lambda])>0));
```

$$C_{[1]} := 0 < 2.87$$

```
> C[[-1]] := subs(lambda = -1,eval(C[lambda])>0));
```

$$C_{[-1]} := 0 < .47$$

```
> W[n] :=
  matrix(5,5,[a[4],a[3],a[2],a[1],a[0],0,a[4],a[3],a[2],a[
  1],0,0,a[4],a[3],a[2],0,0,0,a[4],a[3],0,0,0,0,a[4]]);
```

$$W_n := \begin{bmatrix} 1 & .8 & .55 & .4 & .12 \\ 0 & 1 & .8 & .55 & .4 \\ 0 & 0 & 1 & .8 & .55 \\ 0 & 0 & 0 & 1 & .8 \\ 0 & 0 & 0 & 0 & 1 \end{bmatrix}$$

```
> X[n] :=
  matrix(5,5,[a[4],a[3],a[2],a[1],a[0],a[3],a[2],a[1],a[0]
  ,0,a[2],a[1],a[0],0,0,a[1],a[0],0,0,0,a[0],0,0,0,0]);
```

$$X_n := \begin{bmatrix} 1 & .8 & .55 & .4 & .12 \\ .8 & .55 & .4 & .12 & 0 \\ .55 & .4 & .12 & 0 & 0 \\ .4 & .12 & 0 & 0 & 0 \\ .12 & 0 & 0 & 0 & 0 \end{bmatrix}$$

```
> WXa := evalm(W[n]+X[n]);
```

$$WXa := \begin{bmatrix} 2 & 1.6 & 1.10 & .8 & .24 \\ .8 & 1.55 & 1.2 & .67 & .4 \\ .55 & .4 & 1.12 & .8 & .55 \\ .4 & .12 & 0 & 1 & .8 \\ .12 & 0 & 0 & 0 & 1 \end{bmatrix}$$

```
> WXb := evalm(W[n]-X[n]);
```

$$WXb := \begin{bmatrix} 0 & 0 & 0 & 0 & 0 \\ -.8 & .45 & .4 & .43 & .4 \\ -.55 & -.4 & .88 & .8 & .55 \\ -.4 & -.12 & 0 & 1 & .8 \\ -.12 & 0 & 0 & 0 & 1 \end{bmatrix}$$

Stability Conditions 2: Determinant of inners (k = 1) > 0

```
> eval(WXa[3,3]>0); eval(WXb[3,3]>0);
```

$$0 < 1.12$$

$$0 < .88$$

```
> I3a :=
  array(1..3,1..3,[[WXa[2,2],WXa[2,3],WXa[2,4]],[WXa[3,2],
  WXa[3,3],WXa[3,4]],[WXa[4,2],WXa[4,3],WXa[4,4]]]);
```

$$I3a := \begin{bmatrix} 1.55 & 1.2 & .67 \\ .4 & 1.12 & .8 \\ .12 & 0 & 1 \end{bmatrix}$$

```
> I3b :=
  array(1..3,1..3,[[WXb[2,2],WXb[2,3],WXb[2,4]],[WXb[3,2],
  WXb[3,3],WXb[3,4]],[WXb[4,2],WXb[4,3],WXb[4,4]]]);
```

$$I3b := \begin{bmatrix} .45 & .4 & .43 \\ -.4 & .88 & .8 \\ -.12 & 0 & 1 \end{bmatrix}$$

Stability Conditions 3: Determinant of inners (k = 3) > 0

```
> eval(det(I3a) > 0); eval(det(I3b) > 0);
```

$$0 < 1.281152$$

$$0 < .563008$$

No Conditions are violated. The system is stable

1.4: Stability Criteria for a 6th-Order Discrete-Time System

6th degree characteristic polynomial

```
> C[lambda]:=a[6]*lambda^6 + a[5]*lambda^5 + a[4]*lambda^4
  + a[3]*lambda^3 + a[2]*lambda^2 + a[1]*lambda + a[0];
```

$$C_{\lambda} := a_6 \lambda^6 + a_5 \lambda^5 + a_4 \lambda^4 + a_3 \lambda^3 + a_2 \lambda^2 + a_1 \lambda + a_0$$

Stability Conditions 1: C(1) > 0 and C(-1) > 0

```
> C[[1]] := subs(lambda = 1, eval(C[lambda])>0));
```

$$C_{[1]} := 0 < a_6 + a_5 + a_4 + a_3 + a_2 + a_1 + a_0$$

```
> C[[-1]] := subs(lambda = -1,eval(C[lambda])>0));
```

$$C_{[-1]} := 0 < a_6 - a_5 + a_4 - a_3 + a_2 - a_1 + a_0$$

Form matrices (Wn and Xn) from the coefficients of the polynomial

```
> W[n]:=matrix(7,7,[a[6],a[5],a[4],a[3],a[2],a[1],a[0],0,a
  [6],a[5],a[4],a[3],a[2],a[1],0,0,a[6],a[5],a[4],a[3],a[2
  ],0,0,0,a[6],a[5],a[4],a[3],0,0,0,0,a[6],a[5],a[4],0,0,0
  ,0,0,a[6],a[5],0,0,0,0,0,a[6]]);
```

$$W_n := \begin{bmatrix} a_6 & a_5 & a_4 & a_3 & a_2 & a_1 & a_0 \\ 0 & a_6 & a_5 & a_4 & a_3 & a_2 & a_1 \\ 0 & 0 & a_6 & a_5 & a_4 & a_3 & a_2 \\ 0 & 0 & 0 & a_6 & a_5 & a_4 & a_3 \\ 0 & 0 & 0 & 0 & a_6 & a_5 & a_4 \\ 0 & 0 & 0 & 0 & 0 & a_6 & a_5 \\ 0 & 0 & 0 & 0 & 0 & 0 & a_6 \end{bmatrix}$$

```
> X[n]:=matrix(7,7,[a[6],a[5],a[4],a[3],a[2],a[1],a[0],a[5],
  a[4],a[3],a[2],a[1],a[0],0,a[4],a[3],a[2],a[1],a[0],0,0,a[
  3],a[2],a[1],a[0],0,0,0,a[2],a[1],a[0],0,0,0,0,a[1],a[0],0
  ,0,0,0,0,a[0],0,0,0,0,0,0]);
```

$$X_n := \begin{bmatrix} a_6 & a_5 & a_4 & a_3 & a_2 & a_1 & a_0 \\ a_5 & a_4 & a_3 & a_2 & a_1 & a_0 & 0 \\ a_4 & a_3 & a_2 & a_1 & a_0 & 0 & 0 \\ a_3 & a_2 & a_1 & a_0 & 0 & 0 & 0 \\ a_2 & a_1 & a_0 & 0 & 0 & 0 & 0 \\ a_1 & a_0 & 0 & 0 & 0 & 0 & 0 \\ a_0 & 0 & 0 & 0 & 0 & 0 & 0 \end{bmatrix}$$

Form (Wn + Xn) and (Wn - Xn) matrices:

```
> WXa := evalm(W[n]+X[n]);
```

$$WXa := \begin{bmatrix} 2a_6 & 2a_5 & 2a_4 & 2a_3 & 2a_2 & 2a_1 & 2a_0 \\ a_5 & a_6+a_4 & a_5+a_3 & a_4+a_2 & a_3+a_1 & a_2+a_0 & a_1 \\ a_4 & a_3 & a_6+a_2 & a_5+a_1 & a_4+a_0 & a_3 & a_2 \\ a_3 & a_2 & a_1 & a_6+a_0 & a_5 & a_4 & a_3 \\ a_2 & a_1 & a_0 & 0 & a_6 & a_5 & a_4 \\ a_1 & a_0 & 0 & 0 & 0 & a_6 & a_5 \\ a_0 & 0 & 0 & 0 & 0 & 0 & a_6 \end{bmatrix}$$

```
> WXb := evalm(W[n]-X[n]);
```

$$WXb := \begin{bmatrix} 0 & 0 & 0 & 0 & 0 & 0 & 0 \\ -a_5 & a_6-a_4 & a_5-a_3 & a_4-a_2 & a_3-a_1 & a_2-a_0 & a_1 \\ -a_4 & -a_3 & a_6-a_2 & a_5-a_1 & a_4-a_0 & a_3 & a_2 \\ -a_3 & -a_2 & -a_1 & a_6-a_0 & a_5 & a_4 & a_3 \\ -a_2 & -a_1 & -a_0 & 0 & a_6 & a_5 & a_4 \\ -a_1 & -a_0 & 0 & 0 & 0 & a_6 & a_5 \\ -a_0 & 0 & 0 & 0 & 0 & 0 & a_6 \end{bmatrix}$$

Stability Conditions 2: Determinant of inners (k = 1) > 0

```
> eval(WXa[4,4]>0); eval(WXb[4,4]>0);
```

$$0 < a_6 + a_0$$

$$0 < a_6 - a_0$$

Inners (Wn + Xn) and (Wn - Xn) at k = 3:

```
> I3a:=array(1..3,1..3,[[WXa[3,3],WXa[3,4],WXa[3,5]],[WXa[
  4,3],WXa[4,4],WXa[4,5]],[WXa[5,3],WXa[5,4],WXa[5,5]]]);
```

$$I3a := \begin{bmatrix} a_6+a_2 & a_5+a_1 & a_4+a_0 \\ a_1 & a_6+a_0 & a_5 \\ a_0 & 0 & a_6 \end{bmatrix}$$

```
> I3b:=array(1..3,1..3,[[WXb[3,3],WXb[3,4],WXb[3,5]],[WXb[
  4,3],WXb[4,4],WXb[4,5]],[WXb[5,3],WXb[5,4],WXb[5,5]]]);
```

$$I3b := \begin{bmatrix} a_6-a_2 & a_5-a_1 & a_4-a_0 \\ -a_1 & a_6-a_0 & a_5 \\ -a_0 & 0 & a_6 \end{bmatrix}$$

Stability Conditions 3: Determinant of inners (k = 3) > 0:

```
> eval(det(I3a)>0); eval(det(I3b)>0);
```

$$0 < a_6^3 + a_0 a_6^2 + a_2 a_6^2 + a_6 a_2 a_0 - a_1 a_6 a_5 - a_1^2 a_6 + a_0 a_5^2 + a_0 a_5 a_1 - a_0 a_4 a_6 - a_4 a_0^2 - a_0^2 a_6 - a_0^3$$

$$0 < a_6^3 - a_0 a_6^2 - a_2 a_6^2 + a_6 a_2 a_0 + a_1 a_6 a_5 - a_1^2 a_6 - a_0 a_5^2 + a_0 a_5 a_1 + a_0 a_4 a_6 - a_4 a_0^2 - a_0^2 a_6 + a_0^3$$

Inners (Wn + Xn) and (Wn - Xn) at k = 5:

```
> I5a:=array(1..5,1..5,[[WXa[2,2],WXa[2,3],WXa[2,4],WXa[2,
  5],WXa[2,6]],[WXa[3,2],WXa[3,3],WXa[3,4],WXa[3,5],WXa[3,
  6]],[WXa[4,2],WXa[4,3],WXa[4,4],WXa[4,5],WXa[4,6]],[WXa[
  5,2],WXa[5,3],WXa[5,4],WXa[5,5],WXa[5,6]],[WXa[6,2],WXa[
  6,3],WXa[6,4],WXa[6,5],WXa[6,6]]]);
```

$$I5a := \begin{bmatrix} a_6 + a_4 & a_5 + a_3 & a_4 + a_2 & a_3 + a_1 & a_2 + a_0 \\ a_3 & a_6 + a_2 & a_5 + a_1 & a_4 + a_0 & a_3 \\ a_2 & a_1 & a_6 + a_0 & a_5 & a_4 \\ a_1 & a_0 & 0 & a_6 & a_5 \\ a_0 & 0 & 0 & 0 & a_6 \end{bmatrix}$$

```
> I5b:=array(1..5,1..5,[[WXb[2,2],WXb[2,3],WXb[2,4],WXb[2,5
  ],WXb[2,6]],[WXb[3,2],WXb[3,3],WXb[3,4],WXb[3,5],WXb[3,6]
  ],[WXb[4,2],WXb[4,3],WXb[4,4],WXb[4,5],WXb[4,6]],[WXb[5,2
  ],WXb[5,3],WXb[5,4],WXb[5,5],WXb[5,6]],[WXb[6,2],WXb[6,3]
  ,WXb[6,4],WXb[6,5],WXb[6,6]]]);
```

$$I5b := \begin{bmatrix} a_6 - a_4 & a_5 - a_3 & a_4 - a_2 & a_3 - a_1 & a_2 - a_0 \\ -a_3 & a_6 - a_2 & a_5 - a_1 & a_4 - a_0 & a_3 \\ -a_2 & -a_1 & a_6 - a_0 & a_5 & a_4 \\ -a_1 & -a_0 & 0 & a_6 & a_5 \\ -a_0 & 0 & 0 & 0 & a_6 \end{bmatrix}$$

Stability Conditions 4: Determinant of Inners (k = 5) > 0:

```
> eval(det(I5a)>0); eval(det(I5b)>0);
```

$$0 < -a_0 a_6^2 a_2^2 - a_0 a_2 a_4 a_5^2 - a_0 a_1^2 a_5 a_3 + a_0 a_1 a_5 a_4^2 + a_0^2 a_6 a_5 a_3 + a_2 a_0^2 a_5 a_1 + a_0 a_1 a_2 a_5 a_4 + a_0 a_1 a_5^3 + a_2 a_6^2 a_5 a_3 + 2 a_2 a_0 a_6 a_4^2 + a_2 a_0 a_1 a_6 a_5 - 3 a_2 a_0 a_6 a_1 a_3 - 2 a_2 a_0 a_1^2 a_6 - a_1^2 a_0 a_4 a_6 - a_1^2 a_6 a_2 a_4 + 3 a_1 a_5 a_0^2 a_6 - a_1 a_3 a_5^2 a_6 + a_1 a_5 a_6 a_2^2 - a_1 a_3 a_0 a_4 a_6 + a_1 a_2 a_5 a_6 a_4 + 2 a_1 a_0^2 a_5 a_4 + a_0^2 a_1 a_4 a_3 + a_3 a_0^2 a_5 a_4 + 2 a_2 a_0^2 a_5 a_3 - a_0^2 a_2 a_4^2 + a_0^2 a_4 a_1^2 + a_0^2 a_1^2 a_6 - a_0^2 a_5^2 a_6 + a_0 a_3 a_5^3 + a_0 a_6^2 a_3^2 - a_0 a_2^2 a_5^2 - a_0 a_1^2 a_5^2 - a_0 a_5 a_1^3 + a_0^5 + 2 a_0 a_6 a_2^2 a_4 + a_1^4 a_6 - 2 a_5^2 a_0^3 - a_0^3 a_3^2 + a_2 a_0^4 - a_0^2 a_4^3 + a_4 a_0^4 - a_4^2 a_0^3$$

$$
\begin{aligned}
&+ a_0 a_5^4 + a_0^4 a_6 + a_2 a_6^2 a_5^2 + 3 a_0 a_1 a_6^2 a_5 + a_4 a_1 a_6^2 a_5 - 2 a_4 a_0 a_5^2 a_6 \\
&+ a_4 a_0 a_1 a_6 a_5 + a_3 a_6^2 a_5 a_0 + 2 a_3 a_1 a_6^2 a_4 + a_3 a_1 a_6^2 a_2 - 3 a_3 a_0 a_5 a_6 a_4 \\
&- a_3 a_0 a_5 a_6 a_2 + a_3 a_0 a_1 a_6^2 + a_3 a_6 a_0^2 a_1 - a_6^2 a_2^3 + a_0 a_5^2 a_6^2 - a_0^2 a_4^2 a_6 \\
&- a_4 a_1^2 a_6^2 + a_6 a_0^2 a_3^2 - a_3 a_6^3 a_5 - a_1^2 a_6 a_5^2 + a_1^3 a_6 a_5 + a_6 a_1^3 a_3 - a_1^2 a_6 a_4^2 \\
&- a_1^2 a_6^2 a_2 - a_0 a_1^2 a_6^2 - a_1 a_5^3 a_6 - a_1 a_6^3 a_3 - a_0^2 a_5^2 a_4 - a_3 a_5 a_0^3 - a_0^3 a_1 a_3 \\
&- a_0^3 a_5 a_1 - a_0^2 a_2 a_5^2 + a_6^4 a_0 + a_6^4 a_2 - 2 a_1^2 a_6^3 - 2 a_0^2 a_6^3 - 2 a_0^3 a_6^2 + a_4 a_6^4 \\
&- a_6^3 a_3^2 - a_6^3 a_2^2 + a_6^5 - a_6^2 a_2^2 a_4 - a_1 a_6^3 a_5 + 2 a_2 a_1 a_6^2 a_5 - a_0 a_6 a_2 a_5^2 \\
&- 2 a_0^2 a_4 a_6^2 - 2 a_6^2 a_2 a_0^2 + 2 a_4 a_6^2 a_2 a_0 + 2 a_2 a_0^2 a_4 a_6 \\
0 < &- a_0 a_6^2 a_2^2 - a_0 a_2 a_4 a_5^2 + a_0 a_1^2 a_5 a_3 + a_0 a_1 a_5 a_4^2 + 3 a_0^2 a_6 a_5 a_3 + 3 a_2 a_0^2 a_5 a_1 \\
&- a_0 a_1 a_2 a_5 a_4 + a_0 a_1 a_5^3 + 2 a_6 a_2^2 a_0^2 + a_2 a_6^2 a_5 a_3 + 2 a_2 a_0 a_6 a_4^2 + a_2 a_0 a_1 a_6 a_5 \\
&+ 3 a_2 a_0 a_6 a_1 a_3 - 4 a_2 a_0 a_1^2 a_6 + a_1^2 a_0 a_4 a_6 + a_1^2 a_6 a_2 a_4 - 3 a_1 a_5 a_0^2 a_6 \\
&- a_1 a_3 a_5^2 a_6 - a_1 a_5 a_6 a_2^2 - a_1 a_3 a_0 a_4 a_6 + a_1 a_2 a_5 a_6 a_4 - 2 a_1 a_0^2 a_5 a_4 \\
&- a_0^2 a_1 a_4 a_3 + 3 a_3 a_0^2 a_5 a_4 - 2 a_2 a_0^2 a_5 a_3 + a_0^2 a_2 a_4^2 + a_0^2 a_4 a_1^2 + a_0^2 a_1^2 a_6 \\
&- a_0^2 a_5^2 a_6 + a_0 a_3 a_5^3 + 3 a_0 a_6^2 a_3^2 + a_0 a_2^2 a_5^2 + a_0 a_1^2 a_5^2 - a_0 a_5 a_1^3 - a_0^5 \\
&- 2 a_0 a_6 a_2^2 a_4 + a_1^4 a_6 + 2 a_5^2 a_0^3 + a_0^3 a_3^2 + a_2 a_0^4 - a_0^2 a_4^3 + a_4 a_0^4 + a_4^2 a_0^3 \\
&- a_0 a_5^4 + a_0^4 a_6 - a_2 a_6^2 a_5^2 + 3 a_0 a_1 a_6^2 a_5 - 3 a_4 a_1 a_6^2 a_5 + 4 a_4 a_0 a_5^2 a_6 \\
&- a_4 a_0 a_1 a_6 a_5 - 3 a_3 a_6^2 a_5 a_0 + 2 a_3 a_1 a_6^2 a_4 - 3 a_3 a_1 a_6^2 a_2 - 3 a_3 a_0 a_5 a_6 a_4 \\
&+ a_3 a_0 a_5 a_6 a_2 - 3 a_3 a_0 a_1 a_6^2 + 3 a_3 a_6 a_0^2 a_1 + a_6^2 a_2^3 - a_0 a_5^2 a_6^2 + 2 a_0 a_4 a_6^3 \\
&- 2 a_0 a_4^2 a_6^2 + a_0^2 a_4^2 a_6 + 2 a_4 a_6^3 a_2 + a_4 a_1^2 a_6^2 - 2 a_4 a_0^3 a_6 - 3 a_6 a_0^2 a_3^2 \\
&+ a_3 a_6^3 a_5 - a_1^2 a_6 a_5^2 - a_1^3 a_6 a_5 - a_6 a_1^3 a_3 - a_1^2 a_6 a_4^2 + a_1^2 a_6^2 a_2 + a_0 a_1^2 a_6^2 \\
&+ a_1 a_5^3 a_6 + a_1 a_6^3 a_3 - a_0^2 a_5^2 a_4 - a_3 a_5 a_0^3 - a_0^3 a_1 a_3 - a_0^3 a_5 a_1 - a_0^2 a_2 a_5^2 \\
&- a_6^4 a_0 - a_6^4 a_2 - 2 a_1^2 a_6^3 - 2 a_0^2 a_6^3 + 2 a_0^3 a_6^2 - a_4 a_6^4 - a_6^3 a_3^2 - a_6^3 a_2^2 + a_6^5 \\
&+ 2 a_3 a_1^2 a_6 a_5 - 2 a_6 a_2 a_0^3 - 2 a_2 a_4 a_0^3 - a_6^2 a_2^2 a_4 + a_1 a_6^3 a_5 + 2 a_6^3 a_2 a_0 \\
&+ 2 a_2 a_1 a_6^2 a_5 - a_0 a_6 a_2 a_5^2 - 2 a_0 a_3 a_1 a_5^2
\end{aligned}
$$

1.5: Equilibrium and Stability: Non-Spatial Age-Structured System

(a): Equilibrium and Characteristic Polynomial

```
> with(linalg):
```

Initialize parameters

```
> s1 := 's1': r := 'r': s2 := 's2': s3 := 's3': s4 :=
  's4': a := 'a':
```

Parameter values can be substituted here if necessary

```
> #r := 6.0; s1 := 0.144; s2 := 0.058; a := 0.75; s3 :=
  0.25; s4 := 0.045;
```

Non-spatial age-structured model

```
> f1 := r*y3:
  f2 := s1*y1:
  f3 := s2*y2*exp(-a*z3):
  g1 := y2*(1 - exp(-a*z3)):
  g2 := s3*z1:
  g3 := s4*z2:
```

Equilibrium conditions

```
> sols := solve({f1=y1,f2=y2,f3=y3,g1=z1,g2=z2,g3=z3},
  {y1,y2,y3,z1,z2,z3});
```

$$sols := \{y3 = 0, z1 = 0, y2 = 0, z3 = 0, z2 = 0, y1 = 0\}, \left\{ z1 = -\frac{\ln\left(\frac{1}{s2\ s1\ r}\right)}{a\ s4\ s3}, \right.$$

$$y3 = -\frac{\ln\left(\frac{1}{s2\ s1\ r}\right) s2}{a\ s4\ s3\ (s2\ s1\ r - 1)}, y2 = -\frac{s1\ r \ln\left(\frac{1}{s2\ s1\ r}\right) s2}{a\ s4\ s3\ (s2\ s1\ r - 1)}, z3 = -\frac{\ln\left(\frac{1}{s2\ s1\ r}\right)}{a},$$

$$\left. z2 = -\frac{\ln\left(\frac{1}{s2\ s1\ r}\right)}{a\ s4}, y1 = -\frac{r \ln\left(\frac{1}{s2\ s1\ r}\right) s2}{a\ s4\ s3\ (s2\ s1\ r - 1)} \right\}$$

Jacobian matrix for the system

```
> A:=subs(sols[2],matrix(6,6,[[diff(f1,y1),diff(f1,y2),dif
  f(f1,y3),diff(f1,z1),diff(f1,z2),diff(f1,z3)],[diff(f2,y
  1),diff(f2,y2),diff(f2,y3),diff(f2,z1),diff(f2,z2),diff(
  f2,z3)],[diff(f3,y1),diff(f3,y2),diff(f3,y3),diff(f3,z1)
```

```
,diff(f3,z2),diff(f3,z3)],[diff(g1,y1),diff(g1,y2),diff(
g1,y3),diff(g1,z1),diff(g1,z2),diff(g1,z3)],[diff(g2,y1)
,diff(g2,y2),diff(g2,y3),diff(g2,z1),diff(g2,z2),diff(g2
,z3)],[diff(g3,y1),diff(g3,y2),diff(g3,y3),diff(g3,z1),d
iff(g3,z2),diff(g3,z3)]]);
```

$$A := \begin{bmatrix} 0 & 0 & r & 0 & 0 & 0 \\ s1 & 0 & 0 & 0 & 0 & 0 \\ 0 & s2\, e^{\ln\left(\frac{1}{s2\,s1\,r}\right)} & 0 & 0 & 0 & \dfrac{s2^2\, s1\, r \ln\left(\frac{1}{s2\,s1\,r}\right) e^{\ln\left(\frac{1}{s2\,s1\,r}\right)}}{s4\, s3\,(s2\,s1\,r-1)} \\ 0 & 1-e^{\ln\left(\frac{1}{s2\,s1\,r}\right)} & 0 & 0 & 0 & -\dfrac{s1\, r \ln\left(\frac{1}{s2\,s1\,r}\right) s2\, e^{\ln\left(\frac{1}{s2\,s1\,r}\right)}}{s4\, s3\,(s2\,s1\,r-1)} \\ 0 & 0 & 0 & s3 & 0 & 0 \\ 0 & 0 & 0 & 0 & s4 & 0 \end{bmatrix}$$

Determinant and trace

```
> dA = det(A); TA := trace(A);
```

$$dA = -\frac{s1\, r\, s2 \ln\left(\frac{1}{s2\,s1\,r}\right)}{s2\,s1\,r-1}$$

$$TA := 0$$

Characteristic polynomial

```
> C[lambda] := collect(charpoly(A,lambda),lambda);
```

$$C_\lambda := \lambda^6 + \frac{\left(1+\ln\left(\frac{1}{s2\,s1\,r}\right)\right)-s2\,s1\,r}{s2\,s1\,r-1}\lambda^3 - \frac{s1\, r\, s2 \ln\left(\frac{1}{s2\,s1\,r}\right)}{s2\,s1\,r-1}$$

(b): Stability Analysis

Coefficients from the characteristic polynomial

```
> a[6] := 1: a[5] := 0: a[4] := 0: a[3] :=
  (1+ln(1/(s2*s1*r))-s2*s1*r)/(s2*s1*r-1): a[2] := 0: a[1]
  := 0: a[0] := (s1*r*s2*ln(1/(s2*s1*r)))/(s2*s1*r-1):
```

Test inequalities: Assumptions on s1 and s2 and limits as r approaches infinity

```
> assume(0<s1,s1<1,0<s2,s2<1);
```

Stability Conditions 1: C(1) > 0 and C(-1) > 0:

```
> C[[1]]:=simplify(eval(subs(lambda = 1, C[lambda]))>0);
```

$$C_{[1]} := 0 < \ln(s2) + \ln(s1) - \ln\left(\frac{1}{r}\right)$$

with assumptions on *s2* and *s1*

```
> limit(subs(lambda = 1, C[lambda]), r=infinity);
```

$$\infty$$

```
> C[[-1]] := simplify(eval(subs(lambda = -1,C[lambda]))
  >0);
```

$$C_{[-1]} := 0 < \frac{2\,s2\,s1\,r - 2 + \ln(s2) + \ln(s1) - \ln\left(\frac{1}{r}\right) + s2\,s1\,r\ln(s2) + s2\,s1\,r\ln(s1) - s2\,s1\,r\ln\left(\frac{1}{r}\right)}{s2\,s1\,r - 1}$$

with assumptions on *s2* and *s1*

```
> limit(subs(lambda = -1,C[lambda]), r=infinity);
```

$$\infty$$

Form matrices (Wn and Xn) from coefficients

```
> W[n]:=matrix(7,7,[a[6],a[5],a[4],a[3],a[2],a[1],a[0],0,a
  [6],a[5],a[4],a[3],a[2],a[1],0,0,a[6],a[5],a[4],a[3],a[2
  ],0,0,0,a[6],a[5],a[4],a[3],0,0,0,0,a[6],a[5],a[4],0,0,0
  ,0,0,a[6],a[5],0,0,0,0,0,0,a[6]]);
```

$$W_n := \begin{bmatrix} 1 & 0 & 0 & \%1 & 0 & 0 & \dfrac{s1\,r\,s2\ln\left(\frac{1}{s2\,s1\,r}\right)}{s2\,s1\,r-1} \\ 0 & 1 & 0 & 0 & \%1 & 0 & 0 \\ 0 & 0 & 1 & 0 & 0 & \%1 & 0 \\ 0 & 0 & 0 & 1 & 0 & 0 & \%1 \\ 0 & 0 & 0 & 0 & 1 & 0 & 0 \\ 0 & 0 & 0 & 0 & 0 & 1 & 0 \\ 0 & 0 & 0 & 0 & 0 & 0 & 1 \end{bmatrix}$$

$$\%1 := \frac{1 + \ln\left(\frac{1}{s2\,s1\,r}\right) - s2\,s1\,r}{s2\,s1\,r - 1}$$

with assumptions on *s1* and *s2*

```
> X[n]:=matrix(7,7,[a[6],a[5],a[4],a[3],a[2],a[1],a[0],a[5
```

```
],a[4],a[3],a[2],a[1],a[0],0,a[4],a[3],a[2],a[1],a[0],0,
0,a[3],a[2],a[1],a[0],0,0,0,a[2],a[1],a[0],0,0,0,0,a[1],
a[0],0,0,0,0,0,a[0],0,0,0,0,0,0,0]);
```

$$X_n := \begin{bmatrix} 1 & 0 & 0 & \%1 & 0 & 0 & \%2 \\ 0 & 0 & \%1 & 0 & 0 & \%2 & 0 \\ 0 & \%1 & 0 & 0 & \%2 & 0 & 0 \\ \%1 & 0 & 0 & \%2 & 0 & 0 & 0 \\ 0 & 0 & \%2 & 0 & 0 & 0 & 0 \\ 0 & \%2 & 0 & 0 & 0 & 0 & 0 \\ \%2 & 0 & 0 & 0 & 0 & 0 & 0 \end{bmatrix}$$

$$\%1 := \frac{1 + \ln\left(\frac{1}{s2\ s1\ r}\right) - s2\ s1\ r}{s2\ s1\ r - 1}$$

$$\%2 := \frac{s1\ r\ s2 \ln\left(\frac{1}{s2\ s1\ r}\right)}{s2\ s1\ r - 1}$$

Form (Wn + Xn) and (Wn - Xn) matrices

```
> WXa := evalm(W[n]+X[n]);
```

$$WXa := \begin{bmatrix} 2 & 0 & 0 & 2\,\%1 & 0 & 0 & 2\,\%2 \\ 0 & 1 & \%1 & 0 & \%1 & \%2 & 0 \\ 0 & \%1 & 1 & 0 & \%2 & \%1 & 0 \\ \%1 & 0 & 0 & 1+\%2 & 0 & 0 & \%1 \\ 0 & 0 & \%2 & 0 & 1 & 0 & 0 \\ 0 & \%2 & 0 & 0 & 0 & 1 & 0 \\ \%2 & 0 & 0 & 0 & 0 & 0 & 1 \end{bmatrix}$$

$$\%1 := \frac{1 + \ln\left(\frac{1}{s2\ s1\ r}\right) - s2\ s1\ r}{s2\ s1\ r - 1}$$

$$\%2 := \frac{s1\ r\ s2 \ln\left(\frac{1}{s2\ s1\ r}\right)}{s2\ s1\ r - 1}$$

```
> WXb := evalm(W[n]-X[n]);
```

$$WXb := \begin{bmatrix} 0 & 0 & 0 & 0 & 0 & 0 & 0 \\ 0 & 1 & -\%1 & 0 & \%1 & -\%2 & 0 \\ 0 & -\%1 & 1 & 0 & -\%2 & \%1 & 0 \\ -\%1 & 0 & 0 & 1-\%2 & 0 & 0 & \%1 \\ 0 & 0 & -\%2 & 0 & 1 & 0 & 0 \\ 0 & -\%2 & 0 & 0 & 0 & 1 & 0 \\ -\%2 & 0 & 0 & 0 & 0 & 0 & 1 \end{bmatrix}$$

$$\%1 := \frac{1 + \ln\left(\frac{1}{s2\ s1\ r}\right) - s2\ s1\ r}{s2\ s1\ r - 1}$$

$$\%2 := \frac{s1\ r\ s2 \ln\left(\frac{1}{s2\ s1\ r}\right)}{s2\ s1\ r - 1}$$

Stability Conditions 2: Determinant of inners (k = 1) > 0)

```
> eval(WXa[4,4] > 0);  eval(WXb[4,4]  > 0);
```

$$0 < 1 + \frac{s1\ r\ s2 \ln\left(\frac{1}{s2\ s1\ r}\right)}{s2\ s1\ r - 1}$$

with assumptions on *s1* and *s2*

$$0 < 1 - \frac{s1\ r\ s2 \ln\left(\frac{1}{s2\ s1\ r}\right)}{s2\ s1\ r - 1}$$

with assumptions on *s1* and *s2*

Evaluate limits

```
> limit(WXa[4,4], r= infinity); limit(WXb[4,4], r=
  infinity);
```

$$-\infty$$

$$\infty$$

```
> I3a:=array(1..3,1..3,[[WXa[3,3],WXa[3,4],WXa[3,5]],[WXa[
  4,3],WXa[4,4],WXa[4,5]],[WXa[5,3],WXa[5,4],WXa[5,5]]]);
```

$$I3a := \begin{bmatrix} 1 & 0 & \dfrac{s1\,r\,s2\,\ln\left(\dfrac{1}{s2\,s1\,r}\right)}{s2\,s1\,r-1} \\ 0 & 1+\dfrac{s1\,r\,s2\,\ln\left(\dfrac{1}{s2\,s1\,r}\right)}{s2\,s1\,r-1} & 0 \\ \dfrac{s1\,r\,s2\,\ln\left(\dfrac{1}{s2\,s1\,r}\right)}{s2\,s1\,r-1} & 0 & 1 \end{bmatrix}$$

with assumptions on *s1* and *s2*

```
> I3b:=array(1..3,1..3,[[WXb[3,3],WXb[3,4],WXb[3,5]],[WXb[
  4,3],WXb[4,4],WXb[4,5]],[WXb[5,3],WXb[5,4],WXb[5,5]]]);
```

$$I3b := \begin{bmatrix} 1 & 0 & -\dfrac{s1\,r\,s2\,\ln\left(\dfrac{1}{s2\,s1\,r}\right)}{s2\,s1\,r-1} \\ 0 & 1-\dfrac{s1\,r\,s2\,\ln\left(\dfrac{1}{s2\,s1\,r}\right)}{s2\,s1\,r-1} & 0 \\ -\dfrac{s1\,r\,s2\,\ln\left(\dfrac{1}{s2\,s1\,r}\right)}{s2\,s1\,r-1} & 0 & 1 \end{bmatrix}$$

with assumptions on *s1* and *s2*

Stability Conditions 3: Determinant of inners (k = 3)

```
> eval(det(I3a) > 0);   eval(det(I3b) > 0);
```

$$0 < -\frac{\left(s2\,s1\,r-1+s1\,r\,s2\,\ln\left(\dfrac{1}{s2\,s1\,r}\right)\right)\left(-s2^2\,s1^2\,r^2+2\,s2\,s1\,r-1+s1^2\,r^2\,s2^2\,\ln\left(\dfrac{1}{s2\,s1\,r}\right)^2\right)}{(s2\,s1\,r-1)^3}$$

with assumptions on *s2* and *s1*

$$0 < \frac{\left(-s2\,s1\,r+1+s1\,r\,s2\,\ln\left(\dfrac{1}{s2\,s1\,r}\right)\right)\left(-s2^2\,s1^2\,r^2+2\,s2\,s1\,r-1+s1^2\,r^2\,s2^2\,\ln\left(\dfrac{1}{s2\,s1\,r}\right)^2\right)}{(s2\,s1\,r-1)^3}$$

with assumptions on *s2* and *s1*

Evaluate limits

```
> limit(det(I3a), r = infinity); limit(det(I3b), r=
  infinity);
```

$$\infty$$

$$-\infty$$

```
> I5a:=array(1..5,1..5,[[WXa[2,2],WXa[2,3],WXa[2,4],WXa[2,
  5],WXa[2,6]],[WXa[3,2],WXa[3,3],WXa[3,4],WXa[3,5],WXa[3,
  6]],[WXa[4,2],WXa[4,3],WXa[4,4],WXa[4,5],WXa[4,6]],[WXa[
  5,2],WXa[5,3],WXa[5,4],WXa[5,5],WXa[5,6]],[WXa[6,2],WXa[
  6,3],WXa[6,4],WXa[6,5],WXa[6,6]]]);
```

$$I5a := \begin{bmatrix} 1 & \%1 & 0 & \%1 & \%2 \\ \%1 & 1 & 0 & \%2 & \%1 \\ 0 & 0 & 1+\%2 & 0 & 0 \\ 0 & \%2 & 0 & 1 & 0 \\ \%2 & 0 & 0 & 0 & 1 \end{bmatrix}$$

$$\%1 := \frac{1+\ln\left(\frac{1}{s2\,s1\,r}\right)-s2\,s1\,r}{s2\,s1\,r-1}$$

$$\%2 := \frac{s1\,r\,s2\,\ln\left(\frac{1}{s2\,s1\,r}\right)}{s2\,s1\,r-1}$$

```
> I5b:=array(1..5,1..5,[[WXb[2,2],WXb[2,3],WXb[2,4],WXb[2,
  5],WXb[2,6]],[WXb[3,2],WXb[3,3],WXb[3,4],WXb[3,5],WXb[3,
  6]],[WXb[4,2],WXb[4,3],WXb[4,4],WXb[4,5],WXb[4,6]],[WXb[
  5,2],WXb[5,3],WXb[5,4],WXb[5,5],WXb[5,6]],[WXb[6,2],WXb[
  6,3],WXb[6,4],WXb[6,5],WXb[6,6]]]);
```

$$I5b := \begin{bmatrix} 1 & -\%1 & 0 & \%1 & -\%2 \\ -\%1 & 1 & 0 & -\%2 & \%1 \\ 0 & 0 & 1-\%2 & 0 & 0 \\ 0 & -\%2 & 0 & 1 & 0 \\ -\%2 & 0 & 0 & 0 & 1 \end{bmatrix}$$

$$\%1 := \frac{1+\ln\left(\frac{1}{s2\,s1\,r}\right)-s2\,s1\,r}{s2\,s1\,r-1}$$

$$\%2 := \frac{s1\,r\,s2\,\ln\left(\frac{1}{s2\,s1\,r}\right)}{s2\,s1\,r-1}$$

Stability Conditions 4: Determinant of inners (k = 5):

```
> eval(det(I5a) > 0); eval(det(I5b) > 0);
```

$$0 < \left(s2\ s1\ r - 1 + s1\ r\ s2\ \ln\left(\frac{1}{s2\ s1\ r}\right)\right)\ln\left(\frac{1}{s2\ s1\ r}\right)\left(-2\ s2\ s1\ r + 2 - s1^2\ r^2\ s2^2\ \ln\left(\frac{1}{s2\ s1\ r}\right)\right.$$
$$+ \ln\left(\frac{1}{s2\ s1\ r}\right) + 3\ s1\ r\ s2\ \ln\left(\frac{1}{s2\ s1\ r}\right) + 2\ r\ s1\ s2\ \ln\left(\frac{1}{s2\ s1\ r}\right)^2 + 2\ s1^2\ r^2\ s2^2\ \ln\left(\frac{1}{s2\ s1\ r}\right)^2$$
$$- 2\ s2^2\ s1^2\ r^2 + s1^2\ r^2\ s2^2\ \ln\left(\frac{1}{s2\ s1\ r}\right)^3 + s1^3\ r^3\ s2^3\ \ln\left(\frac{1}{s2\ s1\ r}\right)^3 - 3\ s2^3\ s1^3\ r^3\ \ln\left(\frac{1}{s2\ s1\ r}\right)$$
$$\left. + 2\ s2^3\ s1^3\ r^3\right) \Big/ (s2\ s1\ r - 1)^4$$

with assumptions on *s2* and *s1*

$$0 < -\left(-s2\ s1\ r + 1 + s1\ r\ s2\ \ln\left(\frac{1}{s2\ s1\ r}\right)\right)\ln\left(\frac{1}{s2\ s1\ r}\right)\left(-2\ s2\ s1\ r + 2\right.$$
$$- s1^2\ r^2\ s2^2\ \ln\left(\frac{1}{s2\ s1\ r}\right) + \ln\left(\frac{1}{s2\ s1\ r}\right) + 3\ s1\ r\ s2\ \ln\left(\frac{1}{s2\ s1\ r}\right) + 2\ r\ s1\ s2\ \ln\left(\frac{1}{s2\ s1\ r}\right)^2$$
$$+ 2\ s1^2\ r^2\ s2^2\ \ln\left(\frac{1}{s2\ s1\ r}\right)^2 - 2\ s2^2\ s1^2\ r^2 + s1^2\ r^2\ s2^2\ \ln\left(\frac{1}{s2\ s1\ r}\right)^3 + s1^3\ r^3\ s2^3\ \ln\left(\frac{1}{s2\ s1\ r}\right)^3$$
$$\left. - 3\ s2^3\ s1^3\ r^3\ \ln\left(\frac{1}{s2\ s1\ r}\right) + 2\ s2^3\ s1^3\ r^3\right) \Big/ (s2\ s1\ r - 1)^4$$

with assumptions on *s2* and *s1*

Evaluate limits

```
> limit(det(I5a), r = infinity); limit(det(I5b), r =
  infinity);
```

$$-\infty$$

$$\infty$$

Some conditions evaluate as minus infinity. The non-spatial age-structured system is unstable.

1.6: Equilibrium and Stability in the Kot Model

```
> with(linalg):
> r := 'r': c:= 'c': pi = 'pi':
```

(a): Basic Non-Spatial Kot Model

```
> f := Y*exp(r*(1- Y - Z));
  g := c*Y*Z;
```

$$f := Y\,e^{(r(1-Y-Z))}$$

$$g := c\,Y\,Z$$

Equilibrium conditions

```
> solve({f=Y,g=Z}, {Y,Z});
```

$$\{Y = 0, Z = 0\}, \{Z = 0, Y = 1\}, \{Y = \frac{1}{c}, Z = \frac{c-1}{c}\}$$

Jacobian matrix

```
> A:=subs(Y=1/c,Z=1-1/c,matrix(2,2,[[diff(f,Y),diff(f,Z)],
  [diff(g,Y),diff(g,Z)]]));
```

$$A := \begin{bmatrix} e^0 - \frac{r\,e^0}{c} & -\frac{r\,e^0}{c} \\ \left(1 - \frac{1}{c}\right)c & 1 \end{bmatrix}$$

$$A := \begin{bmatrix} e^0 - \frac{r\,e^0}{c} & -\frac{r\,e^0}{c} \\ \left(1 - \frac{1}{c}\right)c & 1 \end{bmatrix}$$

Determinant and trace

```
> dA := det(A); trA := trace(A);
```

$$dA := \frac{c - 2r + r\,c}{c}$$

$$trA := 2 - \frac{r}{c}$$

Characteristic equation for non-spatial system

```
> CP := collect(charpoly(A,lambda),lambda);
```

$$CP := \lambda^2 + \frac{(r-2c)\lambda}{c} + \frac{c - 2r + r\,c}{c}$$

Stability criteria (May 1974): 2 > 1 + > |trace|

```
> solve({2 > 1 + dA,1 + dA > abs(trA)},{c,r});
```

$$\{r = 2\,c,\ 1 < c,\ c < 2\}$$

Model is stable for $1 < c < 2$ and $0 < r < (4c/3 - c)$ [If c = 2, r ==8]

```
> assume(1<c,c<2,0<r,r<4*c/(3-c));
> is( 1 - trA + dA > 0); is( 1 + trA + dA > 0); is( 1 - dA
  > 0);
```

true

true

true

```
> r := 'r': c:= 'c':
> with(inttrans):
```

(b): Model with 1-D Gaussian Dispersal

Prey and predator SD of dispersal equal (Mean = 0, SD = 1)

```
> Kn1:=(1/sqrt(2*pi))*exp(-(x)^2/(2));
  Kp1:=(1/sqrt(2*pi))*exp(-(x)^2/(2));
```

$$Kn1 := \frac{1}{2}\frac{\sqrt{2}\ e^{(-1/2x^2)}}{\sqrt{\pi}}$$

$$Kp1 := \frac{1}{2}\frac{\sqrt{2}\ e^{(-1/2x^2)}}{\sqrt{\pi}}$$

Fourier Transform of the 1-D dispersal kernels

```
> kn1:=fourier(Kn1,x,omega); kp1 :=fourier(Kp1,x,omega);
```

$$kn1 := \frac{\sqrt{\pi}\ e^{(-1/2\omega^2)}}{\sqrt{\pi}}$$

$$kp1 := \frac{\sqrt{\pi}\ e^{(-1/2\omega^2)}}{\sqrt{\pi}}$$

Matrix of Fourier Transformed dispersal

```
> K := matrix(2,2,[kn1,0,0,kp1]);
```

$$K := \begin{bmatrix} \dfrac{\sqrt{\pi}\ e^{(-1/2\omega^2)}}{\sqrt{\pi}} & 0 \\ 0 & \dfrac{\sqrt{\pi}\ e^{(-1/2\omega^2)}}{\sqrt{\pi}} \end{bmatrix}$$

Characteristic matrix with 1-D equal dispersal

```
> KA1 := evalm(K&*A);
```

$$KA1 := \begin{bmatrix} \dfrac{\sqrt{\pi}\,\%1\left(1-\dfrac{r}{c}\right)}{\sqrt{\pi}} & -\dfrac{\sqrt{\pi}\,\%1\,r}{\sqrt{\pi}\,c} \\ \dfrac{\sqrt{\pi}\,\%1\left(1-\dfrac{1}{c}\right)c}{\sqrt{\pi}} & \dfrac{\sqrt{\pi}\,\%1}{\sqrt{\pi}} \end{bmatrix}$$

$$\%1 := e^{(-1/2\,\omega^2)}$$

Determinant and trace

```
> dA1 := simplify(det(KA1)); trA1 := simplify(trace(KA1));
```

$$dA1 := \frac{\pi\, e^{(-\omega^2)}(c-2\,r+r\,c)}{\pi\,c}$$

$$trA1 := -\frac{\sqrt{\pi}\, e^{(-1/2\,\omega^2)}(r-2\,c)}{\sqrt{\pi}\,c}$$

Characteristic polynomial of 1-D spatial system

```
> CP1 := collect(simplify(charpoly(KA1,lambda)), lambda);
```

$$CP1 := \lambda^2 + \frac{(\sqrt{\pi}\sqrt{\pi}\, e^{(-1/2\,\omega^2)} r - 2\sqrt{\pi}\, c\sqrt{\pi}\, e^{(-1/2\,\omega^2)})\lambda}{\pi\,c} + \frac{-2\,\pi\, e^{(-\omega^2)} r + \pi\, e^{(-\omega^2)} r\,c + \pi\, e^{(-\omega^2)} c}{\pi\,c}$$

Jury Test: Evaluate conditions as limit of c ---> 2 and r ---> 8

```
> C1 := simplify(limit(1 - trA1 + dA1, {c = 2, r = 8}));
```

$$C1 := \frac{\pi^{3/2} + 2\sqrt{\pi}\, e^{(-1/2\,\omega^2)}\pi + \pi\, e^{(-\omega^2)}\sqrt{\pi}}{\pi^{3/2}}$$

```
> C2 := simplify(limit(1 + trA1 + dA1,{c = 2, r = 8}));
```

$$C2 := \frac{\pi^{3/2} - 2\sqrt{\pi}\, e^{(-1/2\,\omega^2)}\pi + \pi\, e^{(-\omega^2)}\sqrt{\pi}}{\pi^{3/2}}$$

Use graph to evaluate the limits

```
> pi := 3.141592654: plot(C2, omega = 0..1); pi := 'pi':
```

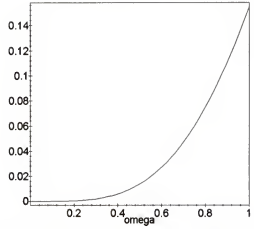


```
> C3 := simplify(limit(1 - dA1, {c = 2, r = 8}));
```

$$C3 := -\frac{-\pi + \pi\, e^{(-\omega^2)}}{\pi}$$

All conditions are positive. Steady-states with 1-D equal prey-predator dispersal are stable.

Prey and predator SD of dispersal unequal (Mean = 0 , SD 2:1 for predator:prey)

```
> Kn2:=(1/(sqrt(2*pi)))*exp(-(x)^2/(2));
  Kp2:=(1/(sqrt(2*pi)*2))*exp(-(x)^2/(2*2^2));
```

$$Kn2 := \frac{1}{2}\frac{\sqrt{2}\, e^{(-1/2\,x^2)}}{\sqrt{\pi}}$$

$$Kp2 := \frac{1}{4}\frac{\sqrt{2}\, e^{(-1/8\,x^2)}}{\sqrt{\pi}}$$

Fourier Transforms of unequal dispersal kernels

```
> kn2:=fourier(Kn2,x,omega); kp2 :=fourier(Kp2,x,omega);
```

$$kn2 := \frac{\sqrt{\pi}\, e^{(-1/2\,\omega^2)}}{\sqrt{\pi}}$$

$$kp2 := \frac{1}{4}\frac{\sqrt{2}\,\sqrt{8}\,\sqrt{\pi}\, e^{(-2\,\omega^2)}}{\sqrt{\pi}}$$

Characteristic matrix with 1-D unequal dispersal

```
> KA2 := evalm(matrix(2,2,[kn2,0,0,kp2])&*A);
```

$$KA2 := \begin{bmatrix} \dfrac{\sqrt{\pi}\, e^{(-1/2\,\omega^2)}\left(1-\dfrac{r}{c}\right)}{\sqrt{\pi}} & -\dfrac{\sqrt{\pi}\, e^{(-1/2\,\omega^2)} r}{\sqrt{\pi}\, c} \\ \dfrac{1}{4}\dfrac{\sqrt{2}\sqrt{8}\sqrt{\pi}\, e^{(-2\,\omega^2)}\left(1-\dfrac{1}{c}\right) c}{\sqrt{\pi}} & \dfrac{1}{4}\dfrac{\sqrt{2}\sqrt{8}\sqrt{\pi}\, e^{(-2\,\omega^2)}}{\sqrt{\pi}} \end{bmatrix}$$

Determinant and trace

```
> dA2 := simplify(det(KA2)); trA2 := simplify(trace(KA2));
```

$$dA2 := \frac{\pi\,(c - 2\,r + r\,c)\, e^{(-5/2\,\omega^2)}}{\pi\, c}$$

$$trA2 := -\frac{\sqrt{\pi}\, e^{(-1/2\,\omega^2)}\,(-c + r - e^{(-3/2\,\omega^2)}\, c)}{\sqrt{\pi}\, c}$$

Characteristic polynomial of 1-D Spatial System with unequal SDs of dispersal

```
> CP2 := collect(simplify(charpoly(KA2,lambda)), lambda);
```

$$CP2 := \lambda^2 - \frac{(-\sqrt{\pi}\sqrt{\pi}\, e^{(-1/2\,\omega^2)} r + \sqrt{\pi}\, c\sqrt{\pi}\, e^{(-2\,\omega^2)} + \sqrt{\pi}\, c\sqrt{\pi}\, e^{(-1/2\,\omega^2)})\,\lambda}{\pi\, c}$$

$$- \frac{2\,\pi\, r\, e^{(-5/2\,\omega^2)} - \pi\, r\, c\, e^{(-5/2\,\omega^2)} - \pi\, c\, e^{(-5/2\,\omega^2)}}{\pi\, c}$$

Jury Test: Stability Conditions with 1-D unequal dispersal

```
> C1 := simplify(limit(1 - trA2 + dA2, {c = 2, r = 8}));
```

$$C1 := -\frac{-\pi^{3/2} - 3\sqrt{\pi}\, e^{(-1/2\,\omega^2)}\,\pi + \sqrt{\pi}\, e^{(-2\,\omega^2)}\,\pi - \pi\, e^{(-5/2\,\omega^2)}\sqrt{\pi}}{\pi^{3/2}}$$

Plot conditions to evaluate

```
> pi := 3.141592654: plot(C1, omega=0..1); pi := 'pi':
```

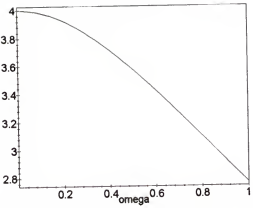


```
> C2 := simplify(limit(1 + trA2 + dA2, {c = 2, r = 8}));
```

$$C2 := \frac{\pi^{3/2} + \sqrt{\pi}\, e^{(-2\omega^2)}\pi - 3\sqrt{\pi}\, e^{(-1/2\omega^2)}\pi + \pi\, e^{(-5/2\omega^2)}\sqrt{\pi}}{\pi^{3/2}}$$

```
> pi := 3.141592654: plot(C2, omega=0..1); pi := 'pi':
```

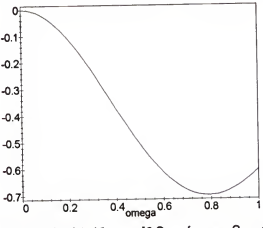


```
> C3 := simplify(limit(1 - dA2, {c = 2, r= 8}));
```

$$C3 := \frac{\pi - \pi\, e^{(-5/2\omega^2)}}{\pi}$$

```
> pi := 3.141592654: plot(C3, omega=0..1); pi := 'pi':
```

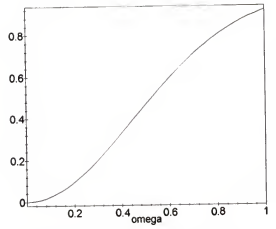

One condition is negative for greater predator dispersal. The system is therefore unstable.

(c): Model with 2-D Gaussian Dispersal

Prey and predator SD of dispersal equal (Mean = 0 and SD = 1)

```
> Knx:=(1/sqrt(2*pi))*exp(-(x)^2/(2));
  Kny:=(1/sqrt(2*pi))*exp(-(y)^2/(2));
```

$$Knx := \frac{1}{2}\frac{\sqrt{2}\, e^{(-1/2x^2)}}{\sqrt{\pi}}$$

$$Kny := \frac{1}{2}\frac{\sqrt{2}\, e^{(-1/2y^2)}}{\sqrt{\pi}}$$

```
> Kpx:=(1/sqrt(2*pi))*exp(-(x)^2/(2));
  Kpy:=(1/sqrt(2*pi))*exp(-(y)^2/(2));
```

$$Kpx := \frac{1}{2}\frac{\sqrt{2}\, e^{(-1/2x^2)}}{\sqrt{\pi}}$$

$$Kpy := \frac{1}{2}\frac{\sqrt{2}\, e^{(-1/2y^2)}}{\sqrt{\pi}}$$

Fourier Transform of 2-D kernels:

```
> kn3:= simplify(fourier(Knx,x,omega)*fourier(Kny,y,u));
```

$$kn3 := \frac{\pi\, e^{(-1/2\omega^2 - 1/2u^2)}}{\pi}$$

```
> kp3 := simplify(fourier(Kpx,x,omega)*fourier(Kpy,y,u));
```

$$kp3 := \frac{\pi\, e^{(-1/2\,\omega^2 - 1/2\,u^2)}}{\pi}$$

Characteristic matrix with 2-D equal dispersal:

```
> KA3 := evalm(matrix(2,2,[kn3,0,0,kp3])&*A);
```

$$KA3 := \begin{bmatrix} \dfrac{\pi\,\%1\left(1-\dfrac{r}{c}\right)}{\pi} & -\dfrac{\pi\,\%1\,r}{\pi\,c} \\ \dfrac{\pi\,\%1\left(1-\dfrac{1}{c}\right)c}{\pi} & \dfrac{\pi\,\%1}{\pi} \end{bmatrix}$$

$$\%1 := e^{(-1/2\,\omega^2 - 1/2\,u^2)}$$

Determinant and trace

```
> dA3 := simplify(det(KA3)); trA3 := simplify(trace(KA3));
```

$$dA3 := \frac{\pi^2\, e^{(-\omega^2 - u^2)}\,(c - 2\,r + r\,c)}{\pi^2\, c}$$

$$trA3 := -\frac{\pi\, e^{(-1/2\,\omega^2 - 1/2\,u^2)}\,(r - 2\,c)}{\pi\, c}$$

Characteristic polynomial of 2-D system

```
> CP3 := collect(simplify(charpoly(KA3,lambda)), lambda);
```

$$CP3 := \lambda^2 + \frac{(\pi\, e^{(-1/2\,\omega^2 - 1/2\,u^2)}\,r\,\pi - 2\,\pi\,c\,\pi\, e^{(-1/2\,\omega^2 - 1/2\,u^2)})\,\lambda}{\pi^2\, c} + \frac{-2\,\pi^2\, e^{(-\omega^2 - u^2)}\,r + \pi^2\, e^{(-\omega^2 - u^2)}\,r\,c + \pi^2\, e^{(-\omega^2 - u^2)}\,c}{\pi^2\, c}$$

Jury Test: Stability conditions with 2-D equal dispersal

```
> C1 := simplify(limit(1 - trA3 + dA3, {c = 2, r=8}));
```

$$C1 := \frac{\pi^2 + 2\,\pi\, e^{(-1/2\,\omega^2 - 1/2\,u^2)}\,\pi + \pi^2\, e^{(-\omega^2 - u^2)}}{\pi^2}$$

```
> C2 := simplify(limit(1 + trA3 + dA3, {c = 2, r=8}));
```

$$C2 := \frac{\pi^2 - 2\,\pi\, e^{(-1/2\,\omega^2 - 1/2\,u^2)}\,\pi + \pi^2\, e^{(-\omega^2 - u^2)}}{\pi^2}$$

```
> pi:=3.141592654: plot3d(C2, omega=0..1, u=
```

```
0..1);pi:='pi':
```

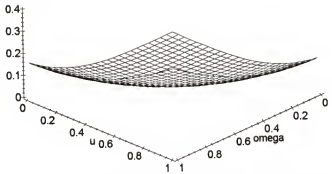


```
> C3 := simplify(limit(1 - dA3, {c = 2, r=8}));
```

$$C3 := \frac{\pi^2 - \pi^2\, e^{(-\omega^2 - u^2)}}{\pi^2}$$

All conditions are positive: Steady-states with 2-D equal dispersal are stable.

Prey and predator SD of dispersal unequal (Mean = 0 , SD 2:1 for predator:prey)

```
> Knx2:=(1/sqrt(2*pi))*exp(-(x)^2/(2));
  Kny2:=(1/sqrt(2*pi))*exp(-(y)^2/(2));
```

$$Knx2 := \frac{\frac{1}{2}\sqrt{2}\, e^{(-1/2x^2)}}{\sqrt{\pi}}$$

$$Kny2 := \frac{\frac{1}{2}\sqrt{2}\, e^{(-1/2y^2)}}{\sqrt{\pi}}$$

```
> Kpx2:=(1/(sqrt(2*pi)*2))*exp(-(x)^2/(2*2^2));
  Kpy2:=(1/(sqrt(2*pi)*2))*exp(-(y)^2/(2*2^2));
```

$$Kpx2 := \frac{\frac{1}{4}\sqrt{2}\, e^{(-1/8x^2)}}{\sqrt{\pi}}$$

$$Kpy2 := \frac{\frac{1}{4}\sqrt{2}\, e^{(-1/8y^2)}}{\sqrt{\pi}}$$

Fourier Transform of 2-D kernels with unequal dispersal

```
> kn4:= simplify(fourier(Knx2,x,omega)*fourier(Kny2,y,u));
```

$$kn4 := \frac{\pi\, e^{(-1/2\omega^2 - 1/2u^2)}}{\pi}$$

```
> kp4 :=
  simplify(fourier(Kpx2,x,omega)*fourier(Kpy2,y,u));
```

$$kp4 := \frac{\pi\, e^{(-2\omega^2 - 2u^2)}}{\pi}$$

Characteristic matrix with 2-D unequal dispersal

```
> KA4 := evalm(matrix(2,2,[kn4,0,0,kp4])&*A);
```

$$KA4 := \begin{bmatrix} \dfrac{\pi\, e^{(-1/2\omega^2 - 1/2u^2)}\left(1 - \dfrac{r}{c}\right)}{\pi} & -\dfrac{\pi\, e^{(-1/2\omega^2 - 1/2u^2)} r}{\pi c} \\ \dfrac{\pi\, e^{(-2\omega^2 - 2u^2)}\left(1 - \dfrac{1}{c}\right) c}{\pi} & \dfrac{\pi\, e^{(-2\omega^2 - 2u^2)}}{\pi} \end{bmatrix}$$

Determinant and trace

```
> dA4 := simplify(det(KA4)); trA4 := simplify(trace(KA4));
```

$$dA4 := \frac{\pi^2 (c - 2r + rc)\, e^{(-5/2\omega^2 - 5/2u^2)}}{\pi^2 c}$$

$$trA4 := -\frac{\pi\, e^{(-1/2\omega^2 - 1/2u^2)}(-c + r - e^{(-3/2\omega^2 - 3/2u^2)} c)}{\pi c}$$

Characteristic polynomial of 2-D system

```
> CP4 := collect(simplify(charpoly(KA4,lambda)), lambda);
```

$$CP4 := \lambda^2 + \frac{(\pi\, e^{(-1/2\omega^2 - 1/2u^2)} r\, \pi - \pi c\, \pi\, e^{(-2\omega^2 - 2u^2)} - \pi c\, \pi\, e^{(-1/2\omega^2 - 1/2u^2)})\lambda}{\pi^2 c}$$

$$+ \frac{-2\pi^2 r\, e^{(-5/2\omega^2 - 5/2u^2)} + \pi^2 r c\, e^{(-5/2\omega^2 - 5/2u^2)} + \pi^2 c\, e^{(-5/2\omega^2 - 5/2u^2)}}{\pi^2 c}$$

Jury Test: Stability conditions with 2-D unequal dispersal:

```
> C1 := simplify(limit(1 - trA4 + dA4, {c = 2, r=8}));
```

$$C1 := \frac{\pi^2 - \pi\, \pi\, e^{(-2\omega^2 - 2u^2)} + 3\pi\, e^{(-1/2\omega^2 - 1/2u^2)}\, \pi + \pi^2 e^{(-5/2\omega^2 - 5/2u^2)}}{\pi^2}$$

```
> pi := 3.141592654: plot3d(C1, omega=0..1, u= 0..1);
  pi:='pi':
```

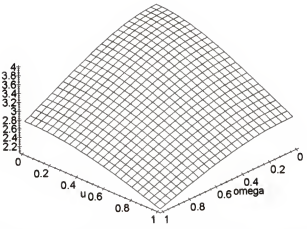


```
> C2 := simplify(limit(1 + trA4 + dA4, {c = 2, r=8}));
```

$$C2 := \frac{\pi^2 + \pi\,\pi\, e^{(-2\omega^2 - 2u^2)} - 3\,\pi\, e^{(-1/2\omega^2 - 1/2u^2)}\,\pi + \pi^2\, e^{(-5/2\omega^2 - 5/2u^2)}}{\pi^2}$$

```
> pi := 3.141592654: plot3d(C2, omega=0..1, u= 0..1);
  pi:='pi':
```

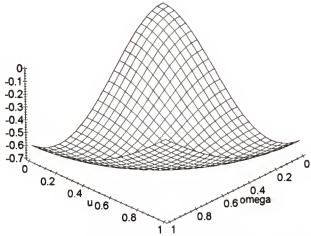


```
> C3 := simplify(limit(1 - dA4, {c = 2, r=8}));
```

$$C3 := \frac{\pi^2 - \pi^2\, e^{(-5/2\omega^2 - 5/2u^2)}}{\pi^2}$$

One condition is negative for greater predator dispersal. The system is unstable.

LITERATURE CITED

Abbass, A.K., A.A. Al-Hitty, A.A. Ali & N.M. Hassan. 1988. Evaluation of various control practices and their time of application against the whitefly (*Bemisia tabaci* Genn.) and some other pests on fall cucumber. J. Agric. Water Res. 7: 123-142.

Abisgold, J.D. & L.D.C. Fishpool. 1990. A method for estimating population sizes of whitefly nymphs (*Bemisia tabaci* Genn.) on cassava. Trop. Pest Manag. 36: 287-292.

Ahmed, A.H.M., E.A. Elhagh & N.H.H. Bashir. 1987. Insecticide resistance in cotton whitefly (*Bemisia tabaci* Genn.) in the Sudan Gezira. Trop. Pest Manag. 33: 67-72, 103, 107.

Al-musa, A.M., I.K. Nazer, N.S. Sharaf & A.N. Mansour. 1985. Muslin and plastic tunnels; effect on incidence of tomato yellow leaf curl, early blight and various growth characteristics of tomatoes. Dirasat 12(6): 101-109.

Alder, F.R. 1993. Migration alone can produce persistence of host-parasitoid models. Am. Nat. 141: 642-650.

Allen, J.C. 1975. Mathematical models of species interactions in time and space. Am. Nat. 109: 319-341.

Allen, J.C., C.C. Brewster, J.F. Paris, D.G. Riley & C.G. Summers. 1996. Spatiotemporal modeling of whitefly dynamics in a regional cropping system using satellite data. In D. Gerling & R. T. Mayer (eds.), *Bemisia*: 1995. taxonomy, biology, damage, control and management. Intercept, Andover, UK. 702pp.

Allen, J.C., W.M. Schaffer & D. Rosko. 1993. Chaos reduces species extinction by amplifying local population noise. Nature 364: 229-232.

Andersen, M. 1991. Properties of some density-dependent integrodifference equation models. Math. BioSci. 104: 135-157.

Avery, T.E. & G.L Berlin. 1992. Fundamentals of remote sensing and airphoto interpretation 5th. edition. Macmillan Publishing Co., New York. 472pp.

Azab, A.K., M.M. Megahed & H.D. El-Mirsawi. 1970. Studies on *Bemisia tabaci* (Genn.) (Hemiptera-Homoptera: Aleyrodidae). Bull. Entomol. Soc. Egypt 53: 339-352.

Azab, A.K., M.M. Megahed & H.D. El-Mirsawi. 1972. On the biology of *Bemisia tabaci* (Genn.) (Hemiptera-Homoptera: Aleyrodidae). Bull. Entomol. Soc. Egypt 55: 305-315.

Banks, H.T., P.M. Kareiva & L. Zia. 1988. Analyzing field studies of insect dispersal using two-dimensional transport equations. Environ. Entomol. 17: 815-820.

Barclay, H.J. 1992. Modeling the effects of population aggregation on the efficiency of insect pest control. Res. Popul. Ecol. 34: 131-141.

Bascompte, J. and R.V. Solé. 1994. Spatially induced bifurcations in single-species population dynamics. J. Anim. Ecol. 63: 256-264.

Baumgärtner, J., V. Delucchi, R. Von Arx & D. Rubli. 1986. Whitefly (*Bemisia tabaci* Genn., Stern.: Aleyrodidae) infestation patterns as influenced by cotton, weather and *Heliothis*: Hypotheses testing by using simulation models. Agric. Ecosystems Environ. 17(1-2): 49-59.

Baumgärtner, J. & E. Yano. 1990. Whitefly population dynamics and modeling. p. 123-146. In D. Gerling (ed.), Whiteflies: Their bionomics, pest status and management. Intercept, Andover, UK.

Beddington, J. R. 1975. Mutual interference between parasites or predators and its effect on searching efficiency. J. Anim. Ecol. 44: 331-340.

Beddington, J.R., C.A. Free & J.H. Lawton. 1975. Dynamic complexity in predator-prey models framed in difference equations. Nature 255: 58-60.

Bellows, T.S., Jr. & K. Arakawa. 1986. Modeling the relationship between transient vector densities and plant disease incidence with special reference to *Bemisia tabaci* (Homoptera: Aleyrodidae) and lettuce infectious virus yellows. J. Econ. Entomol. 79: 1235-1239.

Bellows, T. S., Jr. & K. Arakawa. 1988. Dynamics of preimaginal populations of *Bemisia tabaci* (Homoptera: Aleyrodidae) and *Eretmocerus* sp. (Hymenoptera: Aphelinidae) in southern California cotton. Environ. Entomol. 17: 483-487.

Bellows, T.S., Jr., T.M. Perring, K. Arakawa & C.F. Farrar. 1988. Patterns in diel flight activity of *Bemisia tabaci* (Homoptera: Aleyrodidae) in cropping systems in Southern California. Environ. Entomol. 17: 225-228.

Bellows, T.S., Jr., T.M. Perring, R.J. Gill & D.H. Headrick. 1994. Description of a species of *Bemisia* (Homoptera: Aleyrodidae). Ann. Entomol. Soc. Am. 87: 195-206.

Bentz, J.A., J. Reeves, P. Barbosa & B. Francis. 1995a. Effect of nitrogen fertilizer source and level on ovipositional choice of poinsettia by *Bemisia argentifolii* (Homoptera: Aleyrodidae). J. Econ. Entomol. 88: 1388-1392.

Bentz, J.A., J. Reeves, P. Barbosa & B. Francis. 1995b. Nitrogen fertilizer effect on selection, acceptance and suitability of *Euphorbia pulcherrima* (Euphorbiaceae) as a host plant to *Bemisia tabaci* (Homoptera, Aleyrodidae). Environ. Entomol. 24: 40-45.

Bentz, J.A., J. Reeves, P. Barbosa & B. Francis. 1995c. Within-plant variation in nitrogen and sugar content of poinsettia and its effects on the oviposition pattern, survival, and development of *Bemisia argentifolii* (Homoptera: Aleyrodidae). Environ. Entomol. 24: 271-277.

Bergé, P., Y. Pomeau & C. Vidal. 1984. Order within chaos. Towards a deterministic approach to turbulence. J. Wiley & Sons, New York, 329pp.

Bergh, J.C., T.M. Perring & J.P.R. Le Blanc. 1995. Identification of silverleaf whitefly, *Bemisia argentifolii* Bellows and Perring (Homoptera: Aleyrodidae), in Nova Scotia greenhouses. Can. Entomol. 127: 141-142.

Berlinger, M.J. 1980. A yellow sticky trap for whiteflies: *Trialeurodes vaporariorum* and *Bemisia tabaci* (Aleurodidae). Entomol. Exp. Appl. 27: 98-102.

Berlinger, M.J. 1986. Host plant resistance to *Bemisia tabaci*. Agric. Ecosystems Environ. 17: 69-82.

Berlinger, M.J., D. Dahan & S. Mordechi. 1988. Integrated pest management of organically grown greenhouse tomatoes in Israel. Appl. Agric. Res. 3: 233-238.

Berlinger, M.J. & L.B. Nir. 1989. A population growth model for *Bemisia tabaci*. Phytoparasitica 17: 229-238.

Bethke, J.A., T.D. Paine & G.S. Nuessly. 1991. Comparative biology, morphometrics, and development of two populations of *Bemisia tabaci* (Homoptera: Aleyrodidae) on cotton and poinsettia. Ann. Entomol. Soc. Am. 84: 407-411.

Bink-Moenen, R.M. & L.A. Mound. 1990. Whiteflies diversity biosystematics and evolutionary patterns. p. 1-12. In D. Gerling (ed.), Whiteflies: Their bionomics, pest status, and management. Intercept, Andover, UK.

Blackmer, J.L. & D.N. Byrne. 1993a. Flight behaviour of *Bemisia tabaci* in a vertical flight chamber: Effect of time of day, sex, age and host quality. Physiol. Entomol. 18: 223-232.

Blackmer, J.L. & D.N. Byrne. 1993b. Environmental and physiological factors influencing phototactic flight of *Bemisia tabaci*. Physiol. Entomol. 18: 336-342.

Blua, M.J. & N.C. Toscano. 1994. *Bemisia argentifolii* (Homoptera, Aleyrodidae) development and honeydew production as a function of cotton nitrogen status. Environ. Entomol. 23: 316- 321.

Blua, M.J., T.M. Perring, G.S. Nuessly, J.E. Duffus & N.C. Toscano. 1994. Seasonal cropping pattern effects on abundance of *Bemisia tabaci* (Homoptera: Aleyrodidae) and incidence of lettuce infectious yellows virus. Environ. Entomol. 23: 1422-1427.

Blua. M.J., H.A. Yoshida & N. C. Toscano. 1995. Oviposition preference of two *Bemisia* species (Homoptera: Aleyrodidae). Environ. Entomol. 24: 88-93.

Bock, K. R., E. J. Guthrie & G. Meredith. 1978. Distribution, host range, properties and purification of cassava latent virus, a geminivirus. Ann. Appl. Biol. 90: 361-367.

Borror, D.J., C.A. Triplehorn & N.F. Johnson. 1989. An introduction to the study of insects. 6th. ed. Saunders College Publishing, Philadelphia. 875pp.

Breene, R.G., R.L. Meagher, Jr., A. Nordlund & Y.T. Wang. 1992. Biological control of *Bemisia tabaci* (Homoptera: Aleyrodidae) in a greenhouse using *Chrysopa rufalibris* (Neuroptera: Chrysopidae). Biol. Control 2:9-14.

Broadbent, A.B., R.G. Foottit & G.D. Murphy. 1989. Sweetpotato whitefly *Bemisia tabaci* (Gennadius) (Homoptera: Aleyrodidae), a potential insect pest in Canada. Can. Entomol. 121: 1027-1028.

Brown, J.K. & J.Bird. 1992. Whitefly-transmitted geminiviruses and associated disorders in the Americas and the Caribbean Basin. Plant Dis. 76: 220-225.

Brown, J.K., D.R. Frohlich & R.C. Rosell. 1995. The sweetpotato or silverleaf whiteflies: biotypes of *Bemisia tabaci* or a species complex? Annu. Rev. Entomol. 40: 511-534.

Brown, J.K. & M.R. Nelson. 1984. Geminate particles associated with cotton leaf crumple disease in Arizona. Phytopathology 74: 987-990.

Brown, J.K. & M.R. Nelson. 1986. Whitefly-borne viruses of melons and lettuce in Arizona. Phytopathology 76: 236-239.

Brown, J.K. & M.R. Nelson. 1988. Transmission, host range, and virus-vector relationships of chino del tomate virus (CdTV), a whitefly-transmitted geminivirus from Sinaloa. Plant Dis. 72: 866-869.

Brunt, A.A. & R.H. Kenten. 1973. Cowpea mild mottle, a newly recognized virus infecting cowpeas (*Vigna unguiculata*) in Ghana. Ann. Appl. Sci. 74: 67-74.

Buntin, G.D., D.A. Gilbertz & R.D. Oetting. 1993. Chlorophyll loss and gas exchange in tomato leaves after feeding injury by *Bemisia tabaci* (Homoptera, Aleyrodidae). J. Econ. Entomol. 86:517-522.

Butler, G.D., Jr., T.J. Henneberry & T.E. Clayton. 1983. *Bemisia tabaci* (Homoptera: Aleyrodidae): development, oviposition, and longevity in relation to temperature. Ann. Entomol. Soc. Am. 76: 310-313.

Butler, G.D., Jr., T.J. Henneberry & W.D. Hutchison. 1986. Biology, sampling and population dynamics of *Bemisia tabaci*. p. 167-195. In G. E. Russell (ed.), Agricultural Zoology Reviews. Intercept, Andover, UK.

Butler, G.D., Jr. & F.D. Wilson. 1986. Whitefly adults in okra-leaf and normal-leaf cottons. Arizona Agric. Exp. Stn. P-63: 223-226.

Byrne, D.N. & T.S. Bellows. 1991. Whitefly biology. Annu. Rev. Entomol. 36: 431-457.

Byrne, D.N., T.S. Bellows & M.P. Parrella. 1990. Whiteflies in agricultural systems. p. 227-262. In D. Gerling (ed.), Whiteflies: Their bionomics, pest status and management. Intercept, Andover, UK.

Byrne, D.N., J.L. Blackmer & R.J. Rathman. 1994. Migration and dispersal by the sweetpotato whitefly. Phytoparasitica 22(4): 314.

Byrne, D.N., S.L. Buchmann & H.G. Spangler. 1988. Relationship between wing loading, wingbeat frequency and body mass in homopterous insects. J. Exp. Biol. 135: 9-23.

Byrne, D. N. & E. A. Draeger. 1989. Effect of plant maturity on oviposition and nymphal mortality of *Bemisia tabaci* (Homoptera: Aleyrodidae). Environ. Entomol. 18: 429-434.

Byrne, D.N. & M.A. Houck. 1990. Morphometric identification of wing polymorphism in *Bemisia tabaci* (Gennadius) (Homoptera: Aleyrodidae). Ann. Entomol. Soc. Am. 83: 487-493.

Byrne, D.N. & W.B. Miller. 1990. Carbohydrate and amino acid composition of phloem sap and honeydew produced by *Bemisia tabaci*. J. Insect Physiol. 36: 433-440.

Byrne, D.N., R.J. Rathman, T.V. Orum & J.C. Palumbo. 1996. Localized migration and dispersal by the sweetpotato whitefly, *Bemisia tabaci*. Oecologia 105: 320-328.

Byrne, D.N., P.K. von Bretzel & C.J. Hoffman. 1986. Impact of trap design and placement when monitoring for the banded winged whitefly and the sweetpotato whitefly (Homoptera: Aleyrodidae). Environ. Entomol. 15: 300-304.

Byrne, D.N. & P.K. von Bretzel. 1987. Similarity in flight activity rhythms in coexisting species of Aleyrodidae, *Bemisia tabaci* (Gennadius) and *Trialeurodes abutilonea* (Haldeman). Entomol. Exp. Appl. 43: 215-219.

Byrne, G.R., P.F. Crapper & K.K. Mayo. 1980. Monitoring land cover changes by Principal Component Analysis of multitemporal Landsat data. Remote Sensing of Environ. 10: 175-184.

Cherkasov, V.A. 1986. Effectiveness of the bological method in the greenhouse. Zaschita Rastenii 2:54- 56.

Cheung, P.S.R. & C.W. Roberts. 1980. Implications of disaccharides in sticky cotton processing: honeydew contamination. Textile Res. J. 50:55-59.

Cock, M.J.W. 1986a. *Bemisia tabaci*~A literature survey on the cotton whitefly with an annotated bibliography. CAB International Institute of Biological Control, Ascot, UK, 121pp.

Cock, M.J.W. 1986b. Other control methods. p. 59-61. In M. J. W. Cock (ed.), *Bemisia tabaci*~A literature survey on the cotton whitefly with an annotated bibliography. CAB International Institute of Biological Control, Ascot, UK, 121pp.

Cock, M.J.W. 1993. *Bemisia tabaci*--an update 1986-1992 on the cotton whitefly with an annotated bibliography. CAB International Institute of Biological Control, Ascot, UK, 78pp.

Cohen, J.E. 1995. Unexpected dominance of high frequencies in chaotic nonlinear population models. Nature 378: 610-612.

Cohen, S., J.E. Duffus, R.C. Larsen, H.Y. Liu & R.A. Flock. 1983. Purification, serology, and vector relationships of squash leaf curl virus, a whitefly-transmitted geminivirus. Phytopathology 73: 1669-1673.

Comins, H.N. & D.W.E. Blatt. 1974. Prey-predator models in spatially heterogeneous environments. J. Theor. Biol. 48: 75-83.

Comins, H.N., M.P Hassell & R.M. May. 1992. The spatial dynamics of host-parasitoid systems. J. Anim. Ecol. 61: 735-748.

Congalton, R. 1991. A review of assessing the accuracy of classification of remotely sensed data. Remote Sens. Environ. 37: 35-46.

Conroy, M.J., Y.Cohen, F.C. James, Y.G. Matsinos & B.A. Maurer. 1995. Parameter estimation, reliability, and model improvement for spatially explicit models of animal populations. Ecol. Appl. 5: 17-19.

Corbett, A. & R.E. Plant. 1993. Role of movement in the response of natural enemies to agroecosystem diversification: A theoretical evaluation. Environ. Entomol. 22: 519-531.

Costa, A.S. 1976. Whitefly-transmitted plant diseases. Annu. Rev. Phytopathol. 14: 429-449.

Costa, H.S. & J.K. Brown. 1990. Variability in biological characteristics, isozyme patterns and virus transmission among populations of *Bemisia tabaci* Genn. in Arizona (Abstr.). Phytopathology 80: 888.

Costa, H.S. & J.K. Brown. 1991. Variation in biological characteristics and in esterase patterns among populations of *Bemisia tabaci* Genn. and the association of one population with silverleaf symptom development. Entomol. Exp. Appl. 61: 211-219.

Costa, H.S., J.K. Brown & D.N. Byrne. 1991. Life history traits of the whitefly, *Bemisia tabaci* (Homoptera: Aleyrodidae) on six virus-infected or healthy plant species. Environ. Entomol. 20: 1102-1107.

Costa, H.S., M.W. Johnson & D.E. Ullman. 1994. Row covers effect on sweetpotato whitefly (Homoptera: Aleyrodidae) densities, incidence of silverleaf, and crop yield in zucchini. J. Econ. Entomol. 87: 1616-1621.

Coudriet, D.L., P. Prabhaker, A.N. Kishaba & D.E. Meyerdirk. 1985. Variation in developmental rate on different hosts and overwintering of the sweetpotato whitefly, *Bemisia tabaci* (Homoptera: Alleyrodidae). Environ. Entomol. 14: 516-519.

Cross, M.C. & P.C. Hohenberg. 1994. Spatiotemporal chaos. Science 263: 1569-1570.

Curran, P.J. 1980. Multispectral photographic remote sensing of green vegetation biomass and productivity. Photogam. Eng. Remote Sens. 48: 243-250.

Czosnek, H., R. Ber, Y. Antignus, S. Cohen, N. Navot & D. Zamir. 1988. Isolation of tomato yellow leaf curl virus, a geminivirus. Phytopathology 78: 508-512.

Danzig, E.M. 1964. The whiteflies (Homoptera: Aleyrodidae) of the Caucasus. [In Russian, English translation in Entomol. Rev. 43: 325-330.]. Entomol. Obozrenie 43: 633-646.

Davidson, E.W., B.J. Segura, T. Steele & D.L. Hendrix. 1994. Microorganisms influence the composition of honeydew produced by the silverleaf whitefly, *Bemisia argentifolii*. J. Insect Physiol. 40: 1069-1076.

Dayton, P. & M.J. Tegner. 1984. The importance of scale in community ecology: a kelp forest example with terrestrial analogs. p. 457-481. In P.W Price, C.N. Slobodchikoff & W.S. Gaud (eds.), A new ecology: novel approaches to interactive systems. Wiley, New York.

Dean, D.E. 1994. Predaceous arthropods of the sweetpotato whitefly, *Bemisia tabaci* (Gennadius) on tomatoes in Florida. Ph.D. dissertation, University of Florida. 231pp.

DeGrandi-Hoffman, G., J. Diehl, D. Li, L. Flexner, G. Jackson, W. Jones & J. Debolt. 1994. BIOCONTROL-PARASITE: Parasitoid-host and crop loss assessment simulation model. Environ. Entomol. 23: 1045-1060.

Dennin, M., G. Ahlers & D.S. Cannell. 1996. Spatiotemporal chaos in electroconvection. Science 272: 388-390.

Dennis, B., R.A. Desharnais, J.M. Crushing & R.F. Costantino. 1995. Nonlinear demographic dynamics: Mathematical models, statistical methods, and biological experiments. Ecol. Mono. 65: 261-281.

DePonti, O.M.B., L.R. Romanow & M.J. Berlinger. 1990. Whitefly-plant relationships: plant resistance. p. 91-106. In D. Gerling (ed.), Whiteflies: Their bionomics, pest status, and management. Intercept, Andover, UK.

Dittrich, V., G.H. Ernst, O. Ruesch & S. Uk. 1990. Resistance mechanisms in sweetpotato whitefly (Homoptera: Aleyrodidae) populations from Sudan, Turkey, Guatemala, and Nicaragua. J. Econ. Entomol. 83(5): 1665-1670.

Dittrich, V., S.O. Hassan & G.H. Ernst. 1985. Sudanese cotton and the whitefly: A case study of the emergence of a new primary pest. Crop Prot. 4: 161-176.

Duffus, J.E. 1987. Whitefly transmission of plant diseases. p. 73-91. In K. F. Harris (ed.), Current topics in vector research. Vol. 4. Springer-Verlag, New York.

Duffus, J. E. & R.A. Flock. 1982. Whitefly-transmitted disease complex of the desert southwest. Calif. Agric. 36(11- 12): 4-6.

Duffus, J.E., R.C. Larsen & H. . Liu. 1986. Lettuce infectious yellows virus–a new type of whitefly transmitted virus. Phytopathology 76(1): 97-100.

Dunning, J.B., B.J. Danielson & H.R. Pulliam. 1992. Ecological processes that affect populations in complex landscapes. Okios 65: 169-175.

Dunning, J.B., Jr., D.J. Stewart, B.J. Danielson, B.R. Noon, T.L. Root, R.H. Lamberson, & E.E. Stevens. 1995. Spatially explicit population models: Current forms and future uses. Ecol. Appl. 5: 3-11.

Dunteman, G.H. 1989. Principal component analysis. Sage Publications, Inc. CA., 95 pp.

Edelstein-Keshet, L. 1988. Mathematical models in biology. Birkhauser Mathematical Series. Random House, New York, 586 pp.

Ekbom, B.S. & R. M. Xu. 1990. Sampling and spatial patterns of whiteflies. p. 107-122. In D. Gerling (ed.), Whiteflies: Their bionomics, pest status and management. Intercept, Andover, UK.

El-Helaly, M.S., A.Y. El-Shazli & F.H. El-Gayar. 1971. Morphological studies on immature stages of *Bemisia tabaci* Gennadius (Homoptera: Aleyrodidae). Z. Angew. Entomol. 68: 403- 408.

El-Helaly, M.S., I.A. Rawash & E.G. Ibrahim. 1981a. Phototaxis of the adult whitefly, *Bemisia tabaci* Gennadius to visible light. I. Effect of the exposure period on the insect's response to different wavelengths of the visible light-spectrum using a devised simple technique. Acta Phytopathologica Academiae Scientiarum Hungaricae 16: 181-188.

El-Helaly, M.S., I.A. Rawash & E.G. Ibrahim. 1981b. Phototaxis of the adult whitefly, *Bemisia tabaci* Gennadius to the visible light. II. Effects of both light intensity and sex of the whitefly adults on the insect's response to different wavelengths of light spectrum. Acta Phytopathologica Academiae Scientiarum Hungaricae 16(3-4): 389-398.

Engvall, J.L., J.D. Tubbs & Q.A. Holmes. 1977. pattern recognition of landsat data based upon temporal trend analysis. Remote Sens. Environ. 6: 302-314.

Evans, G.A. 1993. Systematic studies of new world *Encarsia* species and a survey of the parasitoids of *Bemisia tabaci* in Florida, the Caribbean and Latin America. Ph.D. dissertation, University of Florida, 284pp.

Fahrig, L. 1988. A general model of populations in patchy habitats. Appl. Math. Comp. 27: 53-66.

Fahrig, L. & J. Paloheimo. 1988. Effect of spatial arrangement of habitat patches on local population size. Ecol. 69: 468-475.

Faust, R.M. [ed.]. 1992. Conference report and 5-year national research and action plan for development of management and control methodology for the sweetpotato whitefly. Houston, Texas, Feb. 18-21. USDA/ARS ARS-107, 165pp.

Forster, B.C. & J.C. Trinder. 1984. An examination of the effects of resampling on classification accuracy. p. 106-115. Proc. 3rd. Australasian Conf. On Remote Sensing (Landsat '84), Gold Coast Queensland.

Fung, T. & E. LeDrew. 1987. Application of Principal Components analysis to change detection. Photogram. Eng.Remote Sens. 53: 1649-1658.

Gameel, O.I. 1974. Some aspects of the mating and oviposition behaviour of the cotton whitefly *Bemisia tabaci* (Genn.). Rev. Zool. Bot. Afr. 88: 784-788.

Gennadius, P. 1889. Disease of tobacco plantations in the Trikonia. The aleurodid of tobacco. Ellenike Georgia 5: 1-3.

Gerling, D. [ed.]. 1990. Whiteflies: Their bionomics, pest status and management. Intercept Ltd., London.

Gerling, D. 1992. Approaches to the biological control of whiteflies. Fla. Entomol. 75: 446-456.

Gerling, D. & R. Horowitz. 1983. Flight of adult *Bemisia tabaci* as determined in yellow trap catches. Phytoparasitica 11: 64.

Gerling, D. & A.R. Horowitz. 1984. Yellow traps for evaluating the population levels and dispersal patterns of *Bemisia tabaci* (Homoptera: Aleyrodidae). Ann. Entomol. Soc. Am. 77: 753-759.

Gerling, D., A.R. Horowitz & J. Baumgärtner. 1986. Autecology of *Bemisia tabaci*. Agric. Ecosystems Environ. 17: 5-19.

Gerling, D. & V. Kravchenko. 1994. Integrated pest management for the control of *Bemisia* attacking field crops outdoors. Phytoparasitica 22: 354.

Gerling, D., U. Motro & R. Horowitz. 1980. Dynamics of *Bemisia tabaci* (Gennadius) (Homoptera: Aleyrodidae) attacking cotton in the Costal Plain of Israel. Bull. Entomol. Res. 70: 213-219.

Gill, R. J. 1990. The morphology of whiteflies. p. 13-46. In D. Gerling (ed.), Whiteflies: Their bionomics, pest status, and management. Intercept, Andover, UK.

Gill, R. J. 1992. A review of the sweetpotato whitefly in Southern California. Pan-Pacific Entomol. 68(2): 144-152.

Gonzalez, R.A., G.E. Goldman, E.T. Natwick, H.R. Rosenberg, J.I. Grieshop, S.R. Sutter, T. Funakoshi & S. Davila-Garcia. 1992. Whitefly invasion in Imperial Valley costs growers, workers millions in losses. Calif. Agric. 46(5): 7-8.

Goodman, R.M., J. Bird & P. Thongmeearkom. 1977. An unusual viruslike particle associated with golden yellow mosaic of beans. Phytopathol. 67(1): 37-42.

Greathead, A.H. 1986. Host plants. p. 17-25. In M.J.W. Cock (ed.), *Bemisia tabaci*: A literature survey of the cotton whitefly with an annotated bibliography. CAB International Institute of Biological Control, Ascot, UK.

Hamilton, W.D.O., R.C. Sanders, R.H.A. Coutts & K.W. Buck. 1981. Characterization of tomato golden mosaic virus as a geminivirus. FEMS Microbiology Letters. 11: 263-267.

Harrison, B.D. 1985. Advances in geminivirus research. Annu. Rev. Phytopathol. 23: 55-82.

Hassell, M.P. 1975. Density-dependence in single-species populations. J. Anim. Ecol. 44: 283-295.

Hassell, M.P. 1978. The dynamics of arthropod predator-prey systems. Princeton Univ. Press, Princeton, NJ.

Hassell, M.P., Comins, H.N. & R.M. May. 1991. Spatial structure and chaos in insect population dynamics. Nature 353, 255-258.

Hassell, M.P., Comins, H.N. & R.M. May. 1994. Species coexistence and self-organizing spatial dynamics. Nature 370, 290-292.

Hassell, M.P. & R.M. May. 1973. Stability in insect host-parasite models. J. Anim. Ecol. 42: 693-726.

Hassell, M.P. & J.K. Waage. 1984. Host-parasitoid population interactions. Ann. Rev. Entomol. 29: 89-114.

Hastings, A. 1990. Spatial heterogeneity and ecological models. Ecol. 71: 426-428.

Hastings, A. & K. Higgins. 1994. Persistence of transients in spatially structured ecological models. Science 263: 1133-1136.

Hatfield, J.L. 1990. Remote sensing of crop stress: application to plant pathology. Phytopathology 80: 37-39.

Heinz, K. M. & M. P. Parrella. 1994. Biological control of *Bemisia argentifolii* (Homoptera: Aleyrodidae) infesting *Euphorbia pulcherrima*--evaluations of releases of *Encarsia luteola* (Hymenoptera: Aphelinidae) and *Delphastus pusillus* (Coleoptera: Coccinellidae). Environ. Entomol. 23: 1346-1353.

Heinz, K.M. & F.G. Zalom. 1995. Variation in trichome-based resistance to *Bemisia argentifolii* (Homoptera: Aleyrodidae) oviposition on tomato. J. Econ. Entomol. 88: 1494-1502.

Hendi, A., M.I. Abdel-Fattah & A. El-Sayed. 1987. Biological study on the white-fly, *Bemisia tabaci* (Genn.) (Homoptera: Aleyrodidae). Bull. Entomol. Soc. Egypt 65: 101-108.

Hirano, K., E. Budiyanto & S. Winarni. 1993. Biological characteristics and forecasting outbreaks of the whitefly, *Bemisia tabaci*, a vector of virus diseases in soybean fields. Aspac, Technical Bulletin. 135: 1-14.

Hoddle, M.S. & R. Van Driesche. 1996. Evaluation of *Encarsia formosa* (Hymenoptera: Aphelinidae) to control *Bemisia argentifolii* (Homoptera: Aleyrodidae) on Poinsettia (*Euphorbia pulcherrima*): A lifetable analysis. Fla. Entomol. 79: 1-12.

Holt, R.D., S.W. Pacala, T.W. Smith & J. Liu. 1995. Linking contemporary vegetation models with spatially explicit animal population models. Ecol. Appl. 5: 20-27.

Honda, Y., M. Iwaki, Y. Saito, P. Thongmeearkon, K. Kittisak & N. Deema. 1983. Mechanical transmission, purification, and some properties of whitefly-borne mungbean yellow mosaic virus in Thailand. Plant Dis. 67: 801-804.

Hord, R.M. & W. Broone. 1976. Land-use map accuracy criteria. Photogram. Eng. Remote Sens. 42: 671-677.

Horowitz, A. R. 1986. Population dynamics of *Bemisia tabaci* (Gennadius): with special emphasis on cotton fields. Agric. Ecosystems Environ. 17: 37-47.

Horowitz, A.R. & D. Gerling. 1992. Seasonal variation of sex ratio in *Bemisia tabaci* on cotton in Israel. Environ. Entomol. 21: 556-559.

Horowitz, A.R. & I. Ishaaya. 1994. Managing resistance to insect growth regulators in the sweetpotato whitefly (Homoptera: Aleyrodidae). J. Econ. Entomol. 87(4): 866-871.

Horowitz, A.R., Z. Mendelson & I. Ishaaya. 1993. Managing resistance to growth regulators in *Bemisia tabaci* in Israel. Phytoparasitica 21(2): 179.

Horowitz, A.R., H. Podoler & D. Gerling. 1984. Life table analysis of the tobacco whitefly *Bemisia tabaci* (Gennadius) in cotton fields in Israel. Acta Oecologica, Oecologia Appl. 5: 221- 233.

Host, G.E., P.L. Polzer, D.J. Mladenoff, M.A. White & T.R. Crow. 1996. A quantitative approach to developing regional ecosystem classifications. Ecol. Appl. 6: 608-618.

Hudson, W.D. & C.W. Ramm. 1987. Correct formulation of the kappa coefficient of agreement. Photogram. Eng. Remote Sens. 53: 421-422.

Hulspas-Jordaan, P.M. & Lenteren, J.C. van. 1988. Modelling population growth of greenhouse whitefly (*Trialeurodes vaporariorum*) on tomato. Agric. Univ. Wageningen Papers 89(2): 1-54.

Husain, M.A. 1931. A preliminary note on the white-fly of cottons in the Punjab. Agric. J. India 25: 508-526.

Immaraju, J.A. 1989. The whitefly problem in cotton diagnosis and needs. Pesticides 23(8): 19-21.

Imperial County Agricultural Commissioner's Office. 1994. Imperial county agricultural crop and livestock report. El Centro, CA.

Ingebritsen, S.E. & R.J.P. Lyon. 1985. Principal components analysis of multitemporal image pairs. Int. J. Remote Sens. 6: 687-696.

Iwaki, M.,P. Thongmeearkom, Y. Honda & N. Deema. 1983. Soybean crinkle leaf: A new whitefly-borne disease of soybean. Plant Dis. 67: 546-548.

Jagdev, S. & N.S. Butter. 1988. Influence of climatic factors on the buildup of whitefly *Bemisia tabaci* Genn. on cotton. Indian J. Entomol. 47: 359-360.

Jakubauskas, M.E., J.L. Whistler, M.E. Dillworth & E.A. Martinko. 1992. Classifying remotely sensed data for use in an agricultural nonpoint-source pollution model. J. Soil and Water Cons. 47: 179-183.

Jensen, J.R. 1986. Introductory digital image processing. A remote sensing perspective. Prentice-Hall, Englewood Cliffs, NJ, 379 pp.

Johnson, A.R. & B.T. Milne. 1992. Diffusion in fractal landscapes: simulation and experimental studies of tenebrionid beetle movements. Ecol. 73: 1968-1983.

Johnson, C.G. 1969. Migration and dispersal of insects by flight. Metheum & Co. Ltd, London.

Johnson, M. W., N. C. Toscano, H. T. Reynolds, E. S. Sylvester, K. R. Kido & E. T. Natwick. 1982. Whiteflies cause problems for southern California growers. Calif. Agric. 9-10: 24-26.

Jury, E.I. 1964. Theory and application of the z-transform method. Wiley, New York, 330pp.

Jury, E.I. 1971. "Inners" approach to some problems of system theory. IEEE Trans. Automatic Contr., AC-16: 233-240.

Jury, E.I. 1974. Inners and stability of dynamical systems. Wiley, New York.

Kaneko, K. 1989. Spatiotemporal chaos in one- and two-dimensional coupled map lattices. Physica D 37, 60-82.

Kaneko, K. 1990. Supertransients, spatiotemporal intermittency and stability of fully developed spatiotemporal chaos. Phys. Letters A 149: 105-112.

Kaneko, K. 1992. Overview of coupled map lattices. Chaos 2: 279-282.

Kareiva, K.A. & M. Anderson. 1988. Spatial aspects of species interactions: the wedding of models and experiments. pp 35-50. In A. Hastings (ed.), Community ecology. Lecture Notes in Biomathematics 77. Springer-Verlag, Berlin, Germany.

Kot, M. 1989. Diffusion-driven period-doubling bifurcations. BioSyst. 22: 279-287.

Kot, M. & W.M. Schaffer. 1986. Discrete-time growth-dispersal models. Math. BioSci. 80: 109-136.

Kot, M, M.A. Lewis & P. van den Driessche. 1996. Dispersal data and the spread of invading organisms. Ecol. 77: 2027-2042.

Krauss, T.P., L. Shure & J. N. Little. 1993. Signal processing toolbox for use with Matlab. The MathWorks Inc., Natick, MA, 170pp.

Kring, J.B., D.J. Schuster, J.F. Price & G.W. Simone. 1991. Sweetpotato whitefly-vectored geminivirus on tomato in Florida. Plant Dis. 75:1186.

Kuo, J., E. Fox & S. McDonald. 1992. SigmaStat™ statistical software for working scientist. User's manual. Jandel Scientific, San Rafael, CA.

Lavreau, J. 1991. De-hazing landsat thematic mapper images. Photogram. Eng. Remote Sens. 57: 1297-1302.

Leibhold, A.M. & M.L. McManus. 1991. Does larval dispersal cause the expansion of gypsy moth outbreaks? J. Appl. For. 8: 95-98.

Levin, S.A. 1992. The problem of pattern and scale in ecology. Ecol. 73: 1943-1967.

Lewis, E.R. 1977. Network models in population biology (Biomath., vol. 7). Springer-Verlag, New York.

Lewis, M.A. & J.D. Murray. 1993. Modelling territoriality and wolf-deer interactions. Nature 366: 738-740.

Lichtenberg, A.J. & M.A. Lieberman. 1992. Regular and chaotic dynamics. Applied Mathematical Sciences, vol. 38. Springer-Verlag, New York. 692pp.

Liu, T. & P.A. Stansly. 1995. Oviposition by *Bemisia argentifolii* (Homoptera: Aleyrodidae) on tomato: Effects of leaf factors and insecticide resistance. J. Econ. Entomol. 88: 992-997.

Lopez-Avila, A. 1986. Taxonomy and biology. p. 3-11. In M.J.W. Cock (ed.), *Bemisia tabaci*~A literature survey on the cotton whitefly with an annotated bibliography. CAB International Institute of Biological Control, Ascot, UK.

Lopez-Avila, A. & M. J.W. Cook. 1986. Economic Damage. p. 51-53. In M.J.W. Cock (ed.), *Bemisia tabaci*~A literature survey on the cotton whitefly with an annotated bibliography. CAB International Institute of Biological Control, Ascot, UK.

Lui, R. 1989a. Biological growth and spread modeled by systems of recursions. I. Mathematical theory. Math. BioSci. 93: 269-295.

Lui, R. 1989b. Biological growth and spread modeled by systems of recursions. II. Biological theory. Math. BioSci. 93: 297-312.

Lynch, R.E. & A.M. Simmons. 1993. Distribution of immatures and monitoring of adult sweetpotato whitefly, *Bemisia tabaci* (Gennadius) (Homoptera: Aleyrodidae), in peanut, *Arachis hypogaea*. Environ. Entomol. 22: 375-380.

Mahey, R.K., R. Singh, S.S. Sidhu & R.S. Narang. 1990. The use of remote sensing to assess the effects of water stress on wheat. Expl. Agric. 27: 423-429.

Manetsch, T.J. 1976. Time-varying distributed delays and their use in aggregative models of large systems. IEEE Trans. Syst. Man. Cyber. vol SMC-6 (8): 547-553.

Manly, B.F.J. 1986. Multivariate statistical methods. A primer. Chapman and Hall, Ltd., New York.

MathWorks. 1994. MATLAB reference guide. High-performance numeric computation and visualization software. Version 4.2c.1. The MathWorks Inc., Natick, MA.

May, R.M. 1974. Stability and complexity in model ecosystems. Princeton University Press, Princeton, NJ, 265pp.

May, R.M., G.R. Conway, M.P. Hassell & T.R.E Southwood. 1974. Time delays, density dependence and single species oscillations. J. Anim. Ecol. 43: 747-770.

Maynard, D.N. & D.J. Cantliffe. 1989. Squash silverleaf and tomato irregular ripening: new vegetable disorders in Florida. Florida Coop. Ext. Serv., IFAS, Univ. Florida, Veg. Crop Fact Sheet,VC-37, 4pp.

Maynard Smith, J. 1968. Mathematical ideas in biology. Cambridge University Press, New York.

McAuslane, H.J. 1996. Influence of leaf pubescence on ovipositional preference of *Bemisia argentifolii* (Homoptera: Aleyrodidae) on soybean. Environ. Entomol. 24: 834-841.

McAuslane, H.J., F.A. Johnson, D.L. Colvin & B. Sojack. 1995. Influence of foliar pubescence on abundance and parasitism of *Bemisia argentifolii* (Homoptera: Aleyrodidae) on soybean and peanut. Environ. Entomol. 24: 1135-1143.

McAuslane, H.J., F.A. Johnson & D.A. Knauft. 1994. Population levels and parasitism of *Bemisia tabaci* (Gennadius) (Homoptera: Aleyrodidae) on peanut cultivars. Environ. Entomol. 23: 1203-1210.

McAuslane, H.J., F.A. Johnson, D.A. Knauft & D.L. Colvin. 1993. Seasonal abundance and within-plant distribution of parasitoids of *Bemisia tabaci* (Homoptera, Aleyrodidae) in peanuts. Environ. Entomol. 22: 1043-1050.

McAuslane, H.J., D.A. Knauft & F.A. Johnson. 1995. Evaluation of peanut breeding lines for resistance to silverleaf whitefly (Homoptera: Aleyrodidae). Fla. Entomol. 78: 75-81.

Mead, R. & R.N. Curnow. 1983. Statistical methods in agriculture and experimental biology. Chapman and Hall, New York, 335pp.

Melamed-Madjar, V., S. Cohen, M. Chen, S. Tam & D. Rosilio. 1982. A method for monitoring *Bemisia tabaci* and timing spray applications against the pest in cotton fields in Israel. Phytoparasitica 10: 85-91.

Meyerdirk, D. E., D. L. Coudriet & N. Prabhaker. 1986. Population dynamics and control strategy for *Bemisia tabaci* in the Imperial Valley, California. Agric. Ecosystems Environ. 17(1- 2):62-67.

MicroImages. 1995. TNTmips™. The map and image processing system . V5.1 MicroImages, Inc., Lincoln, NE.

Milne, B.T. 1988. Measuring the fractal geometry of landscapes. Appl. Math. Comput. 27: 67-79.

Misra, C.S. & K.S. Lamba. 1929. The cotton white-fly (*Bemisia gossypiperda*, n. sp.). Bull. Agric. Res. Inst., Pusa 196: 1-7.

Molofsky, J. 1994. population dynamics and pattern formation in theoretical populations Ecol. 75: 30-39.

Morris, R.F. 1960. Sampling insect populations. Annu. Rev. Entomol. 5: 243-264.

Mound, L.A. 1962. Studies on the olfaction and colour sensitivity of *Bemisia tabaci* (Genn.) (Homoptera: Aleyrodidae). Entomol. Exp. Appl. 5: 99-104.

Mound, L.A. 1963. Host-correlated variation in *Bemisia tabaci* (Gennadius) (Homoptera: Aleyrodidae). Proc. Royal Entomol. Soc. London, (A) 38: 171-180.

Mound, L.A. 1965. Effect of leaf hair on cotton whitefly populations in the Sudan Gezira. Empire Cotton Growing Rev. 42: 33-40.

Mound, L.A. & S.H. Halsey. 1978. Whitefly of the world. A systematic catalogue of the Aleyrodidae (Homoptera) with host plant and natural enemy data. British Museum (Natural History) and John Wiley & Sons, London, UK, 340 pp.

Murdoch, W.W. 1990. The relevance of pest-enemy models to biological control. p. 1-24. In M. Mackauer, L.E Ehler & J. Roland (eds.), Critical issues in biological control. Intercept, Andover, UK.

Murray, J.D. 1989. Mathematical biology. Biomathematics. Vol. 19. Springer-Verlag, New York, 767pp.

Musuna, A.C.Z. 1986. A method for monitoring whitefly, *Bemisia tabaci* (Genn.), in cotton in Zimbabwe. Agric. Ecosystems Environ. 17(1-2): 29-35.

Naranjo, S.E. & H.M. Flint. 1994. Spatial distribution of preimaginal *Bemisia tabaci* (Homoptera: Aleyrodidae) in cotton and development of fixed-precision sequential sampling plans. Environ. Entomol. 23: 254-266.

Naranjo, S.E., H.M. Flint & T.J. Henneberry. 1995. Comparative analysis of selected sampling methods for adult *Bemisia tabaci* (Homoptera: Aleyrodidae) in cotton. J. Econ. Entomol. 88: 1666-1678.

Natarajan, K., V.T. Sundaramurthy & A.K. Basu. 1986. Meet the menace of whitefly to cotton. Ind. Farm. 36(4): 37, 39, 44.

Neubert. M.G., M. Kot & M.A. Lewis. 1995. Dispersal and pattern formation in a discrete-time predator-prey model. Theor. Popul. Biol. 48: 7-43.

Nicholson, A.J. & V.A. Bailey. 1935. The balance of animal populations. Proc. Zoo. Soc. Lond. 3: 551-598.

Nuessly, G.S. & T.J. Henneberry. 1989. Effect of sweetpotato whitefly population density on cotton fiber stickiness and reducing sugars. p. 281-284. In J.M. Brown & D. A. Richter (ed.), Proceedings Beltwide Cotton Production Conference. National Cotton Council, Memphis, TN.

Ohnesorge, B. & G. Rapp. 1986. Monitoring *Bemisia tabaci*: A review. Agric. Ecosystems Environ. 17(1-2): 21-27.

Ohnesorge, B., N. Sharaf & T. Allawi. 1980. Population studies on the tobacco whitefly *Bemisia tabaci* Genn. (Homoptera, Aleyrodidae) during the winter season. I. The spatial distribution on some host plants. Z. Angew. Entomol. 90: 226-232.

Ohnesorge, B., N. Sharaf & T. Allawi. 1981. Population studies on the tobacco whitefly *Bemisia tabaci* Genn. (Homoptera, Aleyrodidae) during the winter season. II. Some mortality factors of the immature stages. Z. Angew. Entomol. 92: 127-136.

Okubo, A. 1980. Diffusion and Ecological Problems: Mathematical Models, Springer Verlag, Berlin.

O'Neil et al. 1988. Indices of landscape pattern. Landscape Ecol. 1: 153-62.

Onillon, J.C. 1990. The use of natural enemies for the biological control of whiteflies. pp. 287-324. In Gerling. D. (ed.), Whiteflies: Their bionomics, pest status, and management. Intercept, Andover, UK.

Onillon, J.C.& J. Onillon. 1974. Contribution à l'étude de la dynamiquedes populations d'Homoptères inféodes aux Agrumes. III. 2. Modalités de la dispersion de *Cales noacki* (Howard) (Hymenopt., Aphelinidae), parasite d'*Aleurothrixus floccosus* (Maskell) (Homopt., Aleyrodidae). IOBC/WPRS Bulletin, 3: 51-66.

Orbach, R. 1986. Dynamics of fractal networks. Science. 231: 814-819.

Osaki, T. & T. Inouye. 1981. Tobacco leaf curl virus. Commonwealth Mycological Institute and the Association of Applied Biologists. Description of Plant Viruses No. 232, 4pp.

Oster, G. 1978. The dynamics of nonlinear models with age-structure. In S.A. Levin (ed.), Studies in mathematical biology. Part II: Populations and communities. Vol. 16. Math. Assoc. Amer., Washington, DC, 411pp.

Ozgür, A.F. & E. Sekeroglu. 1984. Population developments of *Bemisia tabaci* (Genn.) (Homoptera: Aleyrodidae) on various cotton varieties in Cukurova, Turkey. XVII Int. Congress Entomol. Abstract Vol: 568.

Ozgür, A.F. & E. Sekeroglu. 1986. Population development of *Bemisia tabaci* (Homoptera: Aleurodidae) on various cotton cultivars in Cukurova, Turkey. Agric. Ecosystems. Environ. 17(1-2): 83-88.

Palmer, M.W. 1988. Fractal geometry: a tool for describing spatial patterns of plant communities. Vegatatio. 75: 91-102.

Palumbo, J.C., A. Tonhasca & D.N. Byrne. 1995. Evaluation of three sampling methods for estimating adult sweetpotato whitefly (Homoptera: Aleyrodidae) abundance on cantaloupes. J. Econ. Entomol. 88(5): 1393-1400.

Parrella, M.P., T.S. Bellows, R.J. Gill, J.K. Brown & K.M. Heinz. 1992. Sweetpotato whitefly: Prospects for biological control. Calif. Agric. 46(1): 25-26.

Pearson, J.E. 1993. Complex patterns in a simple system. Science 261: 189-192.

Perring, T.M. 1994. Biological characteristics of *Bemisia tabaci* and closely related species. Phytoparasitica 22(4): 309.

Perring, T.M., A. Cooper & D.J. Kazmer. 1992. Identification of the poinsettia strain of *Bemisia tabaci* (Homoptera, Aleyrodidae) on broccoli by electrophoresis. J. Econ. Entomol. 85: 1278-1284.

Perring, T.M., A. Cooper, D.J. Kazmer, C. Shields & J. Shields. 1991. New strain of sweetpotato whitefly invades California vegetables. Calif. Agric. 45(6): 10-12.

Perring, T.M., A.D. Cooper, R.J. Rodriguez, C.A. Farrar & T.S. Bellows. 1993a. Identification of a whitefly species by genomic and behavioral studies. Science 259: 74-77.

Perring, T.M., C.A. Farrar, T.S. Bellows, A.D. Cooper & R.J. Rodriguez. 1993b. Evidence for a new species of whitefly: UCR findings and implications. Calif. Agric. 47(1): 7-8.

Perring, T.M., C.A. Farrar & A.D. Copper. 1994. Mating behavior and competitive displacement of whiteflies. p. 25. In T. J. Henneberry, N. C. Toscano, R. M. Faust & J. R. Coppedge (eds.), Silverleaf whitefly (formerly sweetpotato whitefly, strain B) 1994 Supplement to the Five-Year National Research and Action Plan. USDA/ARS 125, 24-27 January. Orlando, Florida.

Perring, T.M., C.A. Farrar, A.D. Cooper, T.S. Bellows & R.J. Rodriguez. 1993. Determining whitefly species–response. Science 261: 1334-1335.

Pollard, D.G. 1955. Feeding habits of the cotton whitefly, *Bemisia tabaci* Genn. (Homoptera, Aleyrodidae). Ann. Appl. Biol. 43: 664-671.

Powell, D.A. & T.S. Bellows, Jr. 1992a. Preimaginal development and survival of *Bemisia tabaci* on cotton and cucumber. Environ. Entomol. 21: 359-363.

Powell, D.A. & T.S. Bellows, Jr. 1992b. Adult longevity, fertility and population growth rates for *Bemisia tabaci* (Genn) (Hom, Aleyrodidae) on two host plant species. J. Appl. Entomol. 113: 68-78.

Powell, D.A. & T.S. Bellows, Jr. 1992c. Development and reproduction of two populations of *Eretmocerus* species (Hymenoptera, Aphelinidae) on *Bemisia tabaci* (Homoptera, Aleyrodidae). Environ. Entomol. 21: 651-658.

Prabhaker, N., D.L. Coudriet & D.E. Meyerdirk. 1985. Insecticide resistance in the sweetpotato whitefly, *Bemisia tabaci* (Homoptera: Aleyrodidae). J. Econ. Entomol. 78: 748-752.

Price, J.F., D.J. Schuster & D.E. Short. 1987. Managing sweetpotato whitefly. Greenhouse Grower 35(12): 55-57.

Priesner, H. & M. Hosny. 1934. Contributions to a knowledge of white flies (Aleyrodidae) of Egypt (II). Bull. Ministry Agric. Egypt Tech. Sci. Serv. 139: 1-21.

Quaintance, A.L. 1900. Contribution towards a monograph of the American Aleurodidae. USDA, Tech. Ser. Bur. Entomol. 8: 9-64.

Quattrochi, D.A. & R.E. Pelletier. 1991. Remote sensing for analysis of landscapes: an introduction. pp 51-76. In M.G. Turner & R.H. Gardner (eds.), Quantitative methods in landscape ecology. The analysis and interpretation of landscape heterogeneity. Ecological studies vol. 82. Springer-Verlag, New York. 536pp.

Rahman, S., G. F. Vance & L.C. Munn. 1994. Detecting salinity and soil nutrient deficiencies using spot satellite data. Soil Sci. 158: 31-39.

Reddy, A.S. & N.V. Rao. 1989. Cotton whitefly (*Bemisia tabaci* Genn.): A review. Indian J. Plant Prot. 17: 171-179.

Reeve, J.D. 1988. Environmental variability, migration and persistence in host-parasitiod systems. Am. Nat. 132: 810-836.

Reeve, J.D. 1990. Stability, variability, and persistence in host-parasitoid systems. Ecol. 71: 422-426.

Rey-Benayas, J.M. & K.O. Pope. 1995. Landscape ecology and diversity patterns in the seasonal tropics from landsat TM imagery. Ecol. Appl. 5: 386-394.

Richards, J.A. 1984. Thematic mapping from multitemporal image data using principal components transformation. Remote Sens. Environ. 16: 35-46.

Richards, J.A. 1993. remote sensing digital image analysis. An introduction. Springer-Verlag, New York, 340pp.

Ricker, W.E. 1954. Stock and recruitment. J. Fish. Res. Bd. Can. 11: 559-623.

Riley, D.G. & J.C. Palumbo. 1995. Action threshold for *Bemisia argentifolii* (Homotera: Aleyrodidae) in cantaloupe. J. Econ. Entomol. 88: 1733-1738.

Riley, D. & D. Wolfenbarger. 1993. Cultivated hosts and population dynamics of sweetpotato whitefly in the lower Rio Grande Valley of TX. 1993 Prceedings--Beltwide Cotton Production research Conferences. v2, p. 667-670. Memphis, Tenn.: National Cotton Council of America.

Rosenfield, G.H., K. Fitzpatrick-Lins & H.S. Ling. 1982. Sampling for the thematic map accuracy testing. Photogram. Eng. Remote Sens. 48: 131-137.

Rote, N.B. & S.N. Puri. 1992. Effects of fertilizer application on incidence of whitefly on different cotton cultivars. Maharashtra Agric. Univ. (India) 17(1): 45-48.

Rote, N.B., S.N. Puri, G.D. Butler, Jr. & T.J. Henneberry. 1992. Whitefly population levels, fecundity and developmental period on cotton following insecticidal applications. J. Appl. Zool. Res. 3(1): 1-6.

Rudd, W.G. & R.W. Gandour. 1985. Diffusion model for insect dispersal. J. Econ. Entomol. 78: 295-301

Russell, L.M. 1957. Synonyms of *Bemisia tabaci* (Gennadius) (Homoptera, Aleyrodidae). Bull. Brooklyn Entomol. Soc. 52: 122- 123.

Ruxton, G.D. 1996. Dispersal and chaos in spatially structured models: An individual-level approach. J. Anim. Ecol. 65: 161-169.

Salas, J. & O. Mendoza. 1995. Biology of the sweetpotato whitefly (Homoptera: Aleyrodidae) on tomato. Fla. Entomol. 78(1): 154-160.

Schuster, D.J. 1995. Integration of natural enemies for management of the sweetpotato whitefly and associated disorders on mixed-cropped vegetables. Final report of Sustain. Agric. Res. Educ. (SARE)/Agric. in Concert with the Environment (ACE) Project No. AS92-3. UF/IFAS, Gulf Coast Res. Educ. Center, FL, 69 pp.

Schuster, D.J., J.B. Kring & J.F. Price. 1991. Association of the sweetpotato whitefly with a silverleaf disorder of squash. HortScience 26: 155-156.

Schuster, D.J., T.F. Mueller, J.B. Kring & D.J. Price. 1990. Relationship of the sweetpotato whitefly to a new tomato fruit disorder in Florida. HortScience 25: 1618-1620.

Schuster, D.J., J.E. Polston & J.F. Price. 1992. Reservoirs of the sweetpotato whitefly for tomatoes in west-central Florida. Proc. Fla. State. Hort. Soc. 105: 311-314.

Schuster,, D.J., & J.F. Price. 1987. The western flower thrips and the sweetpotato whitefly: New pests threatening Florida tomato production. Gulf Coast. Res. Educ. Res. Rep. BRA1987, . Univ. of Fla., Gainesville.

Schreier, H., R. Wiart & S. Smith. 1988. Quantifying organic matter degradation in agricultural fields using PC-based image analysis. J. Soil Water Cons. : 421-424.

Segel, L.A. & J.L. Jackson. 1972. Dissipative structure: An explanation and an ecological example. J. Theor. Biol. 37: 545-559.

Sela, I.,I. Assouline, E. Tanne, S. Cohen & S. Marco. 1980. Isolation and characterization of a rod-shaped, whitefly-transmissible, DNA-containing plant virus. Phytopathology 70: 226- 228.

Sharaf, N. & Y. Batta. 1985. Effect of some factors on the relationship between the whitefly *Bemisia tabaci* Genn. (Homoptera: Aleyrodidae) and the parasitoid *Eretmocerus mundus* Mercet (Hymenoptera: Aphelinidae) in Jordan. Z. Angew. Entomol. 99: 267-276.

Silverman, B.W. 1986. Density estimation for statistics and data analysis. Chapman and Hall, New York.

Simmons, A.M. 1994. Oviposition on vegetables by *Bemisia tabaci* (Homoptera, Aleyrodidae)--temporal and leaf surface factors. Environ. Entomol. 23: 381-389.

Simmons, A.M. & K.D. Elsey. 1995. Overwintering and cold tolerance of *Bemisia argentifolii* (Homoptera: Aleyrodidae) in coastal South Carolina. J. Entomol. Sci. 30: 497-506.

Simmons, G.S. & O.P.J.M. Minkenberg. 1994. Field-cage evaluation of augmentative biological control of *Bemisia argentifolii* (Homoptera: Aleyrodidae) in Southern California cotton with the parasitoid *Eretmocerus* nr. *californicus* (Hymenoptera: Aphelinidae). Environ. Entomol. 23: 1552-1557.

Slatkin, M. 1973. Gene flow and selection in a cline. Genetics 75: 733-756.

Sokal, R.R. & N.L. Oden. 1978. Spatial autocorrelation in biology 1. Methodology. Biol. J. Linn. Soc. 10: 199-228.

Solé, R.V. & J. Valls. 1991. Characterization of spatiotemporal chaos from macroscopic measures. Physics Letters A 161: 241-246

Southwood, T.R.E. 1978. Ecological methods: With particular reference to the study of insect populations. Chapman and Hall, London, UK.

Stearns, S.D. & R.A. David. 1996. Signal processing algorithms in Matlab. Prentice Hall Englewood Cliffs, NJ, 372pp.

Stinner, R.E., C.S. Barfield, J.L. Stimac & L. Dohse. 1983. Dispersal and movement of insect pests. Ann. Rev. Entomol. 28: 319-335.

Strahler, A.H. 1980. The use of prior probabilities in maximum likelihood classification of remotely sensed data. Remote Sens. Environ. 10: 135-163.

Strong, D., J. Lawton & R. Southwood. 1984. Insects on plants: Community patterns and mechanisms. Blackwell Scientific, Oxford.

Summers, C.G. & D. Estrada. 1996. Chlorotic streak of bell-pepper: A new toxicogenic disorder induced by feeding of the silverleaf whitefly, *Bemisia argentifolii*. Plant Dis. 80: 822.

Taylor, A.D. 1988. Large-scale spatial structure and population dynamics in arthropod predator-prey systems. Annales Zoologici Fennici 25: 63-74.

Taylor, A.D. 1990. Metapopulation, dispersal, and predator-prey dynamics: An overview. Ecol. 71: 429-433.

Thompson, C.M. & L. Shure. 1995. Image processing toolbox for use with Matlab. The MathWorks Inc., Natick, MA, 170pp

Tonhasca, A., J.C. Palumbo & D.N. Byrne. 1994. Distribution patterns of *Bemisia tabaci* (Homoptera: Aleyrodidae) in cantaloupe fields in Arizona. Environ. Entomol. 23: 949-954.

Tou, J.T. & R.C. Gonzalez. 1974. Pattern recognition principles. Addison-Wesley Publishing Co., Reading, MA, 377pp.

Tsai, J.H. & K. Wang. 1996. Development and reproduction of *Bemisia argentifolii* (Homoptera: Aleyrodidae) on five host plants. Environ. Entomol. 25: 810-816.

Turner, M.G., G.J. Arthaud, R.T. Engstrom, S.J. Hejl, J. Liu, S. Loeb & K. McKelvey. 1995. Usefulness of spatially explicit population models in land management. Ecol. Appl. 5: 12-16.

Van Genderen, J.L., B.F. Lock, & P.A. Vass. 1978. Remote sensing: statistical testing of thematic map accuracy. Remote Sens. Environ. 7: 3-14.

Van Giessen, W.A., C. Mollema & K.D. Elsey. 1995. Design and use of a simulation model to evaluate germplasm for antibiotic resistance to the greenhouse whitefly (*Trialeurodes vaporariorum*) and the sweetpotato whitefly (*Bemisia tabaci*). Entomol. Exp. Appl. 76: 271-286.

Van Lenteren, J.C. & L.P.J. Noldus. 1990. Whitefly-plant relationships behavioral and ecological aspects. p. 47-90. In D. Gerling (ed.), Whiteflies: Their bionomics, pest status, and management. Intercept, Andover, UK.

van Roermund, H.J.W. & J.C. van Lenteren. 1992. Life-history parameters of the greenhouse whitefly, *Trialeurodes vaporariorum* and the parasitoid *Encarsia formosa*. Wageningen Agric. Univ. Papers 92-3: 106-147.

Vansickle, J. Attrition in distributed delay models. IEEE Transactions on Syst. Man. Cyber. SMC-7 (9): 635-638.

Varma, P.M. 1963. Transmission of plant viruses by whiteflies. Bull. Natl. Inst. Sci. India 24: 11-33.

von Arx, R., J. Baumgartner & V. Delucchi. 1983. A model to stimulate the population dynamics of *Bemisia tabaci* Genn. (Stern., Aleyrodidae) on cotton in the Sudan Gezira. Z. Angew. Entomol. 96: 341-363.

von Arx, R.V., J. Baumgärtner & V. Delucchi. 1984. Sampling of *Bemisia tabaci* (Genn.) (Sternorrhyncha: Aleyrodidae) in Sudanese cotton fields. J. Econ. Entomol. 77: 1130-1136.

Wagner, T.L. 1995. Temperature-dependent development, mortality, and adult size of sweetpotato whitefly biotype B (Hompotera: Aleyrodidae) on cotton. Environ. Entomol. 24: 1179-1188.

Wang, K. & J.H. Tsai. 1996. Temperature effect on development and reproduction of silverleaf whitefly (Homoptera: Aleyrodidae). Ann. Entomol. Soc. Am. 89: 375-384.

Wiens, J.A. 1989. Spatial scaling in ecology. Func. Ecol. 3: 385-397.

Wilhoit, L., S. Schoenig, D. Supkoff & B. Johnson. 1994. A regional simulation model for silverleaf whitefly in the Imperial Valley. PM 94-01, Pest Management Analysis and Planning Program, State of California, EPA, Sacramento, CA.

With, K.A. & T.O. Crist. 1995. Critical thresholds in species' responses to landscape structure. Ecol. 76(8): 2446-2459.

Woods, M. 1988. Scientists take aim on lettuce menaces. Agric. Res., USA 36(8): 10-12.

Worner, S.P. 1992. Performance of phenological models under variable temperature regimes: Consequences of the Kaufmann or rate summation effect. Environ. Entomol. 21: 689-699.

Xu R.M. 1987. A system model for host plant-whitefly-*Encarsia* relationships to investigate optimal biological control strategies. Bull. IOBC, WPRS/EPRS. 1987/X/2: 183-187

Xu R.M. 1991a. Improvements of the plant-pest-parasitoid PPP model and its application on whitefly *Encarsia* population dynamics under different release methods. J. Appl. Entomol. 112(3): 274-287.

Xu R.M. 1991b. Spatio-temporal dynamics of population abundance–A systems approach on greenhouse whiteflies. Beijing Normal Univ. Press, Beijing.

Xu R.M., L.F. Liu, Q. Zhu & J.J. Shen. 1981. Application of a dimension-changeable matrix model on the simulation of the population dynamics of greenhouse whiteflies. Acta Ecologica Sinica 1(2): 147-148.

Yano, E., J.C. van Lanteren, R. Rabbinge & P.M. Hulspas-Jordaan. 1988a. The parasite-host relationship between *Encarsia formosa* Gahan (Hymenoptera, Aphelinidae) and *Trialeurodes vaporarium* (Westwood) (Homoptera, Aleyrodidae). XXXI. Simulation studies of the population growth of the greenhouse whitefly on tomatoes. Agric. Univ., Wageningen Papers 89(2), 55-73.

Yano, E., J.C. van Lenteren, R. Rabbinge. & P.M. Hulspas-Jordaan. 1988b. The parasite-host relationship between *Encarsia formosa* Gahan (Hymenoptera, Aphelinidae) and *Trialeurodes vaporarium* (Westwood) (Homoptera, Aleyrodidae). XXXII. Simulation studies of the population growth of the greenhouse whitefly on eggplants, cucumbers, sweet peppers and gerberas. Agric. Univ., Wageningen Papers 89(2): 75-100.

Yee, W.L. & N.C. Toscano. 1996. Ovipositional preference and development of *Bemisia argentifolii* (Homotera: Aleyrodidae) in relation to alfalfa. Environ. Entomol. 89: 870-876.

Yokomi, R.K., D.R. Jimenez, L.S. Osborne & J.P. Shapiro. 1995. Comparison of silverleaf whitefly-induced and chlormequat chloride-induced leaf silvering in *Cucurbita pepo*. Plant Dis. 79(9): 950-955.

Youngman, R.R., N.C. Toscano, V.P. Jones, K. Kido & E.T. Natwick. 1986. Correlations of seasonal trap counts of *Bemisia tabaci* (Homoptera: Aleyrodidae) in southeastern California. J. Econ. Entomol. 79: 67-70.

Zalom, F.G., E.T. Natwick & N.C. Toscano. 1985. Temperature regulation of *Bemisia tabaci* (Homoptera: Aleyrodidae) populations in Imperial Valley cotton. J. Econ. Entomol. 78: 61-64.

Zar, J.H. 1984. Biostatistical analysis, 2nd edition. Prentice-Hall, Inc., Englewood Cliffs, NJ, 718pp.

BIOGRAPHICAL SKETCH

Carlyle Christopher Brewster was born on November 2, 1957, to Mr. and Mrs. Christopher Brewster of Port-of-Spain, Trinidad and Tobago. Carlyle graduated from Fatima College in 1977 and in 1979 entered the Eastern Caribbean Institute of Agriculture and Forestry (ECIAF),Trinidad, where he received training in practical and theoretical agriculture. He graduated with a diploma in 1981 and spent one year as a quarantine and plant inspection officer with the Ministry of Agriculture. In 1982, he entered the University of the West Indies (UWI),Trinidad, and received his Bachelor of Science degree in agriculture in 1986. Carlyle worked in the Entomology section of the Central Experiment Station, Trinidad, and in 1988 was awarded a USDA/ARS Caribbean Basin fellowship that allowed him to undertake studies at the Entomology and Nematology Department, University of Florida (UF). He obtained his master's in 1990 and returned to Trinidad and to his job at the Central Experiment Station where he worked on the control of vegetable insect pests such as thrips and whiteflies. In 1992, he again entered the Entomology and Nematology Department at UF and began his doctoral studies on the dynamics and modeling of insect populations and the development of methods for studying these dynamics in large regional systems.

I certify that I have read this study and that in my opinion it conforms to acceptable standards of scholarly presentation and is fully adequate, in scope and quality, as a dissertation for the degree of Doctor of Philosophy.

Jon C. Allen, Chair
Professor of Entomology and Nematology

I certify that I have read this study and that in my opinion it conforms to acceptable standards of scholarly presentation and is fully adequate, in scope and quality, as a dissertation for the degree of Doctor of Philosophy.

Jerry L. Stimac
Professor of Entomology and Nematology

I certify that I have read this study and that in my opinion it conforms to acceptable standards of scholarly presentation and is fully adequate, in scope and quality, as a dissertation for the degree of Doctor of Philosophy.

Heather J. McAuslane
Assistant Professor of Entomology and Nematology

I certify that I have read this study and that in my opinion it conforms to acceptable standards of scholarly presentation and is fully adequate, in scope and quality, as a dissertation for the degree of Doctor of Philosophy.

James W. Jones
Professor of Agricultural and Biological Engineering

I certify that I have read this study and that in my opinion it conforms to acceptable standards of scholarly presentation and is fully adequate, in scope and quality, as a dissertation for the degree of Doctor of Philosophy.

Robert M. Peart
Graduate Research Professor of
Agricultural and Biological
Engineering

This dissertation was submitted to the Graduate Faculty of the College of Agriculture and to the Graduate School and was accepted as partial fulfillment of the requirements for the degree of Doctor of Philosophy.

December 1996

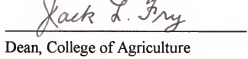

Dean, College of Agriculture

Dean, Graduate School